iScience

CellPress

Article

Atroposelective Synthesis of Biaryl Diamines and Amino Alcohols via Chiral Phosphoric Acid Catalyzed *para*-Aminations of Anilines and Phenols

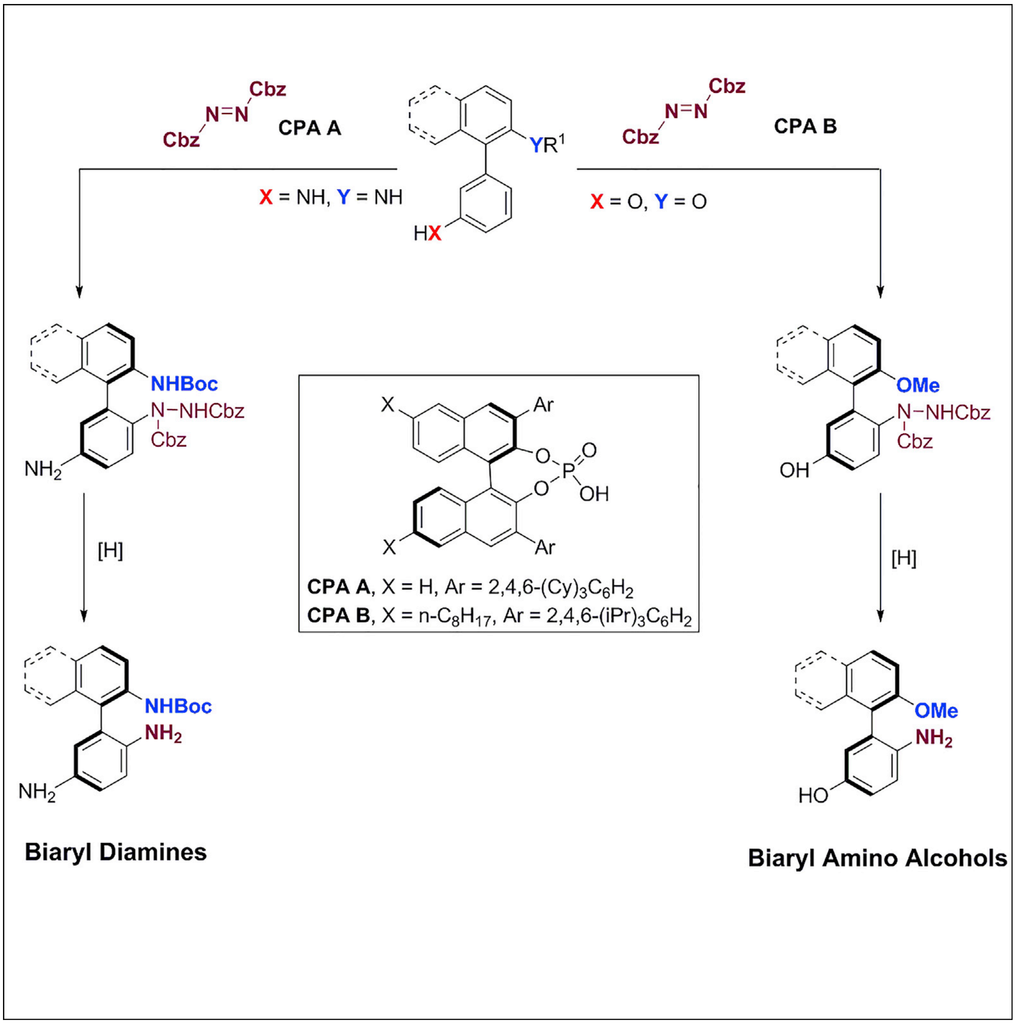

Donglei Wang,
Wei Liu, Mengyao
Tang, Na Yu,
Xiaoyu Yang

yangxy1@shanghaitech.edu.cn

HIGHLIGHTS

Versatile methods for asymmetric synthesis of biaryl diamines and amino alcohols

Atroposelective *para*-aminations of biaryl anilines and phenols

Kinetic resolution of racemic biaryl anilines

Facile transformations of chiral products

Wang et al., iScience *22*, 195–205
December 20, 2019 © 2019
The Author(s).
https://doi.org/10.1016/j.isci.2019.11.024

iScience

CellPress

Article

Atroposelective Synthesis of Biaryl Diamines and Amino Alcohols via Chiral Phosphoric Acid Catalyzed *para*-Aminations of Anilines and Phenols

Donglei Wang,[1,2,3] Wei Liu,[1,2,3] Mengyao Tang,[1,2] Na Yu,[1] and Xiaoyu Yang[1,4,*]

SUMMARY

A versatile method for atroposelective synthesis of chiral biaryl diamines and amino alcohols has been developed via *para*-amination of anilines and phenols with azodicarboxylates enabled by chiral phosphoric acid catalysis. Meanwhile, highly efficient kinetic resolution of the racemic biaryl anilines has also been realized through these reactions, giving selectivity factor up to 246. The gram-scale reaction and facile derivatizations of the chiral products well demonstrate the potential of these reactions in the development of novel chiral ligands and catalysts.

INTRODUCTION

Biaryl compounds possessing axial chirality are ubiquitous among biologically active natural products and pharmaceuticals (Bringmann et al., 2011; Kozlowski et al., 2009) and have been extensively exploited as chiral ligands/catalysts in asymmetric catalysis (Brunel, 2005, 2007; Chen et al., 2003; Kočovský et al., 2003; McCarthy and Guiry, 2001). To this end, their highly efficient and asymmetric catalytic synthesis has drawn increasing research interests, and various elegant methods have been developed in the last two decades (Bencivenni, 2015; Bonne and Rodriguez, 2018; Liao et al., 2019; Ma and Sibi, 2015; Nguyen, 2019; Renzi, 2017; Wang and Tan, 2018; Wencel-Delord et al., 2015; Zilate et al., 2018). However, in contrast to the numerous well-developed methods for asymmetric synthesis of BINOL-type biaryl diols (Chen et al., 2015; Egami et al., 2010; Guo et al., 2007; Jarvo et al., 2001; Jolliffe et al., 2017; Li et al., 2003; Luo et al., 2002; Ma et al., 2014; Moliterno et al., 2016; Moustafa et al., 2018; Narute et al., 2016; Wang et al., 2016; Xu et al., 2017), methods for enantioselective synthesis of other functionalized chiral biaryls are relatively limited. 1,1′-Binaphthyl-2,2′-diamine (BINAM), a representative chiral biaryl diamine, has been widely exploited in the development of chiral ligands and organocatalysts (Galzerano et al., 2009; Tan et al., 2011; Telfer and Kuroda, 2003; Uraguchi et al., 2009; Wang et al., 2005). However, only limited asymmetric catalytic methods (Brown et al., 1985; Chang et al., 2019) have been developed for its enantioselective synthesis, including asymmetric [3,3]-sigmatropic rearrangement (De et al., 2013; Li et al., 2013) and kinetic resolution (Cheng et al., 2014). 2-Amino-2′-hydroxy-1,1′-binaphthyl (NOBIN) (Smrcina et al., 1992, 1993), which is considered as the hybrid analogue of BINOL and BINAM, represents one type of privileged biaryl amino alcohol scaffold for constructing chiral ligands (Ding et al., 2005a, 2005b; Kočovský et al., 2003). However, methods for their asymmetric catalytic synthesis was also limited to kinetic resolutions (Lu et al., 2014; Shirakawa et al., 2013) and enantioselective direct arylation of 2-naphthylamines (Chen et al., 2017). Although the aforementioned elegant methods have provided access to enantioenriched biaryl diamines and amino alcohols, respectively, versatile methods for their asymmetric synthesis remain elusive. Recently, Tan and co-workers reported the asymmetric synthesis of BINAM- and NOBIN-type biaryls via enantioselective additions of 2-naphthols and 2-naphthylamines with 2-azonaphthalenes, which represented the first versatile protocol for their asymmetric synthesis, although two different catalytic systems were required (Qi et al., 2019).

Asymmetric Friedel-Crafts aminations of naphthols and naphthylamines with azodicarboxylates have been well employed in asymmetric synthesis of N-containing chiral scaffolds. For instance, Jørgensen group (Brandes et al., 2006a, 2006b) and Zhang group (Bai et al., 2019) developed asymmetric construction of C-N axial chirality by chiral amine and phosphoric acid-catalyzed *ortho*-amination of 2-naphthols and 2-naphthyl amines, respectively (Scheme 1A). You group (Wang et al., 2015; Xia et al., 2019) and Luan group (Nan et al., 2015) reported asymmetric dearomatization of naphthols via direct aminations of naphthols with azodicarboxylates enabled by chiral Brønsted/Lewis acid catalysis, constructing N-containing chiral quaternary centers (Scheme 1B). Nevertheless, most of these methods are still limited to *ortho*-aminations

---

[1] School of Physical Science and Technology, ShanghaiTech University, Shanghai 201210, China

[2] University of Chinese Academy of Sciences, Beijing 100049, China

[3] These authors contributed equally

[4] Lead Contact

*Correspondence: yangxy1@shanghaitech.edu.cn

https://doi.org/10.1016/j.isci.2019.11.024

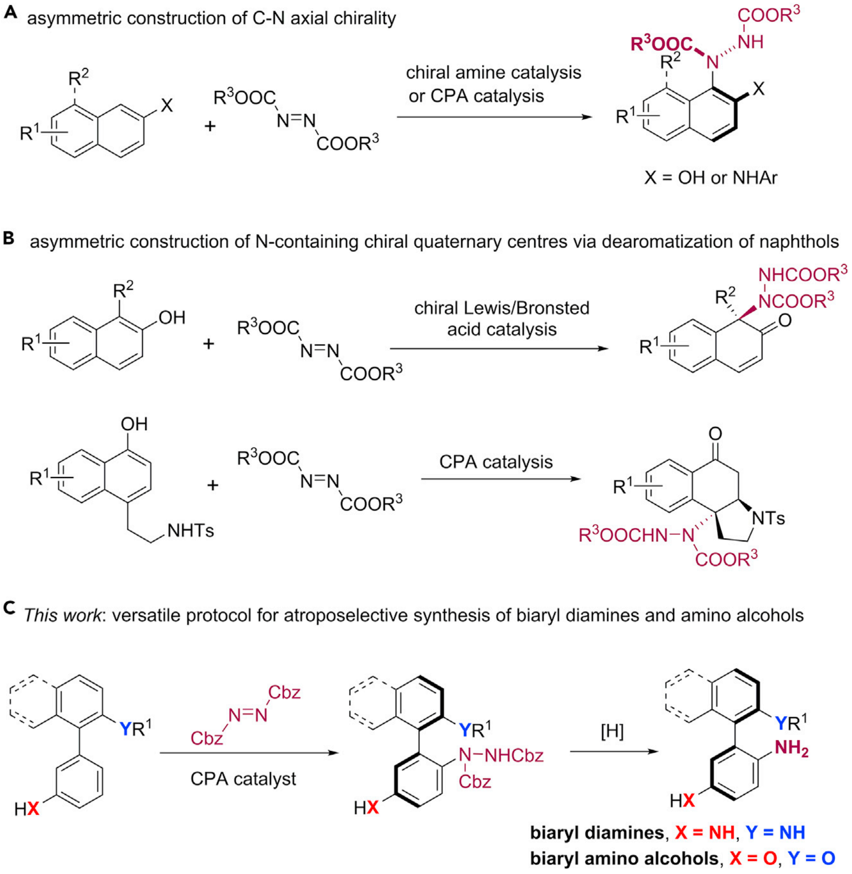

Scheme 1. Asymmetric Friedel-Crafts Amination with Azodicarboxylates

(A) construction of C-N axial chirality, (B) construction of N-containing chiral quaternary centers, and (C) atroposelective synthesis of biaryl diamines and amino alcohols.

of naphthols and naphthylamines; asymmetric reactions involving *para*-aminations of common anilines and phenols (Leblanc and Boudreault, 1995; Tang et al., 2017; Yadav et al., 2002; Zaltsgendler et al., 1993) are still elusive. Herein, we report a versatile protocol for atroposelective synthesis of biaryl diamines and amino alcohols via *para*-aminations of anilines and phenols (Diener et al., 2015; Gustafson et al., 2010; Miyaji et al., 2015, 2017; Mori et al., 2013a, b) with azodicarboxylates via chiral phosphoric acid catalysis (Akiyama, 2007; Akiyama et al., 2004; Akiyama and Mori, 2015; Li and Song, 2018; Parmar et al., 2014; Terada, 2010; Uraguchi and Terada, 2004) (Scheme 1C).

RESULTS AND DISCUSSION

Optimization of Reaction Conditions

Our study commenced with using biaryl aniline **1a** as substrate and dibenzyl azodicarboxylate **2** as amination reagent under the catalysis of CPA catalysts (Table 1). Interestingly, in the presence of CPA catalyst **A1** (10 mol %), the amination reaction between **1a** and azodicarboxylate **2** (1.1 equiv.) in toluene (with 5 Å molecular sieves) proceeded smoothly at ambient temperature to afford the triazane **4a** (Egger et al., 1983; Tang et al., 2017) as the major product (60% yield), whereas the desired *para*-amination product **3a** was obtained only in 13% yield with 47% enantiomeric excess (ee) (entry 1). Next, a variety of BINOL-derived chiral phosphoric acid catalysts were examined (entries 2–7), and encouragingly the TCYP catalyst (cat **A7**) provided the desired product **3a** in 80% yield with 98% ee, with the undesired *N*-amination product **4a** and diamination product **5a** isolated in <10% yield (entry 7). Next, a range of solvents were also investigated (entries 8–10), and $CHCl_3$ turned out to be the optimal one, in which the desired product **3a** was produced in 91% yield with 98% ee (entry 9). The role of the molecular sieves was also demonstrated; in the absence of 5-Å molecular sieves, the axially chiral biaryl **3a** was obtained only in 66% yield (entry 11).

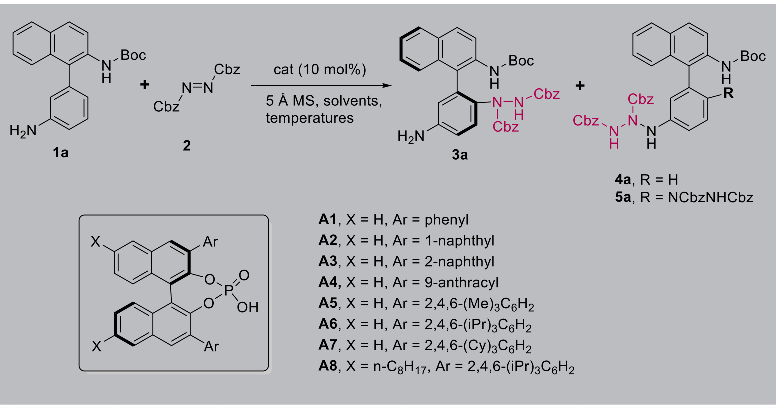

A1, X = H, Ar = phenyl
A2, X = H, Ar = 1-naphthyl
A3, X = H, Ar = 2-naphthyl
A4, X = H, Ar = 9-anthracyl
A5, X = H, Ar = 2,4,6-$(Me)_3C_6H_2$
A6, X = H, Ar = 2,4,6-$(iPr)_3C_6H_2$
A7, X = H, Ar = 2,4,6-$(Cy)_3C_6H_2$
A8, X = n-C_8H_{17}, Ar = 2,4,6-$(iPr)_3C_6H_2$

Entry[a]	Cat.	Sol.	4a Yield[b] (%)	5a Yield[b] (%)	3a Yield[b] (%)	3a ee[c] (%)
1	A1	Tol	60	16	13	47
2	A2	Tol	35	22	19	81
3	A3	Tol	58	22	5	46
4	A4	Tol	20	22	28	94
5	A5	Tol	48	17	5	85
6	A6	Tol	7	17	54	98
7	A7	Tol	9	6	80	98
8	A7	DCM	14	22	56	98
9	A7	$CHCl_3$	–	–	91	98
10	A7	Et_2O	44	22	16	96
11[d]	A7	$CHCl_3$	–	17	66	97
12[e]	A7	$CHCl_3$	7	18	74	98
13[e,f]	A7	$CHCl_3$	–	–	87	98

Table 1. Optimization of the Reaction Conditions

[a] Unless otherwise noted, reactions were performed with **1a** (0.1 mmol), **2** (0.11 mmol), CPA catalyst (0.01 mmol), and 5 Å MS (30 mg) in solvents (0.5 mL) for 16 h at ambient temperature.

[b] Yield was isolated yield.

[c] Enantiomeric excess (ee) was determined by HPLC analysis on a chiral stationary phase.

[d] Reaction was performed without 5 Å MS.

[e] Reaction was performed with 5 mol % catalyst.

[f] Reaction was performed at 40°C.

The reduction of catalyst loading was also studied; however, decreasing the catalyst loading to 5 mol % at room temperature led to a diminished yield (entry 12). Interestingly, conducting this reaction with 5 mol % catalyst at 40°C gave product **3a** in 87% yield with the same ee (entry 13). The axially chiral biaryl product **3a** has high configurational stability, whose ee was retained after storing on bench for more than 2 months at ambient temperature and heating at 100°C in toluene for 36 h.

Substrate Scope

With the optimal conditions in hand, we next sought to explore the compatibility of substrate scope of this reaction (Scheme 2). A range of substituted 2-naphthylamine moieties could be well tolerated in the biaryl aniline substrates, affording the axially chiral amination products with high enantioselectivities (**3b-3d**). A series of substitutions at the *ortho*- and *meta*-positions of the aniline moieties in substrates was also compatible with the optimal conditions (**3f-3h**). It is worth mentioning that the direct amination of substrates **1g** and **1h** afforded products as inseparable diastereomer mixtures due to the presence of extra

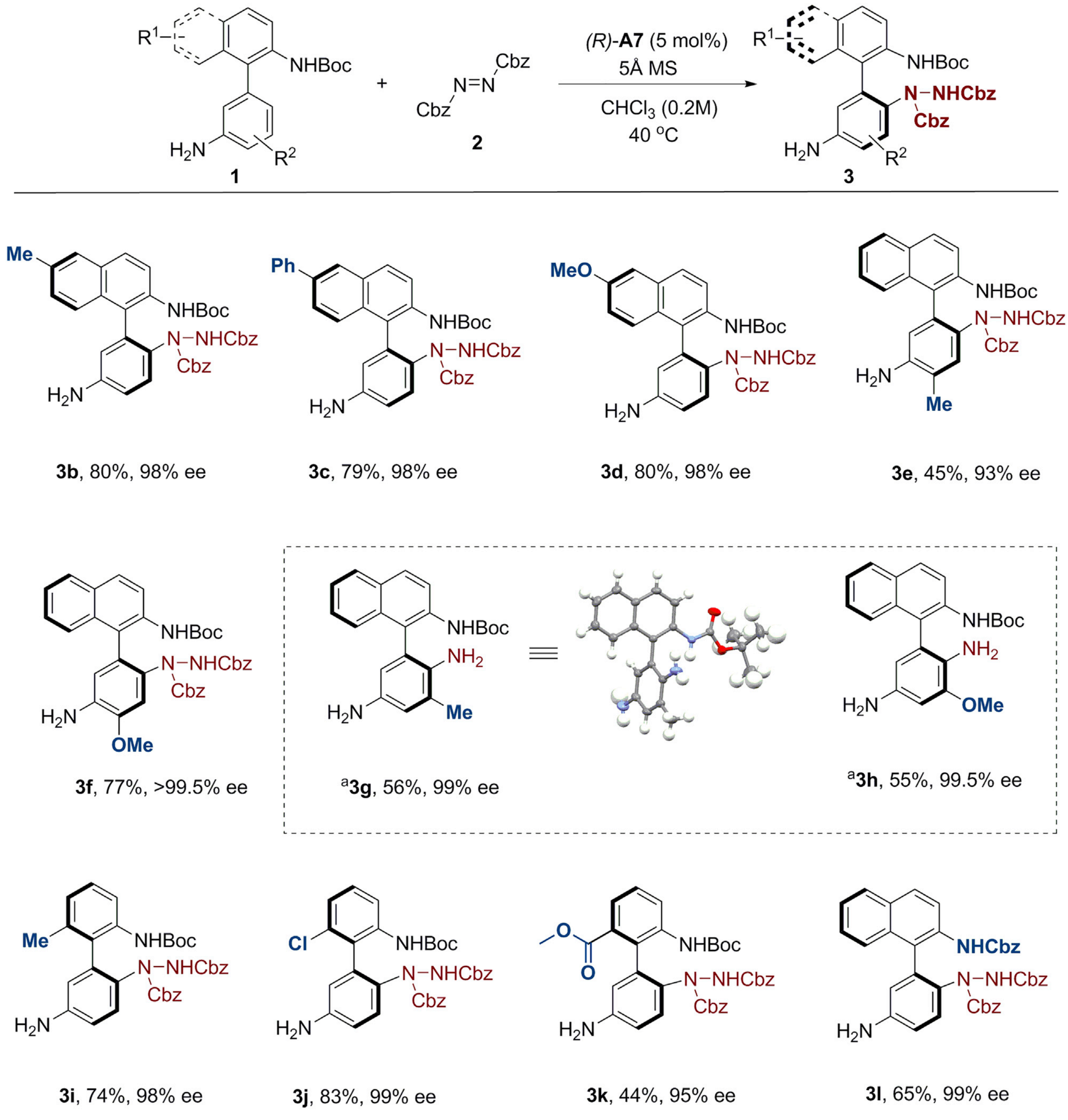

3b, 80%, 98% ee

3c, 79%, 98% ee

3d, 80%, 98% ee

3e, 45%, 93% ee

3f, 77%, >99.5% ee

[a]**3g**, 56%, 99% ee

[a]**3h**, 55%, 99.5% ee

3i, 74%, 98% ee

3j, 83%, 99% ee

3k, 44%, 95% ee

3l, 65%, 99% ee

Scheme 2. Substrate Scope for Asymmetric Synthesis of Biaryl Diamines via *Para*-aminations of Anilines

Reactions were performed with **1** (0.1 mmol), **2** (0.11 mmol), (*R*)-cat **A7** (0.005 mmol), and 5 Å MS (30 mg) in $CHCl_3$ (0.5 mL) at 40°C overnight. Yield was isolated yield. Ee was determined by HPLC analysis on a chiral stationary phase.

[a] The amination products were subjected into catalytic hydrogenation (1 atm) with Pd/C (10 mol %) as catalyst to afford **3g** and **3h**.

C-N axial chirality; therefore, these products were directly converted into $–NH_2$-containing product **3g** and **3h** by catalytic hydrogenations. The absolute configurations of the axially chiral products **3** were assigned as (*S*) by analogy to product **3g**, whose structure was unambiguously confirmed by X-ray crystallography (see Supplemental Information). The 2-naphthylamine scaffold in the substrates could also be switched to 3-substituted anilines (**3i-3k**), which also produced the biaryl amination products with high enantioselectivities under the standard conditions. Switching the N-protecting group from -Boc to –Cbz was also well

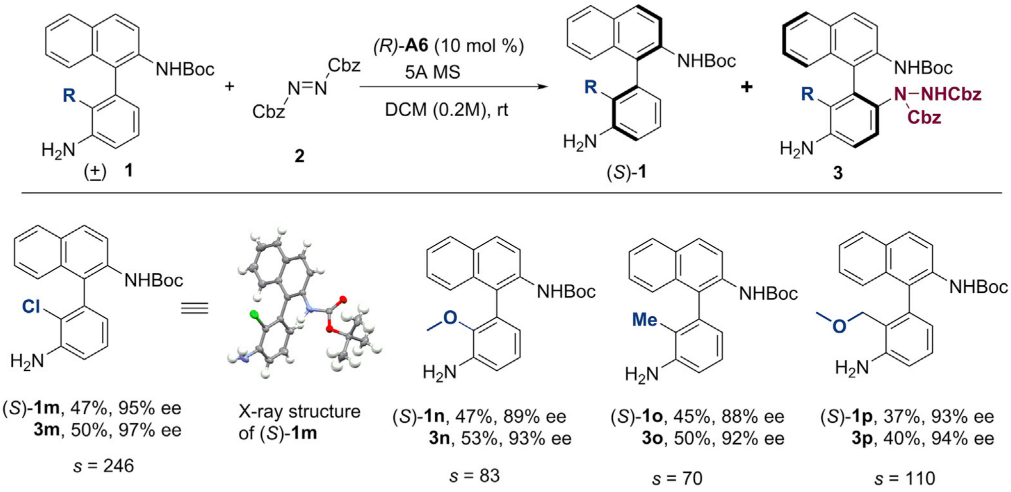

Scheme 3. Substrate Scope for Kinetic Resolution of Biaryl Anilines by *Para*-aminations

Reactions were performed with **1** (0.1 mmol), **2** (0.06 mmol), (*R*)-cat **A6** (0.01 mmol), and 5 Å MS (30 mg) in CH_2Cl_2 (0.5 mL) at room temperature overnight. Yield was isolated yield. Ee was determined by HPLC analysis on a chiral stationary phase.

tolerated with the optimal conditions, which produced product **3l** with excellent enantioselectivity. However, using the N-protecting group-free biaryl aniline as substrates provided the triazane product as the major product.

With the excellent performance of constructing chiral biaryl diamines via asymmetric *para*-amination reactions, we envisioned that these reactions could also be adopted in the kinetic resolution of racemic biaryl anilines. Thus, a variety of 2-substituted biaryl anilines possessing axial chirality were synthesized and their kinetic resolution via *para*-amination reactions with azodicarboxylate **2** (0.6 equiv.) was investigated (Scheme 3). Under the catalysis of (*R*)-TRIP catalyst (cat **A6,** 10 mol %) in DCM at room temperature, the kinetic resolutions of these substrates proceeded with high efficiencies to afford both recovered aniline substrates and *para*-amination products with high enantioselectivities (with *s* factor up to 246, **3m**-**3p**). The absolute configurations of the axially chiral products and recovered starting materials were assigned by analogy to recovered **1m**, whose structure was unambiguously confirmed by X-ray crystallography (see Supplemental Information).

To achieve enantioselective synthesis of biaryl amino alcohols, the 2-naphthylamine moieties in the substrates were switched to 2-naphthol moieties. However, the amination reactions of the corresponding biaryl anilines **6′** provided only *N*-amination triazane products **7′** (Scheme 4). Interestingly, the desired biaryl amino alcohols were obtained while phenols **6** were employed as electron-rich arenes instead of anilines. Under the catalysis of (*R*)-C_8-TRIP catalyst (cat **A8**) in $CHCl_3$ at ambient temperature, the *para*-amination of biaryl phenol **6a** with azodicarboxylate **2** afforded the biaryl amino alcohol **7a** in 56% yield with 86% ee (for further details, see Table S1 in the Supplemental Information). Switching the protecting group from *O*-Me to *O*-MOM was compatible with the optimal conditions, providing the axially chiral amination product with comparable stereoselectivity (**7b**). The substrate scope for the 2-naphthol moieties in the substrates were explored under the standard conditions, which showed that a range of substituted 2-naphthol scaffolds (with various substitutions at the 4-, 6-, and 7-positions) could be accommodated, affording biaryl amino alcohols in good yields and high enantioselectivities (**7c–7g**). The absolute configurations of these biaryl amino alcohols **7** were assigned by analogy to product **7c**, whose structure was also confirmed by X-ray crystallography (Supplemental Information). It is worth mentioning that biaryl phenol substrate without O-Me protecting group afforded the *para*-amination product with diminished enantioselectivity under the optimal conditions.

Mechanistic Discussion

To gain more insight into the reaction mechanism, several control experiments were performed (Scheme 5). The amination reaction of *N*-Me biaryl aniline substrate **1q** proceeded smoothly under

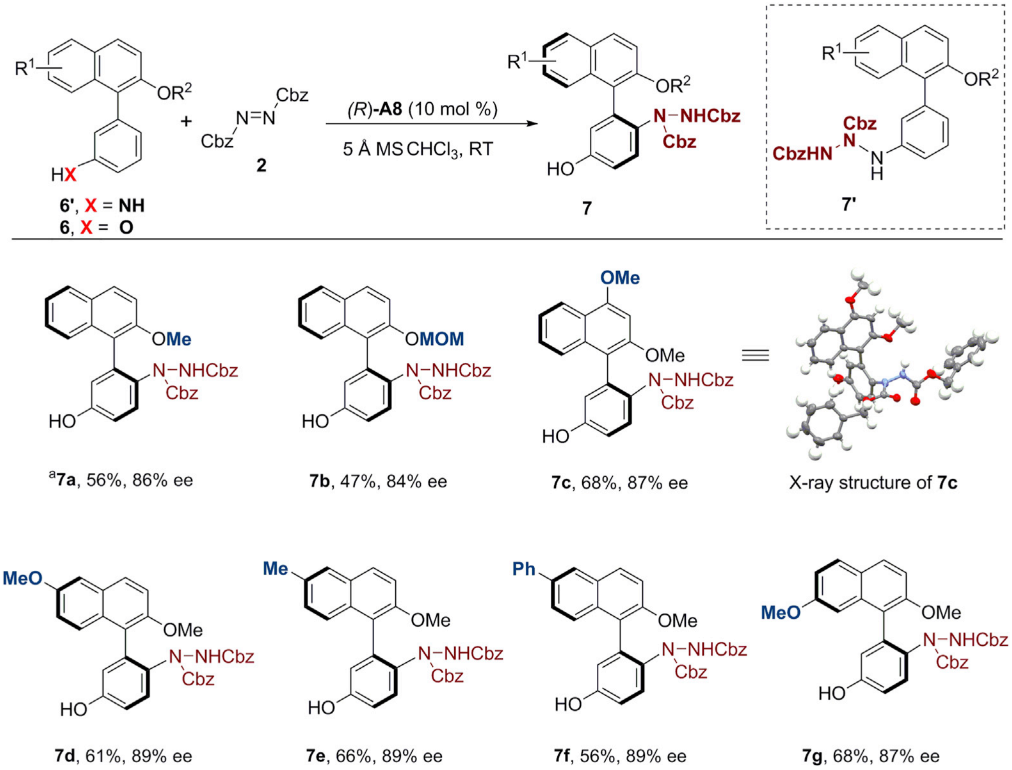

[a]7a, 56%, 86% ee

7b, 47%, 84% ee

7c, 68%, 87% ee

X-ray structure of 7c

7d, 61%, 89% ee

7e, 66%, 89% ee

7f, 56%, 89% ee

7g, 68%, 87% ee

Scheme 4. Substrate Scope for Asymmetric Synthesis of Biaryl Amino Alcohols via *Para*-amination of Phenols

Reactions were performed with **6** (0.1 mmol), **2** (0.3 mmol), (*R*)-cat **A8** (0.01 mmol), and 5 Å MS (30 mg) in $CHCl_3$ (0.5 mL) at ambient temperature for 36 h. Yield was isolated yield. Ees was determined by HPLC analysis on a chiral stationary phase. [a]Reaction was performed with **2** (0.15 mmol).

the standard conditions to give the desired *para*-amination product **3q** in 56% yield with 92% ee. However, applying the same conditions on *N*,*N*-dimethyl aniline substrate **1r** provided only the *para*-amination product **3r** in 25% yield with 5% ee (with the N-amination product as the major by-product), which indicated that the potential hydrogen bonding between CPA catalyst and the aniline N-H group played a key role in controlling both chemoselectivity and stereoselectivity in this reaction (Scheme 5A). Interestingly, subjection of the N-amination triazane product **4a** into the optimal conditions without adding azodicarboxylate **2** also gave the *para*-amination product **3a** in 58% yield with 98% ee after 16 h, with the aniline substrate **1a** isolated in 28% yield, which suggested the reversible nature of the triazane formation step (Scheme 5B). Based on the above-mentioned experimental study and previous work (Bai et al., 2019; Drouet et al., 2011; Dumoulin et al., 2015), a plausible reaction mechanism is proposed, in which bifunctional activation (Parmar et al., 2014; Simón and Goodman, 2008; Yamanaka et al., 2007) of both the aniline substrate and azodicarboxylate via dual hydrogen-bonding interaction with the CPA catalyst is postulated (Scheme 5C). Under the catalysis of CPA catalyst, there are two alternative reaction pathways between aniline substrates and azodicarboxylates: (1) direct nucleophilic addition of the $–NH_2$ group to the azodicarboxylate facilitated the generation of the triazane products (path a), which is also reversible under these conditions; and (2) the *para*-selective amination of aniline substrates would give the dearomatized addition product **INT A**, possessing a chiral center (path b). On subsequent aromatization, **INT A** underwent the central-to-axial chirality transfer (Qi et al., 2017; Raut et al., 2017) to provide the axial biaryl diamine products.

Transformations of Products

To evaluate the practicability of these reactions, a gram-scale amination reaction of **1a** was performed, which provided the axially chiral biaryl **3a** in 70% yield with 99% ee, with reduced catalyst loading (2 mol %, Scheme 6A). The derivatizations of the chiral products were also studied to prove the value of these reactions. By means of the Sandmeyer reaction, the directing $–NH_2$ group was transformed into

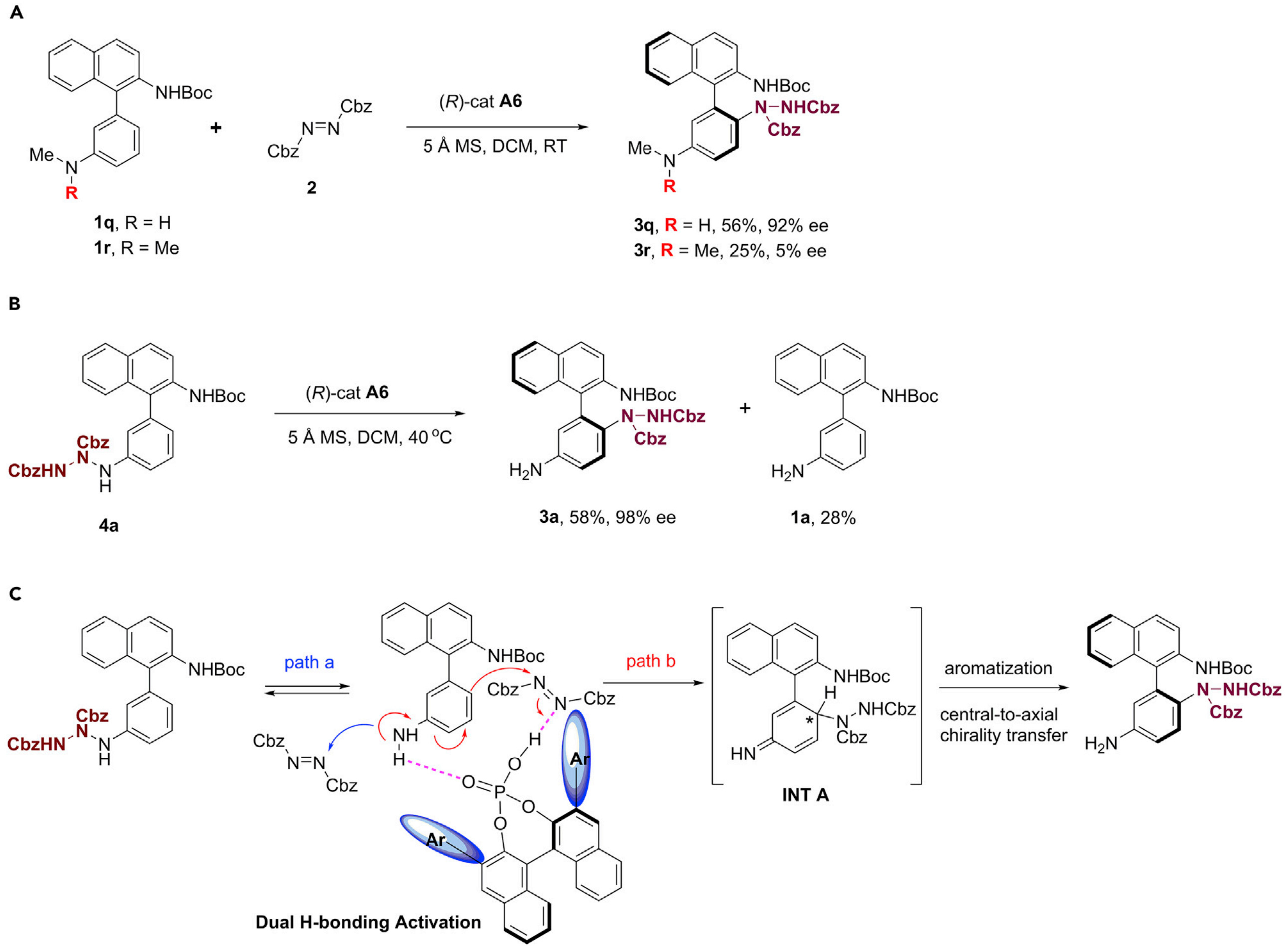

Scheme 5. Preliminary Mechanistic Study and Proposed Mechanism

an iodide group via diazotization of **3a** with $NaNO_2$ followed by treatment with NaI to afford **8a**, which could be further employed in Suzuki coupling with phenylboronic acid to give product **9a** in 81% yield (Scheme 6B). Notably, the ee of chiral biaryl product was retained through these steps of transformations, including the Suzuki coupling step (105°C, overnight), again demonstrating the high configurational stability of these atropisomeric products. The catalytic hydrogenation of **7a** using Pd/C as catalyst facilely reduced the substituted hydrazine moiety to give the biaryl product **10a** in 90% yield (Scheme 6C). A two-step procedure of catalytic hydrogenation followed by deprotection of the N-Boc group converted chiral product **3n** into biaryl diamine **11n** in 82% yield, without erosion of the enantioselectivity (Scheme 6D). Finally, a primary-amine/thiourea bifunctional catalyst **13a** was straightforwardly synthesized from the chiral product **3a** within 4 steps, with complete retention of the enantiomeric purity (Scheme 6E). The application of this bifunctional catalyst was preliminarily demonstrated in an asymmetric Michael reaction of 3-methyl oxindole **14** with cinnamaldehyde **15** (Galzerano et al., 2009), which readily provided the product **16** (after reduction) in 53% yield with 6:1 d.r. and 73% ee without optimization (Scheme 6F).

Conclusion

We have disclosed a versatile method for asymmetric synthesis of biaryl diamines and amino alcohols, which was realized through chiral phosphoric acid catalyzed enantioselective *para*-aminations of biaryl anilines and phenols with azodicarboxylates. These reactions are also well employed in the highly efficient kinetic resolution of racemic biaryl anilines, which give *s* factor up to 246. Preliminary mechanistic studies were performed to elucidate the reaction mechanism, in which a dual hydrogen-bonding activation mode was proposed in the key chirality induction step. The facile transformations of chiral products into atropisomeric biaryl diamine

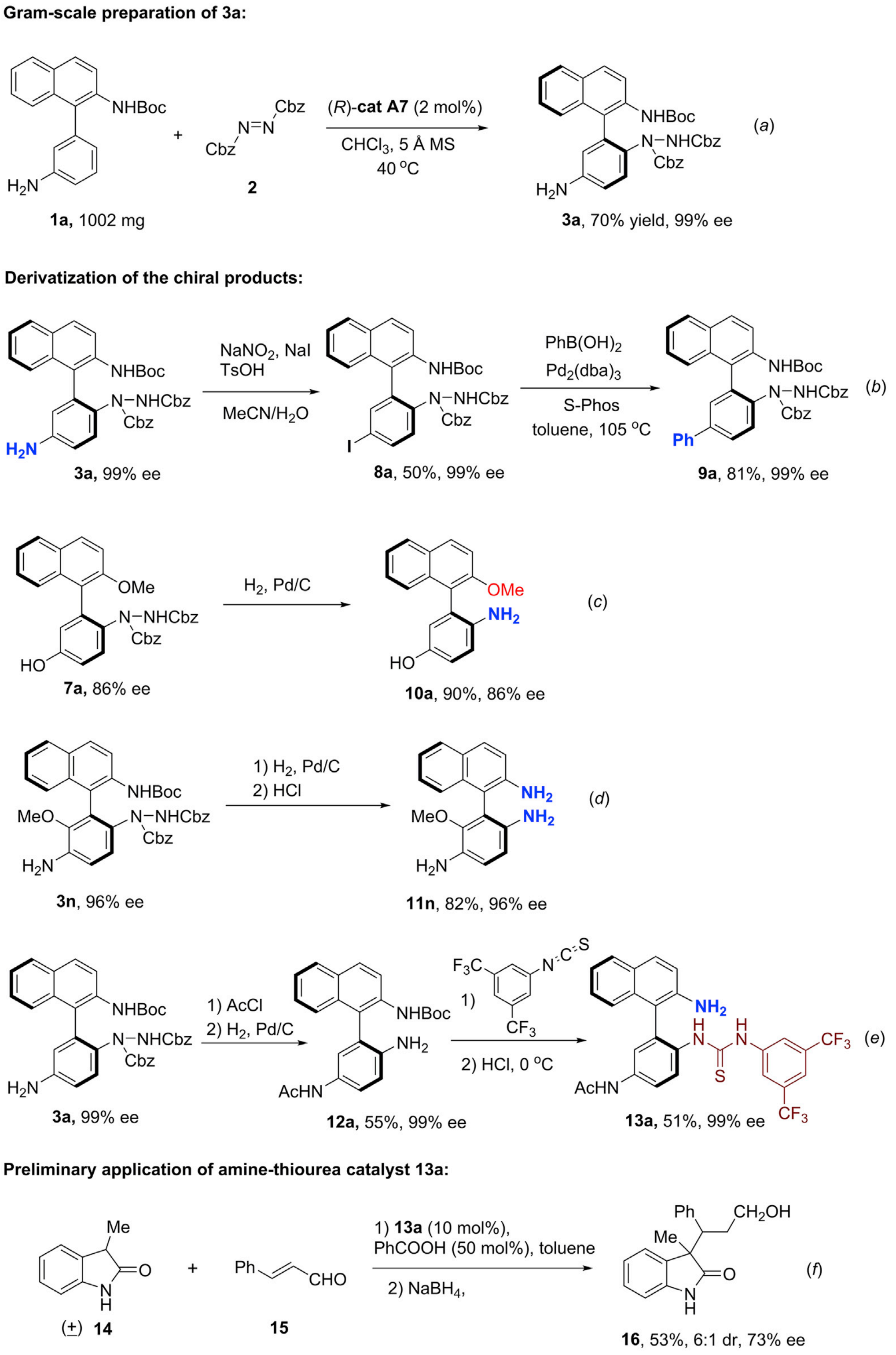

Scheme 6. Gram-Scale Synthesis of 3a and Derivatizations of the Chiral Products

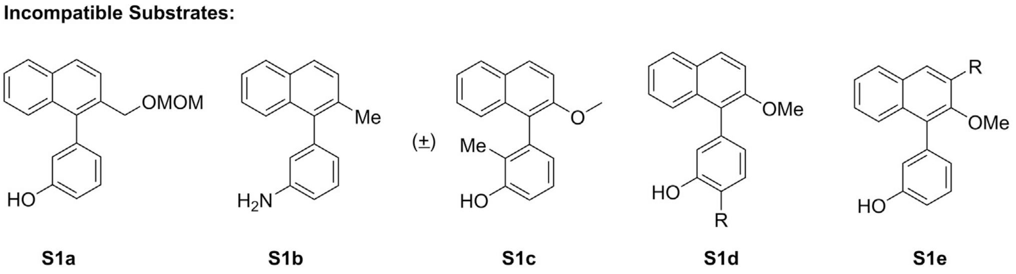

Scheme 7. Incompatible Substrates

and amino alcohol derivatives with novel and diversified scaffolds well demonstrate the value of these reactions, especially in the field of developments of novel chiral catalysts and ligands.

Limitations of the Study

The synthesis of the substrates usually needs multiple steps. Different directing groups are required in the synthesis of biaryl diamines and biaryl amino alcohols.

There are also some limitations of the substrate scope (Scheme 7): (1) electron-donating groups were required at the 2-position of the naphthyl moiety; substrates with alkyl groups at this position barely provided the *para*-amination products (**S1a** and **S1b**); (2) kinetic resolution of racemic biaryl phenol substrate did not provide good kinetic resolution performance (**S1c**); (3) substitutions at the 2-position of the phenol moiety and 3-position of the naphthol moiety were not compatible in the asymmetric *para*-amination reactions of biaryl phenols (**S1d** and **S1e**).

METHODS

All methods can be found in the accompanying Transparent Methods supplemental file.

DATA AND CODE AVAILABILITY

The X-ray crystallographic coordinates for structures reported in this study have been deposited at the Cambridge Crystallographic Data Centre (CCDC) under accession number CCDC: 1923360 (**3g**), 1938295 (**7c**), and 1923362 ((*S*)-**1m**). These data can be obtained free of charge from The Cambridge Crystallographic Data Centre via www.ccdc.cam.ac.uk/data_request/cif.

SUPPLEMENTAL INFORMATION

Supplemental Information can be found online at https://doi.org/10.1016/j.isci.2019.11.024.

ACKNOWLEDGMENTS

We gratefully acknowledge NSFC (Grant No. 21702138), ''Thousand Talents Plan'' Youth Program, and ShanghaiTech University start-up funding for financial support. We thank the Analytical Instrumentation Centre of ShanghaiTech for facilities and services of characterization of compounds.

AUTHOR CONTRIBUTIONS

D.W., W.L., and M.T. performed the experiments. N.Y. performed the crystallographic studies. X.Y. conceived the concept, directed the project, and wrote the paper.

DECLARATION OF INTERESTS

The authors declare no competing interests.

Received: September 29, 2019
Revised: October 29, 2019
Accepted: November 12, 2019
Published: December 20, 2019

REFERENCES

Akiyama, T. (2007). Stronger Brønsted acids. Chem. Rev. *107*, 5744–5758.

Akiyama, T., Itoh, J., Yokota, K., and Fuchibe, K. (2004). Enantioselective Mannich-type reaction catalyzed by a chiral Brønsted acid. Angew. Chem. Int. Ed. *43*, 1566–1568.

Akiyama, T., and Mori, K. (2015). Stronger Brønsted acids: recent progress. Chem. Rev. *115*, 9277–9306.

Bai, H.-Y., Tan, F.-X., Liu, T.-Q., Zhu, G.-D., Tian, J.-M., Ding, T.-M., Chen, Z.-M., and Zhang, S.-Y. (2019). Highly atroposelective synthesis of nonbiaryl naphthalene-1,2-diamine N-C atropisomers through direct enantioselective C-H amination. Nat. Commun. *10*, 3063.

Bencivenni, G. (2015). Organocatalytic strategies for the synthesis of axially chiral compounds. Synlett *26*, 1915–1922.

Bonne, D., and Rodriguez, J. (2018). A bird's eye view of atropisomers featuring a five-membered ring. Eur. J. Org. Chem. *2018*, 2417–2431.

Brandes, S., Bella, M., Kjærsgaard, A., and Jørgensen, K.A. (2006a). Chirally aminated 2-naphthols—organocatalytic synthesis of non-biaryl atropisomers by asymmetric Friedel–Crafts amination. Angew. Chem. Int. Ed. *45*, 1147–1151.

Brandes, S., Niess, B., Bella, M., Prieto, A., Overgaard, J., and Jørgensen, K.A. (2006b). Non-biaryl atropisomers in organocatalysis. Chem. Eur. J. *12*, 6039–6052.

Bringmann, G., Gulder, T., Gulder, T.A.M., and Breuning, M. (2011). Atroposelective total synthesis of axially chiral biaryl natural products. Chem. Rev. *111*, 563–639.

Brown, K.J., Berry, M.S., and Murdoch, J.R. (1985). Synthesis of optically active 2,2′-dihalo-1,1′-binaphthyls via stable diazonium salts. J. Org. Chem. *50*, 4345–4349.

Brunel, J.M. (2005). BINOL: A versatile chiral reagent. Chem. Rev. *105*, 857–898.

Brunel, J.M. (2007). Update 1 of: BINOL: A versatile chiral reagent. Chem. Rev. *107*, PR1–PR45.

Chang, X., Zhang, Q., and Guo, C. (2019). Switchable smiles rearrangement for enantioselective O-aryl amination. Org. Lett. *21*, 4915–4918.

Chen, Y.-H., Cheng, D.-J., Zhang, J., Wang, Y., Liu, X.-Y., and Tan, B. (2015). Atroposelective synthesis of axially chiral biaryldiols via organocatalytic arylation of 2-naphthols. J. Am. Chem. Soc. *137*, 15062–15065.

Chen, Y.-H., Qi, L.-W., Fang, F., and Tan, B. (2017). Organocatalytic atroposelective arylation of 2-naphthylamines as a practical approach to axially chiral biaryl amino alcohols. Angew. Chem. Int. Ed. *56*, 16308–16312.

Chen, Y., Yekta, S., and Yudin, A.K. (2003). Modified BINOL ligands in asymmetric catalysis. Chem. Rev. *103*, 3155–3212.

Cheng, D.-J., Yan, L., Tian, S.-K., Wu, M.-Y., Wang, L.-X., Fan, Z.-L., Zheng, S.-C., Liu, X.-Y., and Tan, B. (2014). Highly enantioselective kinetic resolution of axially chiral BINAM derivatives catalyzed by a Brønsted acid. Angew. Chem. Int. Ed. *53*, 3684–3687.

De, C.K., Pesciaioli, F., and List, B. (2013). Catalytic asymmetric benzidine rearrangement. Angew. Chem. Int. Ed. *52*, 9293–9295.

Diener, M.E., Metrano, A.J., Kusano, S., and Miller, S.J. (2015). Enantioselective synthesis of 3-arylquinazolin-4(3H)-ones via peptide-catalyzed atroposelective bromination. J. Am. Chem. Soc. *137*, 12369–12377.

Ding, K., Guo, H., Li, X., Yuan, Y., and Wang, Y. (2005a). Synthesis of NOBIN derivatives for asymmetric catalysis. Top. Catal. *35*, 105–116.

Ding, K., Li, X., Ji, B., Guo, H., and Kitamura, M. (2005b). Ten years of research on NOBIN chemistry. Curr. Org. Syn. *2*, 499–545.

Drouet, F., Lalli, C., Liu, H., Masson, G., and Zhu, J. (2011). Chiral calcium organophosphate-catalyzed enantioselective electrophilic amination of enamides. Org. Lett. *13*, 94–97.

Dumoulin, A., Lalli, C., Retailleau, P., and Masson, G. (2015). Catalytic, highly enantioselective, direct amination of enecarbamates. Chem. Commun. (Camb.) *51*, 5383–5386.

Egami, H., Matsumoto, K., Oguma, T., Kunisu, T., and Katsuki, T. (2010). Enantioenriched synthesis of C1-symmetric BINOLs: iron-catalyzed cross-coupling of 2-naphthols and some mechanistic insight. J. Am. Chem. Soc. *132*, 13633–13635.

Egger, N., Hoesch, L., and Dreiding, A.S. (1983). Azimine. VII. Herstellung durch Oxydation von Triazenen. Helv. Chim. Acta *66*, 1599–1607.

Galzerano, P., Bencivenni, G., Pesciaioli, F., Mazzanti, A., Giannichi, B., Sambri, L., Bartoli, G., and Melchiorre, P. (2009). Asymmetric iminium ion catalysis with a novel bifunctional primary amine thiourea: controlling adjacent quaternary and tertiary stereocenters. Chem. Eur. J. *15*, 7846–7849.

Guo, Q.-X., Wu, Z.-J., Luo, Z.-B., Liu, Q.-Z., Ye, J.-L., Luo, S.-W., Cun, L.-F., and Gong, L.-Z. (2007). Highly enantioselective oxidative couplings of 2-naphthols catalyzed by chiral bimetallic oxovanadium complexes with either oxygen or air as oxidant. J. Am. Chem. Soc. *129*, 13927–13938.

Gustafson, J.L., Lim, D., and Miller, S.J. (2010). Dynamic kinetic resolution of biaryl atropisomers via peptide-catalyzed asymmetric bromination. Science *328*, 1251.

Jarvo, E.R., Evans, C.A., Copeland, G.T., and Miller, S.J. (2001). Fluorescence-based screening of asymmetric acylation catalysts through parallel enantiomer analysis. Identification of a catalyst for tertiary alcohol resolution. J. Org. Chem. *66*, 5522–5527.

Jolliffe, J.D., Armstrong, R.J., and Smith, M.D. (2017). Catalytic enantioselective synthesis of atropisomeric biaryls by a cation-directed O-alkylation. Nat. Chem. *9*, 558.

Kočovský, P., Vyskočil, Š., and Smrčina, M. (2003). Non-symmetrically substituted 1,1′-binaphthyls in enantioselective catalysis. Chem. Rev. *103*, 3213–3246.

Kozlowski, M.C., Morgan, B.J., and Linton, E.C. (2009). Total synthesis of chiral biaryl natural products by asymmetric biaryl coupling. Chem. Soc. Rev. *38*, 3193–3207.

Leblanc, Y., and Boudreault, N. (1995). Para-directed amination of electron-rich arenes with bis(2,2,2-trichloroethyl) azodicarboxylate. J. Org. Chem. *60*, 4268–4271.

Li, G.-Q., Gao, H., Keene, C., Devonas, M., Ess, D.H., and Kürti, L. (2013). Organocatalytic aryl–aryl bond formation: an atroposelective [3,3]-Rearrangement approach to BINAM derivatives. J. Am. Chem. Soc. *135*, 7414–7417.

Li, X., Hewgley, J.B., Mulrooney, C.A., Yang, J., and Kozlowski, M.C. (2003). Enantioselective oxidative biaryl coupling reactions catalyzed by 1,5-diazadecalin metal Complexes: efficient formation of chiral functionalized BINOL derivatives. J. Org. Chem. *68*, 5500–5511.

Li, X., and Song, Q. (2018). Recent advances in asymmetric reactions catalyzed by chiral phosphoric acids. Chin. Chem. Lett. *29*, 1181–1192.

Liao, G., Zhou, T., Yao, Q.-J., and Shi, B.-F. (2019). Recent advances in the synthesis of axially chiral biaryls via transition metal-catalysed asymmetric C–H functionalization. Chem. Commun. (Camb.) *55*, 8514–8523.

Lu, S., Poh, S.B., and Zhao, Y. (2014). Kinetic resolution of 1,1′-biaryl-2,2′-diols and amino alcohols through NHC-catalyzed atroposelective acylation. Angew. Chem. Int. Ed. *53*, 11041–11045.

Luo, Z., Liu, Q., Gong, L., Cui, X., Mi, A., and Jiang, Y. (2002). The rational design of novel chiral oxovanadium(iv) complexes for highly enantioselective oxidative coupling of 2-naphthols. Chem. Commun. (Camb.), 914–915.

Ma, G., Deng, J., and Sibi, M.P. (2014). Fluxionally chiral DMAP catalysts: kinetic resolution of axially chiral biaryl compounds. Angew. Chem. Int. Ed. *53*, 11818–11821.

Ma, G., and Sibi, M.P. (2015). Catalytic kinetic resolution of biaryl compounds. Chemistry *21*, 11644–11657.

McCarthy, M., and Guiry, P.J. (2001). Axially chiral bidentate ligands in asymmetric catalysis. Tetrahedron *57*, 3809–3844.

Miyaji, R., Asano, K., and Matsubara, S. (2015). Bifunctional organocatalysts for the enantioselective synthesis of axially chiral isoquinoline N-oxides. J. Am. Chem. Soc. *137*, 6766–6769.

Miyaji, R., Asano, K., and Matsubara, S. (2017). Induction of axial chirality in 8-arylquinolines through halogenation reactions using bifunctional organocatalysts. Chem. Eur. J. *23*, 9996–10000.

Moliterno, M., Cari, R., Puglisi, A., Antenucci, A., Sperandio, C., Moretti, E., Di Sabato, A., Salvio, R., and Bella, M. (2016). Quinine-catalyzed asymmetric synthesis of 2,2′-binaphthol-type biaryls under mild reaction conditions. Angew. Chem. Int. Ed. *55*, 6525–6529.

Mori, K., Ichikawa, Y., Kobayashi, M., Shibata, Y., Yamanaka, M., and Akiyama, T. (2013a). Enantioselective synthesis of multisubstituted biaryl skeleton by chiral phosphoric acid catalyzed desymmetrization/kinetic resolution sequence. J. Am. Chem. Soc. *135*, 3964–3970.

Mori, K., Ichikawa, Y., Kobayashi, M., Shibata, Y., Yamanaka, M., and Akiyama, T. (2013b). Prediction of suitable catalyst by 1H NMR: asymmetric synthesis of multisubstituted biaryls by chiral phosphoric acid catalyzed asymmetric bromination. Chem. Sci. *4*, 4235–4239.

Moustafa, G.A.I., Oki, Y., and Akai, S. (2018). Lipase-catalyzed dynamic kinetic resolution of C1- and C2-symmetric racemic axially chiral 2,2′-Dihydroxy-1,1′-biaryls. Angew. Chem. Int. Ed. *57*, 10278–10282.

Nan, J., Liu, J., Zheng, H., Zuo, Z., Hou, L., Hu, H., Wang, Y., and Luan, X. (2015). Direct asymmetric dearomatization of 2-naphthols by scandium-catalyzed electrophilic amination. Angew. Chem. Int. Ed. *54*, 2356–2360.

Narute, S., Parnes, R., Toste, F.D., and Pappo, D. (2016). Enantioselective oxidative homocoupling and cross-coupling of 2-naphthols catalyzed by chiral iron phosphate complexes. J. Am. Chem. Soc. *138*, 16553–16560.

Nguyen, T.T. (2019). Traceless point-to-axial chirality exchange in the atropselective synthesis of biaryls/heterobiaryls. Org. Bio. Chem. *17*, 6952–6963.

Parmar, D., Sugiono, E., Raja, S., and Rueping, M. (2014). Complete field guide to asymmetric BINOL-phosphate derived Brønsted acid and metal catalysis: history and classification by mode of activation; Brønsted acidity, hydrogen bonding, ion pairing, and Metal Phosphates. Chem. Rev. *114*, 9047–9153.

Qi, L.-W., Li, S., Xiang, S.-H., Wang, J., and Tan, B. (2019). Asymmetric construction of atropisomeric biaryls via a redox neutral cross-coupling strategy. Nat. Catal. *2*, 314–323.

Qi, L.-W., Mao, J.-H., Zhang, J., and Tan, B. (2017). Organocatalytic asymmetric arylation of indoles enabled by azo groups. Nat.Chem. *10*, 58.

Raut, V.S., Jean, M., Vanthuyne, N., Roussel, C., Constantieux, T., Bressy, C., Bugaut, X., Bonne, D., and Rodriguez, J. (2017). Enantioselective syntheses of furan atropisomers by an oxidative central-to-axial chirality conversion strategy. J. Am. Chem. Soc. *139*, 2140–2143.

Renzi, P. (2017). Organocatalytic synthesis of axially chiral atropisomers. Org. Bio. Chem. *15*, 4506–4516.

Shirakawa, S., Wu, X., and Maruoka, K. (2013). Kinetic resolution of axially chiral 2-amino-1,1′-biaryls by phase-transfer-catalyzed N-allylation. Angew. Chem. Int. Ed. *52*, 14200–14203.

Simón, L., and Goodman, J.M. (2008). Theoretical study of the mechanism of Hantzsch ester hydrogenation of imines catalyzed by chiral BINOL-phosphoric acids. J. Am. Chem. Soc. *130*, 8741–8747.

Smrcina, M., Lorenc, M., Hanus, V., Sedmera, P., and Kocovsky, P. (1992). Synthesis of enantiomerically pure 2,2′-dihydroxy-1,1′-binaphthyl, 2,2′-diamino-1,1′-binaphthyl, and 2-amino-2′-hydroxy-1,1′-binaphthyl. Comparison of processes operating as diastereoselective crystallization and as second order asymmetric transformation. J. Org. Chem. *57*, 1917–1920.

Smrcina, M., Polakova, J., Vyskocil, S., and Kocovsky, P. (1993). Synthesis of enantiomerically pure binaphthyl derivatives. Mechanism of the enantioselective, oxidative coupling of naphthols and designing a catalytic cycle. J. Org. Chem. *58*, 4534–4538.

Tan, B., Candeias, N.R., and Barbas Iii, C.F. (2011). Construction of bispirooxindoles containing three quaternary stereocentres in a cascade using a single multifunctional organocatalyst. Nat. Chem. *3*, 473.

Tang, R.-J., Milcent, T., and Crousse, B. (2017). Hexafluoro-2-propanol promotes para-selective C–H amination of free anilines with azodicarboxylates. Eur. J. Org. Chem. *2017*, 4753–4757.

Telfer, S.G., and Kuroda, R. (2003). 1,1′-Binaphthyl-2,2′-diol and 2,2′-diamino-1,1′-binaphthyl: versatile frameworks for chiral ligands in coordination and metallosupramolecular chemistry. Coord. Chem. Rev. *242*, 33–46.

Terada, M. (2010). Chiral phosphoric acids as versatile catalysts for enantioselective carbon-carbon bond forming reactions. Synthesis *2010*, 1929–1982.

Uraguchi, D., Nakashima, D., and Ooi, T. (2009). Chiral arylaminophosphonium barfates as a new class of charged Brønsted acid for the enantioselective activation of nonionic Lewis bases. J. Am. Chem. Soc. *131*, 7242–7243.

Uraguchi, D., and Terada, M. (2004). Chiral BRØNSTED acid-catalyzed direct Mannich reactions via electrophilic activation. J. Am. Chem. Soc. *126*, 5356–5357.

Wang, J.-Z., Zhou, J., Xu, C., Sun, H., Kürti, L., and Xu, Q.-L. (2016). Symmetry in cascade chirality-transfer processes: a catalytic atroposelective direct arylation approach to BINOL derivatives. J. Am. Chem. Soc. *138*, 5202–5205.

Wang, J., Li, H., Duan, W., Zu, L., and Wang, W. (2005). Organocatalytic asymmetric Michael addition of 2,4-pentandione to nitroolefins. Org. Lett. *7*, 4713–4716.

Wang, S.G., Yin, Q., Zhuo, C.X., and You, S.L. (2015). Asymmetric dearomatization of β-naphthols through an amination reaction catalyzed by a chiral phosphoric acid. Angew. Chem. Int. Ed. *54*, 647–650.

Wang, Y.-B., and Tan, B. (2018). Construction of axially chiral compounds via asymmetric organocatalysis. Acc. Chem. Res. *51*, 534–547.

Wencel-Delord, J., Panossian, A., Leroux, F.R., and Colobert, F. (2015). Recent advances and new concepts for the synthesis of axially stereoenriched biaryls. Chem. Soc. Rev. *44*, 3418–3430.

Xia, Z.-L., Zheng, C., Xu, R.-Q., and You, S.-L. (2019). Chiral phosphoric acid catalyzed aminative dearomatization of α-naphthols/ Michael addition sequence. Nat. Commun. *10*, 3150.

Xu, C., Zheng, H., Hu, B., Liu, X., Lin, L., and Feng, X. (2017). Chiral cobalt(ii) complex catalyzed Friedel–Crafts aromatization for the synthesis of axially chiral biaryldiols. Chem. Commun. (Camb.) *53*, 9741–9744.

Yadav, J.S., Reddy, B.V.S., Veerendhar, G., Rao, R.S., and Nagaiah, K. (2002). Sc(OTf)3 catalyzed electrophilic amination of arenes: an expeditious synthesis of aryl hydrazides. Chem. Lett. *31*, 318–319.

Yamanaka, M., Itoh, J., Fuchibe, K., and Akiyama, T. (2007). Chiral Brønsted acid catalyzed enantioselective Mannich-type reaction. J. Am. Chem. Soc. *129*, 6756–6764.

Zaltsgendler, I., Leblanc, Y., and Bernstein, M.A. (1993). Synthesis of aromatic amines from electron-rich arenes and bis(2,2,2-trichloroethyl) azodicarboxylate. Tetrahedron Lett. *34*, 2441–2444.

Zilate, B., Castrogiovanni, A., and Sparr, C. (2018). Catalyst-controlled stereoselective synthesis of atropisomers. ACS Catal. *8*, 2981–2988.

ISCI, Volume *22*

Supplemental Information

Atroposelective Synthesis of Biaryl Diamines and Amino Alcohols via Chiral Phosphoric Acid Catalyzed *para*-Aminations of Anilines and Phenols

Donglei Wang, Wei Liu, Mengyao Tang, Na Yu, and Xiaoyu Yang

Table S1. Reaction conditions optimization for *para*-amination of biaryl phenol **6a**, related to **Scheme 4**.

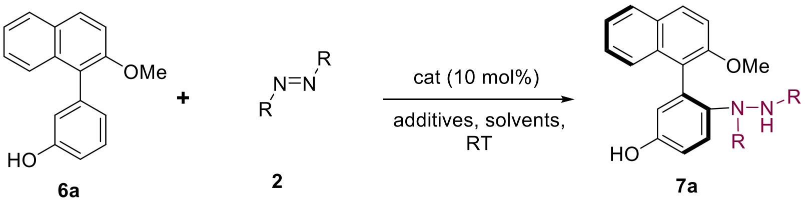

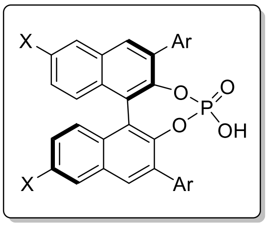

A1, X = H, Ar = phenyl
A2, X = H, Ar = 1-naphthyl
A3, X = H, Ar = 2-naphthyly
A4, X = H, Ar = 9-anthracyl
A5, X = H, Ar = 2,4,6-$(Me)_3C_6H_2$
A6, X = H, Ar = 2,4,6-$(iPr)_3C_6H_2$
A7, X = H, Ar = 2,4,6-$(Cy)_3C_6H_2$
A8, X = n-C_8H_{17}, Ar = 2,4,6-$(iPr)_3C_6H_2$

Entry[a]	R	Catalyst	Solvent	Additives	Yield[b] (%)	Ee[b] (%)
1	COOEt	**A6**	$CHCl_3$	-	52	40
2	Boc	**A6**	$CHCl_3$	-	45	61
3	Cbz	**A6**	$CHCl_3$	-	38	69
4	Cbz	**A6**	$CHCl_3$	4 Å MS	64	73
5	Cbz	**A6**	$CHCl_3$	5 Å MS	63	83
6	Cbz	**A6**	Toluene	5 Å MS	46	66
7	Cbz	**A6**	DCM	5 Å MS	46	78
8	Cbz	**A6**	CCl_4	5 Å MS	37	74
9	Cbz	**A6**	Et_2O	5 Å MS	NR	-
10	Cbz	**A2**	$CHCl_3$	5 Å MS	42	55
11	Cbz	**A3**	$CHCl_3$	5 Å MS	49	35
12	Cbz	**A4**	$CHCl_3$	5 Å MS	60	13
13	Cbz	**A5**	$CHCl_3$	5 Å MS	58	37
14	Cbz	**A7**	$CHCl_3$	5 Å MS	51	84
15	Cbz	**A8**	$CHCl_3$	5 Å MS	56	86

[a] Unless otherwise noted, reactions were performed with **6a** (0.1 mmol), **2** (0.15 mmol), CPA catalyst (0.01 mmol) in solvents (0.5 mL) for 36 h at ambient temperature. [b] Yields were isolated yields. [c] Enantiomeric excesses (ees) were determined by HPLC analysis on a chiral stationary phase.

Supplemental Figures for HPLC spectra:

Figure S1. HPLC spectrum of racemic-**3a**, related to **Table 1**.

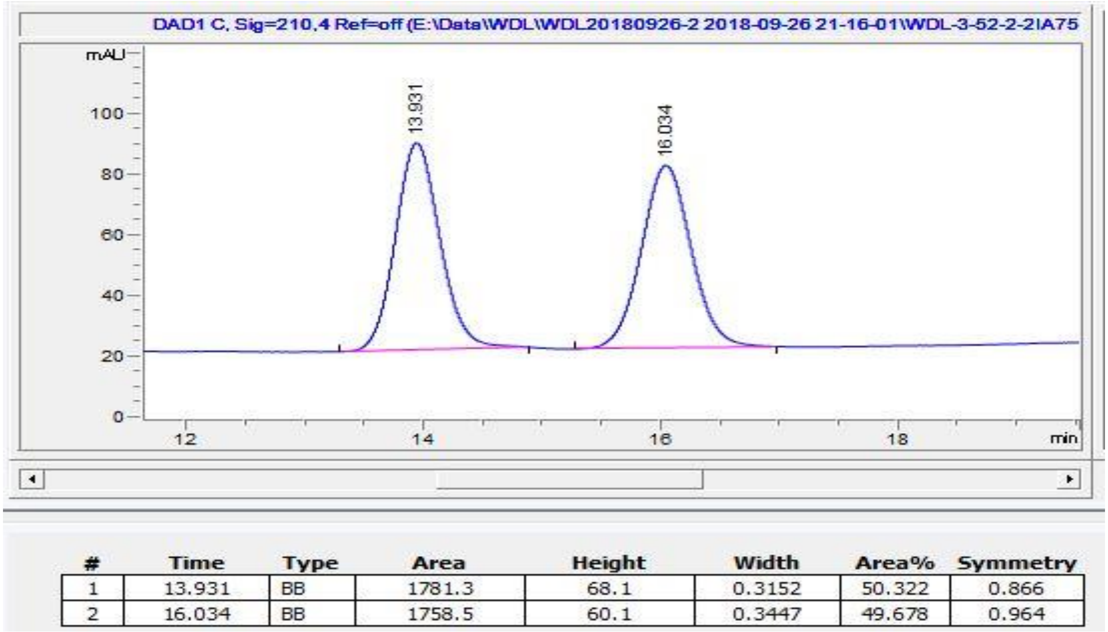

#	Time	Type	Area	Height	Width	Area%	Symmetry
1	13.931	BB	1781.3	68.1	0.3152	50.322	0.866
2	16.034	BB	1758.5	60.1	0.3447	49.678	0.964

Figure S2. HPLC spectrum of **3a**, related to **Table 1**.

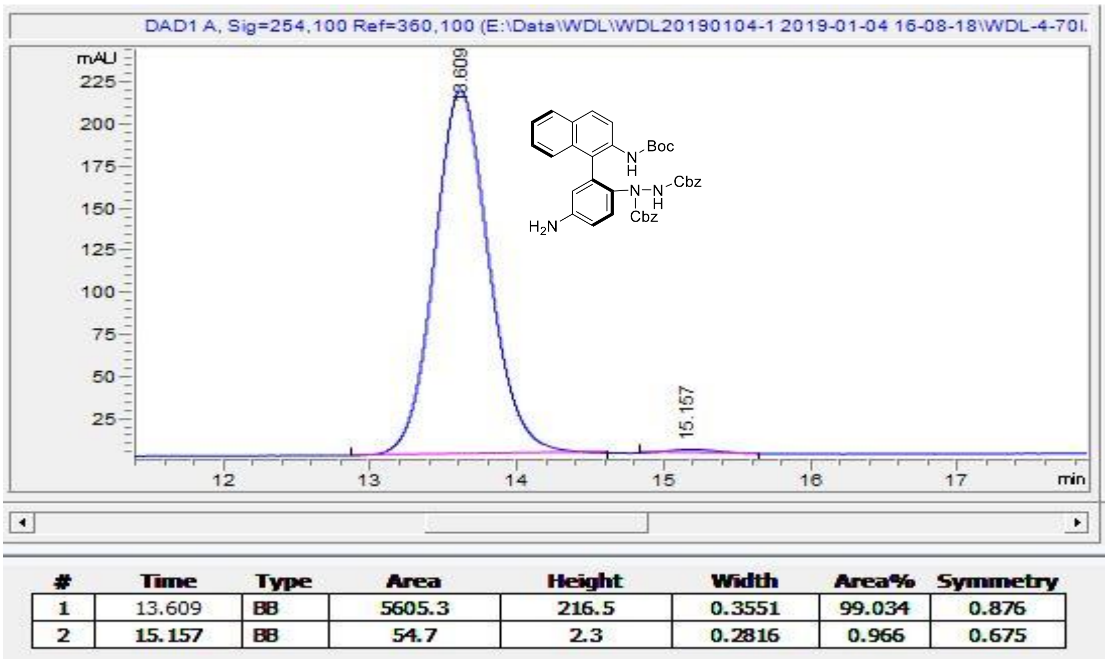

#	Time	Type	Area	Height	Width	Area%	Symmetry
1	13.609	BB	5605.3	216.5	0.3551	99.034	0.876
2	15.157	BB	54.7	2.3	0.2816	0.966	0.675

Figure S3. Full HPLC spectrum of **3a**, related to **Table 1**.

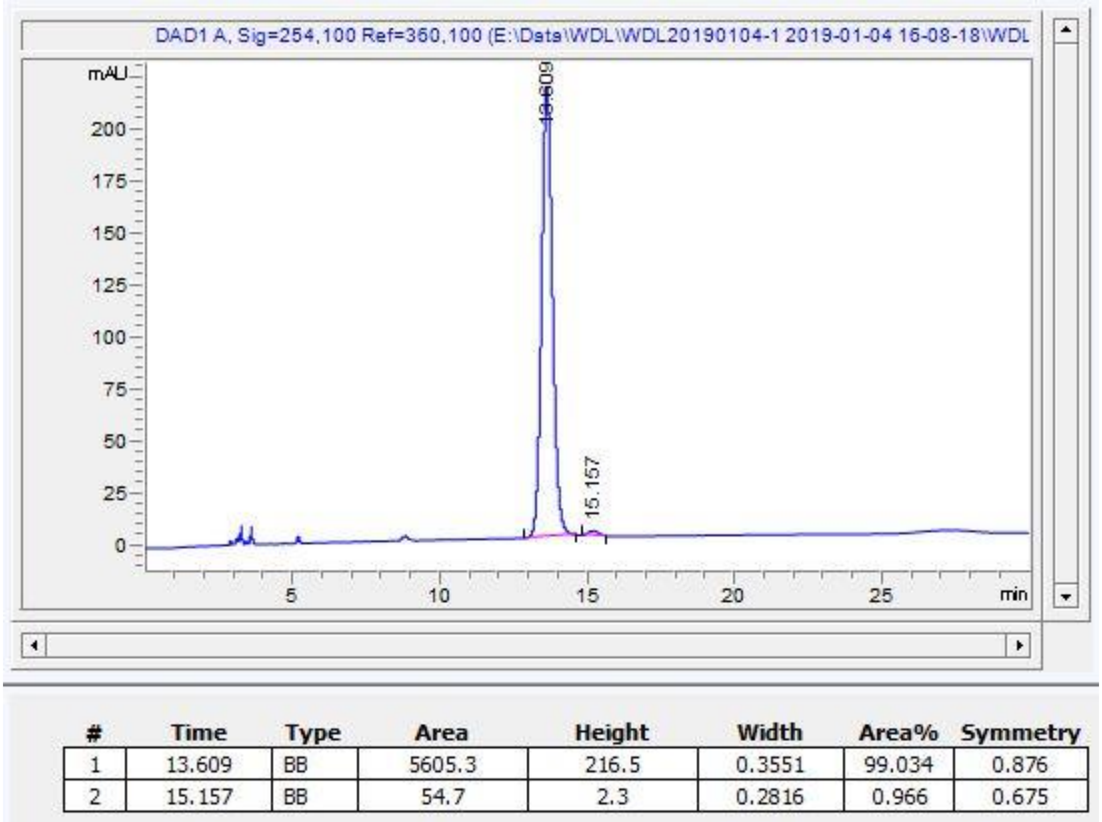

#	Time	Type	Area	Height	Width	Area%	Symmetry
1	13.609	BB	5605.3	216.5	0.3551	99.034	0.876
2	15.157	BB	54.7	2.3	0.2816	0.966	0.675

Figure S4. HPLC spectrum of racemic-**3b**, related to **Scheme 2**.

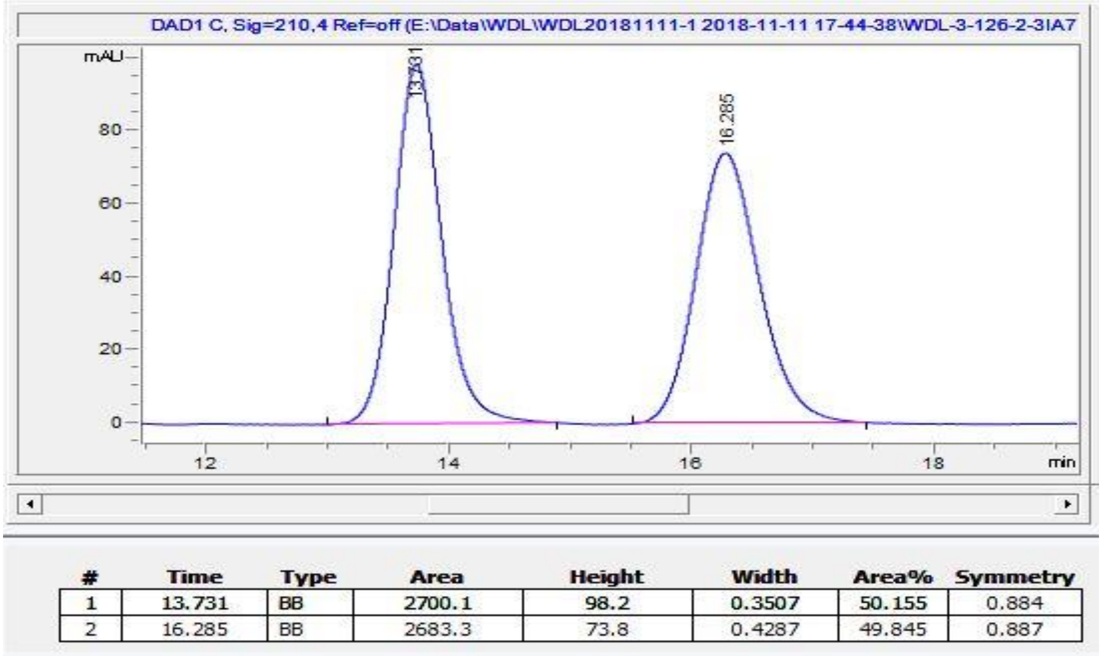

#	Time	Type	Area	Height	Width	Area%	Symmetry
1	13.731	BB	2700.1	98.2	0.3507	50.155	0.884
2	16.285	BB	2683.3	73.8	0.4287	49.845	0.887

Figure S5. HPLC spectrum of **3b**, related to **Scheme 2**.

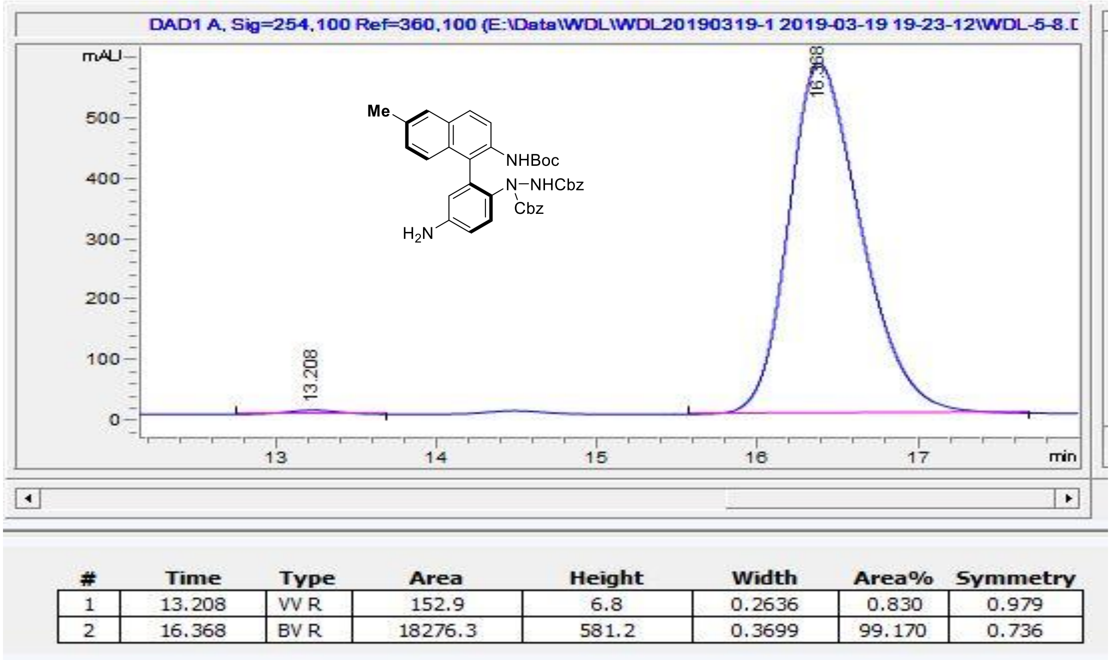

#	Time	Type	Area	Height	Width	Area%	Symmetry
1	13.208	VV R	152.9	6.8	0.2636	0.830	0.979
2	16.368	BV R	18276.3	581.2	0.3699	99.170	0.736

Figure S6. Full HPLC spectrum of **3b**, related to **Scheme 2**.

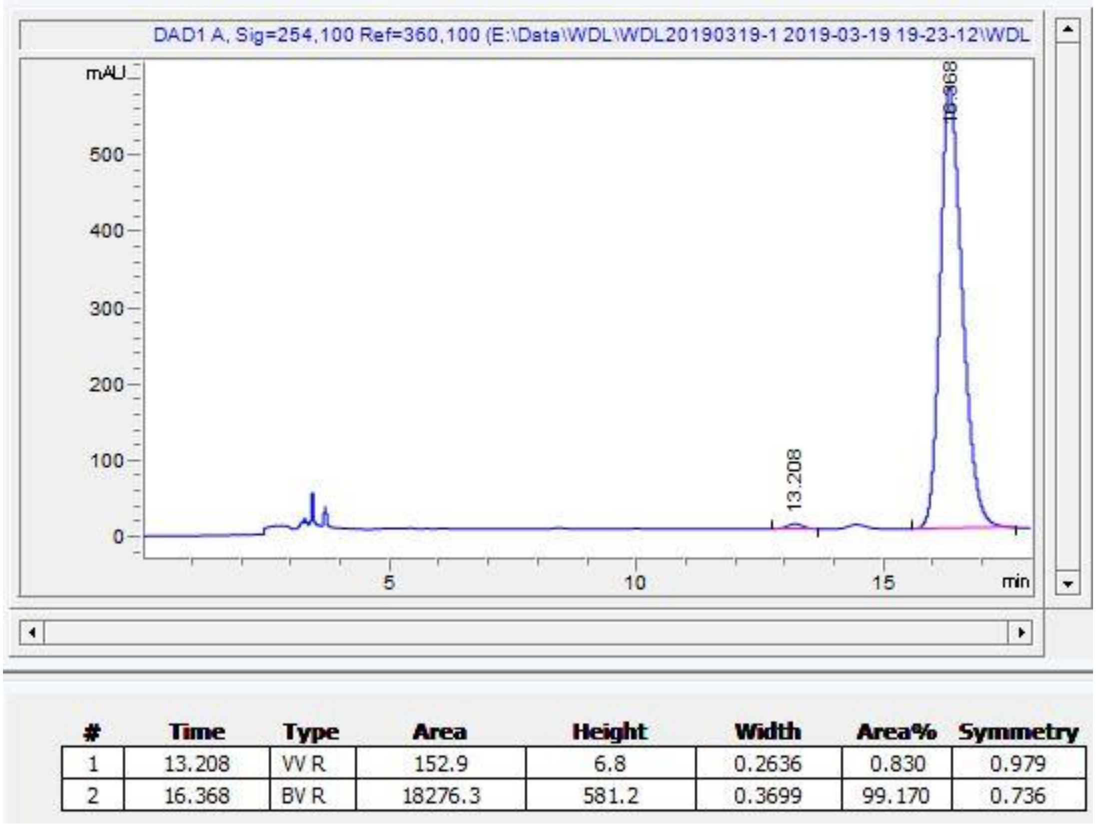

#	Time	Type	Area	Height	Width	Area%	Symmetry
1	13.208	VV R	152.9	6.8	0.2636	0.830	0.979
2	16.368	BV R	18276.3	581.2	0.3699	99.170	0.736

Figure S7. HPLC spectrum of racemic-**3c**, related to **Scheme 2.**

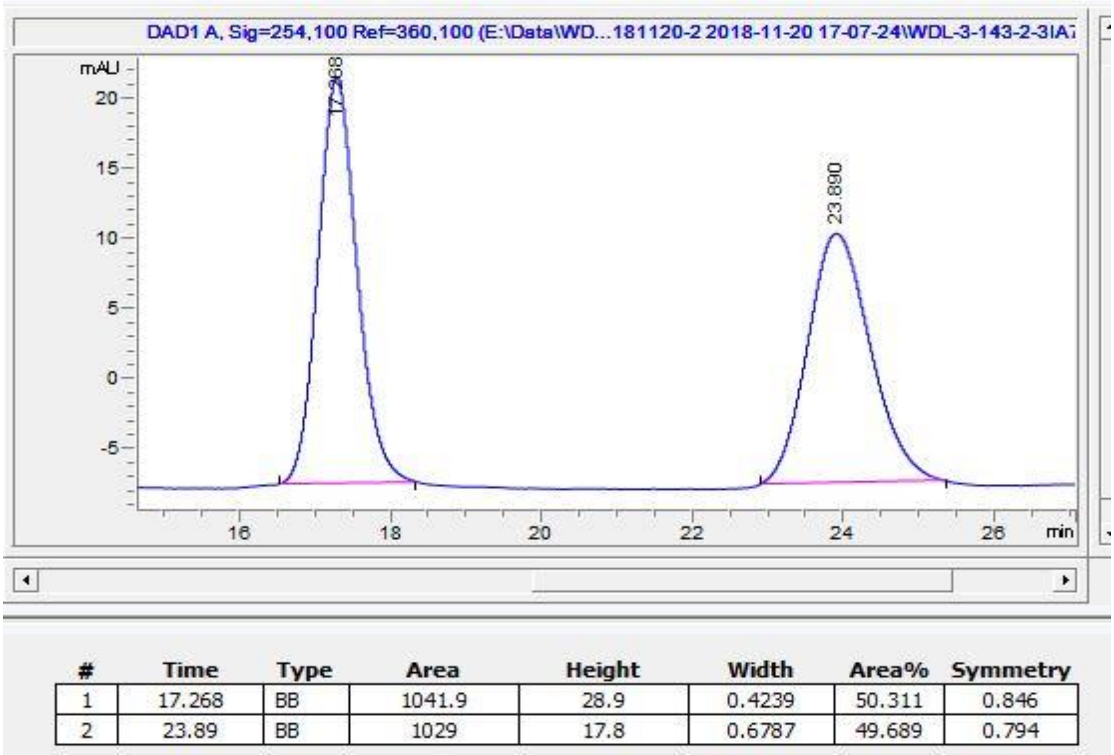

#	Time	Type	Area	Height	Width	Area%	Symmetry
1	17.268	BB	1041.9	28.9	0.4239	50.311	0.846
2	23.89	BB	1029	17.8	0.6787	49.689	0.794

Figure S8. HPLC spectrum of **3c**, related to **Scheme 2.**

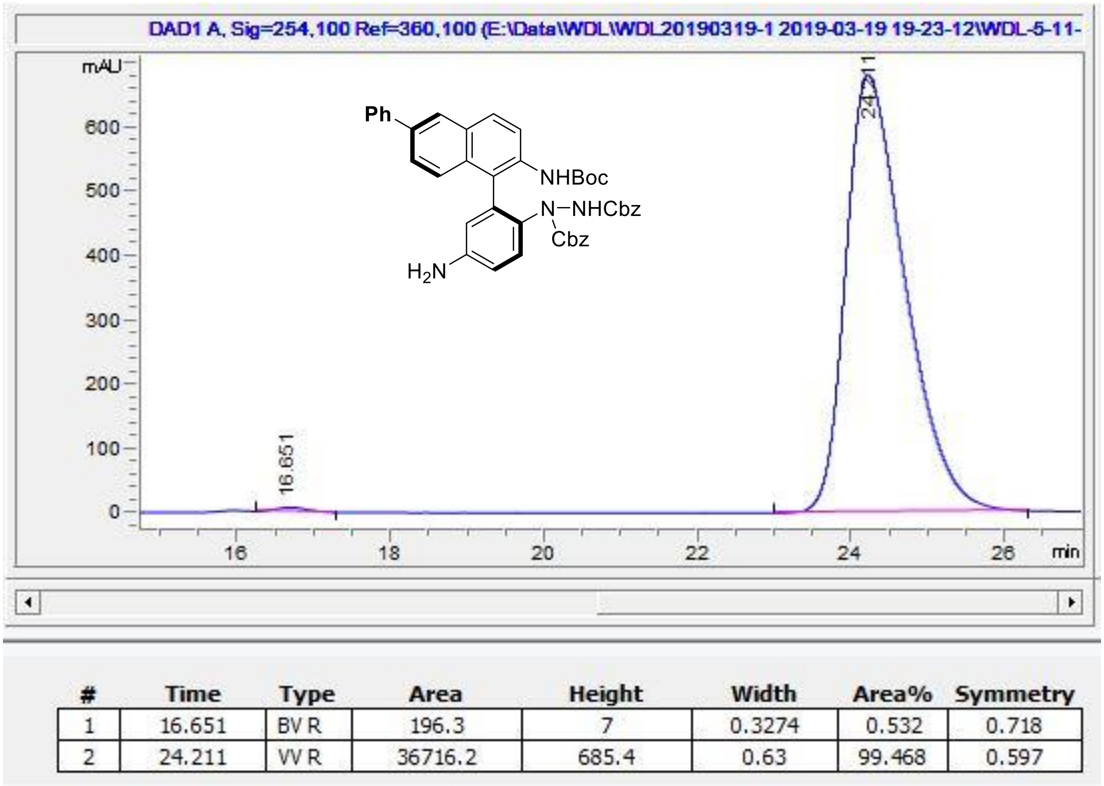

#	Time	Type	Area	Height	Width	Area%	Symmetry
1	16.651	BV R	196.3	7	0.3274	0.532	0.718
2	24.211	VV R	36716.2	685.4	0.63	99.468	0.597

Figure S9. Full HPLC spectrum of **3b**, related to **Scheme 2.**

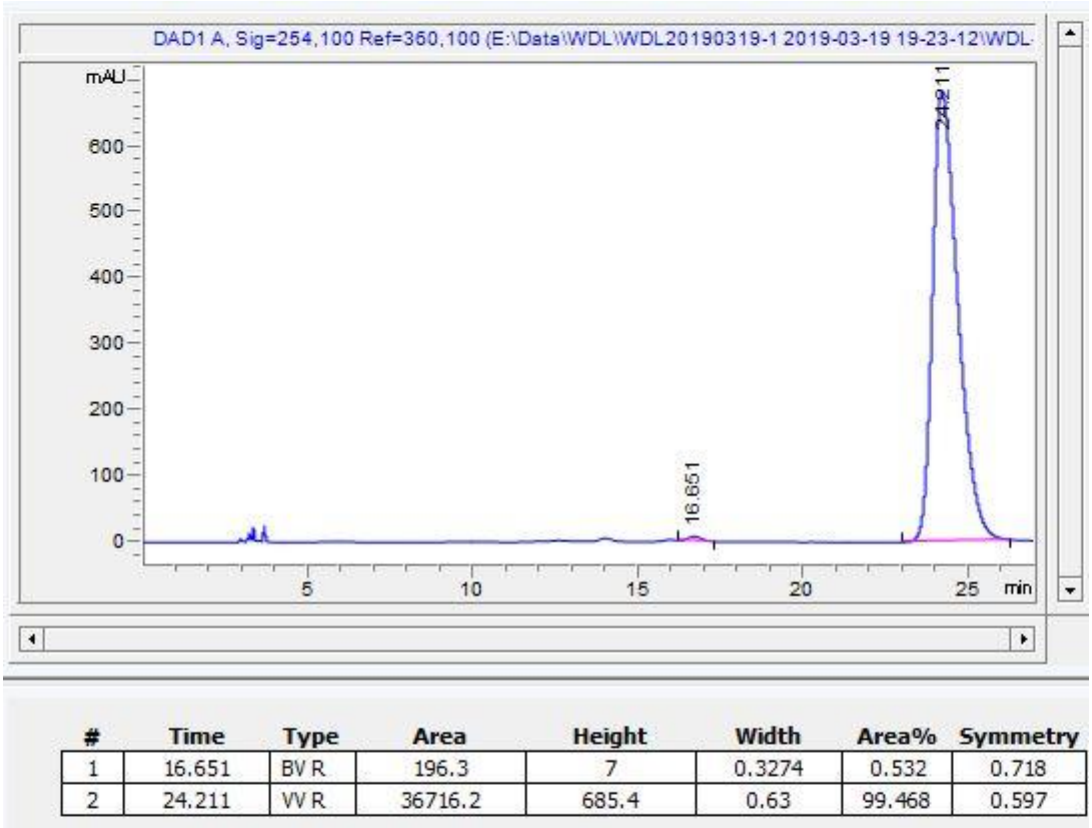

DAD1 A, Sig=254,100 Ref=360,100 (E:\Data\WDL\WDL20190319-1 2019-03-19 19-23-12\WDL-

#	Time	Type	Area	Height	Width	Area%	Symmetry
1	16.651	BV R	196.3	7	0.3274	0.532	0.718
2	24.211	VV R	36716.2	685.4	0.63	99.468	0.597

Figure S10. HPLC spectrum of racemic-**3d**, related to **Scheme 2.**

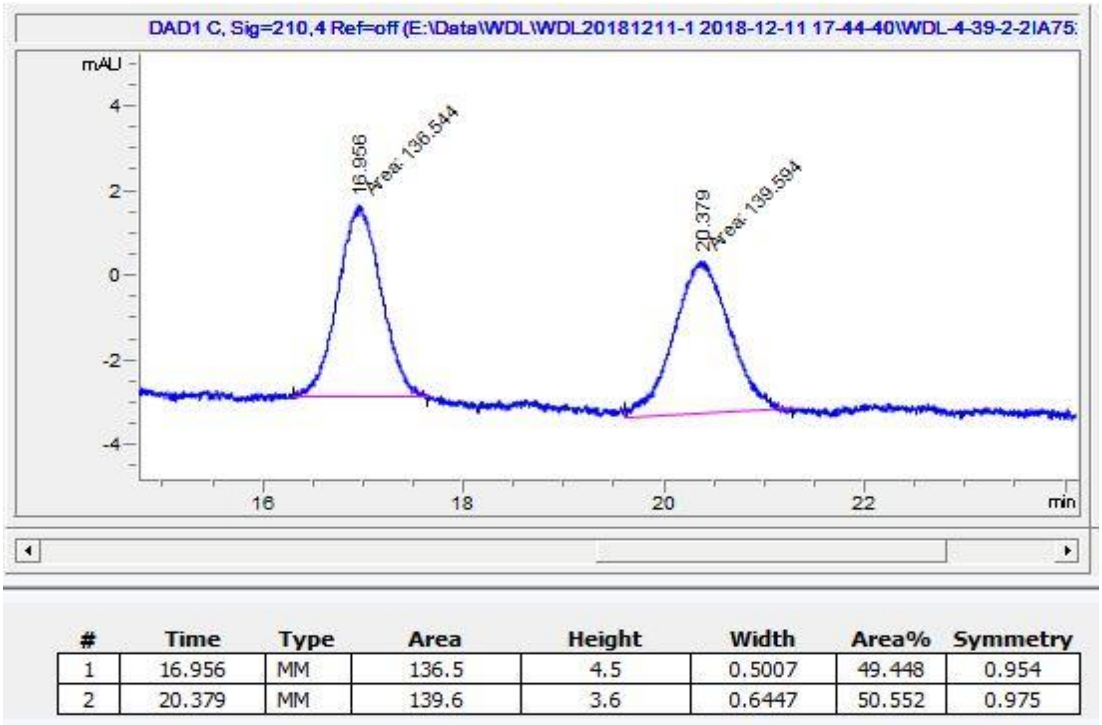

DAD1 C, Sig=210,4 Ref=off (E:\Data\WDL\WDL20181211-1 2018-12-11 17-44-40\WDL-4-39-2-2IA75:

#	Time	Type	Area	Height	Width	Area%	Symmetry
1	16.956	MM	136.5	4.5	0.5007	49.448	0.954
2	20.379	MM	139.6	3.6	0.6447	50.552	0.975

Figure S11. HPLC spectrum of **3d**, related to **Scheme 2.**

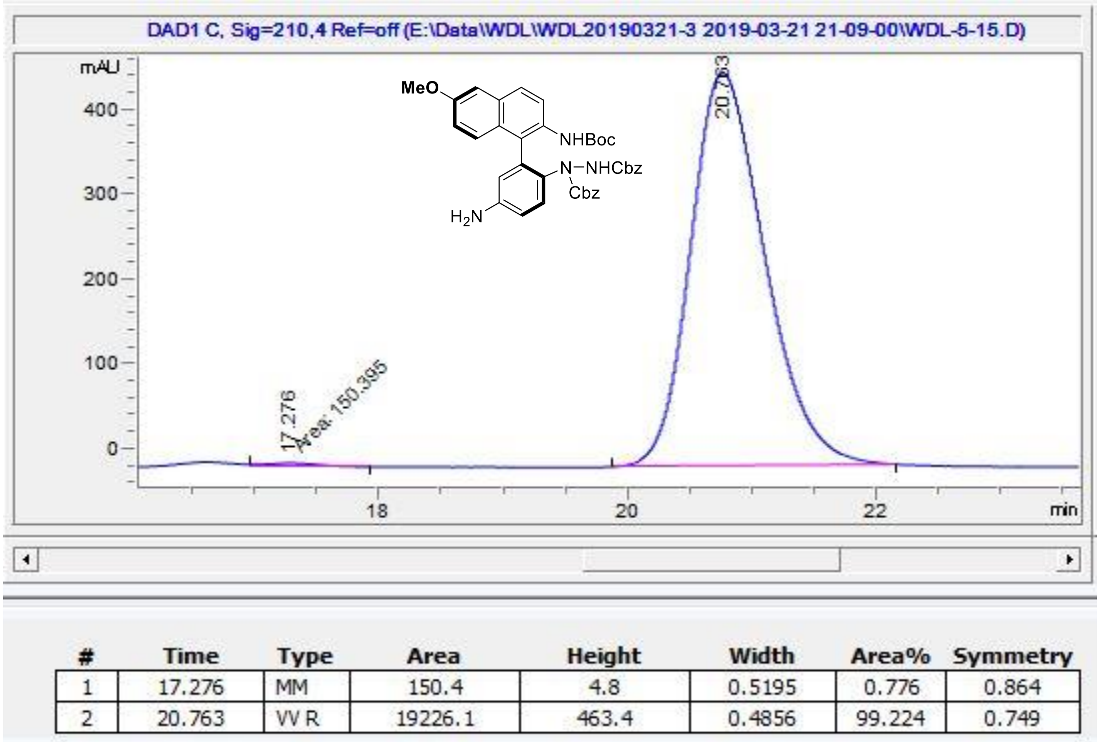

#	Time	Type	Area	Height	Width	Area%	Symmetry
1	17.276	MM	150.4	4.8	0.5195	0.776	0.864
2	20.763	VV R	19226.1	463.4	0.4856	99.224	0.749

Figure S12. Full HPLC spectrum of **3b**, related to **Scheme 2.**

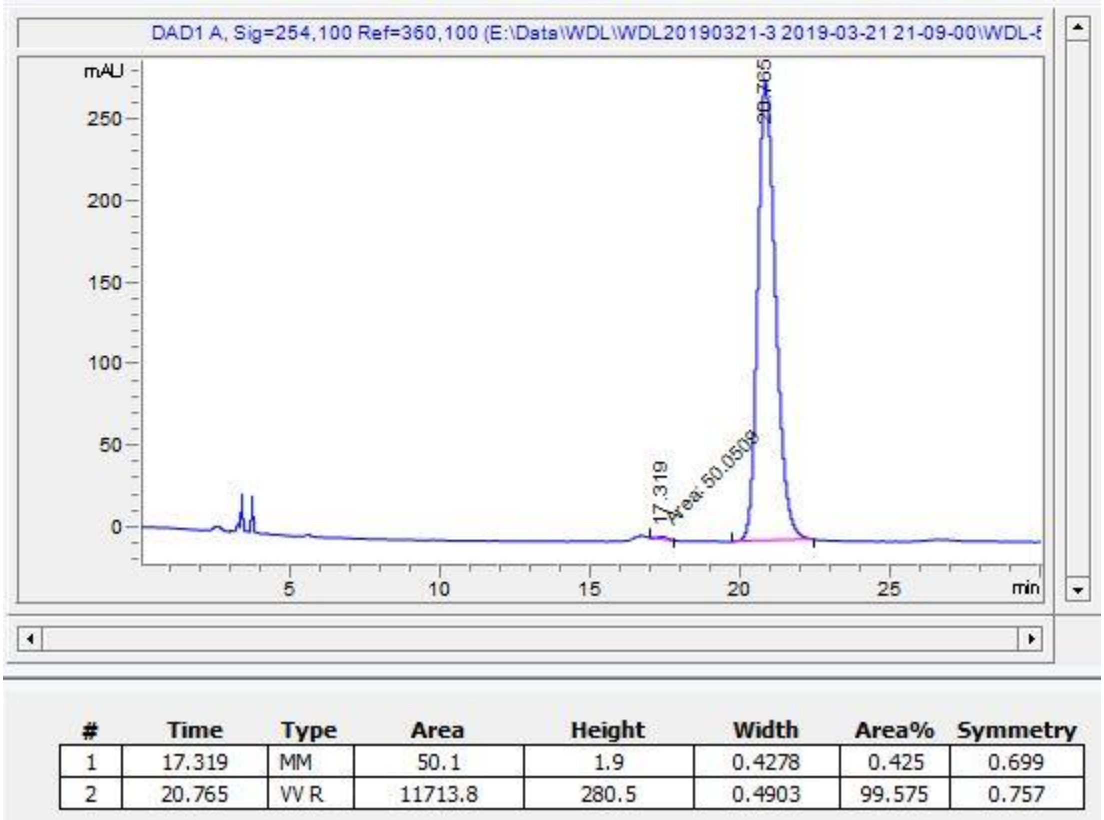

#	Time	Type	Area	Height	Width	Area%	Symmetry
1	17.319	MM	50.1	1.9	0.4278	0.425	0.699
2	20.765	VV R	11713.8	280.5	0.4903	99.575	0.757

Figure S13. HPLC spectrum of racemic-**3e**, related to **Scheme 2.**

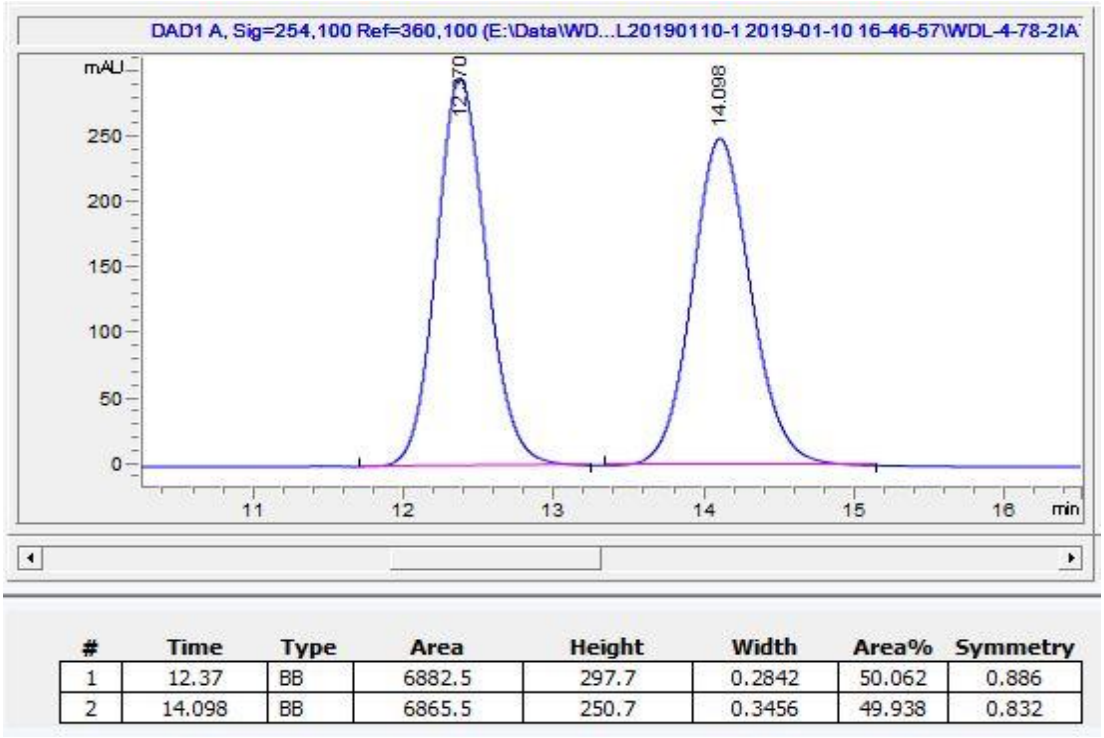
DAD1 A, Sig=254,100 Ref=360,100 (E:\Data\WD...L20190110-1 2019-01-10 16-46-57\WDL-4-78-2.D)

#	Time	Type	Area	Height	Width	Area%	Symmetry
1	12.37	BB	6882.5	297.7	0.2842	50.062	0.886
2	14.098	BB	6865.5	250.7	0.3456	49.938	0.832

Figure S14. HPLC spectrum of **3e**, related to **Scheme 2.**

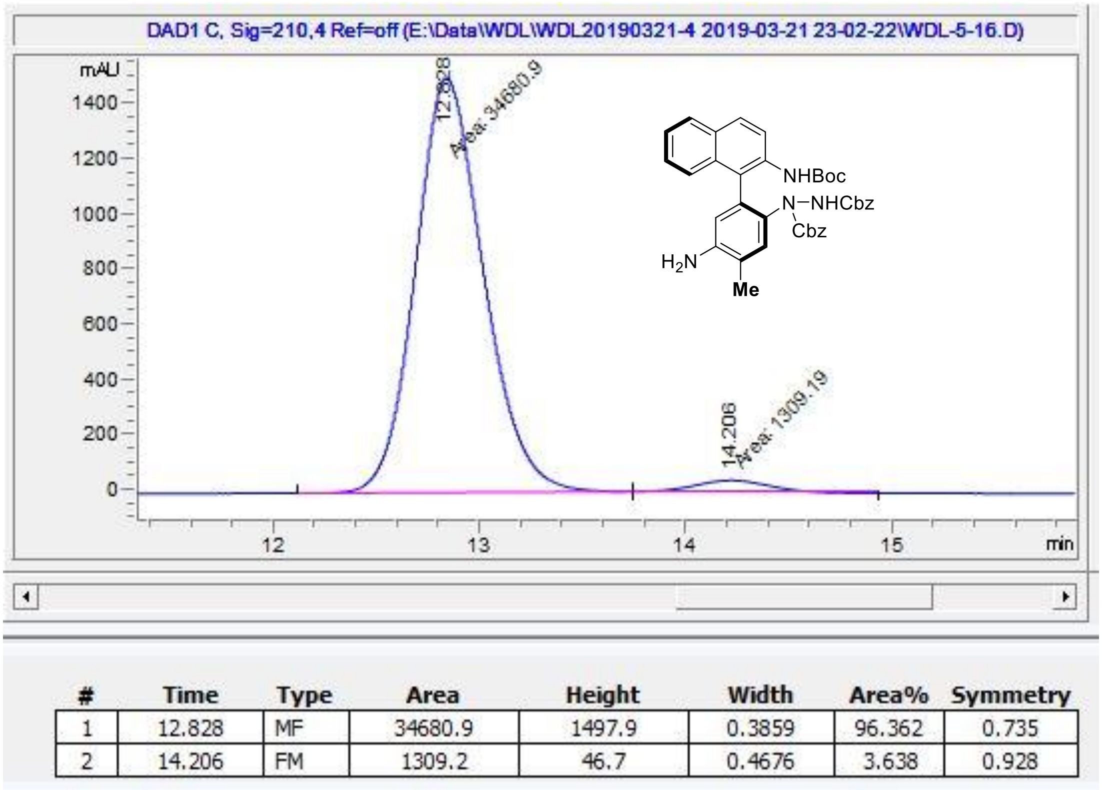
DAD1 C, Sig=210,4 Ref=off (E:\Data\WDL\WDL20190321-4 2019-03-21 23-02-22\WDL-5-16.D)

#	Time	Type	Area	Height	Width	Area%	Symmetry
1	12.828	MF	34680.9	1497.9	0.3859	96.362	0.735
2	14.206	FM	1309.2	46.7	0.4676	3.638	0.928

Figure S15. Full HPLC spectrum of **3b**, related to **Scheme 2.**

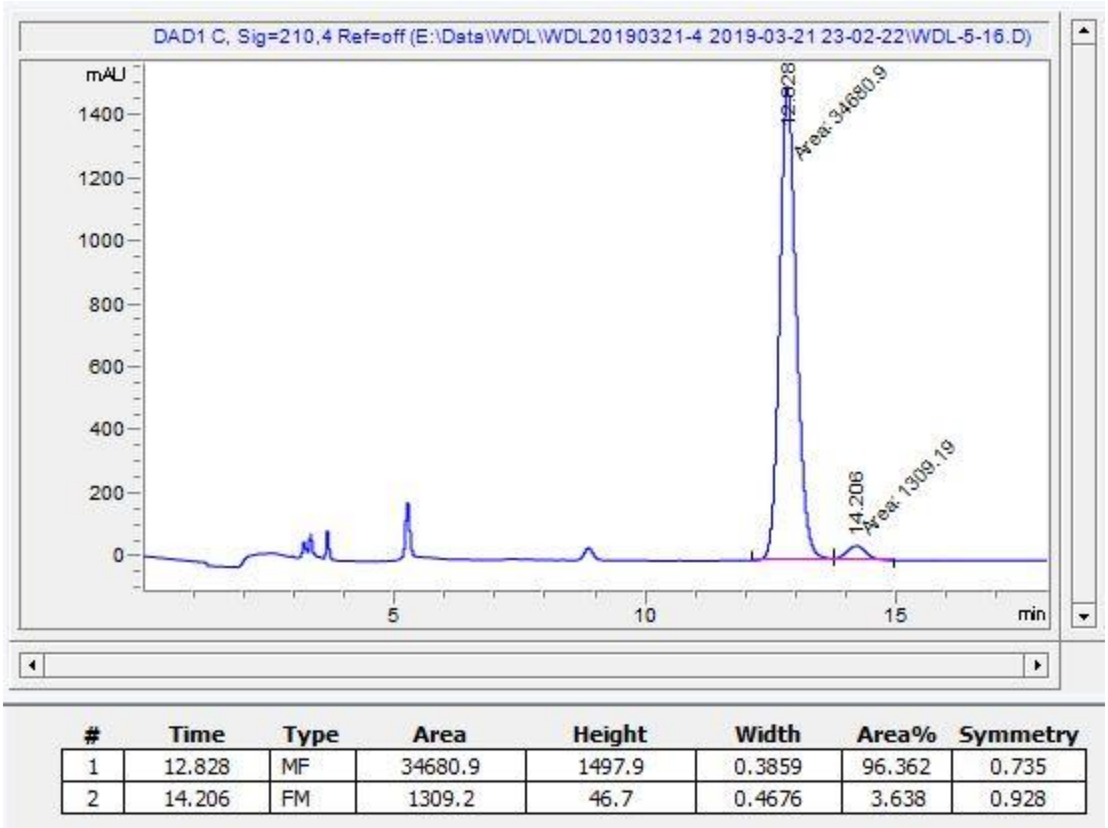

DAD1 C, Sig=210,4 Ref=off (E:\Data\WDL\WDL20190321-4 2019-03-21 23-02-22\WDL-5-16.D)

#	Time	Type	Area	Height	Width	Area%	Symmetry
1	12.828	MF	34680.9	1497.9	0.3859	96.362	0.735
2	14.206	FM	1309.2	46.7	0.4676	3.638	0.928

Figure S16. HPLC spectrum of racemic-**3f**, related to **Scheme 2.**

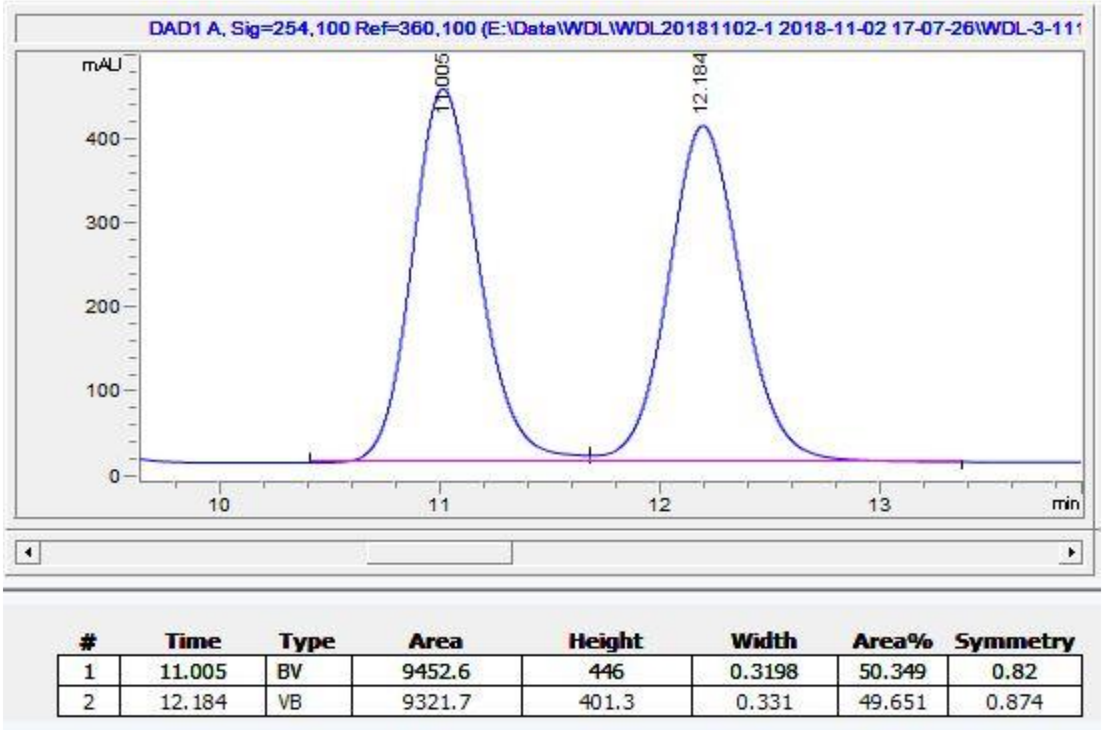

DAD1 A, Sig=254,100 Ref=360,100 (E:\Data\WDL\WDL20181102-1 2018-11-02 17-07-26\WDL-3-11

#	Time	Type	Area	Height	Width	Area%	Symmetry
1	11.005	BV	9452.6	446	0.3198	50.349	0.82
2	12.184	VB	9321.7	401.3	0.331	49.651	0.874

Figure S17. HPLC spectrum of **3f**, related to **Scheme 2.**

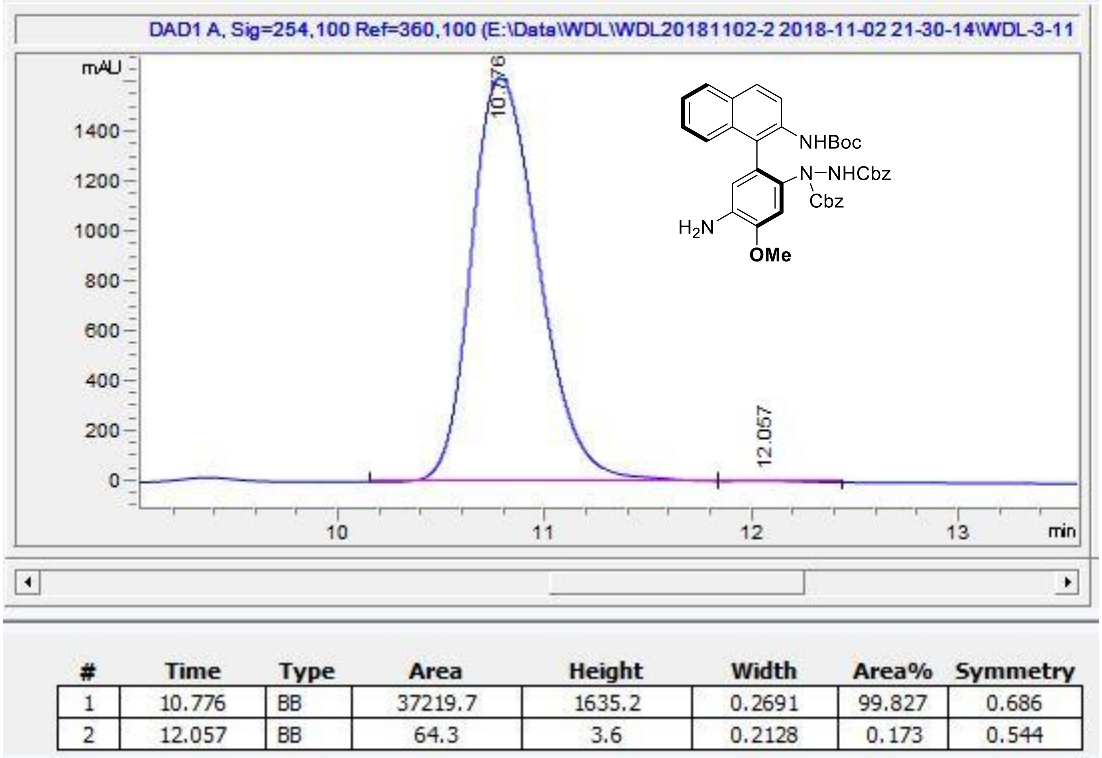

DAD1 A, Sig=254,100 Ref=360,100 (E:\Data\WDL\WDL20181102-2 2018-11-02 21-30-14\WDL-3-11

#	Time	Type	Area	Height	Width	Area%	Symmetry
1	10.776	BB	37219.7	1635.2	0.2691	99.827	0.686
2	12.057	BB	64.3	3.6	0.2128	0.173	0.544

Figure S18. Full HPLC spectrum of **3b**, related to **Scheme 2.**

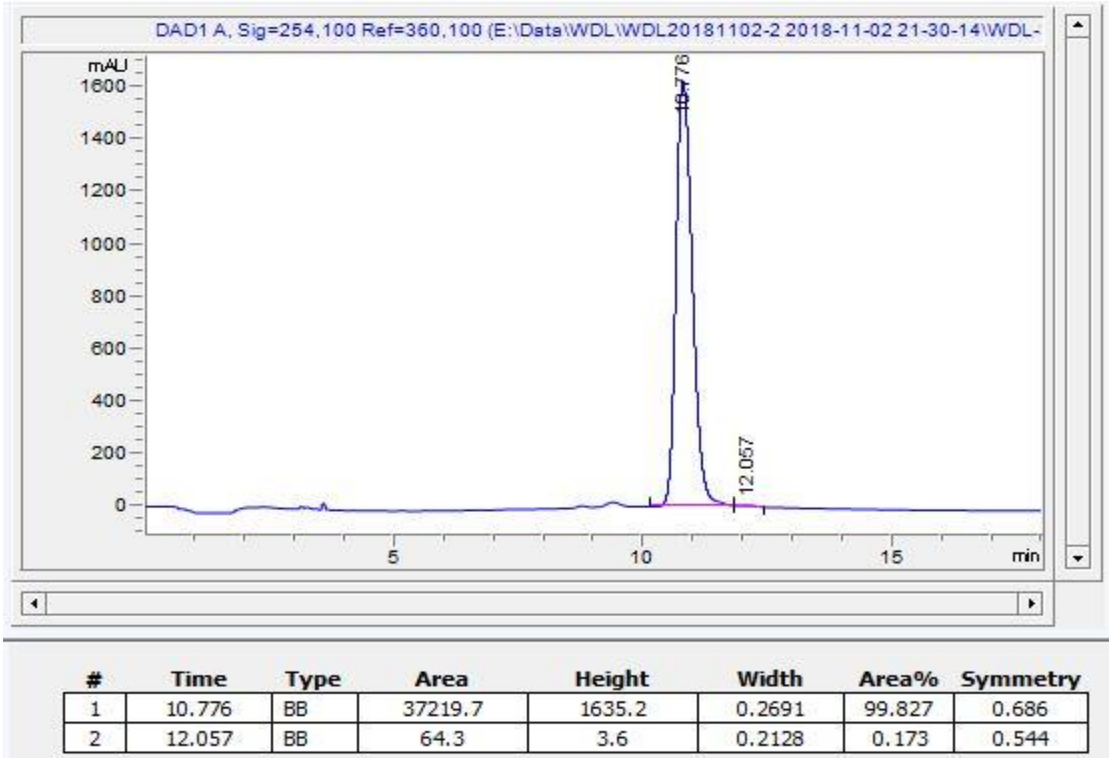

DAD1 A, Sig=254,100 Ref=360,100 (E:\Data\WDL\WDL20181102-2 2018-11-02 21-30-14\WDL-

#	Time	Type	Area	Height	Width	Area%	Symmetry
1	10.776	BB	37219.7	1635.2	0.2691	99.827	0.686
2	12.057	BB	64.3	3.6	0.2128	0.173	0.544

Figure S19. HPLC spectrum of racemic-**3g**, related to **Scheme 2.**

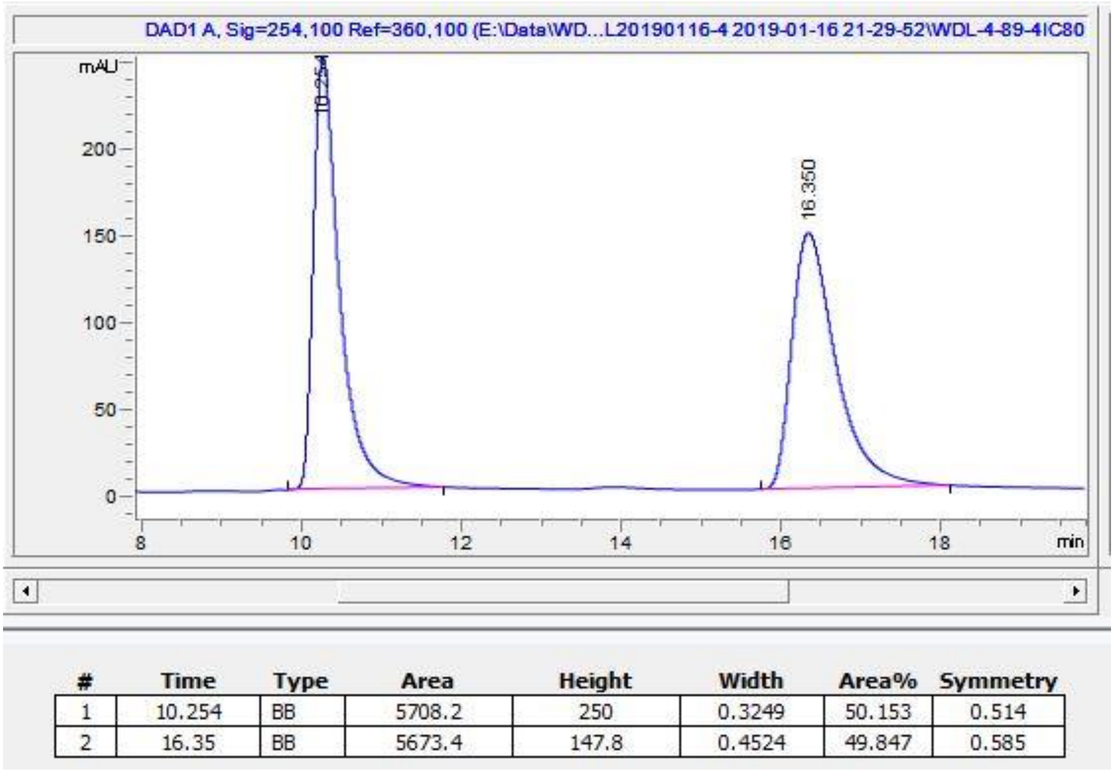

#	Time	Type	Area	Height	Width	Area%	Symmetry
1	10.254	BB	5708.2	250	0.3249	50.153	0.514
2	16.35	BB	5673.4	147.8	0.4524	49.847	0.585

Figure S20. HPLC spectrum of **3g**, related to **Scheme 2.**

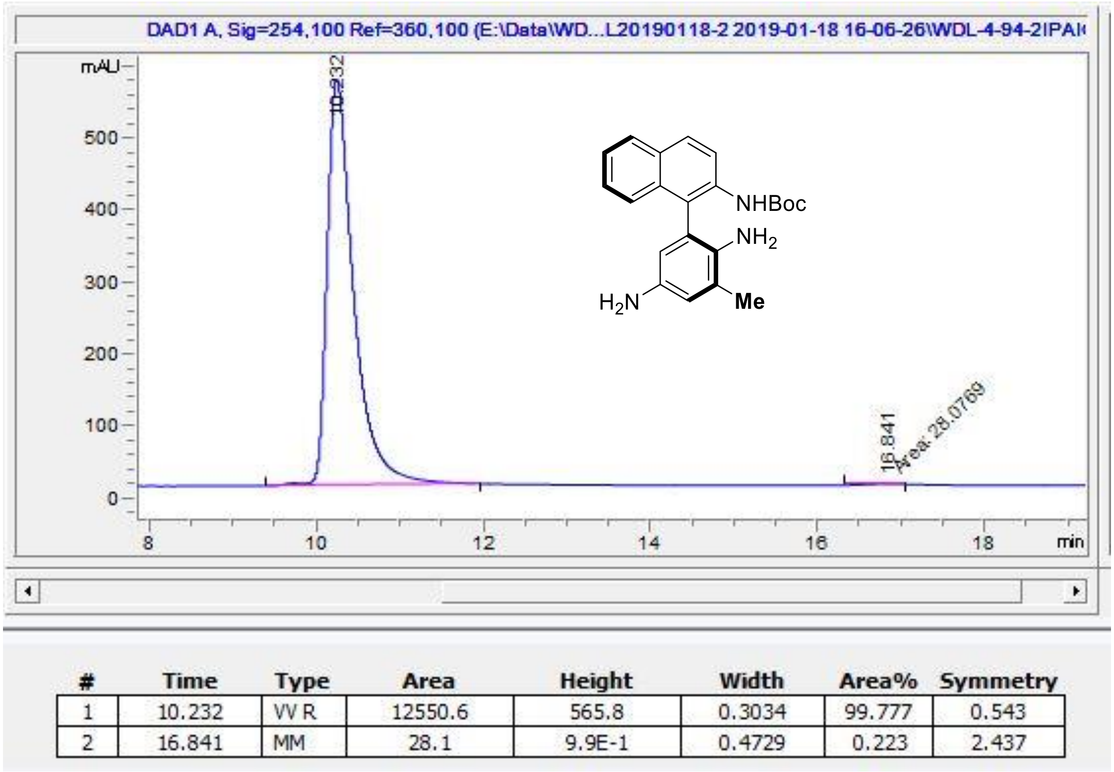

#	Time	Type	Area	Height	Width	Area%	Symmetry
1	10.232	VV R	12550.6	565.8	0.3034	99.777	0.543
2	16.841	MM	28.1	9.9E-1	0.4729	0.223	2.437

Figure S21. Full HPLC spectrum of **3b**, related to **Scheme 2.**

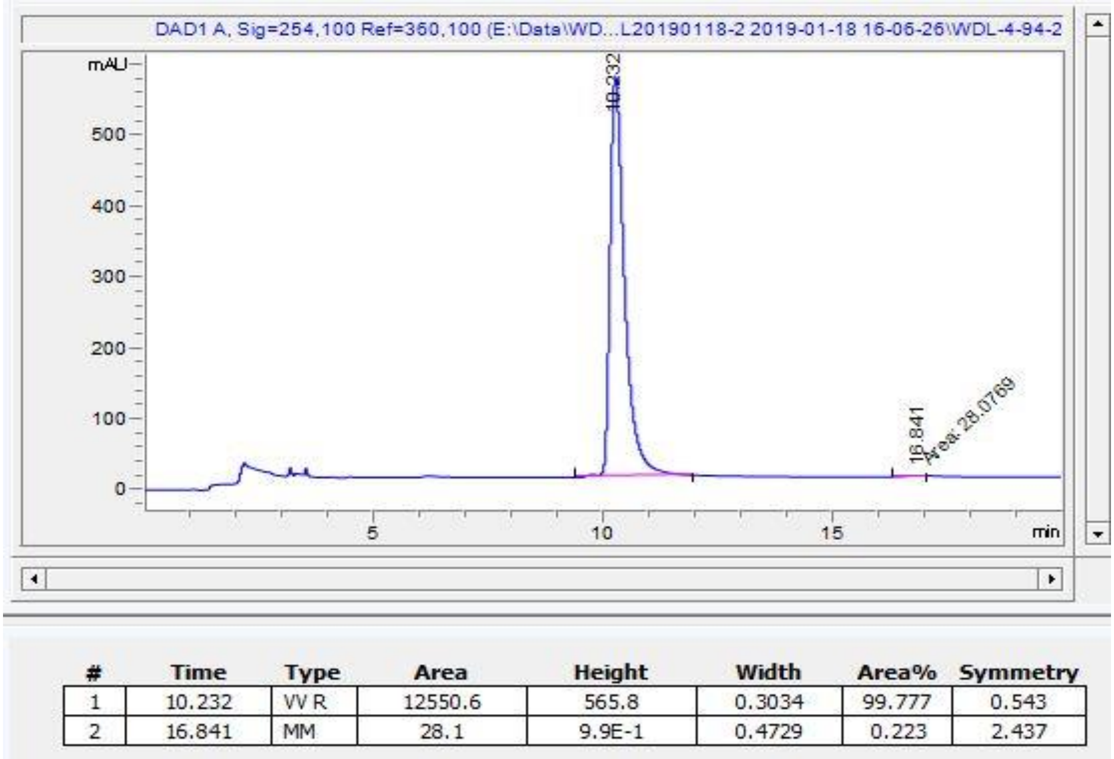

#	Time	Type	Area	Height	Width	Area%	Symmetry
1	10.232	VV R	12550.6	565.8	0.3034	99.777	0.543
2	16.841	MM	28.1	9.9E-1	0.4729	0.223	2.437

Figure S22. HPLC spectrum of racemic-**3h**, related to **Scheme 2.**

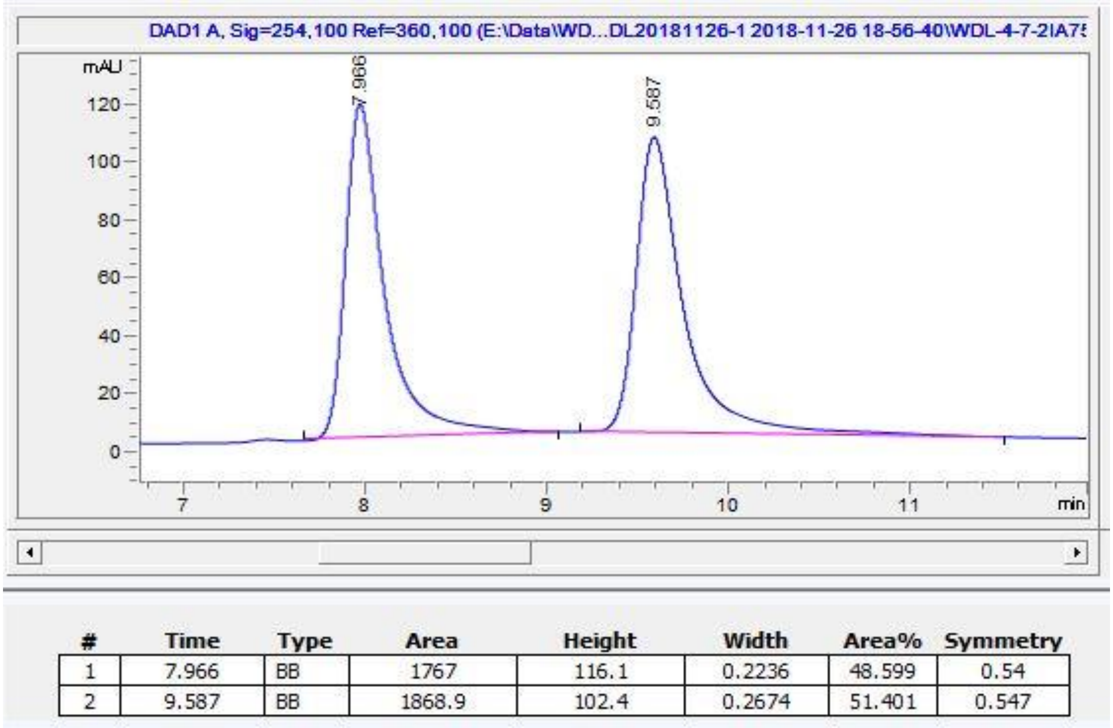

#	Time	Type	Area	Height	Width	Area%	Symmetry
1	7.966	BB	1767	116.1	0.2236	48.599	0.54
2	9.587	BB	1868.9	102.4	0.2674	51.401	0.547

Figure S23. HPLC spectrum of **3h**, related to **Scheme 2.**

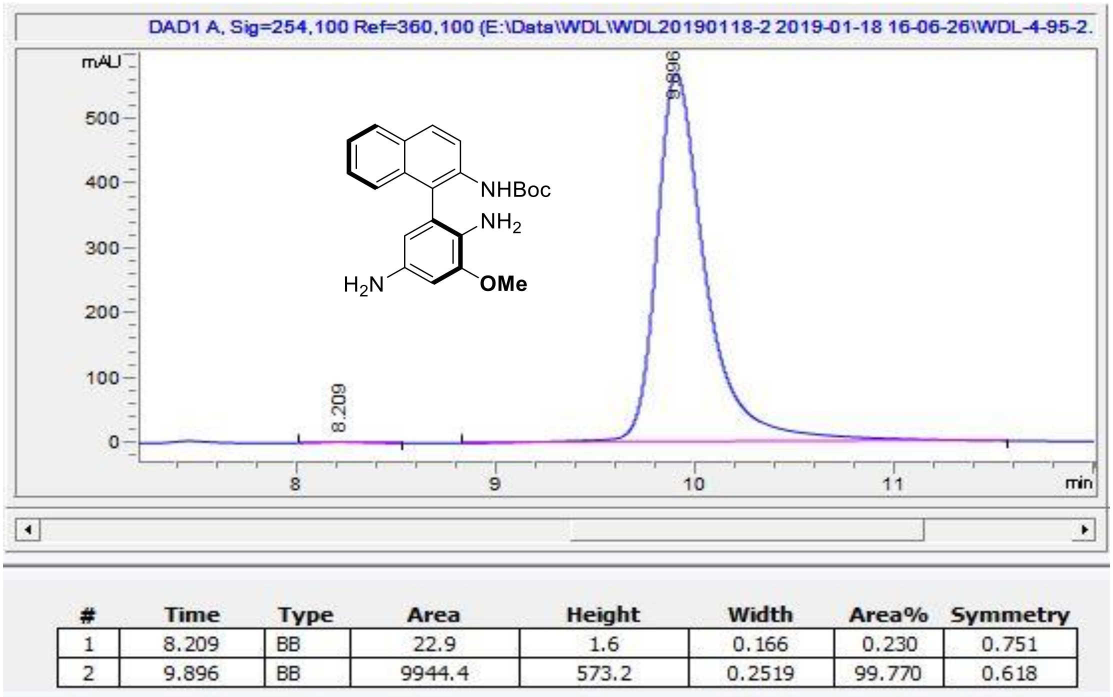

#	Time	Type	Area	Height	Width	Area%	Symmetry
1	8.209	BB	22.9	1.6	0.166	0.230	0.751
2	9.896	BB	9944.4	573.2	0.2519	99.770	0.618

Figure S24. Full HPLC spectrum of **3b**, related to **Scheme 2.**

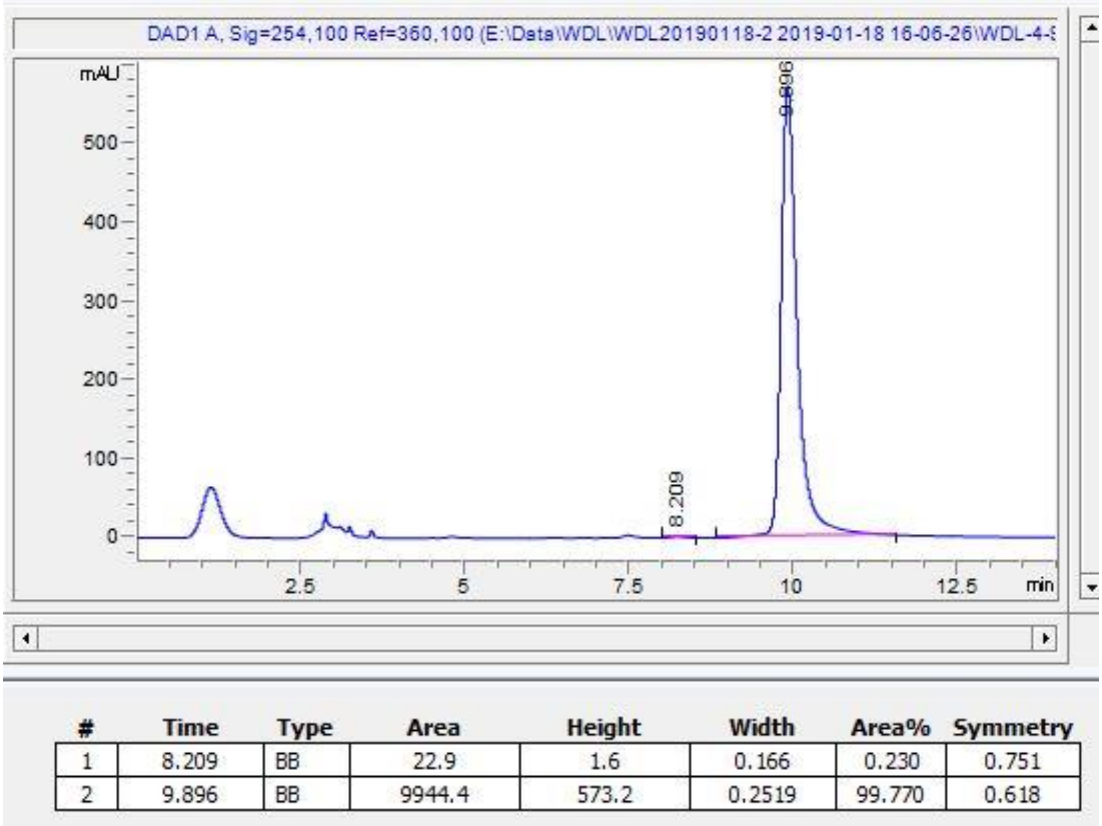

#	Time	Type	Area	Height	Width	Area%	Symmetry
1	8.209	BB	22.9	1.6	0.166	0.230	0.751
2	9.896	BB	9944.4	573.2	0.2519	99.770	0.618

Figure S25. HPLC spectrum of racemic-**3i**, related to **Scheme 2.**

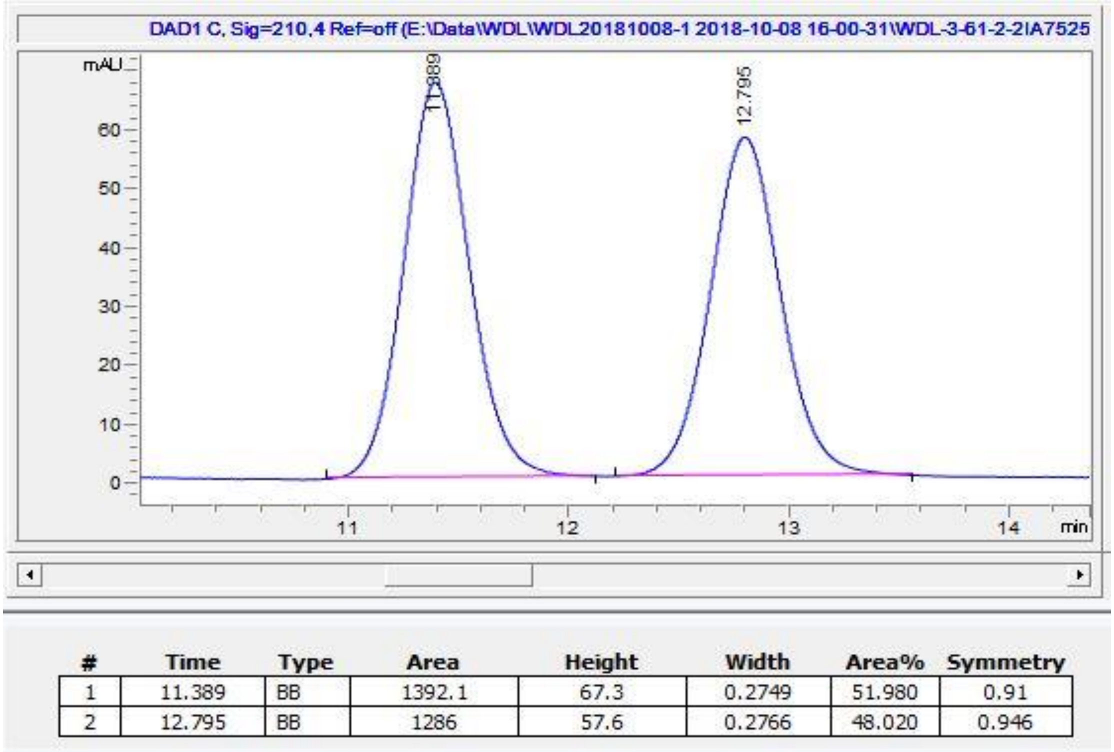

#	Time	Type	Area	Height	Width	Area%	Symmetry
1	11.389	BB	1392.1	67.3	0.2749	51.980	0.91
2	12.795	BB	1286	57.6	0.2766	48.020	0.946

Figure S26. HPLC spectrum of **3i**, related to **Scheme 2.**

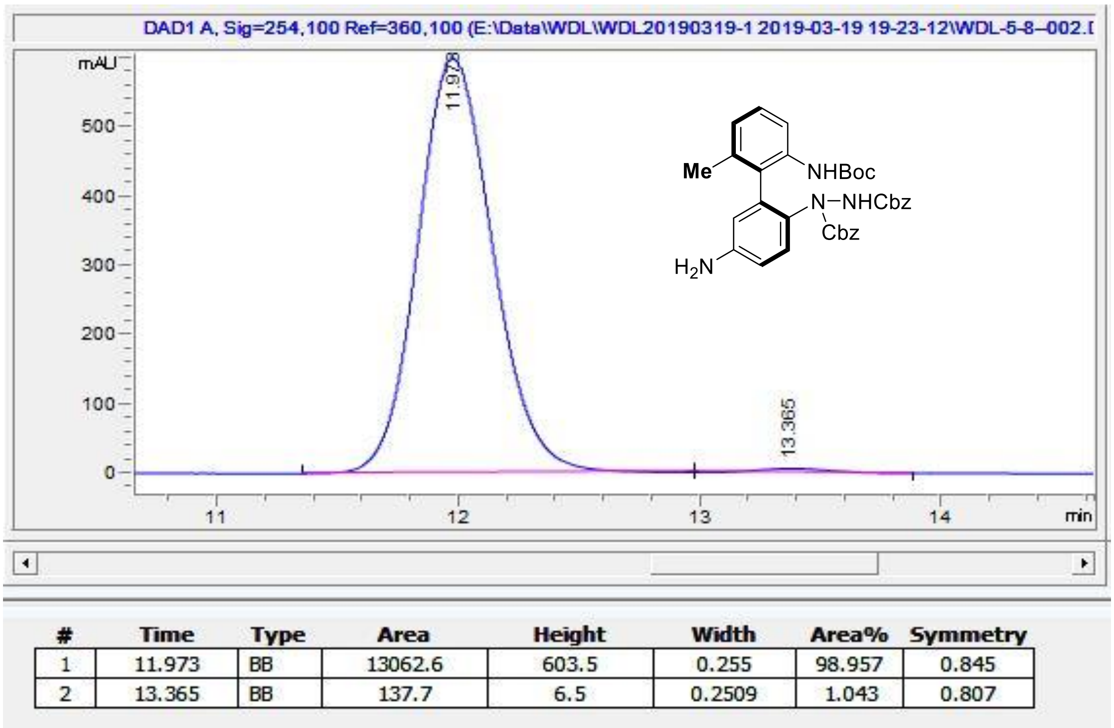

#	Time	Type	Area	Height	Width	Area%	Symmetry
1	11.973	BB	13062.6	603.5	0.255	98.957	0.845
2	13.365	BB	137.7	6.5	0.2509	1.043	0.807

Figure S27. Full HPLC spectrum of **3b**, related to **Scheme 2.**

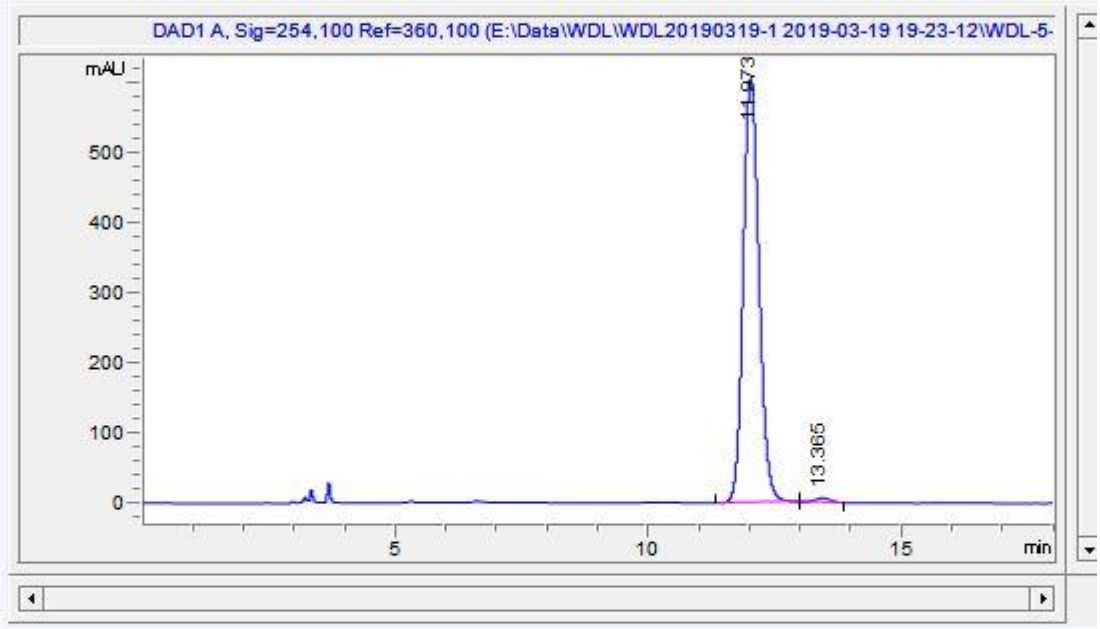

#	Time	Type	Area	Height	Width	Area%	Symmetry
1	11.973	BB	13062.6	603.5	0.255	98.957	0.845
2	13.365	BB	137.7	6.5	0.2509	1.043	0.807

Figure S28. HPLC spectrum of racemic-**3j**, related to **Scheme 2.**

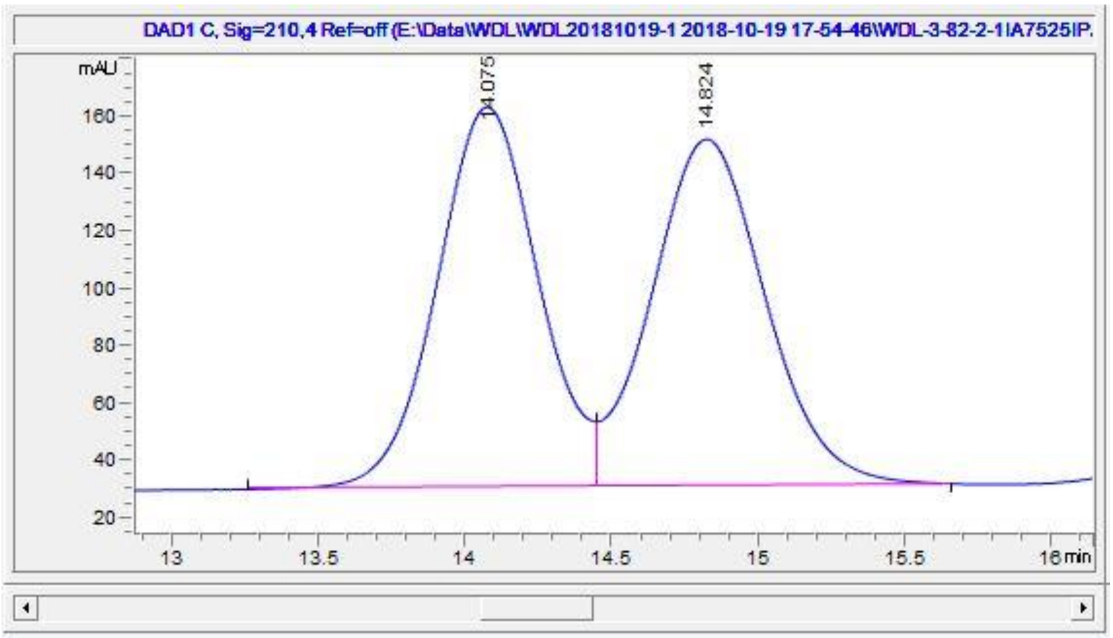

#	Time	Type	Area	Height	Width	Area%	Symmetry
1	14.075	VV R	3210.1	133.1	0.2848	49.400	0.987
2	14.824	VV R	3288	121.2	0.3261	50.600	0.897

Figure S29. HPLC spectrum of **3j**, related to **Scheme 2.**

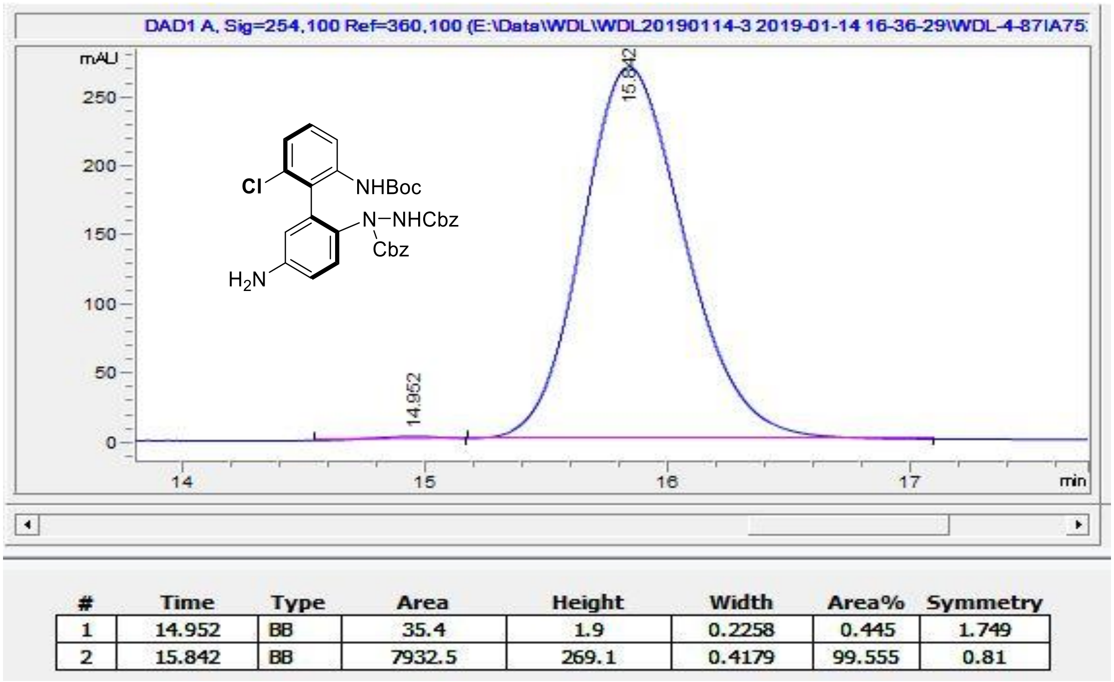

#	Time	Type	Area	Height	Width	Area%	Symmetry
1	14.952	BB	35.4	1.9	0.2258	0.445	1.749
2	15.842	BB	7932.5	269.1	0.4179	99.555	0.81

Figure S30. Full HPLC spectrum of **3b**, related to **Scheme 2.**

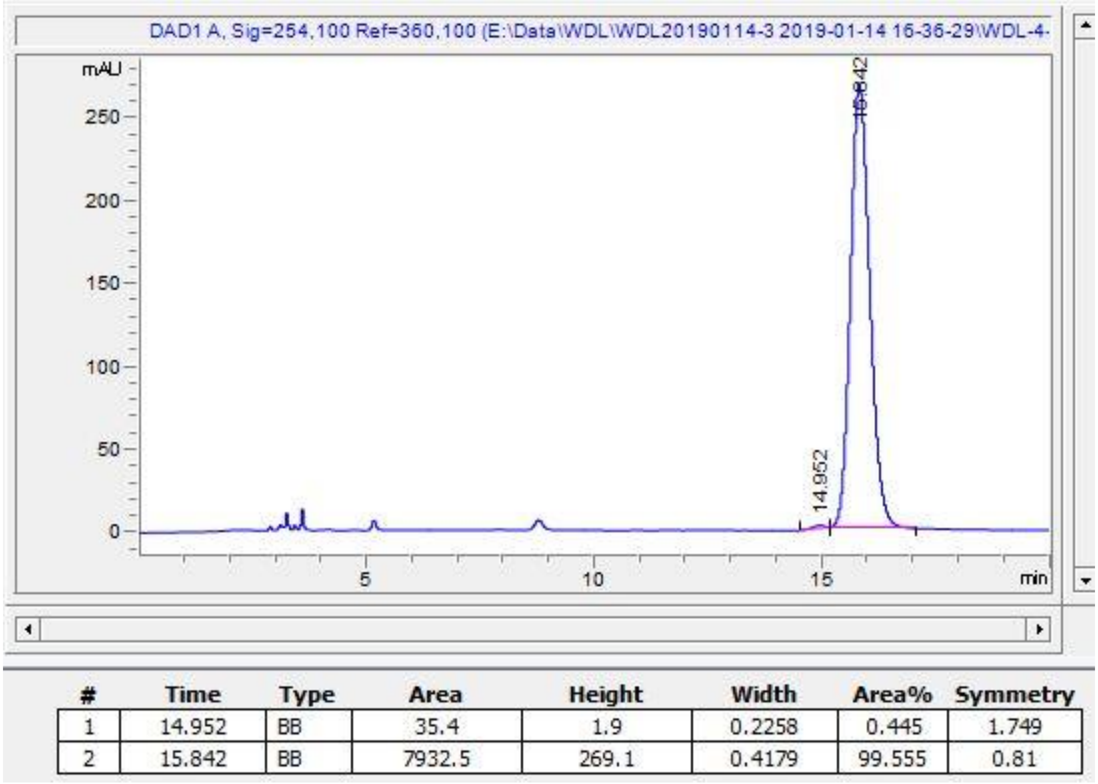

#	Time	Type	Area	Height	Width	Area%	Symmetry
1	14.952	BB	35.4	1.9	0.2258	0.445	1.749
2	15.842	BB	7932.5	269.1	0.4179	99.555	0.81

Figure S31. HPLC spectrum of racemic-**3k**, related to **Scheme 2.**

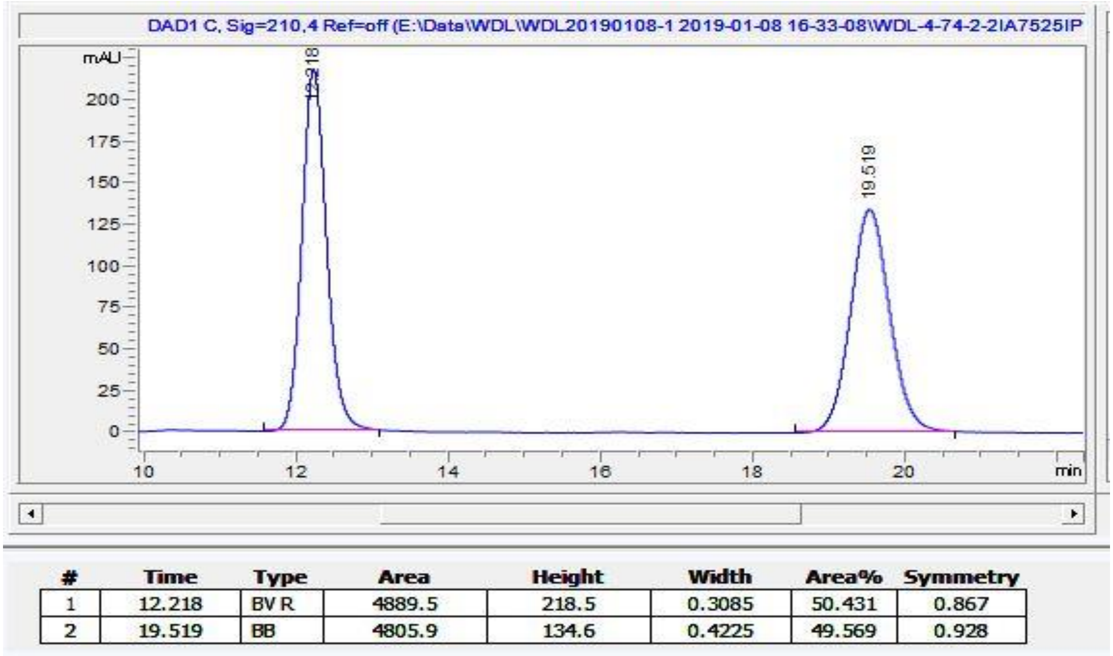

#	Time	Type	Area	Height	Width	Area%	Symmetry
1	12.218	BV R	4889.5	218.5	0.3085	50.431	0.867
2	19.519	BB	4805.9	134.6	0.4225	49.569	0.928

Figure S32. HPLC spectrum of **3k**, related to **Scheme 2.**

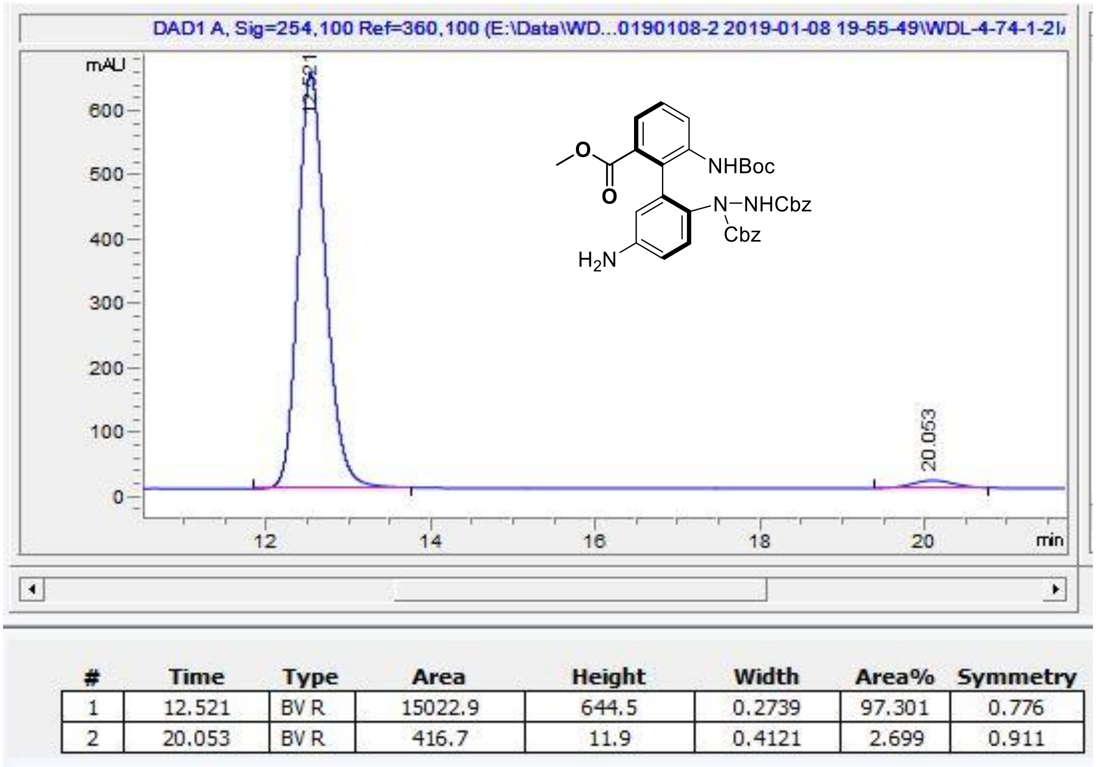

#	Time	Type	Area	Height	Width	Area%	Symmetry
1	12.521	BV R	15022.9	644.5	0.2739	97.301	0.776
2	20.053	BV R	416.7	11.9	0.4121	2.699	0.911

Figure S33. Full HPLC spectrum of **3k**, related to **Scheme 2.**

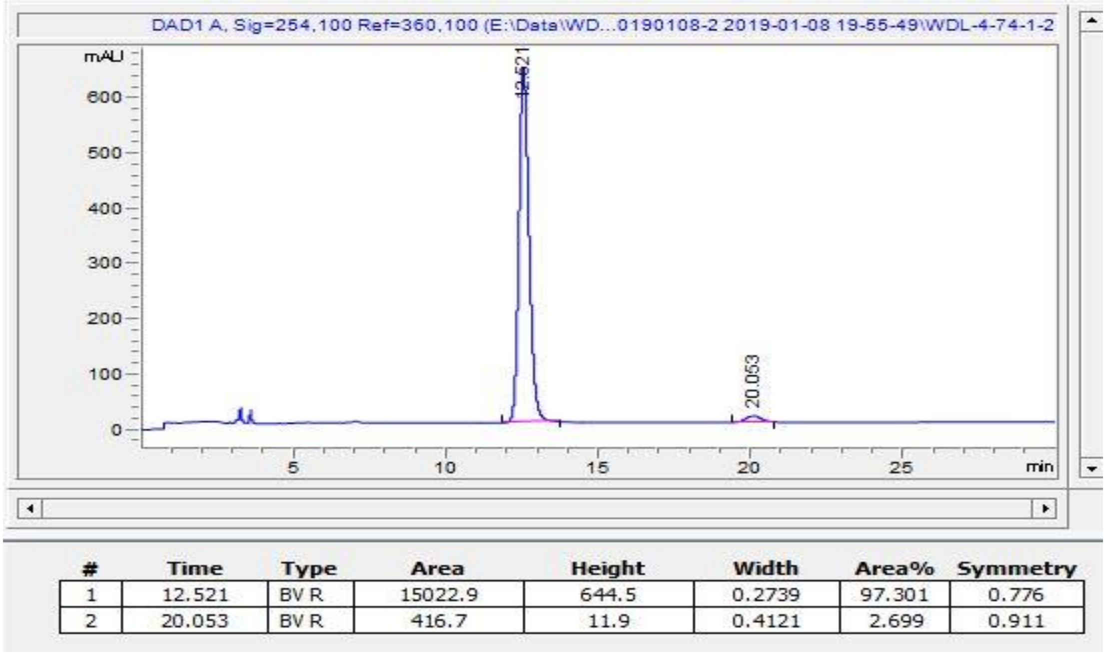

DAD1 A, Sig=254,100 Ref=360,100 (E:\Data\WD...0190108-2 2019-01-08 19-55-49\WDL-4-74-1-2

#	Time	Type	Area	Height	Width	Area%	Symmetry
1	12.521	BV R	15022.9	644.5	0.2739	97.301	0.776
2	20.053	BV R	416.7	11.9	0.4121	2.699	0.911

Figure S34. HPLC spectrum of racemic-**3l**, related to **Scheme 2.**

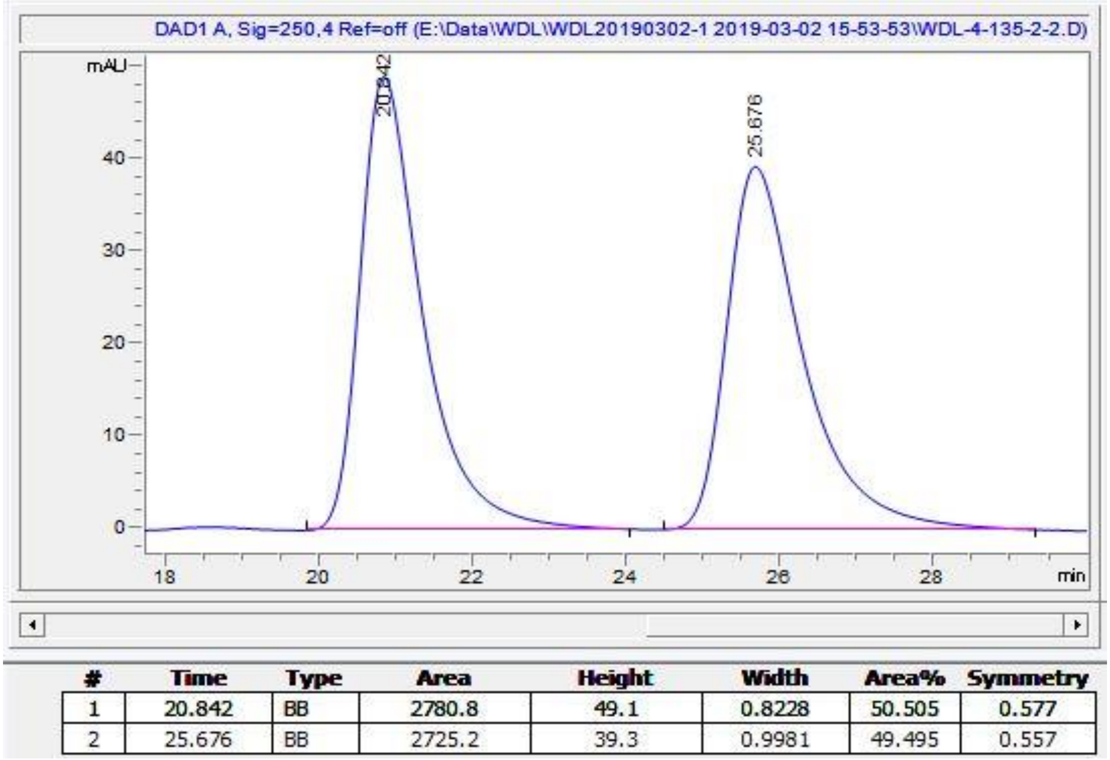

DAD1 A, Sig=250,4 Ref=off (E:\Data\WDL\WDL20190302-1 2019-03-02 15-53-53\WDL-4-135-2-2.D)

#	Time	Type	Area	Height	Width	Area%	Symmetry
1	20.842	BB	2780.8	49.1	0.8228	50.505	0.577
2	25.676	BB	2725.2	39.3	0.9981	49.495	0.557

Figure S35. HPLC spectrum of **3l**, related to **Scheme 2.**

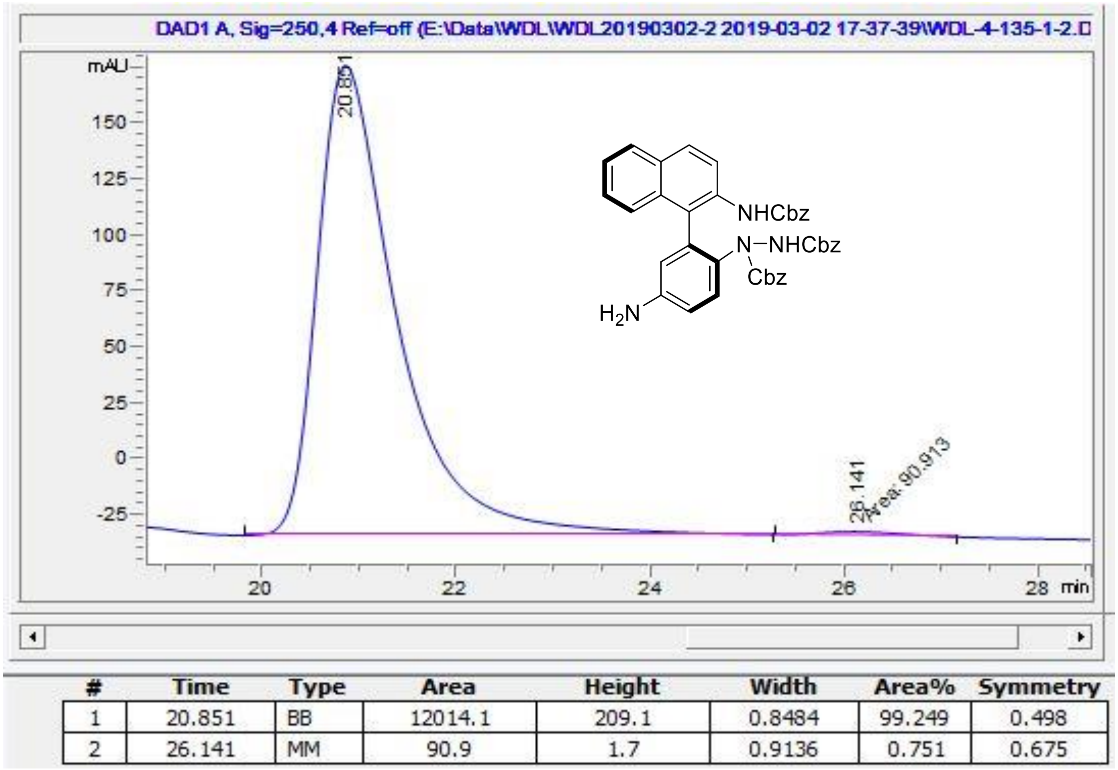

#	Time	Type	Area	Height	Width	Area%	Symmetry
1	20.851	BB	12014.1	209.1	0.8484	99.249	0.498
2	26.141	MM	90.9	1.7	0.9136	0.751	0.675

Figure S36. Full HPLC spectrum of **3b**, related to **Scheme 2.**

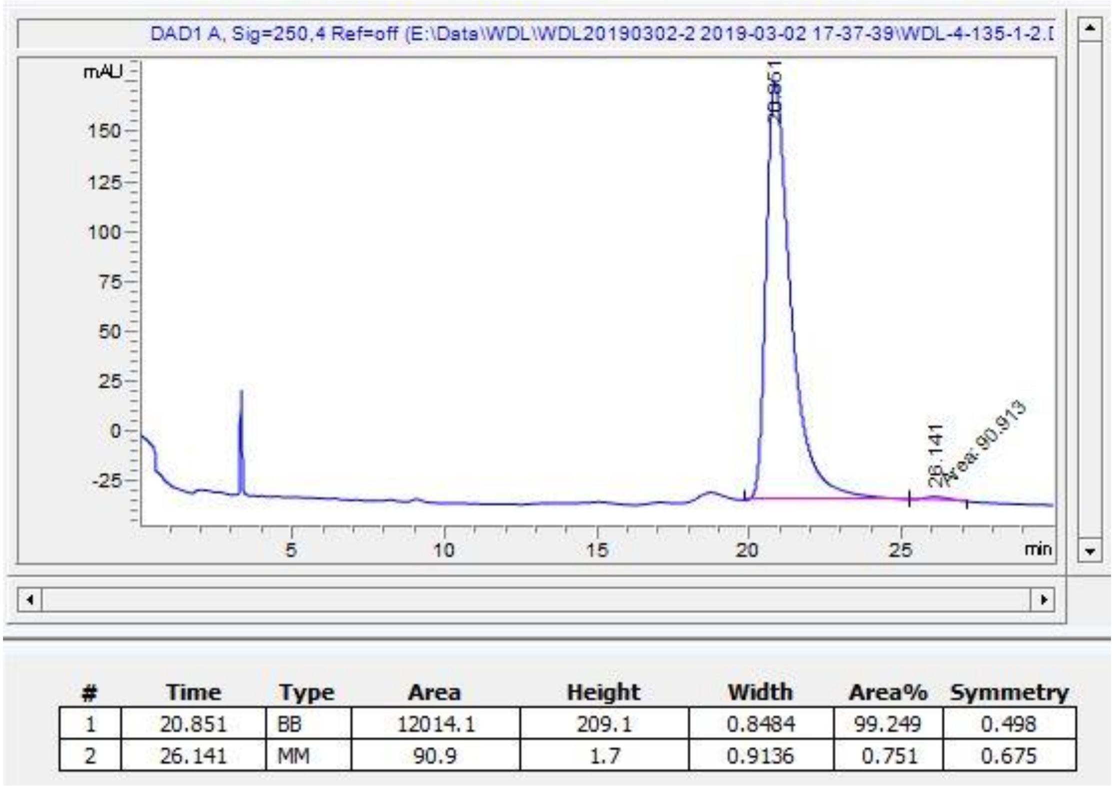

#	Time	Type	Area	Height	Width	Area%	Symmetry
1	20.851	BB	12014.1	209.1	0.8484	99.249	0.498
2	26.141	MM	90.9	1.7	0.9136	0.751	0.675

Figure S37. HPLC spectrum of racemic-**1m**, related to **Scheme 3.**.

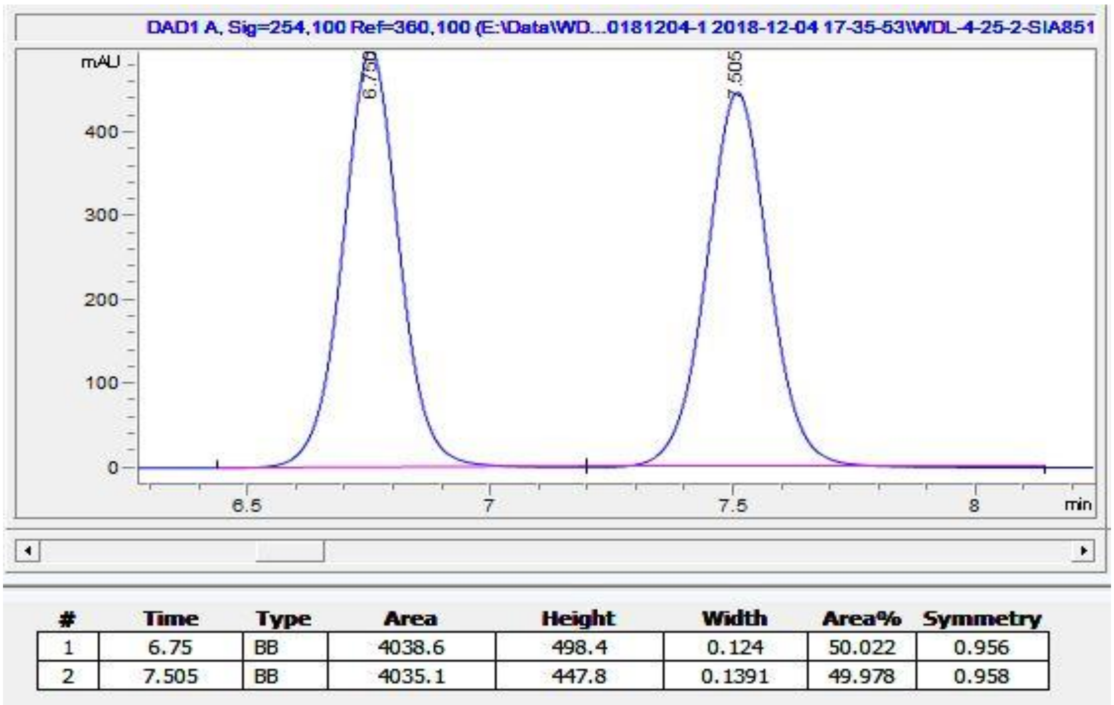

#	Time	Type	Area	Height	Width	Area%	Symmetry
1	6.75	BB	4038.6	498.4	0.124	50.022	0.956
2	7.505	BB	4035.1	447.8	0.1391	49.978	0.958

Figure S38. HPLC spectrum of (S)-**1m**, related to **Scheme 3.**

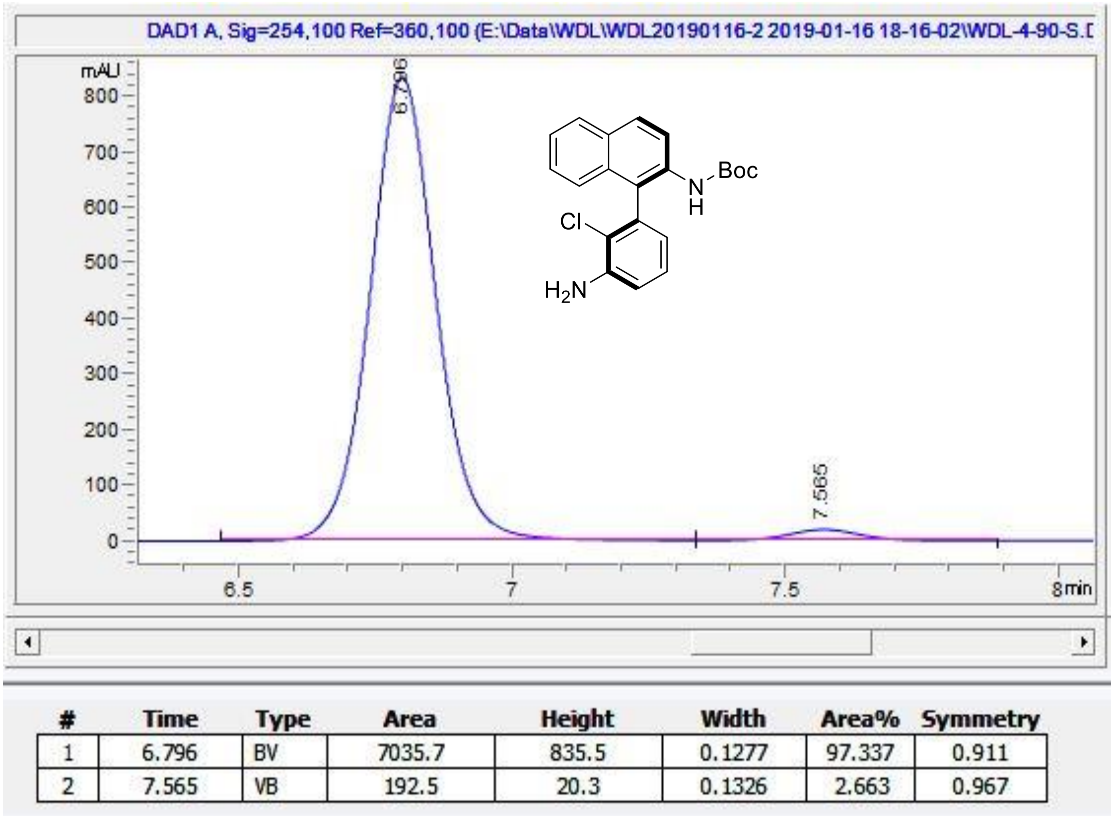

#	Time	Type	Area	Height	Width	Area%	Symmetry
1	6.796	BV	7035.7	835.5	0.1277	97.337	0.911
2	7.565	VB	192.5	20.3	0.1326	2.663	0.967

Figure S39. Full HPLC spectrum of (S)**-1m**, related to **Scheme 3.**

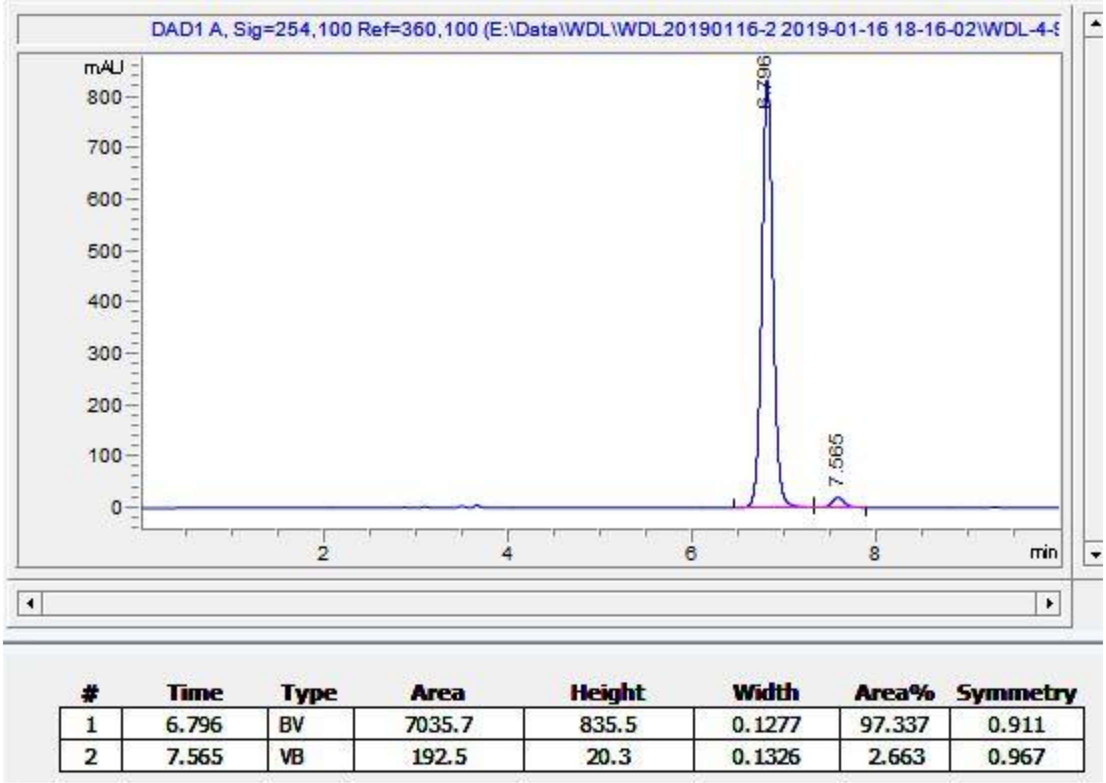
DAD1 A, Sig=254,100 Ref=360,100 (E:\Data\WDL\WDL20190116-2 2019-01-16 18-16-02\WDL-4-

#	Time	Type	Area	Height	Width	Area%	Symmetry
1	6.796	BV	7035.7	835.5	0.1277	97.337	0.911
2	7.565	VB	192.5	20.3	0.1326	2.663	0.967

Figure S40. HPLC spectrum of racemic-**3m**, related to **Scheme 3.**

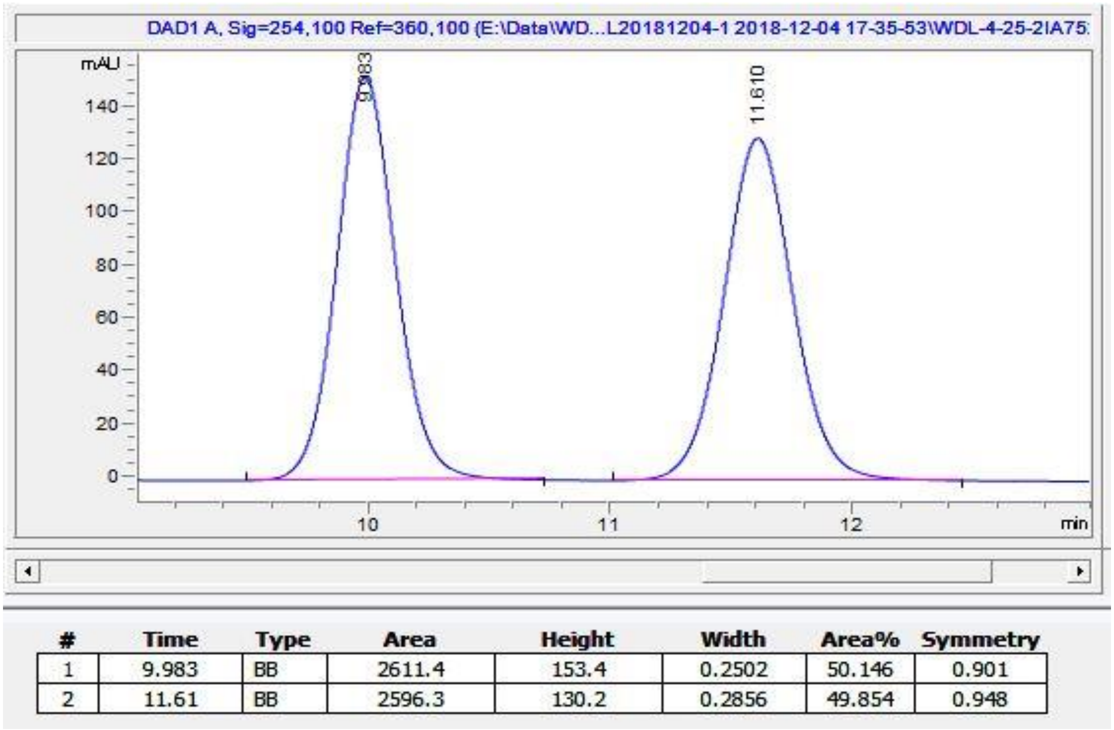
DAD1 A, Sig=254,100 Ref=360,100 (E:\Data\WD...L20181204-1 2018-12-04 17-35-53\WDL-4-25-2IA75

#	Time	Type	Area	Height	Width	Area%	Symmetry
1	9.983	BB	2611.4	153.4	0.2502	50.146	0.901
2	11.61	BB	2596.3	130.2	0.2856	49.854	0.948

Figure S41. HPLC spectrum of **3m**, related to **Scheme 3.**

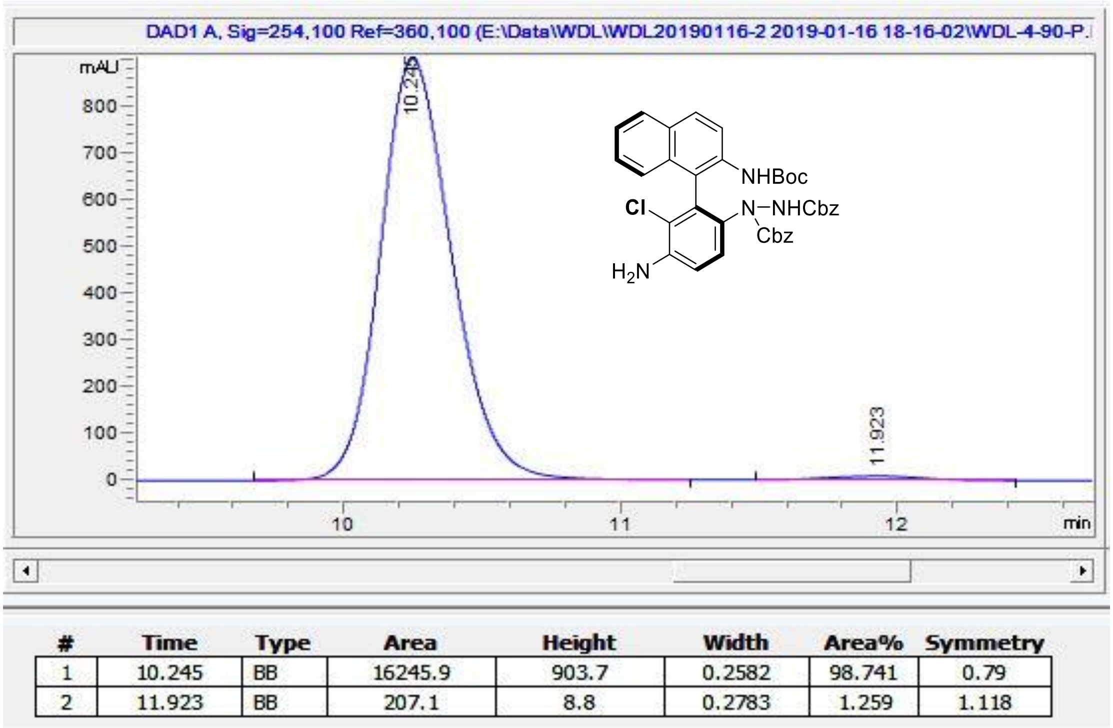
DAD1 A, Sig=254,100 Ref=360,100 (E:\Data\WDL\WDL20190116-2 2019-01-16 18-16-02\WDL-4-90-P.

#	Time	Type	Area	Height	Width	Area%	Symmetry
1	10.245	BB	16245.9	903.7	0.2582	98.741	0.79
2	11.923	BB	207.1	8.8	0.2783	1.259	1.118

Figure S42. Full HPLC spectrum of **3m**, related to **Scheme 3.**

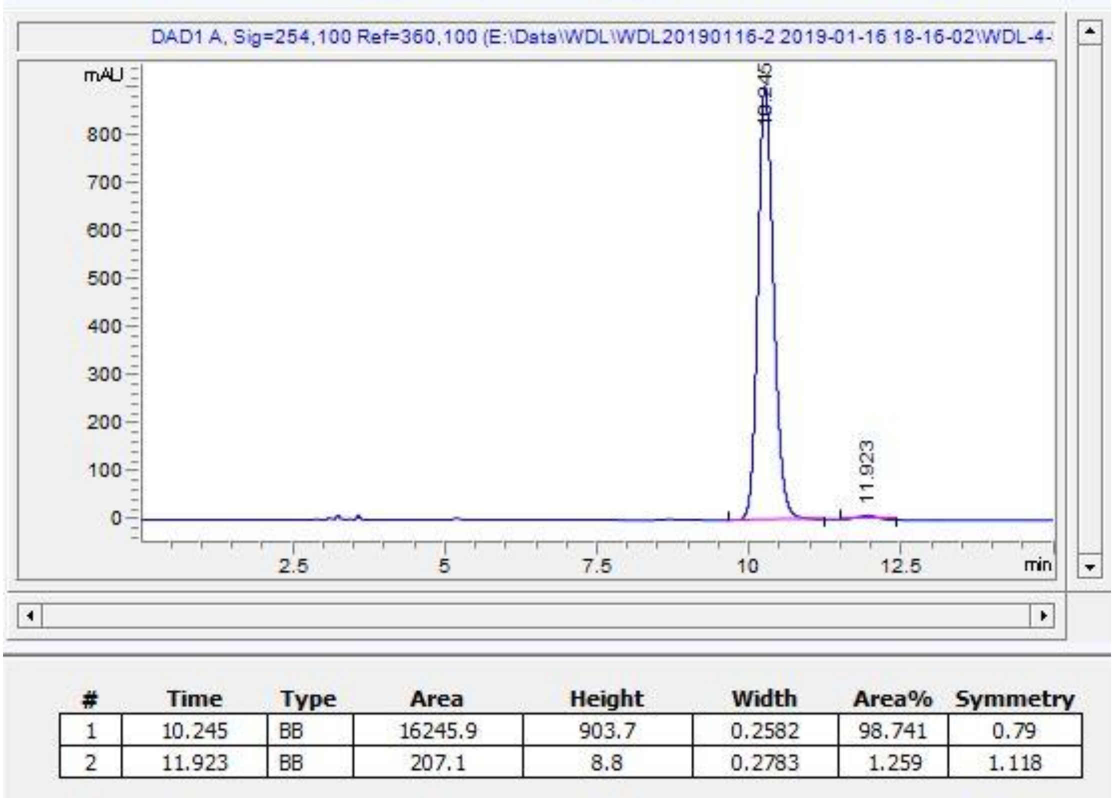
DAD1 A, Sig=254,100 Ref=360,100 (E:\Data\WDL\WDL20190116-2 2019-01-16 18-16-02\WDL-4-

#	Time	Type	Area	Height	Width	Area%	Symmetry
1	10.245	BB	16245.9	903.7	0.2582	98.741	0.79
2	11.923	BB	207.1	8.8	0.2783	1.259	1.118

Figure S43. HPLC spectrum of racemic-**1n**, related to **Scheme 3.**

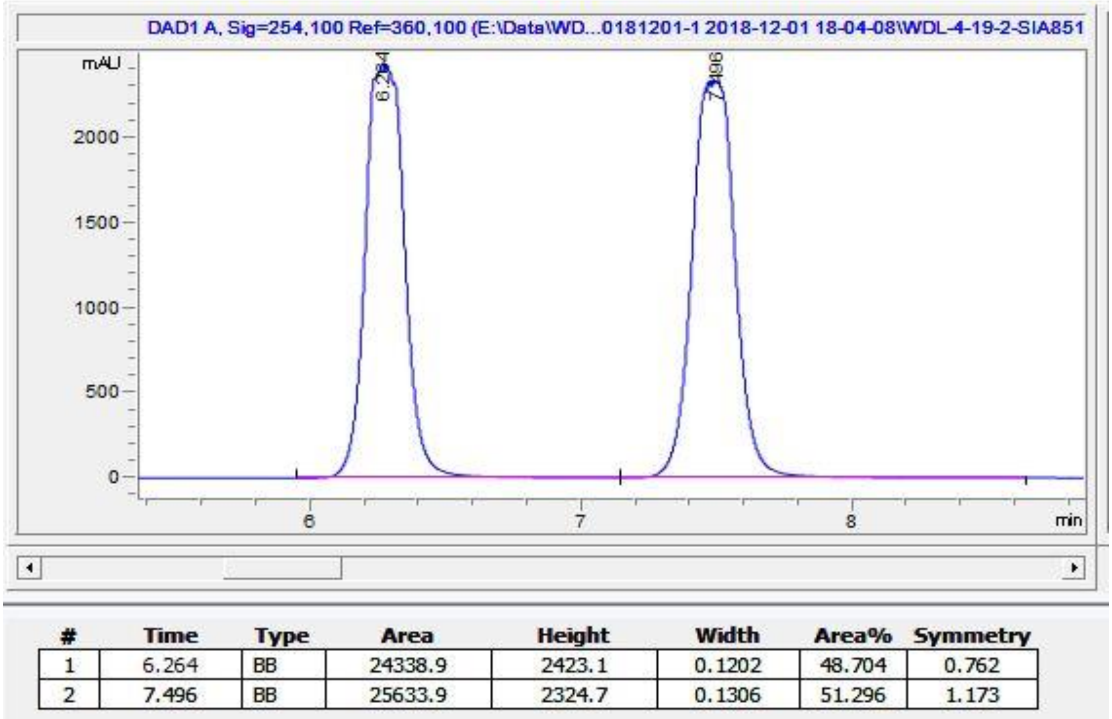

#	Time	Type	Area	Height	Width	Area%	Symmetry
1	6.264	BB	24338.9	2423.1	0.1202	48.704	0.762
2	7.496	BB	25633.9	2324.7	0.1306	51.296	1.173

Figure S44. HPLC spectrum of (S)-**1n**, related to **Scheme 3.**

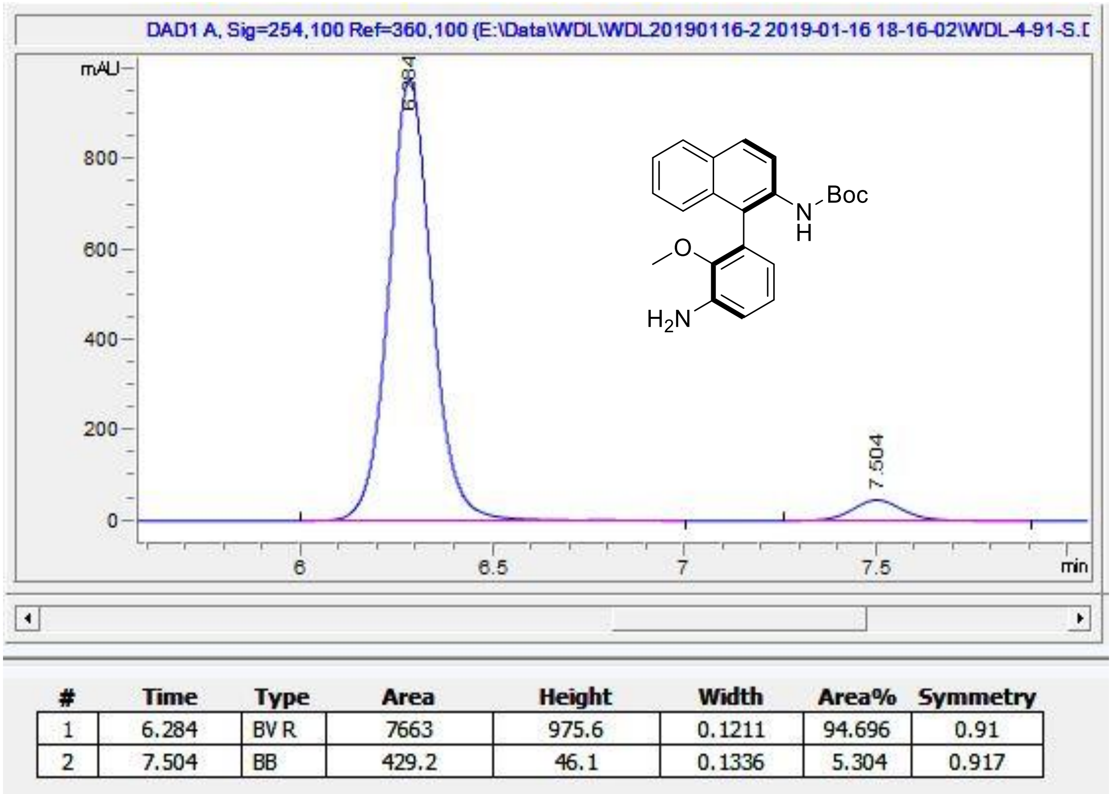

#	Time	Type	Area	Height	Width	Area%	Symmetry
1	6.284	BV R	7663	975.6	0.1211	94.696	0.91
2	7.504	BB	429.2	46.1	0.1336	5.304	0.917

Figure S45. Full HPLC spectrum of (S)-**1n**, related to **Scheme 3.**

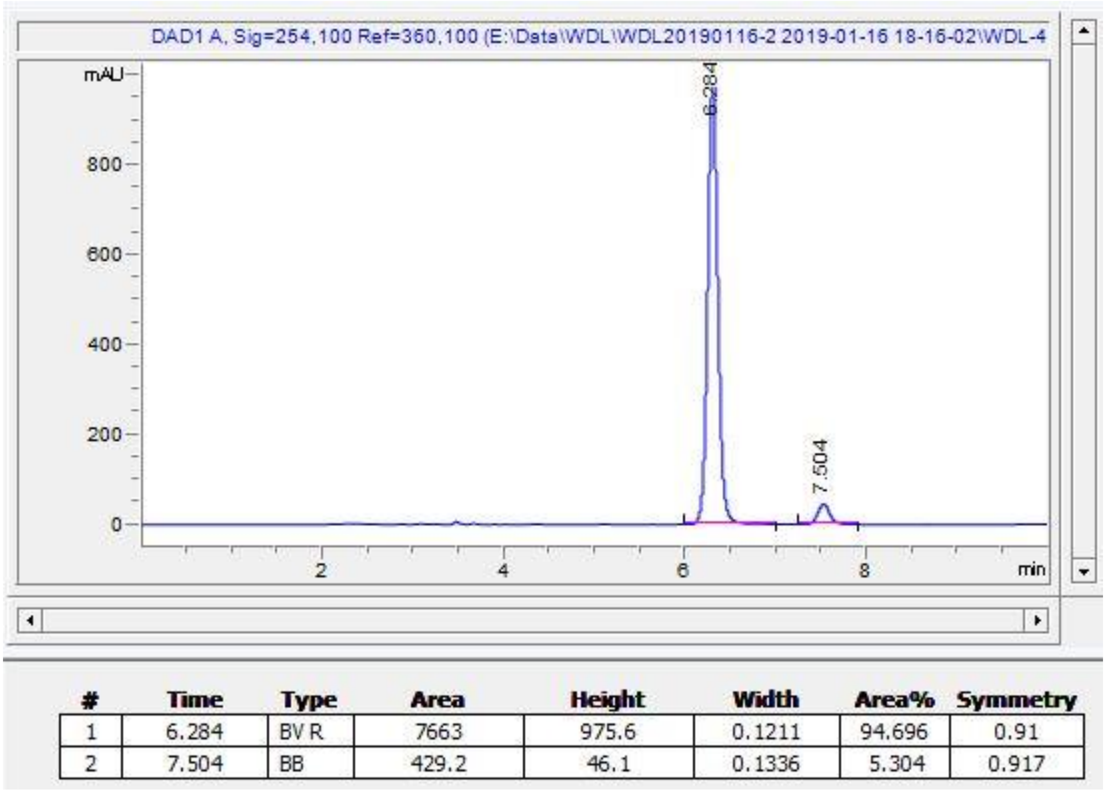

#	Time	Type	Area	Height	Width	Area%	Symmetry
1	6.284	BV R	7663	975.6	0.1211	94.696	0.91
2	7.504	BB	429.2	46.1	0.1336	5.304	0.917

Figure S46. HPLC spectrum of racemic-**3n**, related to **Scheme 3.**

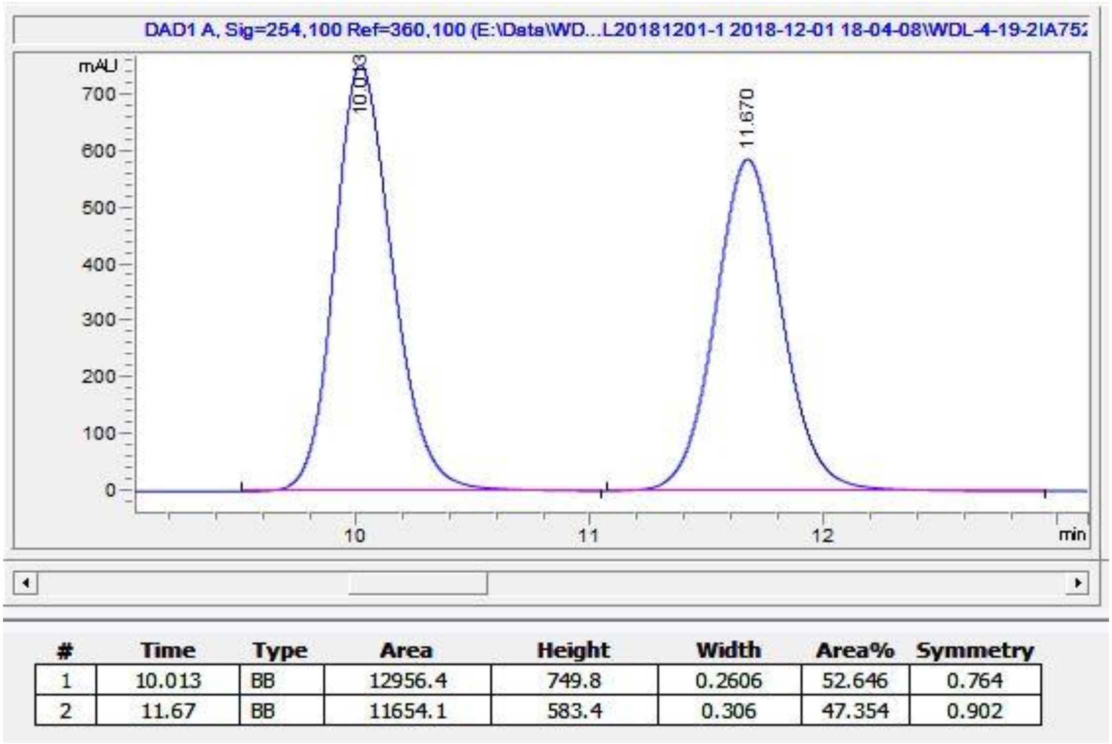

#	Time	Type	Area	Height	Width	Area%	Symmetry
1	10.013	BB	12956.4	749.8	0.2606	52.646	0.764
2	11.67	BB	11654.1	583.4	0.306	47.354	0.902

Figure S47. HPLC spectrum of **3n**, related to **Scheme 3.**

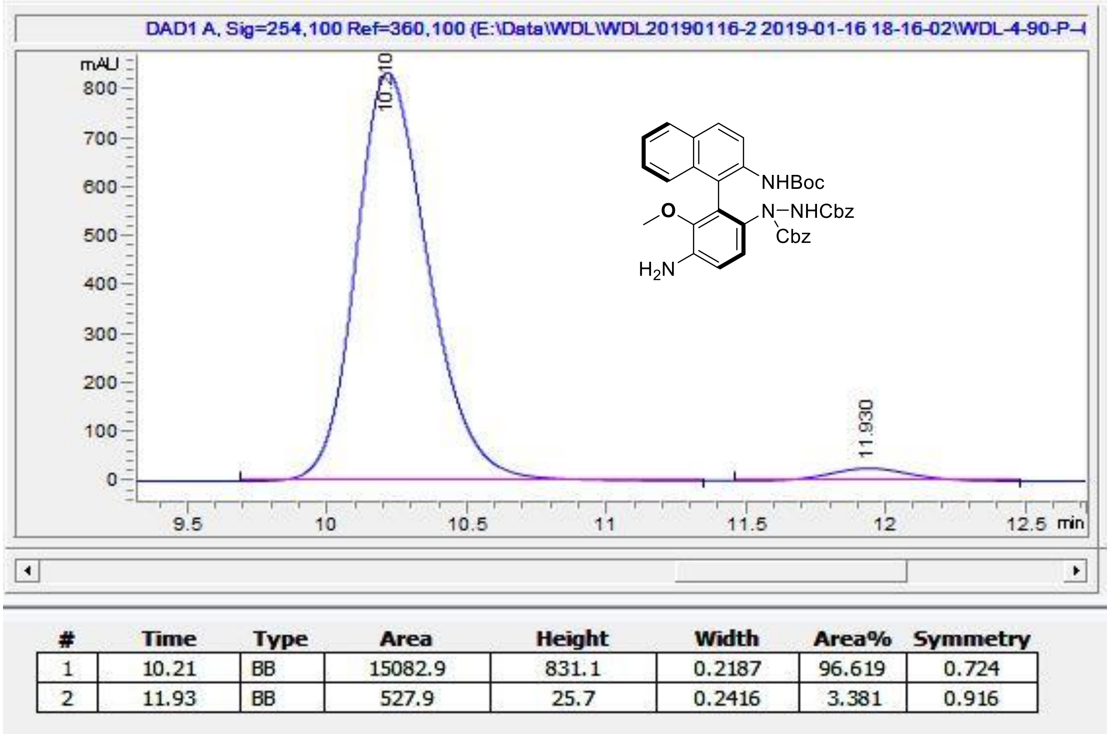

#	Time	Type	Area	Height	Width	Area%	Symmetry
1	10.21	BB	15082.9	831.1	0.2187	96.619	0.724
2	11.93	BB	527.9	25.7	0.2416	3.381	0.916

Figure S48. Full HPLC spectrum of **3n**, related to **Scheme 3.**

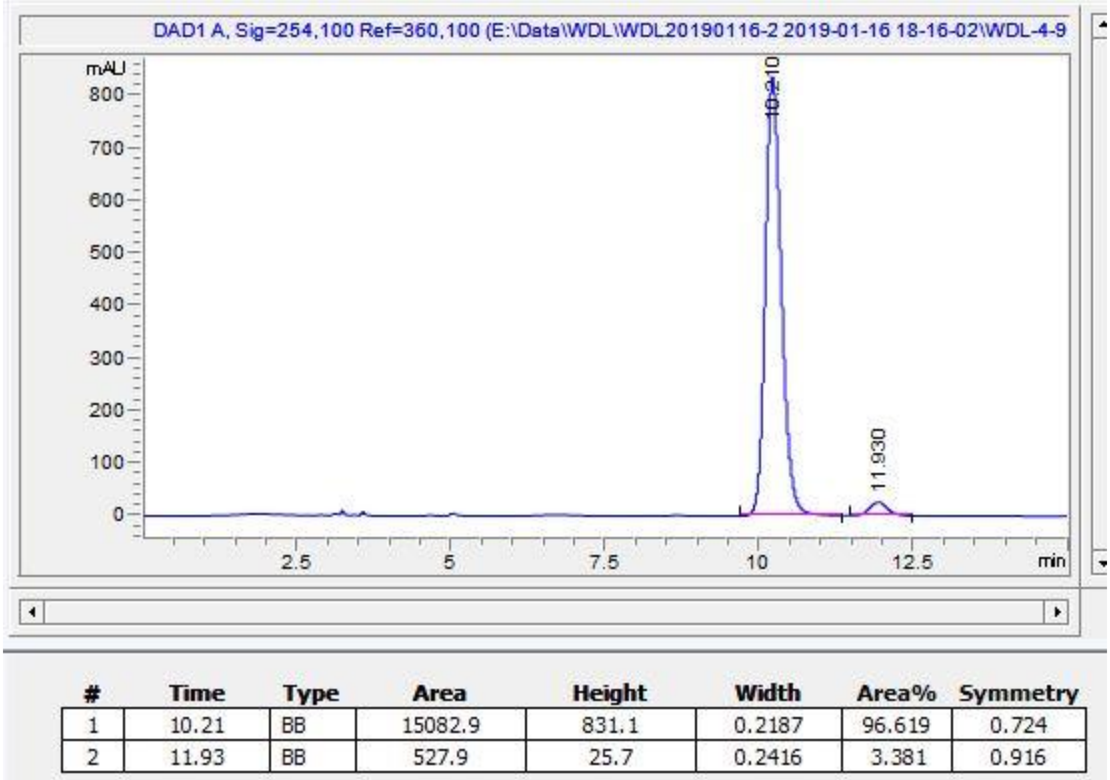

#	Time	Type	Area	Height	Width	Area%	Symmetry
1	10.21	BB	15082.9	831.1	0.2187	96.619	0.724
2	11.93	BB	527.9	25.7	0.2416	3.381	0.916

Figure S49. HPLC spectrum of racemic-**1o**, related to **Scheme 3.**

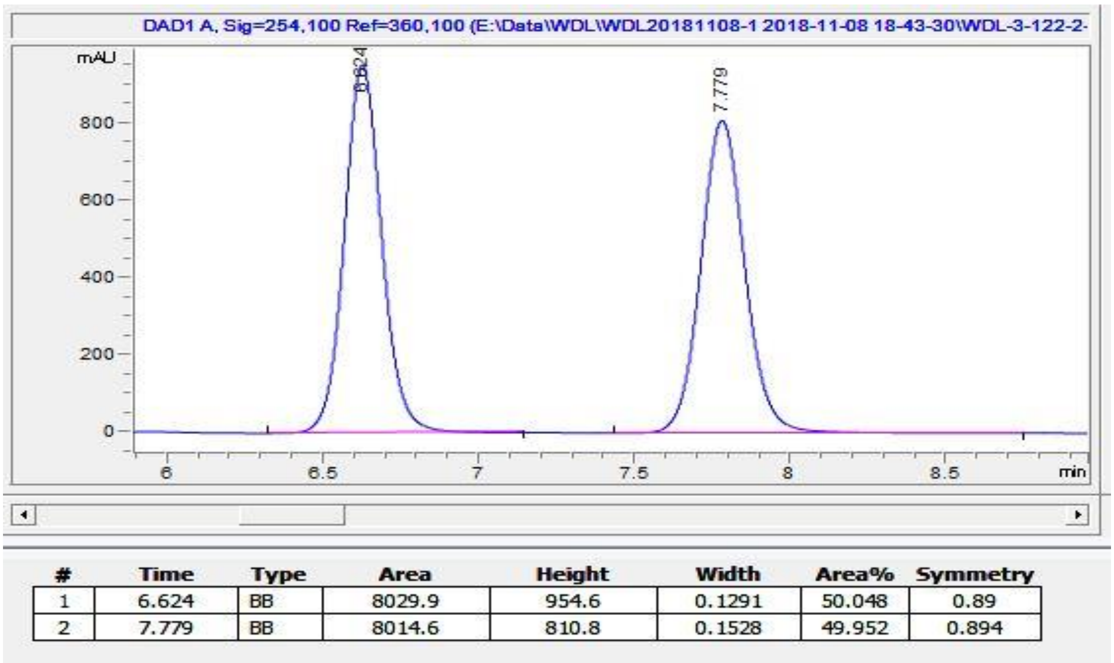

#	Time	Type	Area	Height	Width	Area%	Symmetry
1	6.624	BB	8029.9	954.6	0.1291	50.048	0.89
2	7.779	BB	8014.6	810.8	0.1528	49.952	0.894

Figure S50. HPLC spectrum of (S)-**1o**, related to **Scheme 3.**

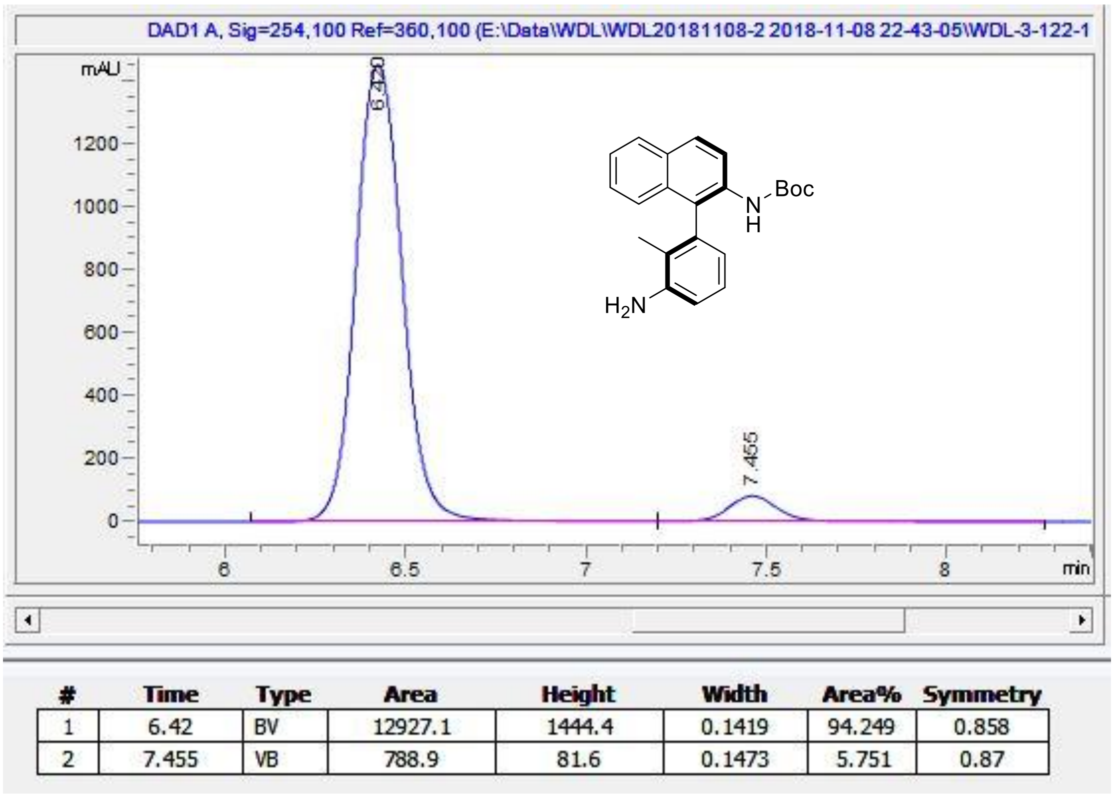

#	Time	Type	Area	Height	Width	Area%	Symmetry
1	6.42	BV	12927.1	1444.4	0.1419	94.249	0.858
2	7.455	VB	788.9	81.6	0.1473	5.751	0.87

Figure S51. Full HPLC spectrum of (S)-**1o**, related to **Scheme 3.**

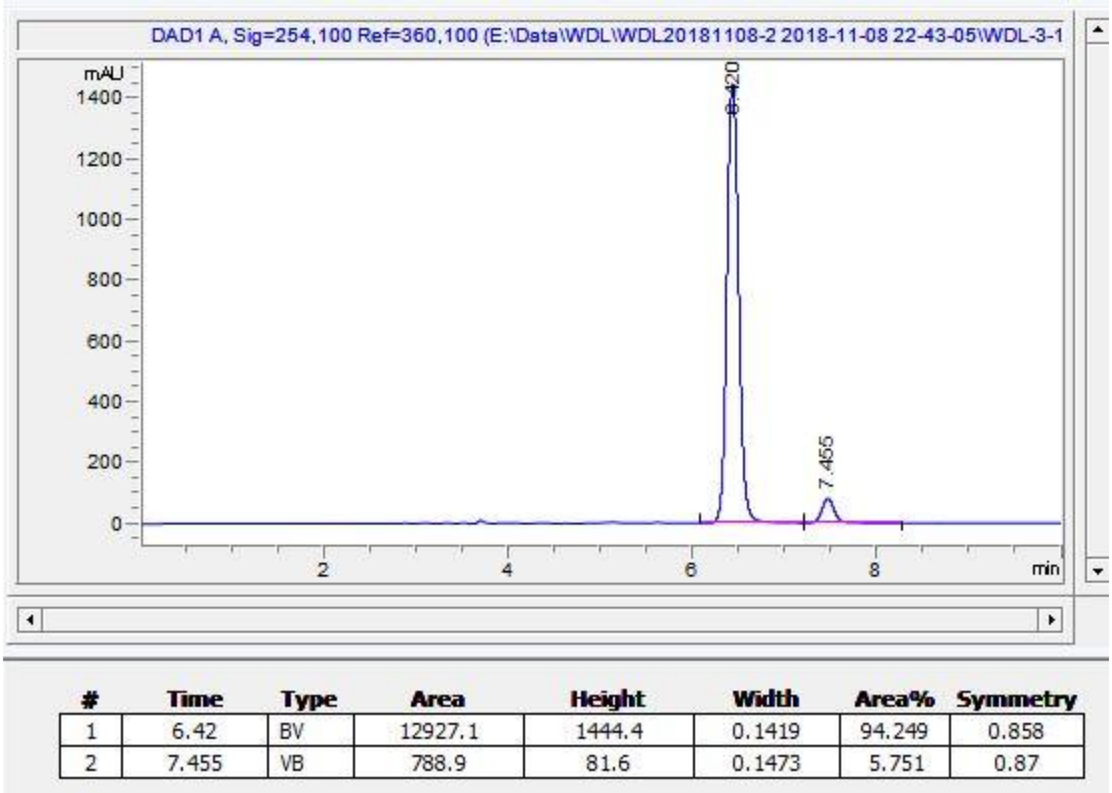

#	Time	Type	Area	Height	Width	Area%	Symmetry
1	6.42	BV	12927.1	1444.4	0.1419	94.249	0.858
2	7.455	VB	788.9	81.6	0.1473	5.751	0.87

Figure S52. HPLC spectrum of racemic-**3o**, related to **Scheme 3.**

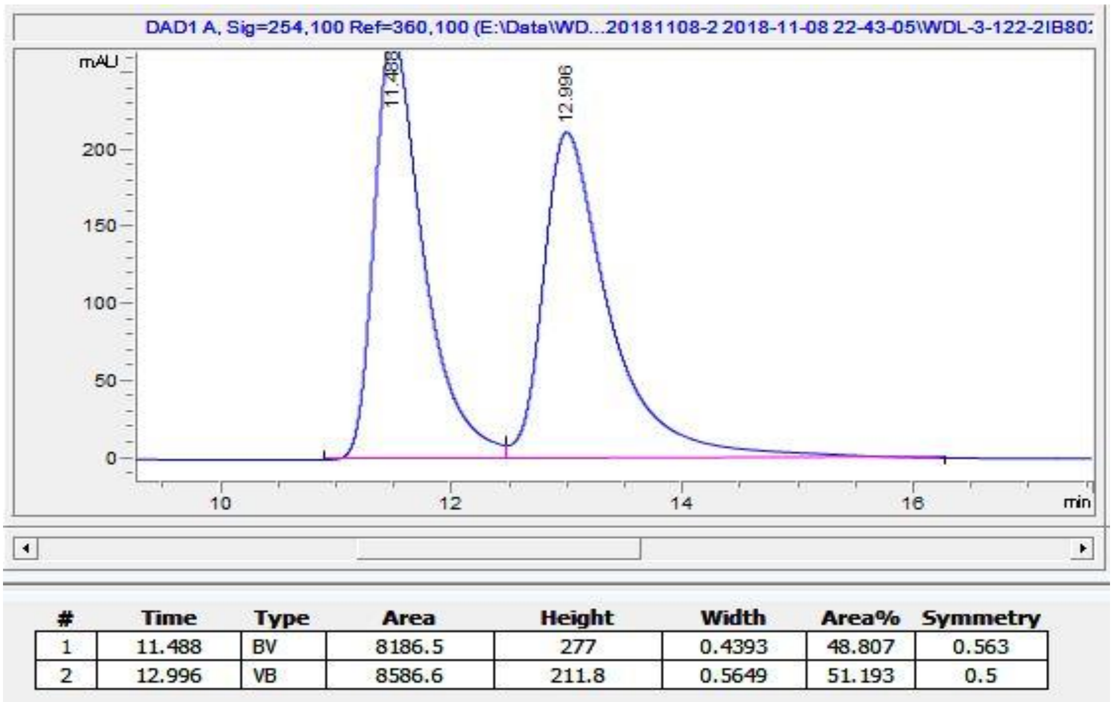

#	Time	Type	Area	Height	Width	Area%	Symmetry
1	11.488	BV	8186.5	277	0.4393	48.807	0.563
2	12.996	VB	8586.6	211.8	0.5649	51.193	0.5

Figure S53. HPLC spectrum of **3o**, related to **Scheme 3.**

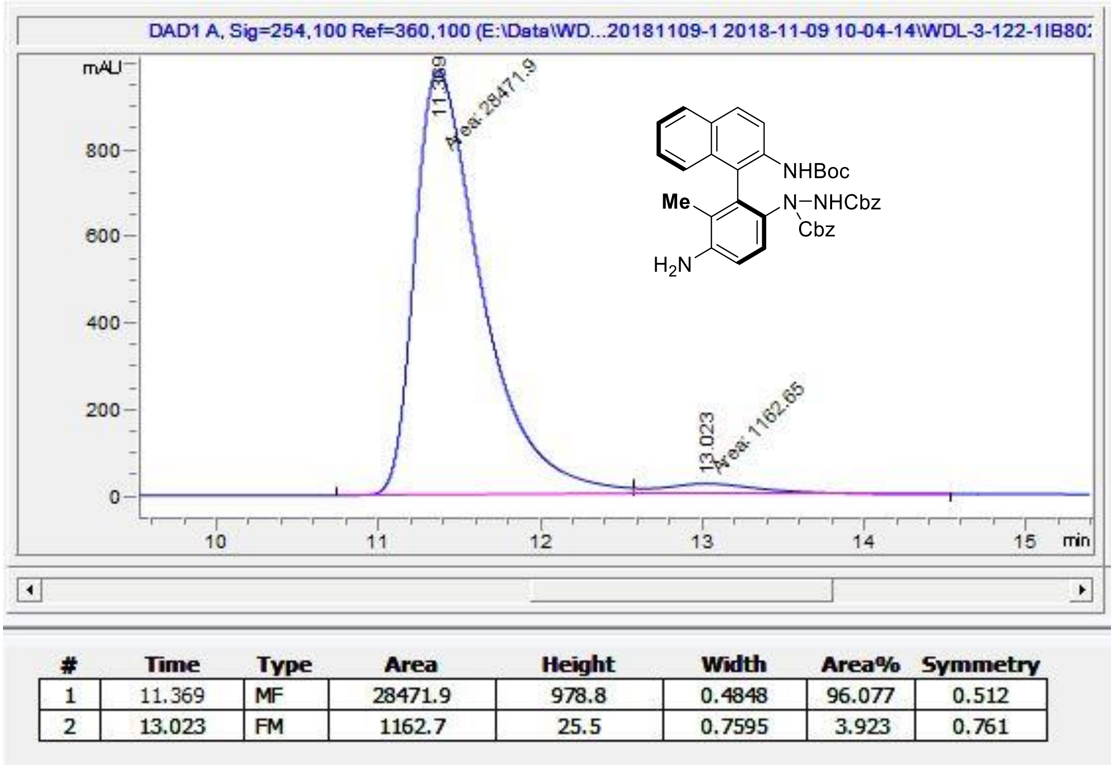

#	Time	Type	Area	Height	Width	Area%	Symmetry
1	11.369	MF	28471.9	978.8	0.4848	96.077	0.512
2	13.023	FM	1162.7	25.5	0.7595	3.923	0.761

Figure S54. Full HPLC spectrum of **3o**, related to **Scheme 3.**

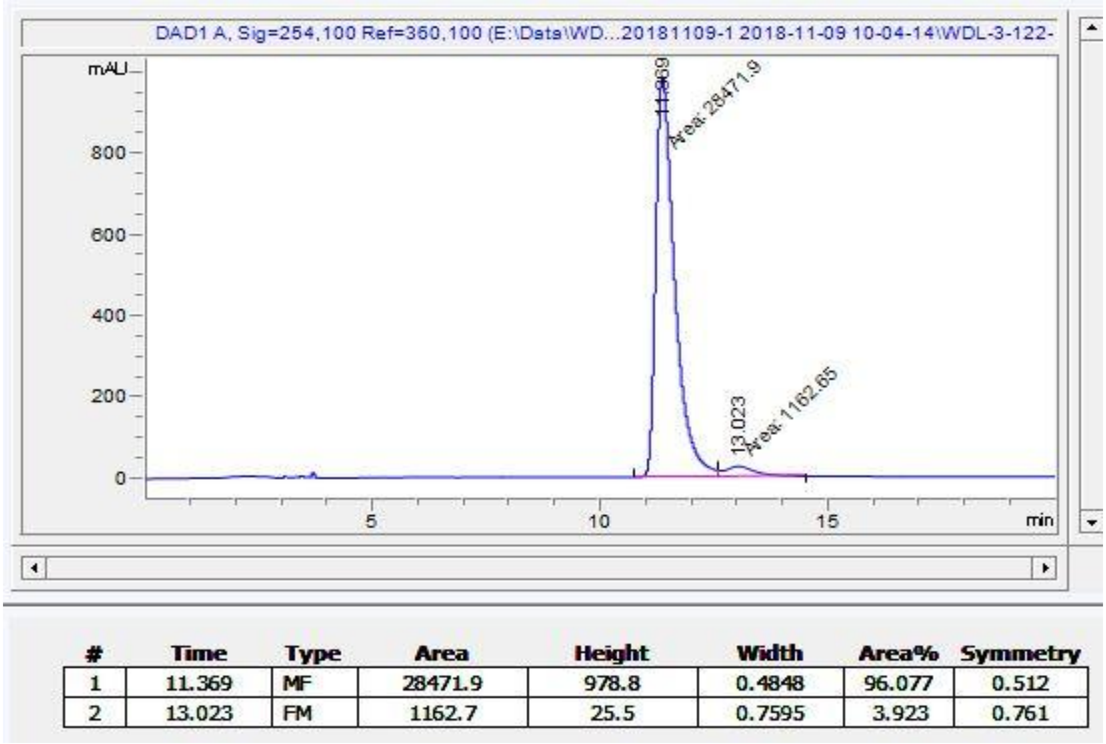

#	Time	Type	Area	Height	Width	Area%	Symmetry
1	11.369	MF	28471.9	978.8	0.4848	96.077	0.512
2	13.023	FM	1162.7	25.5	0.7595	3.923	0.761

Figure S55. HPLC spectrum of racemic-**1p**, related to **Scheme 3.**

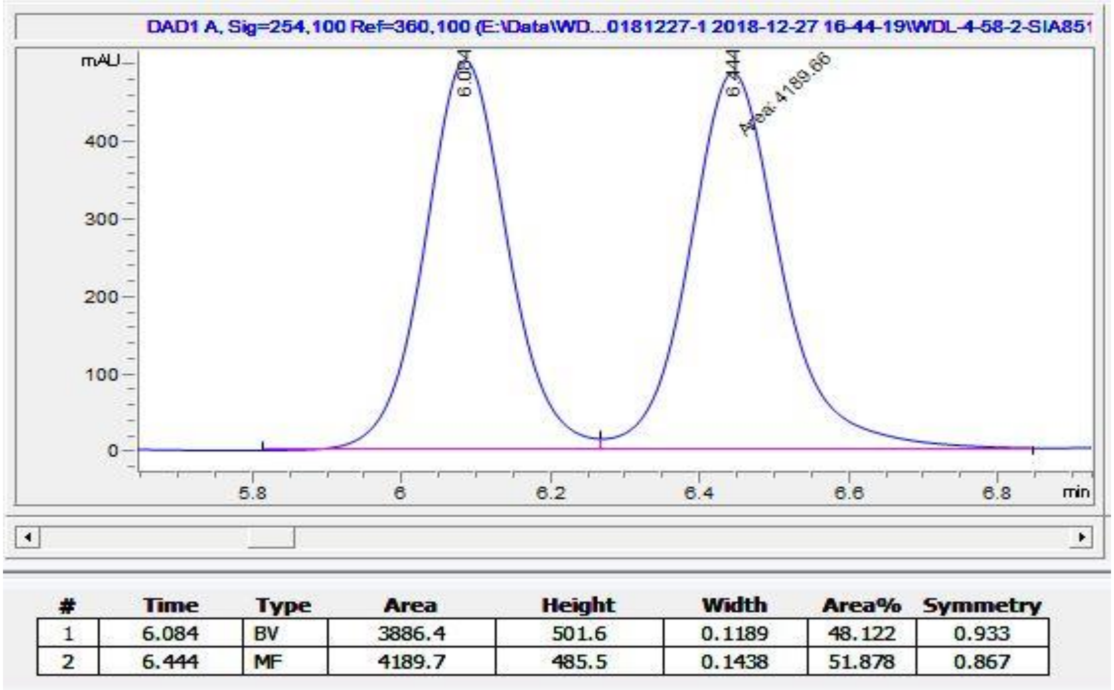

#	Time	Type	Area	Height	Width	Area%	Symmetry
1	6.084	BV	3886.4	501.6	0.1189	48.122	0.933
2	6.444	MF	4189.7	485.5	0.1438	51.878	0.867

Figure S56. HPLC spectrum of (S)-**1p**, related to **Scheme 3.**

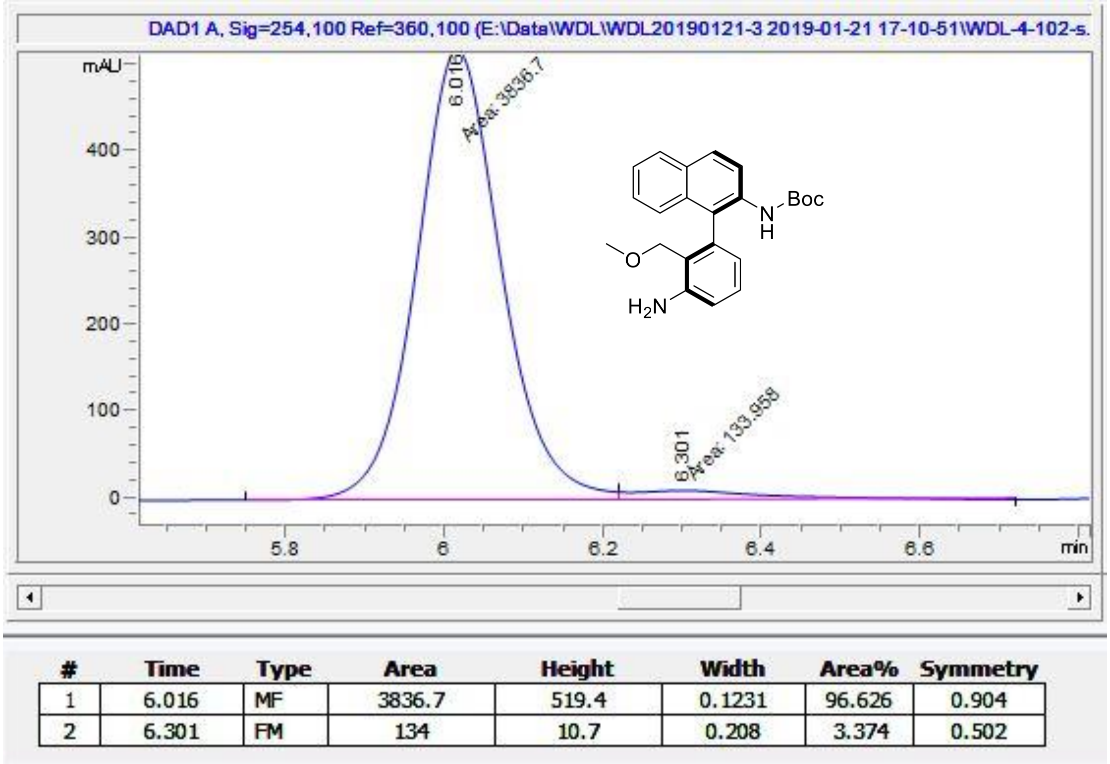

#	Time	Type	Area	Height	Width	Area%	Symmetry
1	6.016	MF	3836.7	519.4	0.1231	96.626	0.904
2	6.301	FM	134	10.7	0.208	3.374	0.502

Figure S57. Full HPLC spectrum of (S)-**1p**, related to **Scheme 3.**

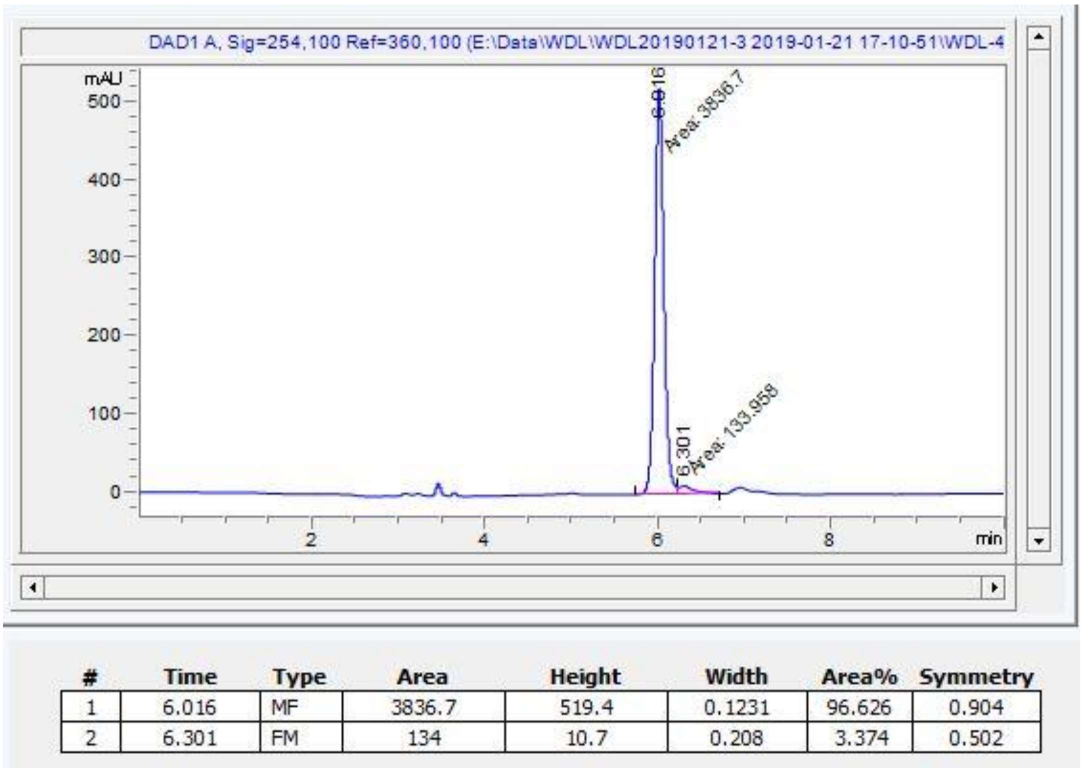

#	Time	Type	Area	Height	Width	Area%	Symmetry
1	6.016	MF	3836.7	519.4	0.1231	96.626	0.904
2	6.301	FM	134	10.7	0.208	3.374	0.502

Figure S58. HPLC spectrum of racemic-**3p**, related to **Scheme 3.**

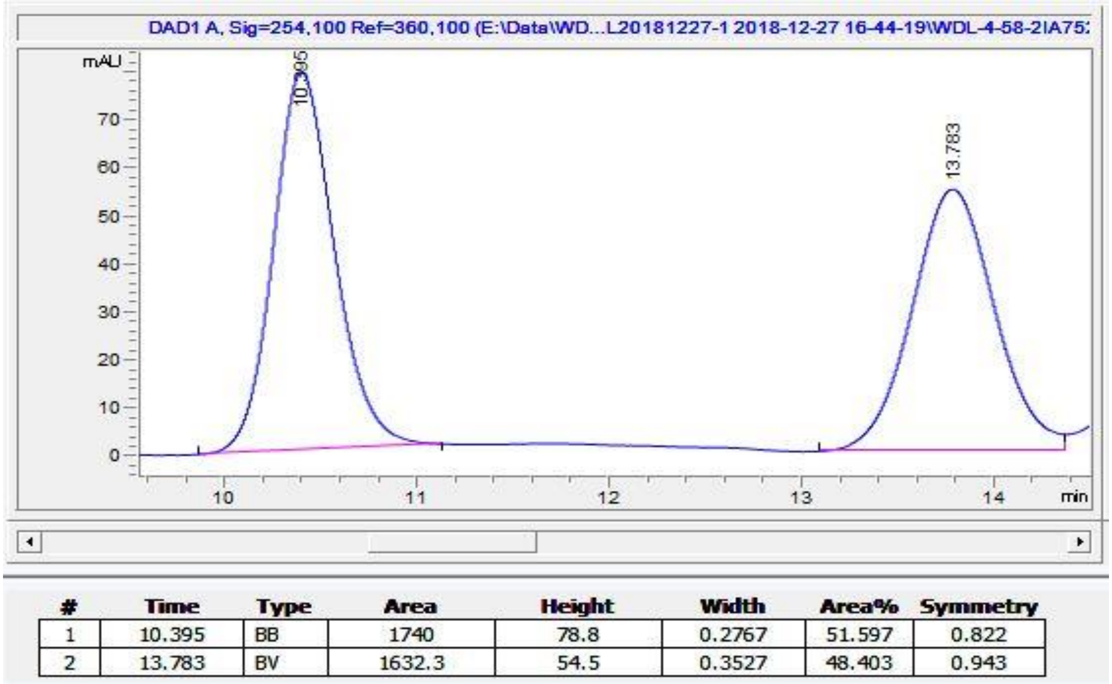

#	Time	Type	Area	Height	Width	Area%	Symmetry
1	10.395	BB	1740	78.8	0.2767	51.597	0.822
2	13.783	BV	1632.3	54.5	0.3527	48.403	0.943

Figure S59. HPLC spectrum of **3p**, related to **Scheme 3.**

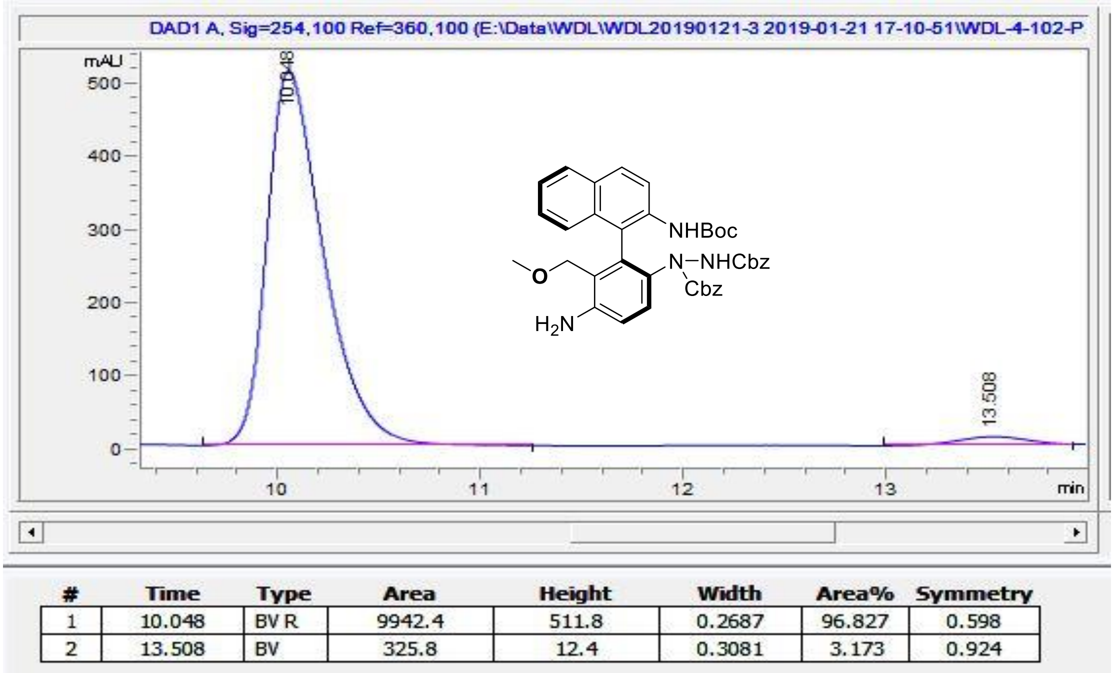

DAD1 A, Sig=254,100 Ref=360,100 (E:\Data\WDL\WDL20190121-3 2019-01-21 17-10-51\WDL-4-102-P

#	Time	Type	Area	Height	Width	Area%	Symmetry
1	10.048	BV R	9942.4	511.8	0.2687	96.827	0.598
2	13.508	BV	325.8	12.4	0.3081	3.173	0.924

Figure S60. Full HPLC spectrum of racemic-**3p**, related to **Scheme 3.**

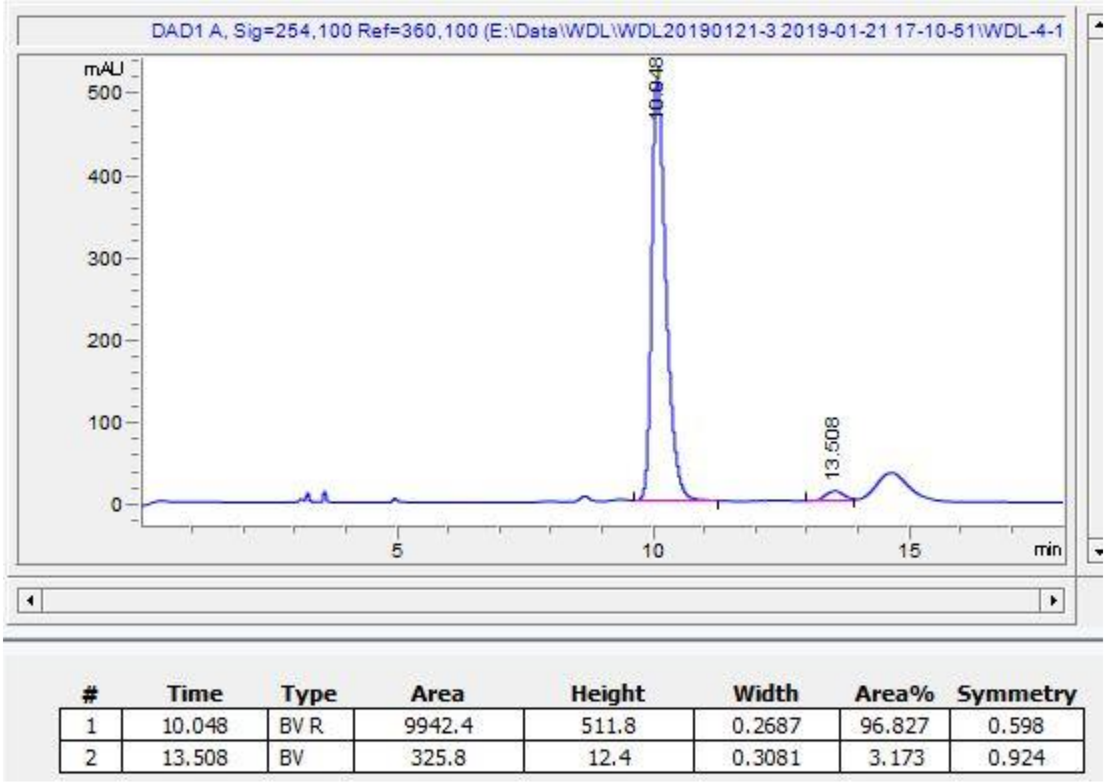

DAD1 A, Sig=254,100 Ref=360,100 (E:\Data\WDL\WDL20190121-3 2019-01-21 17-10-51\WDL-4-1

#	Time	Type	Area	Height	Width	Area%	Symmetry
1	10.048	BV R	9942.4	511.8	0.2687	96.827	0.598
2	13.508	BV	325.8	12.4	0.3081	3.173	0.924

Figure S61. HPLC spectrum of racemic-**7a**, related to **Scheme 4**

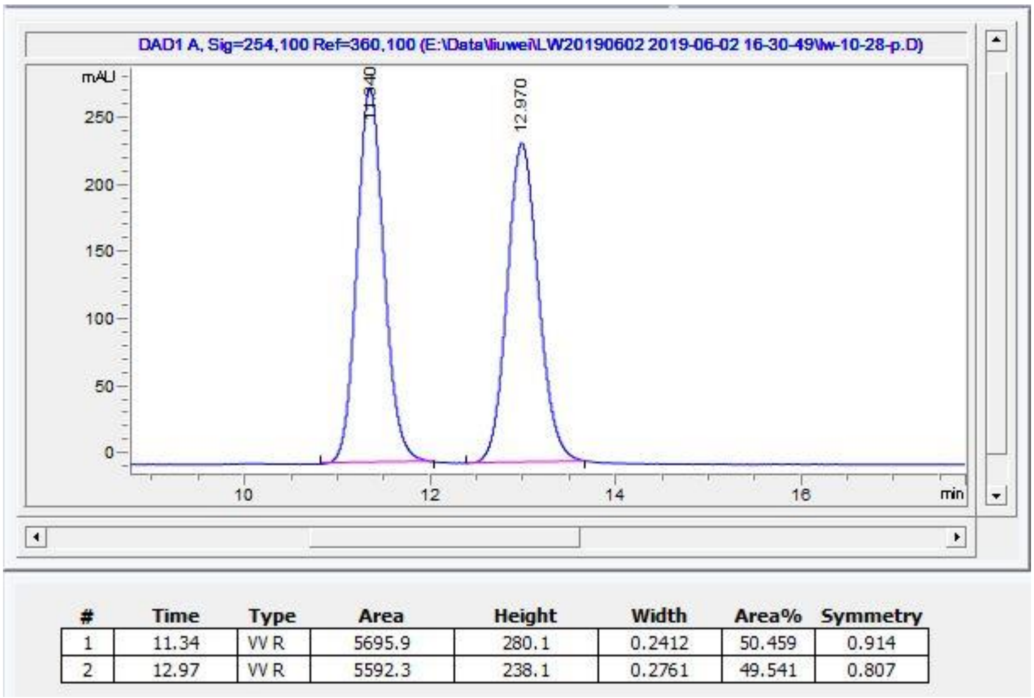

#	Time	Type	Area	Height	Width	Area%	Symmetry
1	11.34	VV R	5695.9	280.1	0.2412	50.459	0.914
2	12.97	VV R	5592.3	238.1	0.2761	49.541	0.807

Figure S62. HPLC spectrum of **7a**, related to **Scheme 4**

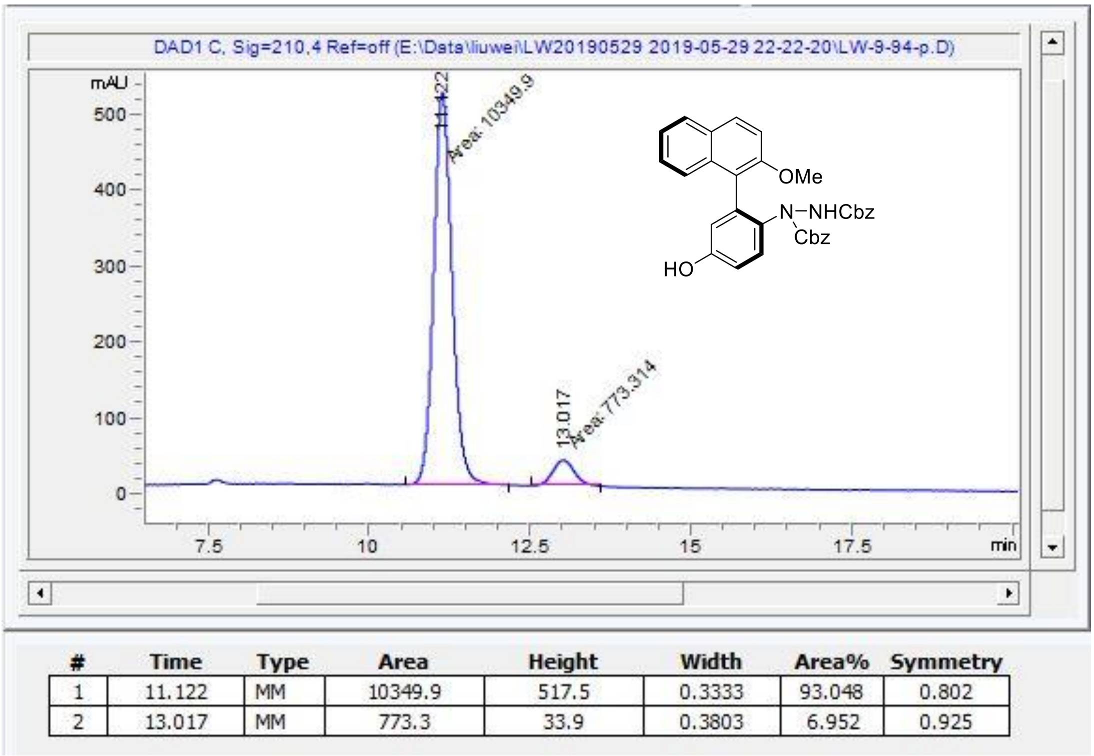

#	Time	Type	Area	Height	Width	Area%	Symmetry
1	11.122	MM	10349.9	517.5	0.3333	93.048	0.802
2	13.017	MM	773.3	33.9	0.3803	6.952	0.925

Figure S63. Full HPLC spectrum of racemic-**7a**, related to **Scheme 4**

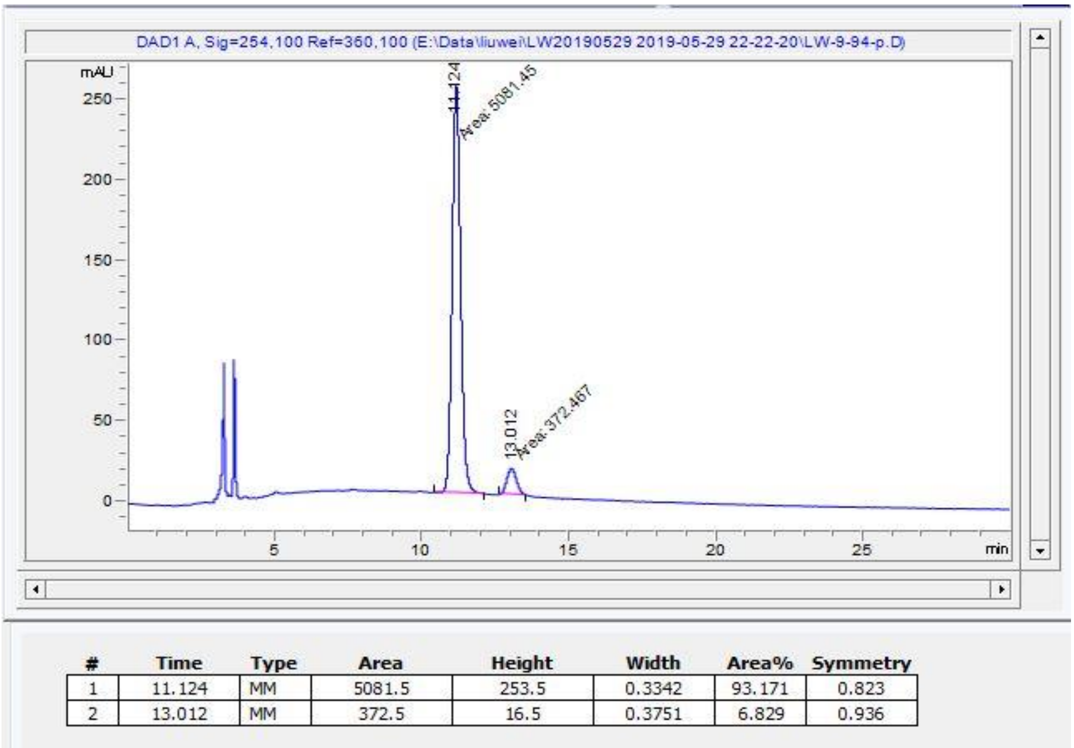

#	Time	Type	Area	Height	Width	Area%	Symmetry
1	11.124	MM	5081.5	253.5	0.3342	93.171	0.823
2	13.012	MM	372.5	16.5	0.3751	6.829	0.936

Figure S64. HPLC spectrum of racemic-**7b**, related to **Scheme 4**

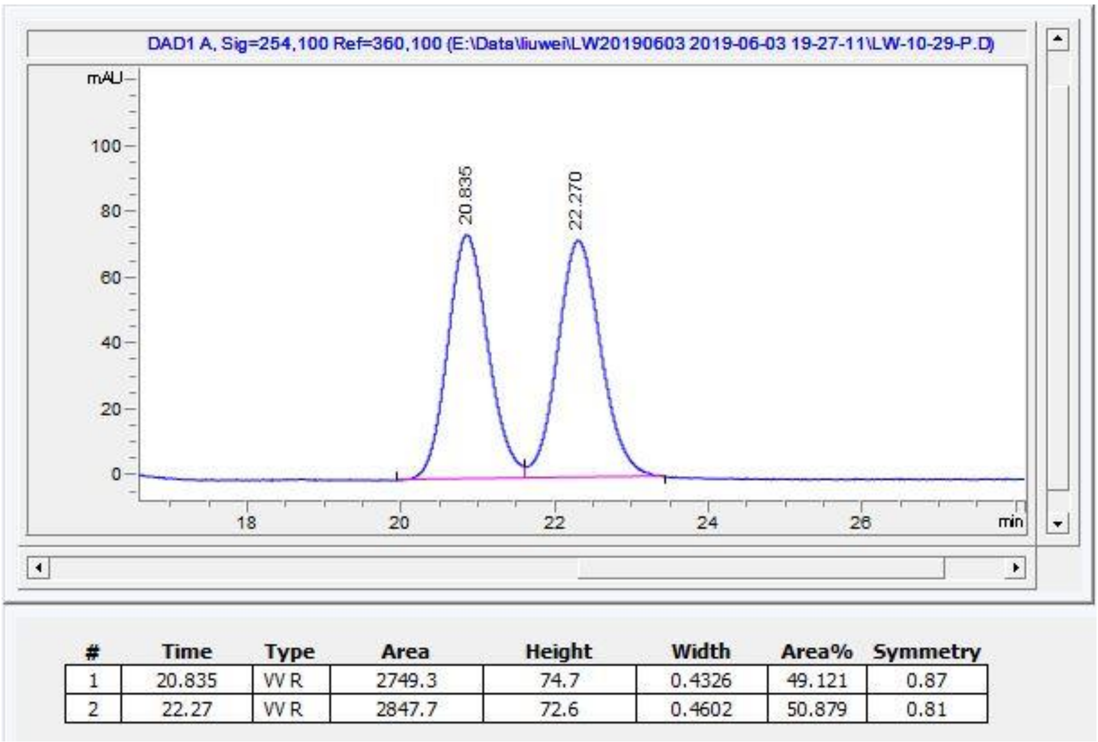

#	Time	Type	Area	Height	Width	Area%	Symmetry
1	20.835	VV R	2749.3	74.7	0.4326	49.121	0.87
2	22.27	VV R	2847.7	72.6	0.4602	50.879	0.81

Figure S65. HPLC spectrum of **7b**, related to **Scheme 4**

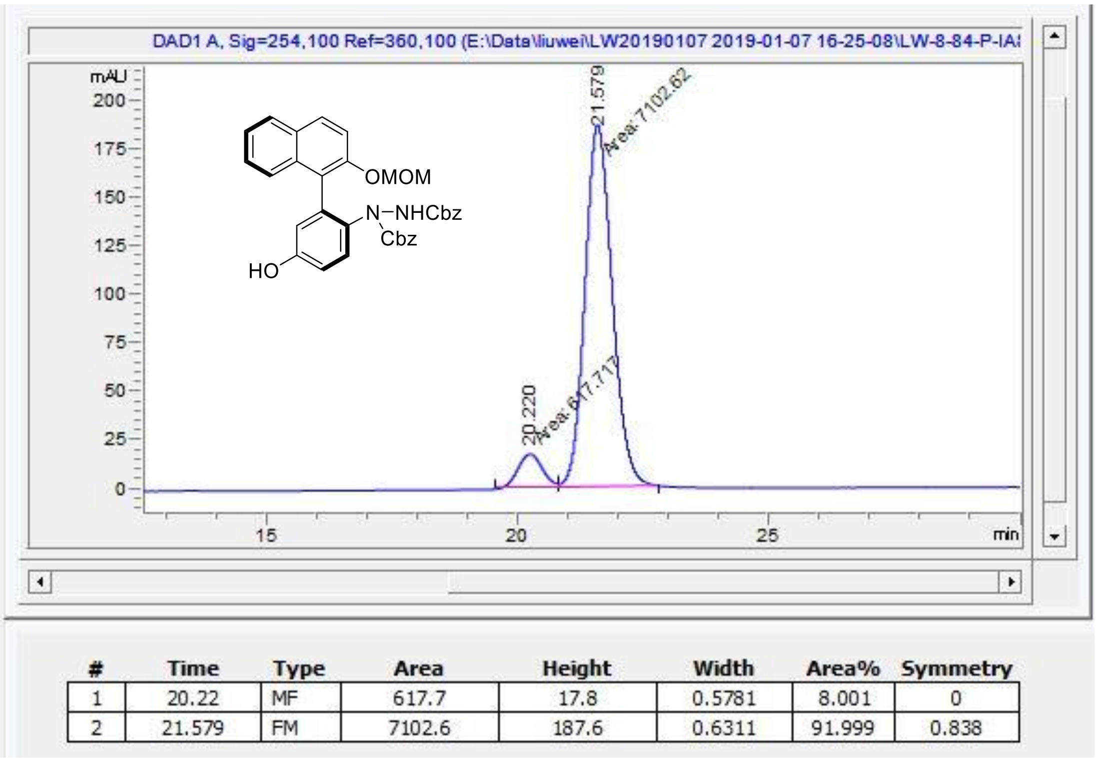

#	Time	Type	Area	Height	Width	Area%	Symmetry
1	20.22	MF	617.7	17.8	0.5781	8.001	0
2	21.579	FM	7102.6	187.6	0.6311	91.999	0.838

Figure S66. Full HPLC spectrum of **7b**, related to **Scheme 4**

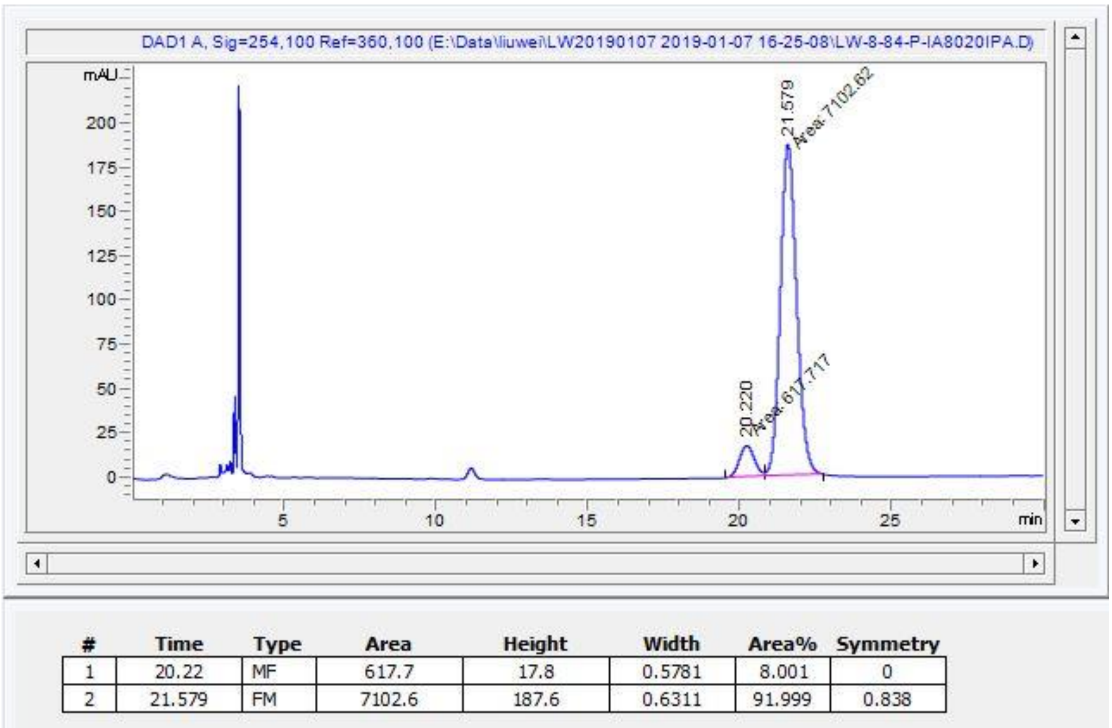

#	Time	Type	Area	Height	Width	Area%	Symmetry
1	20.22	MF	617.7	17.8	0.5781	8.001	0
2	21.579	FM	7102.6	187.6	0.6311	91.999	0.838

Figure S67. HPLC spectrum of racemic-**7c**, related to **Scheme 4**

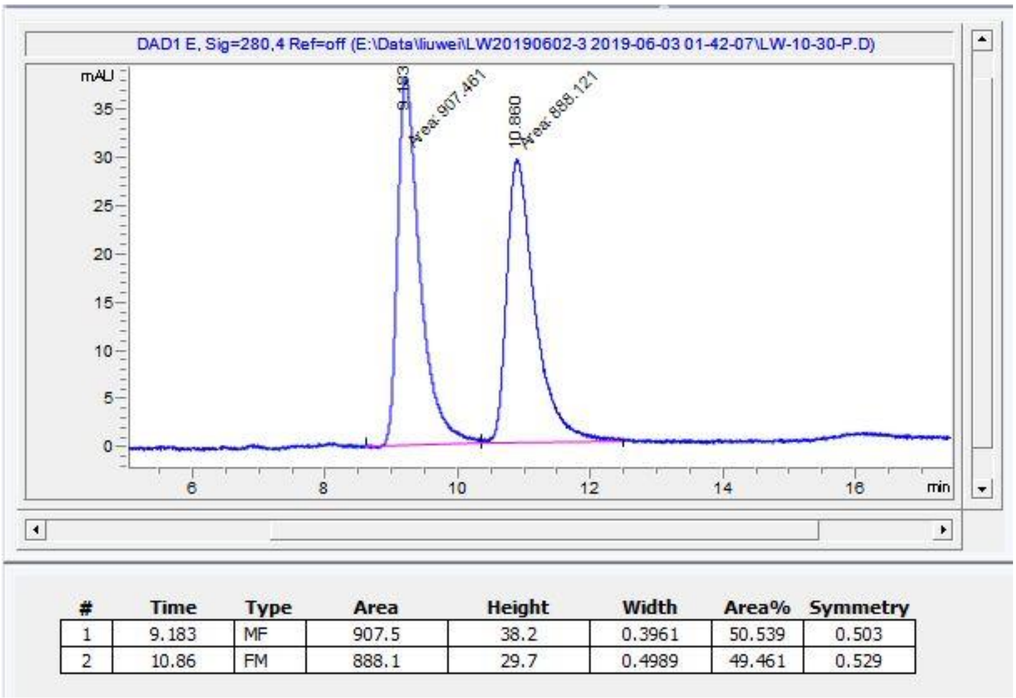

#	Time	Type	Area	Height	Width	Area%	Symmetry
1	9.183	MF	907.5	38.2	0.3961	50.539	0.503
2	10.86	FM	888.1	29.7	0.4989	49.461	0.529

Figure S68. HPLC spectrum of **7c**, related to **Scheme 4**

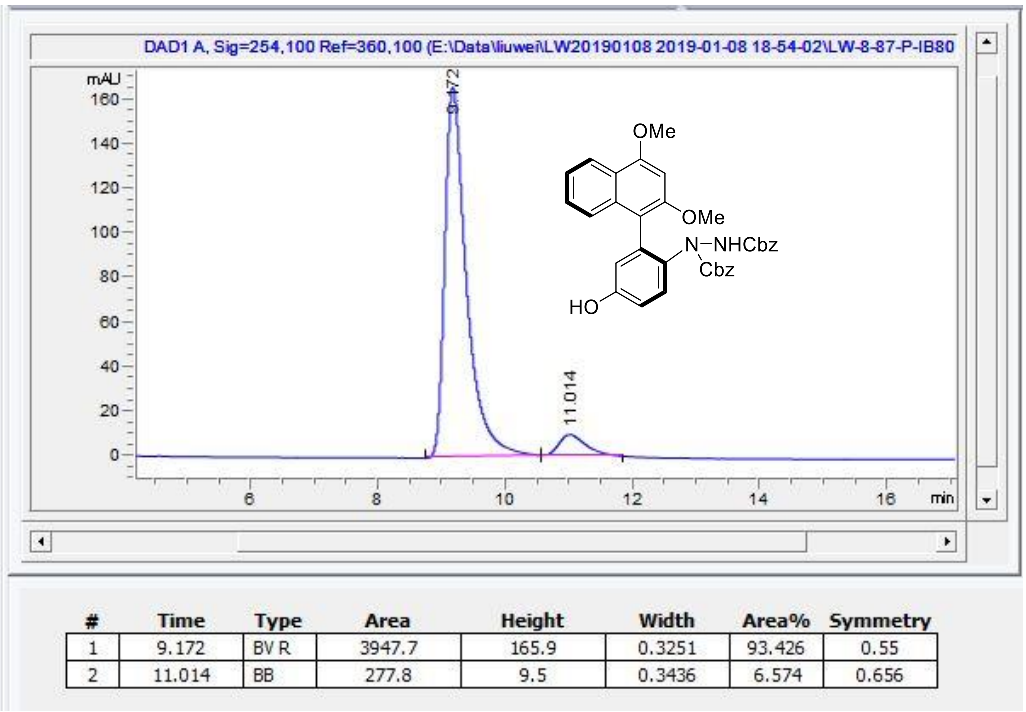

#	Time	Type	Area	Height	Width	Area%	Symmetry
1	9.172	BV R	3947.7	165.9	0.3251	93.426	0.55
2	11.014	BB	277.8	9.5	0.3436	6.574	0.656

Figure S69. Full HPLC spectrum of **7c**, related to **Scheme 4**

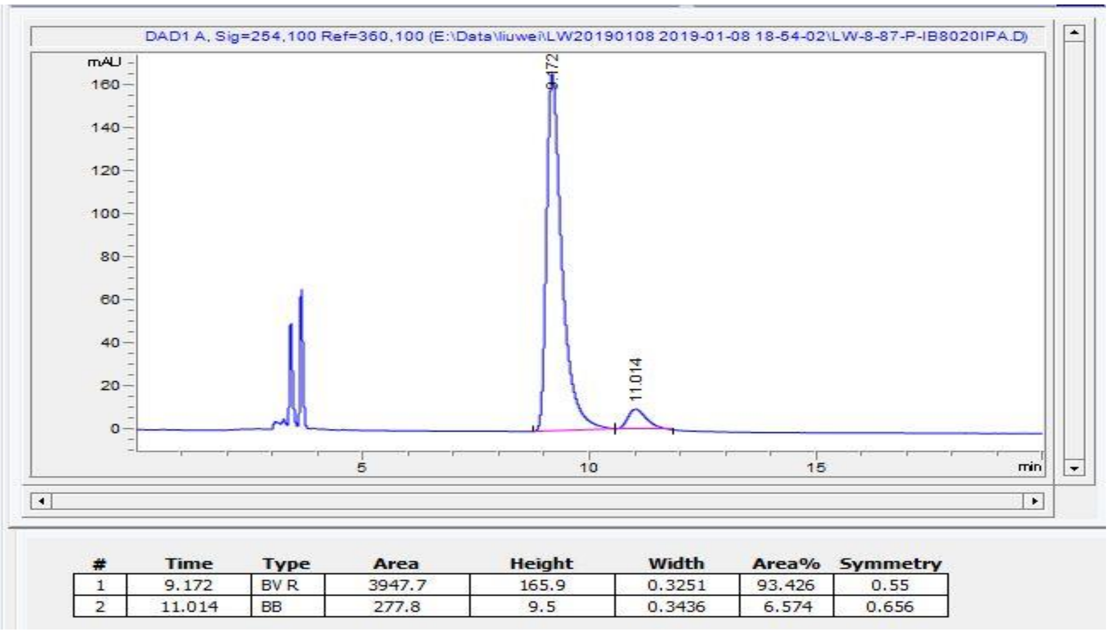

#	Time	Type	Area	Height	Width	Area%	Symmetry
1	9.172	BV R	3947.7	165.9	0.3251	93.426	0.55
2	11.014	BB	277.8	9.5	0.3436	6.574	0.656

Figure S70. HPLC spectrum of racemic-**7d**, related to **Scheme 4**

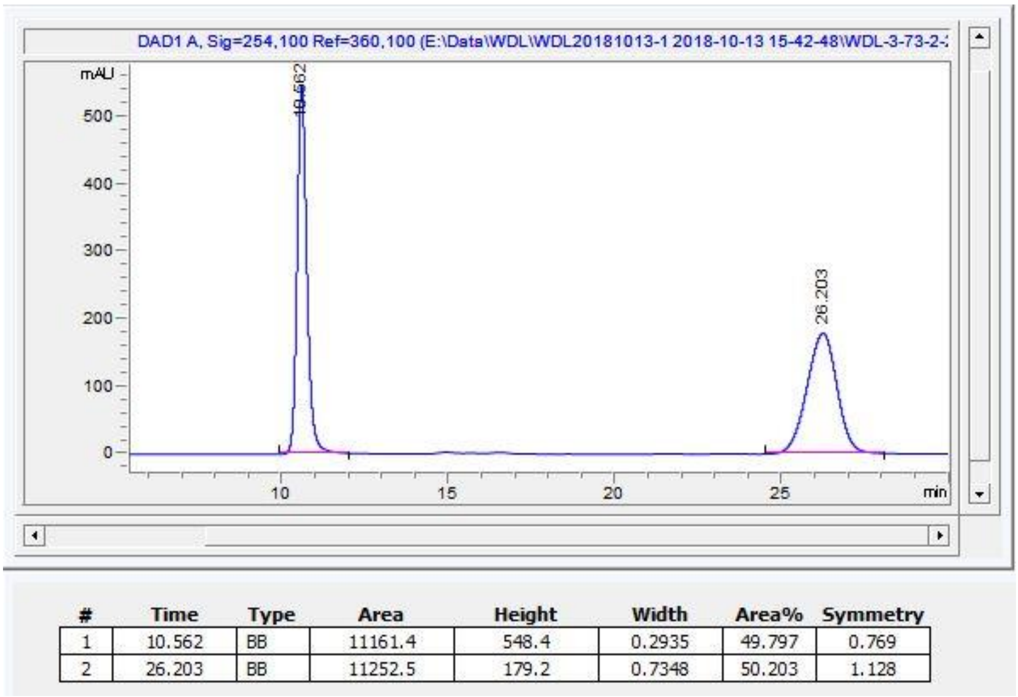

#	Time	Type	Area	Height	Width	Area%	Symmetry
1	10.562	BB	11161.4	548.4	0.2935	49.797	0.769
2	26.203	BB	11252.5	179.2	0.7348	50.203	1.128

Figure S71. HPLC spectrum of **7d**, related to **Scheme 4**

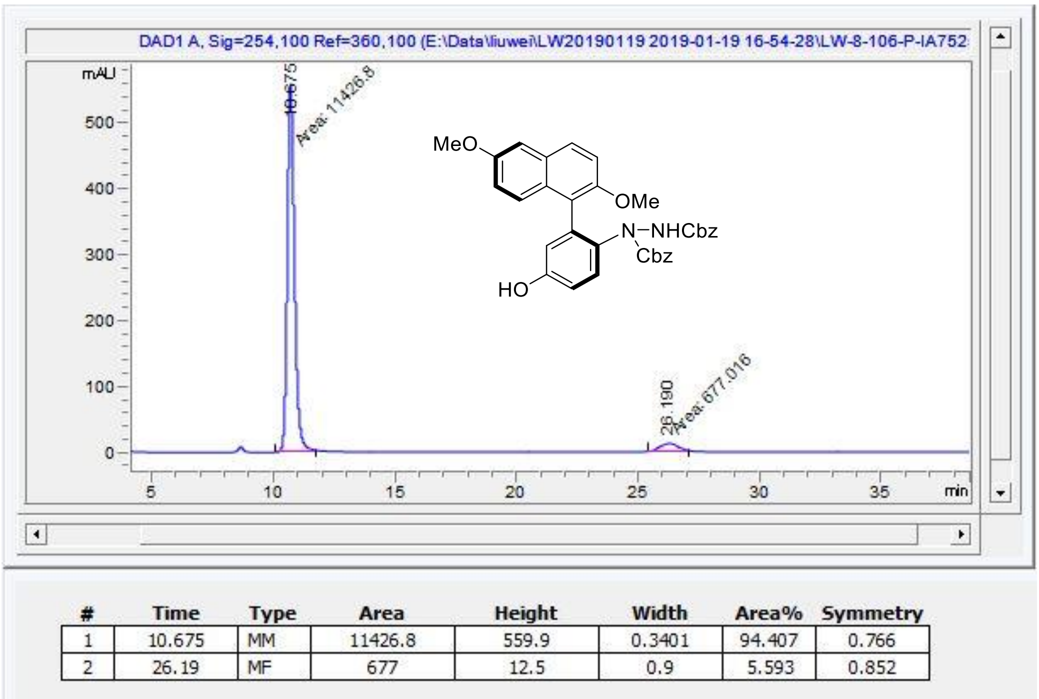

#	Time	Type	Area	Height	Width	Area%	Symmetry
1	10.675	MM	11426.8	559.9	0.3401	94.407	0.766
2	26.19	MF	677	12.5	0.9	5.593	0.852

Figure S72. Full HPLC spectrum of **7a**, related to **Scheme 4**

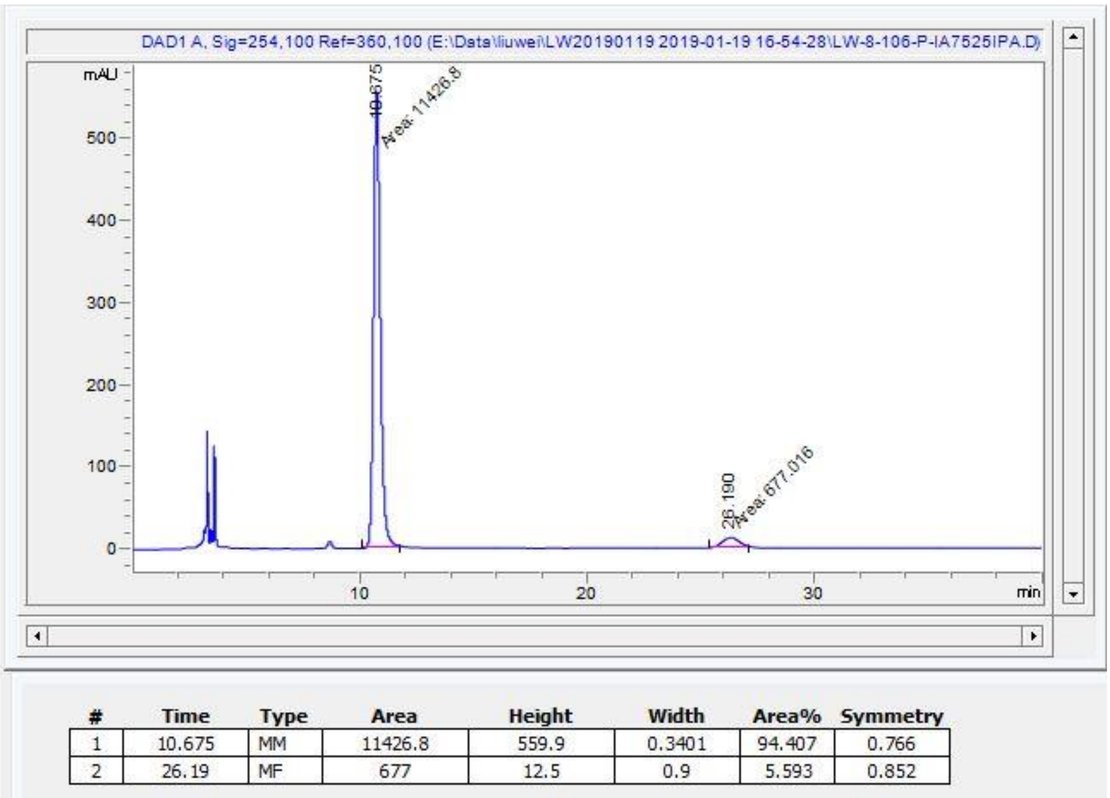

#	Time	Type	Area	Height	Width	Area%	Symmetry
1	10.675	MM	11426.8	559.9	0.3401	94.407	0.766
2	26.19	MF	677	12.5	0.9	5.593	0.852

Figure S73. HPLC spectrum of racemic-**7e**, related to **Scheme 4**

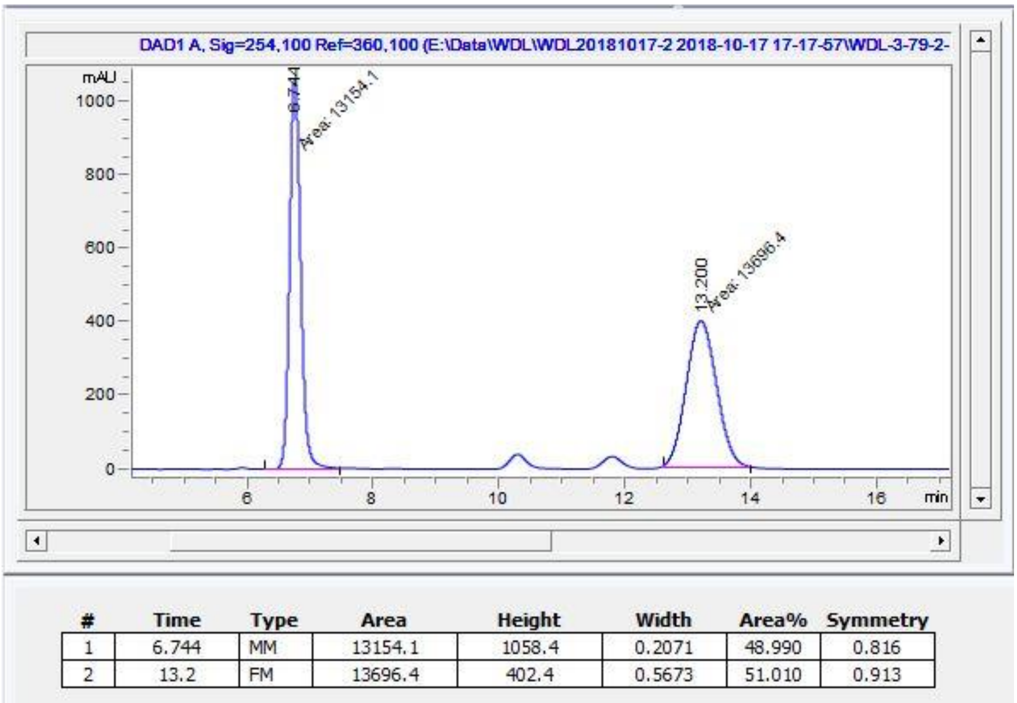

DAD1 A, Sig=254,100 Ref=360,100 (E:\Data\WDL\WDL20181017-2 2018-10-17 17-17-57\WDL-3-79-2-

#	Time	Type	Area	Height	Width	Area%	Symmetry
1	6.744	MM	13154.1	1058.4	0.2071	48.990	0.816
2	13.2	FM	13696.4	402.4	0.5673	51.010	0.913

Figure S74. HPLC spectrum of **7e**, related to **Scheme 4**

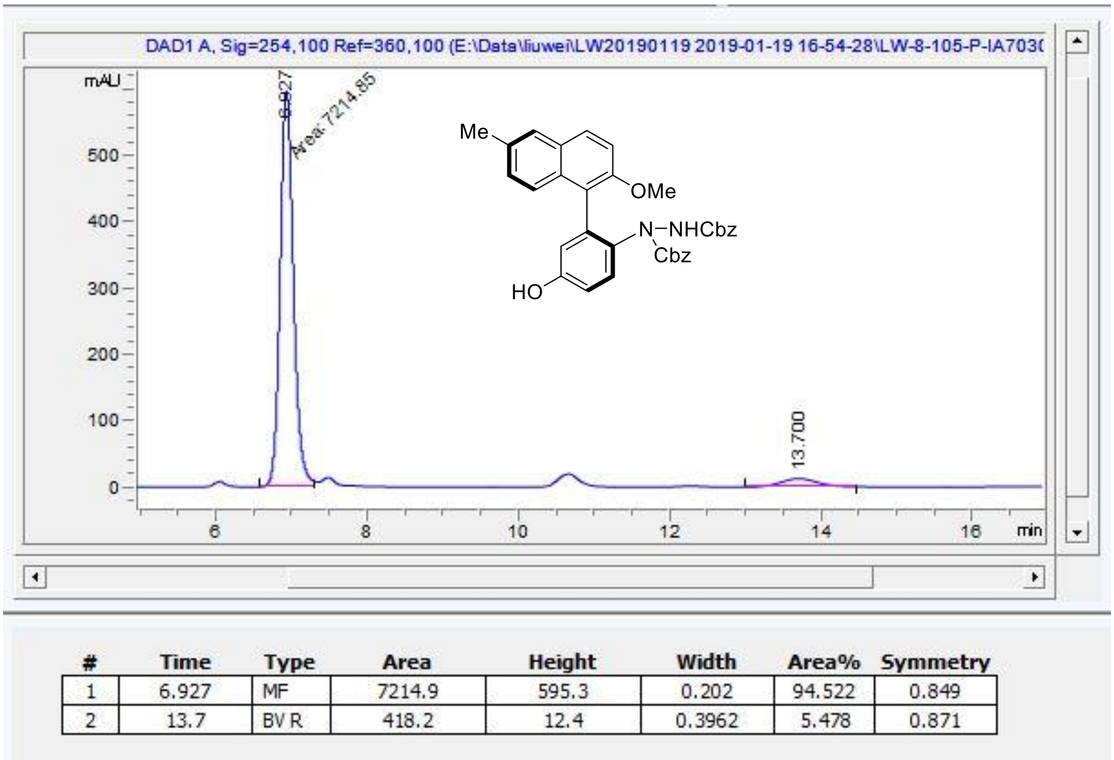

DAD1 A, Sig=254,100 Ref=360,100 (E:\Data\liuwei\LW20190119 2019-01-19 16-54-28\LW-8-105-P-IA703(

#	Time	Type	Area	Height	Width	Area%	Symmetry
1	6.927	MF	7214.9	595.3	0.202	94.522	0.849
2	13.7	BV R	418.2	12.4	0.3962	5.478	0.871

Figure S75. Full HPLC spectrum of **7e**, related to **Scheme 4**

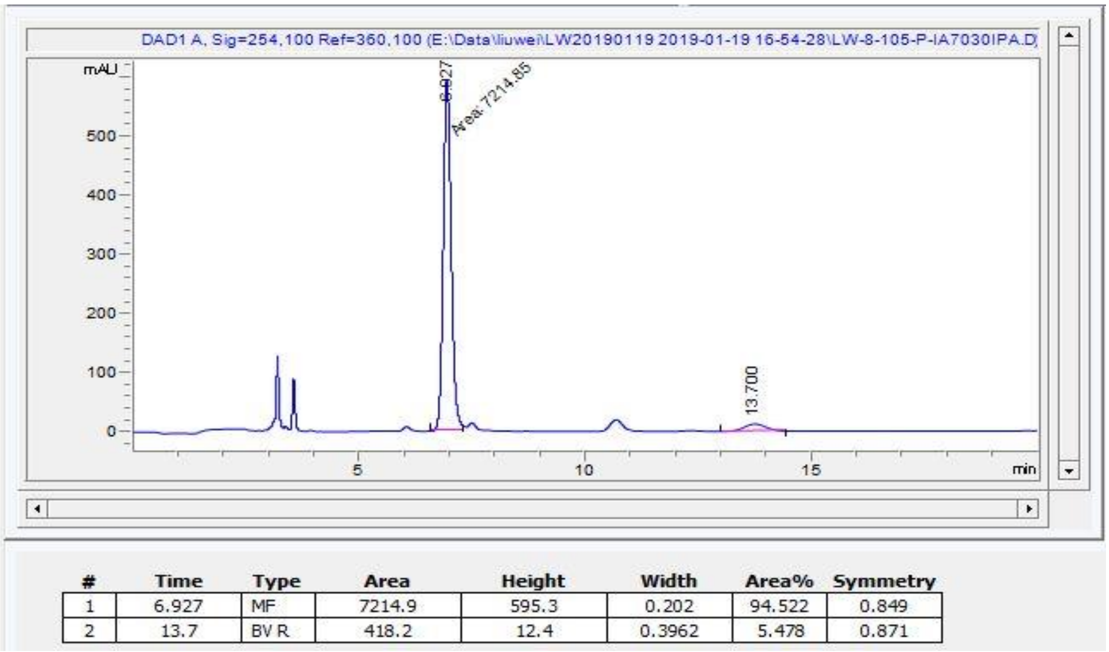

DAD1 A, Sig=254,100 Ref=360,100 (E:\Data\liuwei\LW20190119 2019-01-19 16-54-28\LW-8-105-P-IA7030IPA.D)

#	Time	Type	Area	Height	Width	Area%	Symmetry
1	6.927	MF	7214.9	595.3	0.202	94.522	0.849
2	13.7	BV R	418.2	12.4	0.3962	5.478	0.871

Figure S76. HPLC spectrum of racemic-**7f**, related to **Scheme 4**

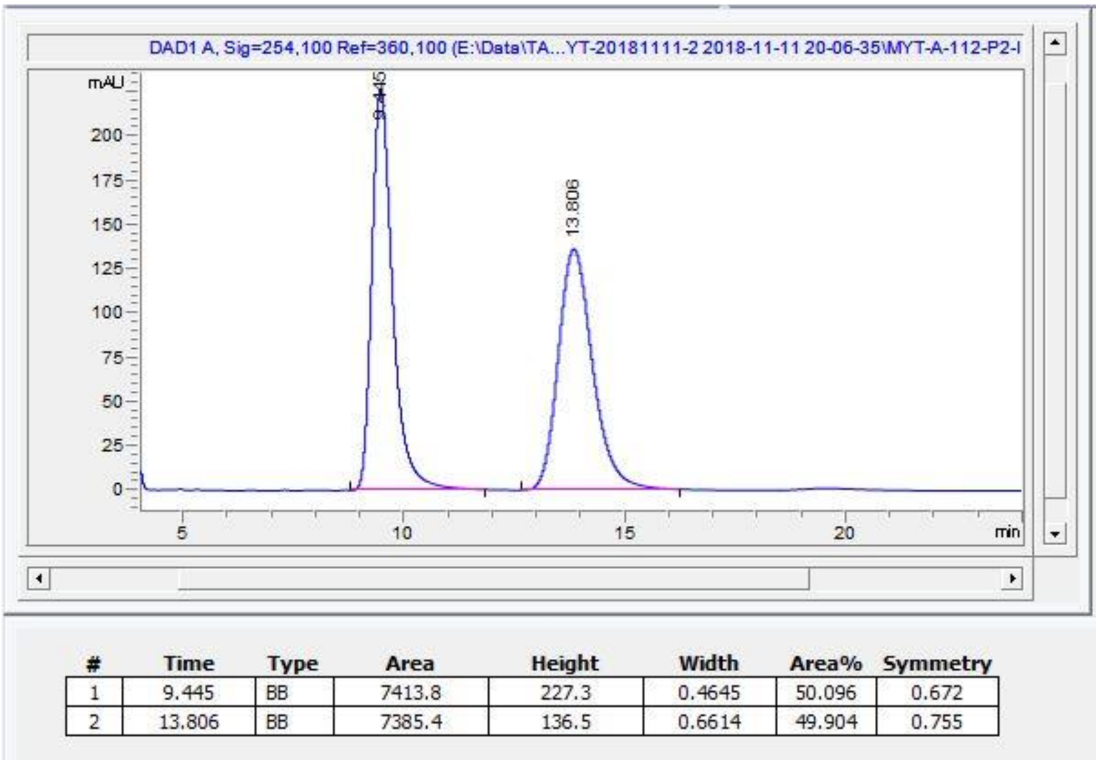

DAD1 A, Sig=254,100 Ref=360,100 (E:\Data\TA...YT-20181111-2 2018-11-11 20-06-35\MYT-A-112-P2-I

#	Time	Type	Area	Height	Width	Area%	Symmetry
1	9.445	BB	7413.8	227.3	0.4645	50.096	0.672
2	13.806	BB	7385.4	136.5	0.6614	49.904	0.755

Figure S77. HPLC spectrum of **7f**, related to **Scheme 4**

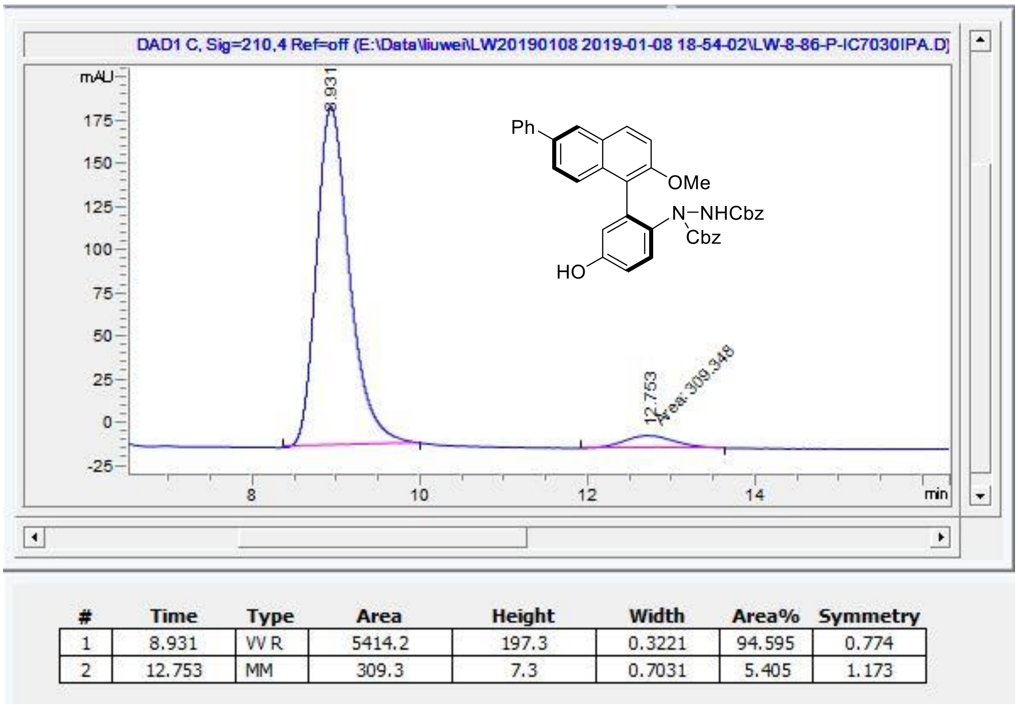

#	Time	Type	Area	Height	Width	Area%	Symmetry
1	8.931	VV R	5414.2	197.3	0.3221	94.595	0.774
2	12.753	MM	309.3	7.3	0.7031	5.405	1.173

Figure S78. Full HPLC spectrum of **7f**, related to **Scheme 4**

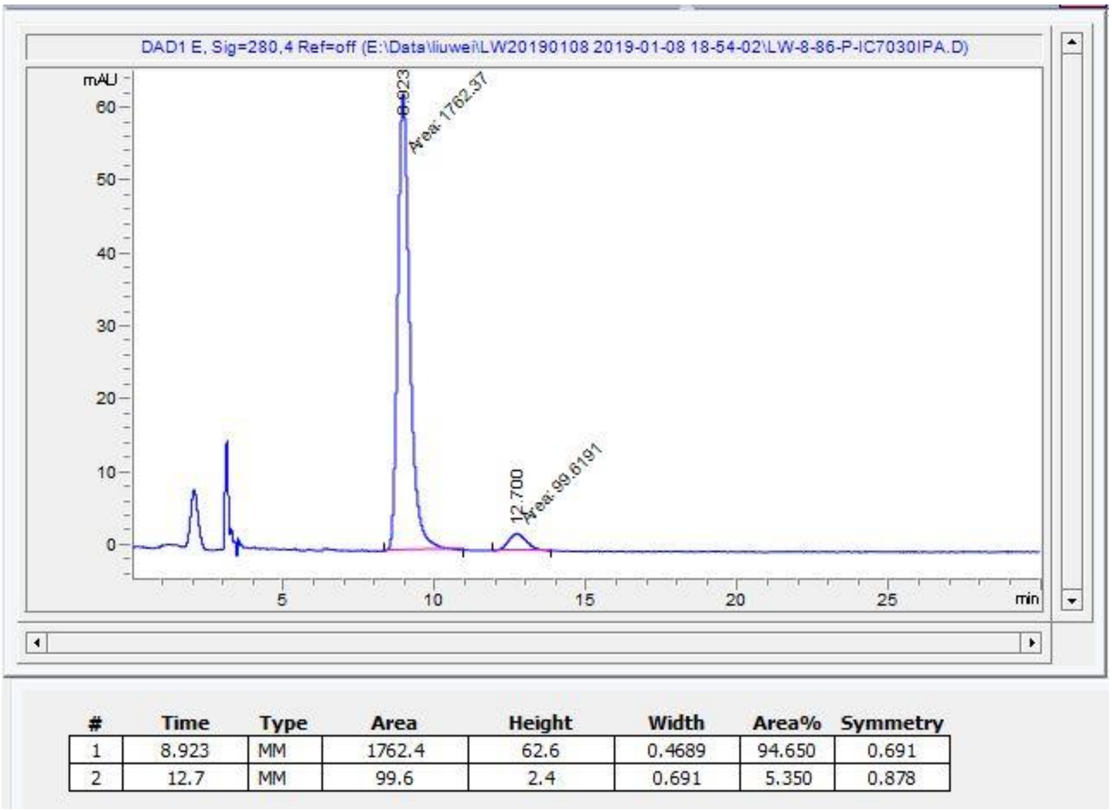

#	Time	Type	Area	Height	Width	Area%	Symmetry
1	8.923	MM	1762.4	62.6	0.4689	94.650	0.691
2	12.7	MM	99.6	2.4	0.691	5.350	0.878

Figure S79. HPLC spectrum of racemic-**7g**, related to **Scheme 4**

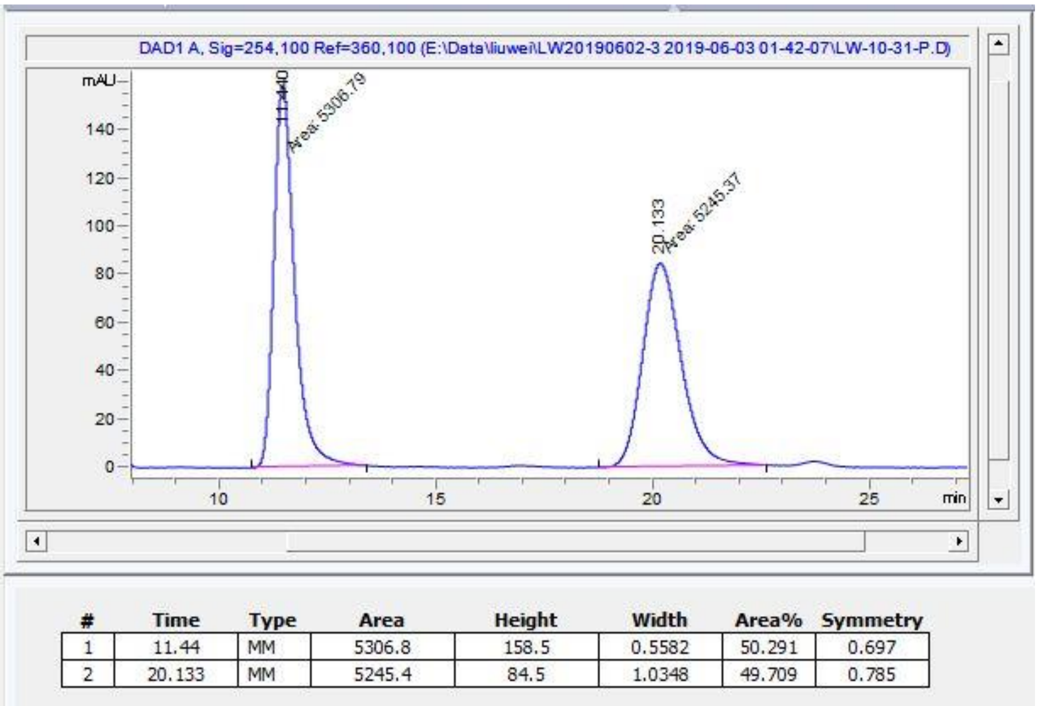

#	Time	Type	Area	Height	Width	Area%	Symmetry
1	11.44	MM	5306.8	158.5	0.5582	50.291	0.697
2	20.133	MM	5245.4	84.5	1.0348	49.709	0.785

Figure S80. HPLC spectrum of **7g**, related to **Scheme 4**

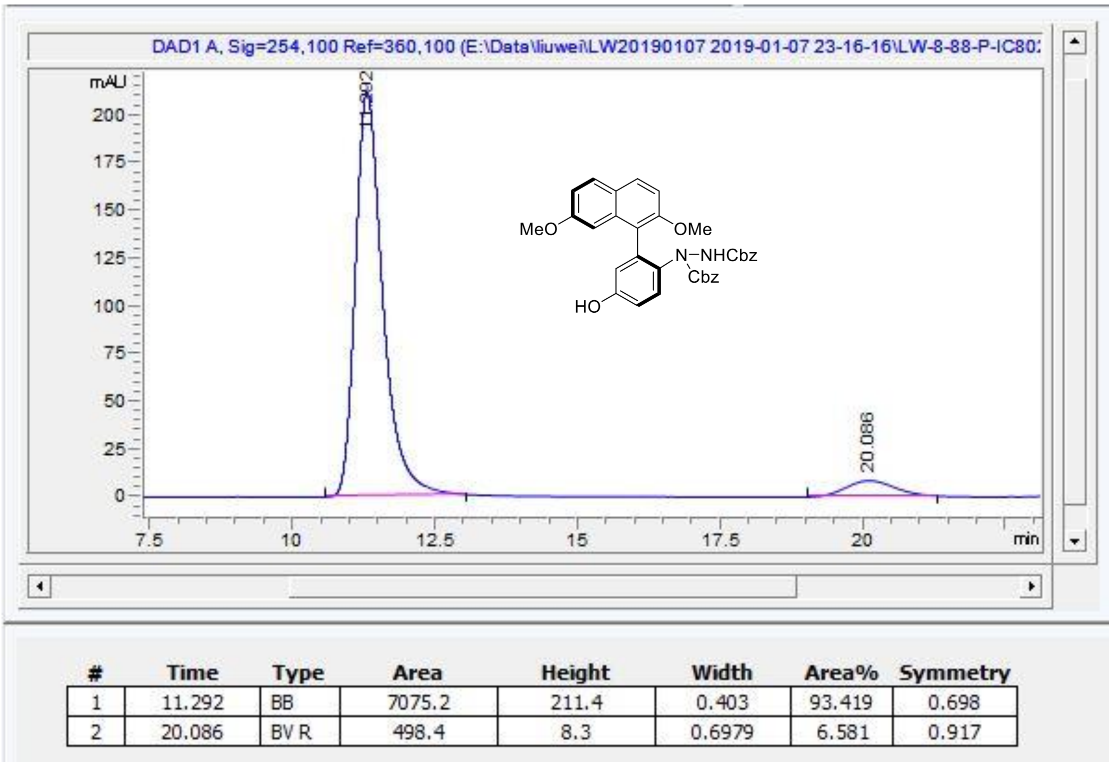

#	Time	Type	Area	Height	Width	Area%	Symmetry
1	11.292	BB	7075.2	211.4	0.403	93.419	0.698
2	20.086	BV R	498.4	8.3	0.6979	6.581	0.917

Figure S81. Full HPLC spectrum of **7g**, related to **Scheme 4**

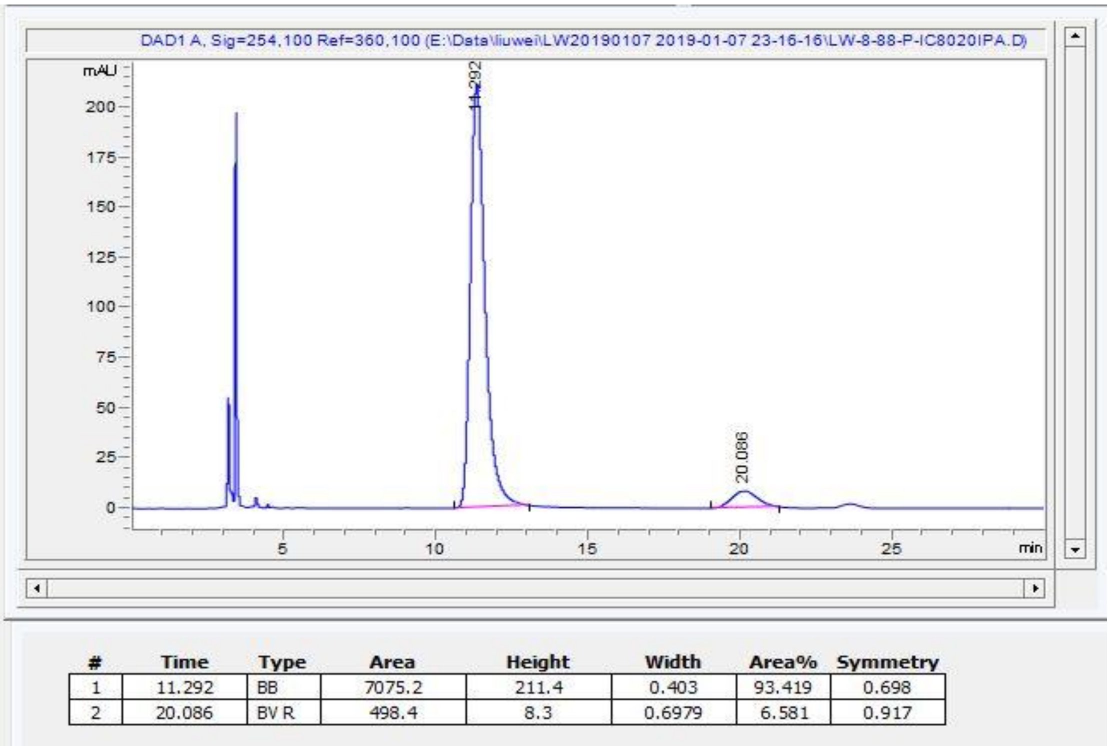
DAD1 A, Sig=254,100 Ref=360,100 (E:\Data\liuwei\LW20190107 2019-01-07 23-16-16\LW-8-88-P-IC8020IPA.D)

#	Time	Type	Area	Height	Width	Area%	Symmetry
1	11.292	BB	7075.2	211.4	0.403	93.419	0.698
2	20.086	BV R	498.4	8.3	0.6979	6.581	0.917

Figure S82. HPLC spectrum of racemic-**8a**, related to **Scheme 6**.

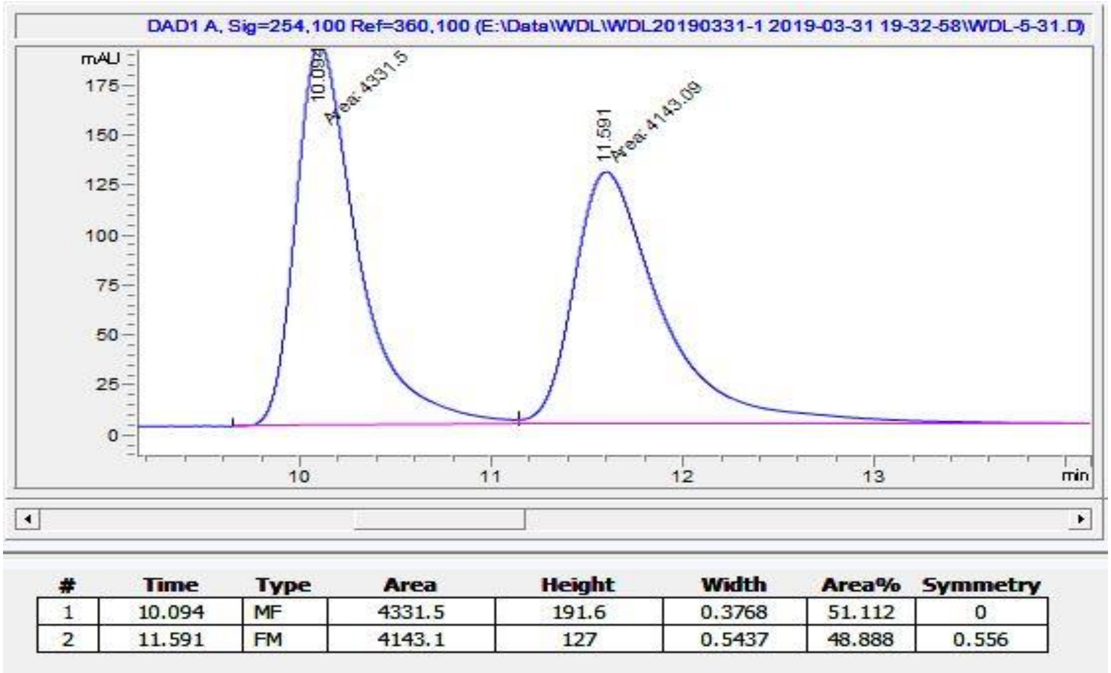
DAD1 A, Sig=254,100 Ref=360,100 (E:\Data\WDL\WDL20190331-1 2019-03-31 19-32-58\WDL-5-31.D)

#	Time	Type	Area	Height	Width	Area%	Symmetry
1	10.094	MF	4331.5	191.6	0.3768	51.112	0
2	11.591	FM	4143.1	127	0.5437	48.888	0.556

Figure S83. HPLC spectrum of **8a**, related to **Scheme 6**.

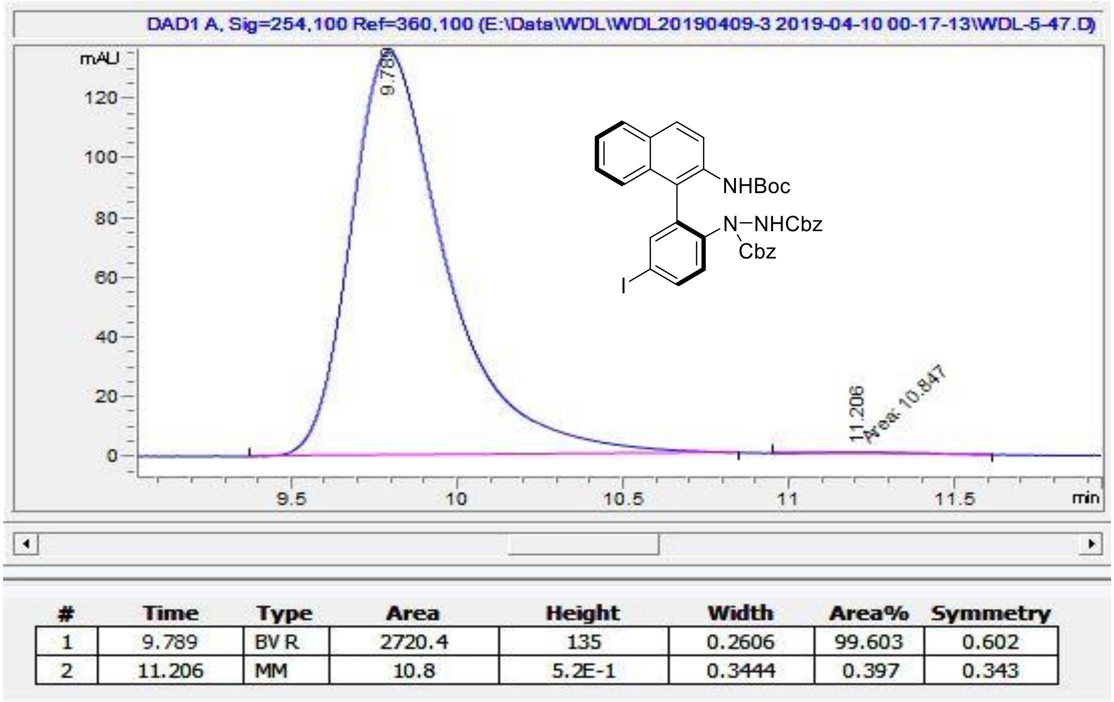
DAD1 A, Sig=254,100 Ref=360,100 (E:\Data\WDL\WDL20190409-3 2019-04-10 00-17-13\WDL-5-47.D)

#	Time	Type	Area	Height	Width	Area%	Symmetry
1	9.789	BV R	2720.4	135	0.2606	99.603	0.602
2	11.206	MM	10.8	5.2E-1	0.3444	0.397	0.343

Figure S84. Full HPLC spectrum of **8a**, related to **Scheme 6**.

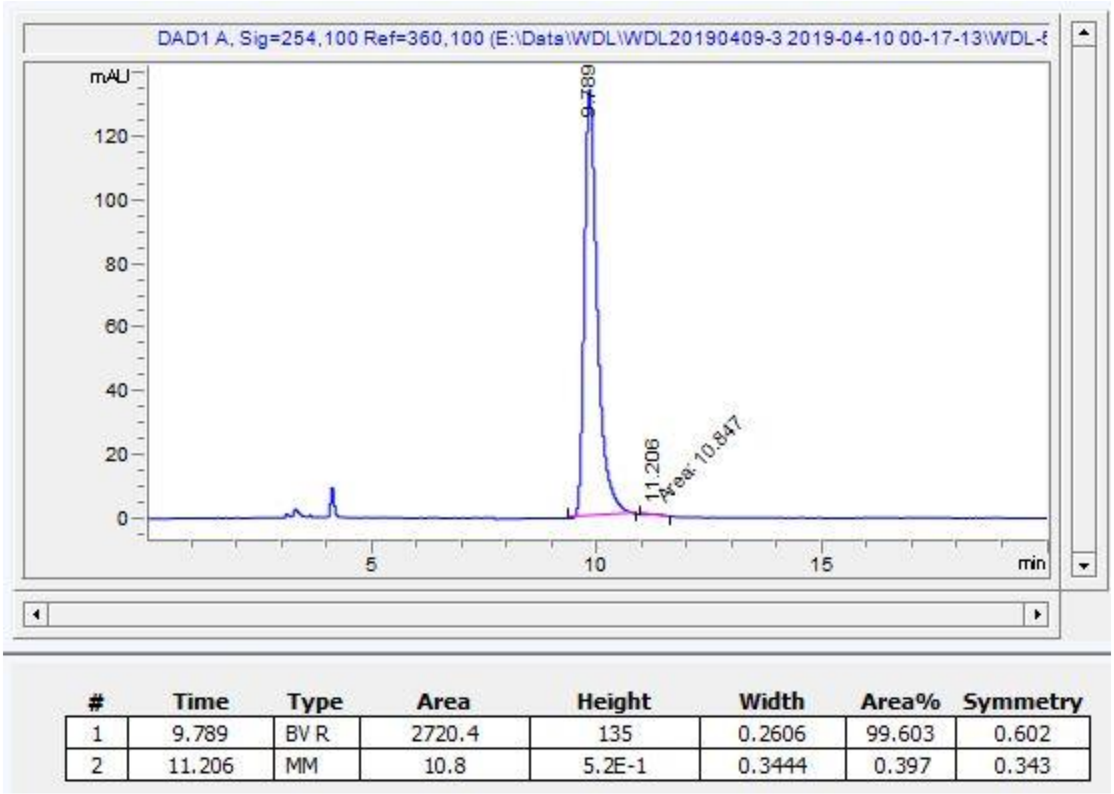
DAD1 A, Sig=254,100 Ref=360,100 (E:\Data\WDL\WDL20190409-3 2019-04-10 00-17-13\WDL-

#	Time	Type	Area	Height	Width	Area%	Symmetry
1	9.789	BV R	2720.4	135	0.2606	99.603	0.602
2	11.206	MM	10.8	5.2E-1	0.3444	0.397	0.343

Figure S85. HPLC spectrum of racemic-**9a**, related to **Scheme 6**.

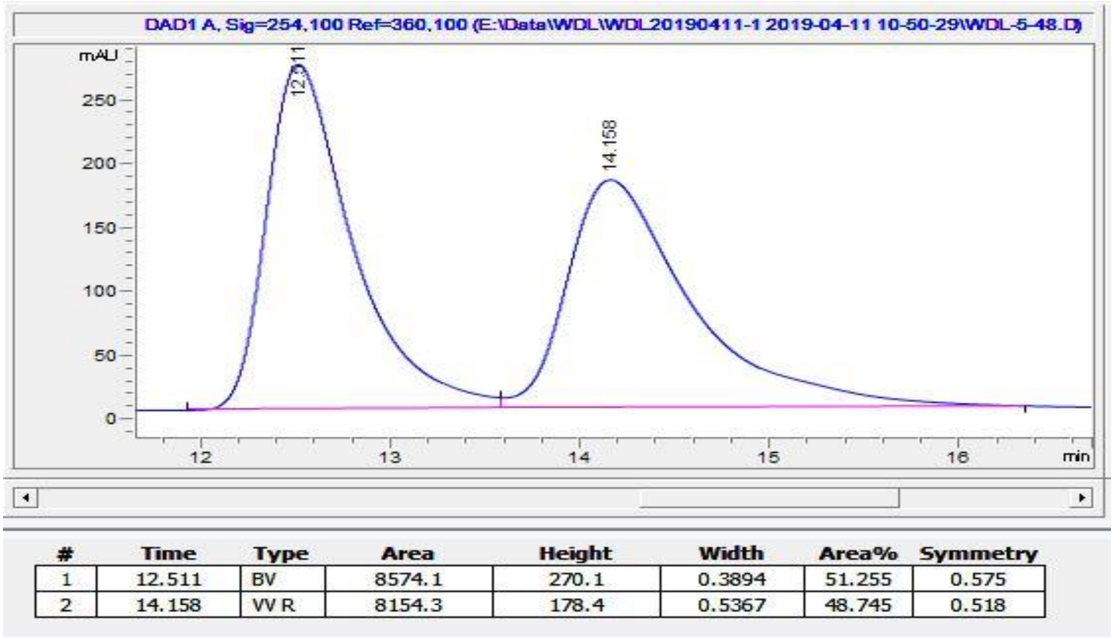

#	Time	Type	Area	Height	Width	Area%	Symmetry
1	12.511	BV	8574.1	270.1	0.3894	51.255	0.575
2	14.158	VV R	8154.3	178.4	0.5367	48.745	0.518

Figure S86. HPLC spectrum of **9a**, related to **Scheme 6**.

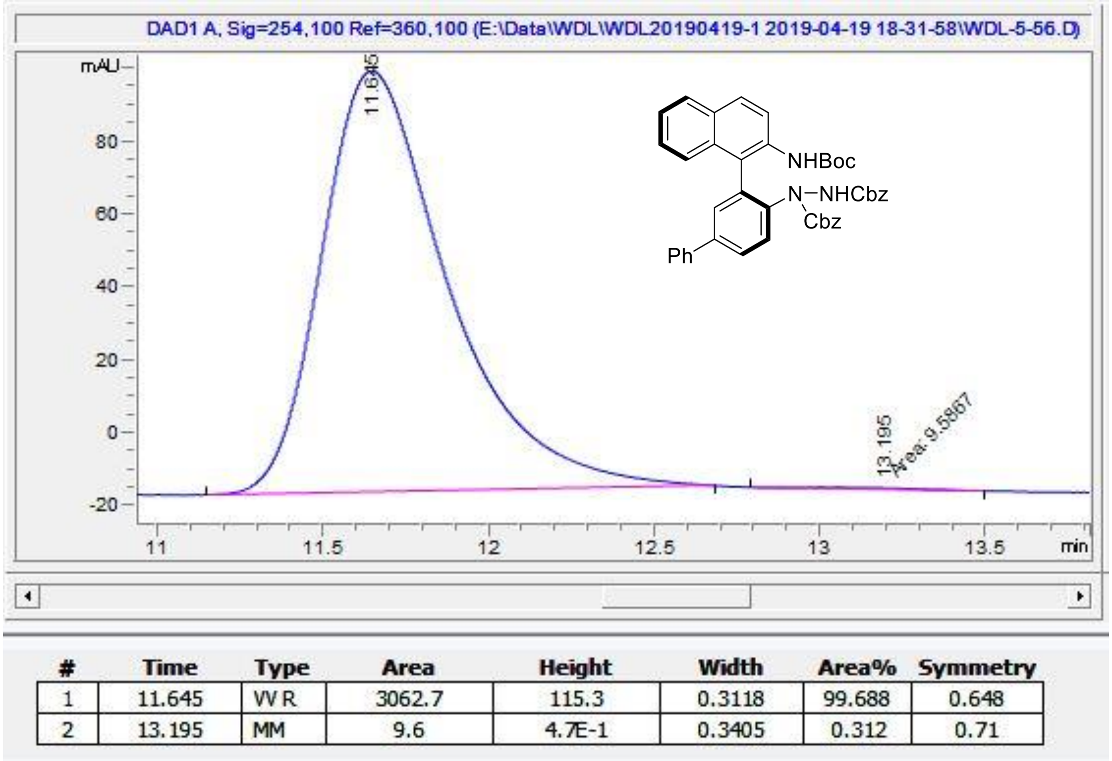

#	Time	Type	Area	Height	Width	Area%	Symmetry
1	11.645	VV R	3062.7	115.3	0.3118	99.688	0.648
2	13.195	MM	9.6	4.7E-1	0.3405	0.312	0.71

Figure S87. Full HPLC spectrum of **9a**, related to **Scheme 6**.

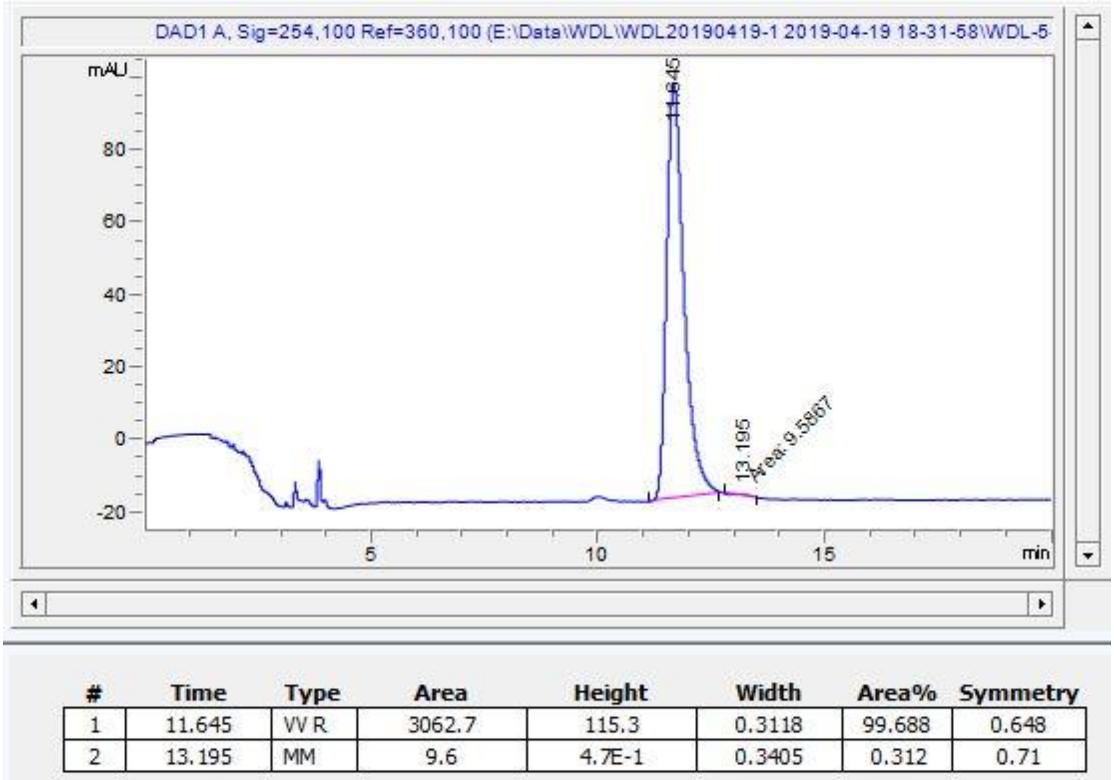

#	Time	Type	Area	Height	Width	Area%	Symmetry
1	11.645	VV R	3062.7	115.3	0.3118	99.688	0.648
2	13.195	MM	9.6	4.7E-1	0.3405	0.312	0.71

Figure S88. HPLC spectrum of racemic-**10a**, related to **Scheme 6**.

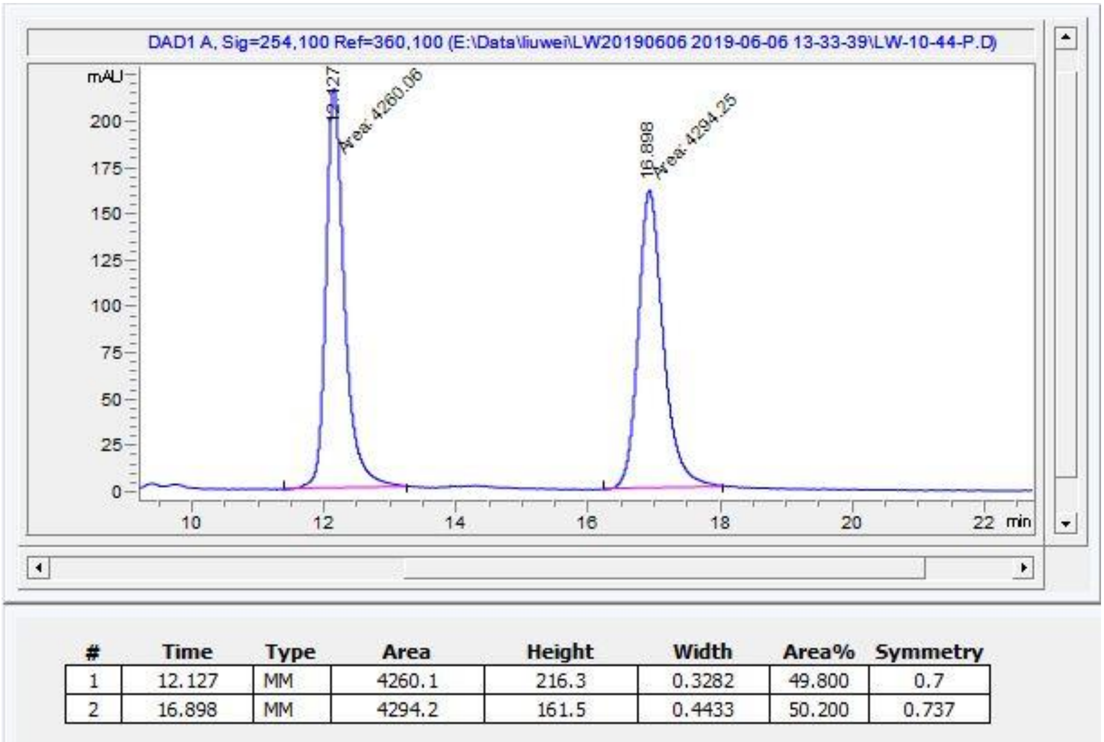

#	Time	Type	Area	Height	Width	Area%	Symmetry
1	12.127	MM	4260.1	216.3	0.3282	49.800	0.7
2	16.898	MM	4294.2	161.5	0.4433	50.200	0.737

Figure S89. HPLC spectrum of **10a**, related to **Scheme 6**.

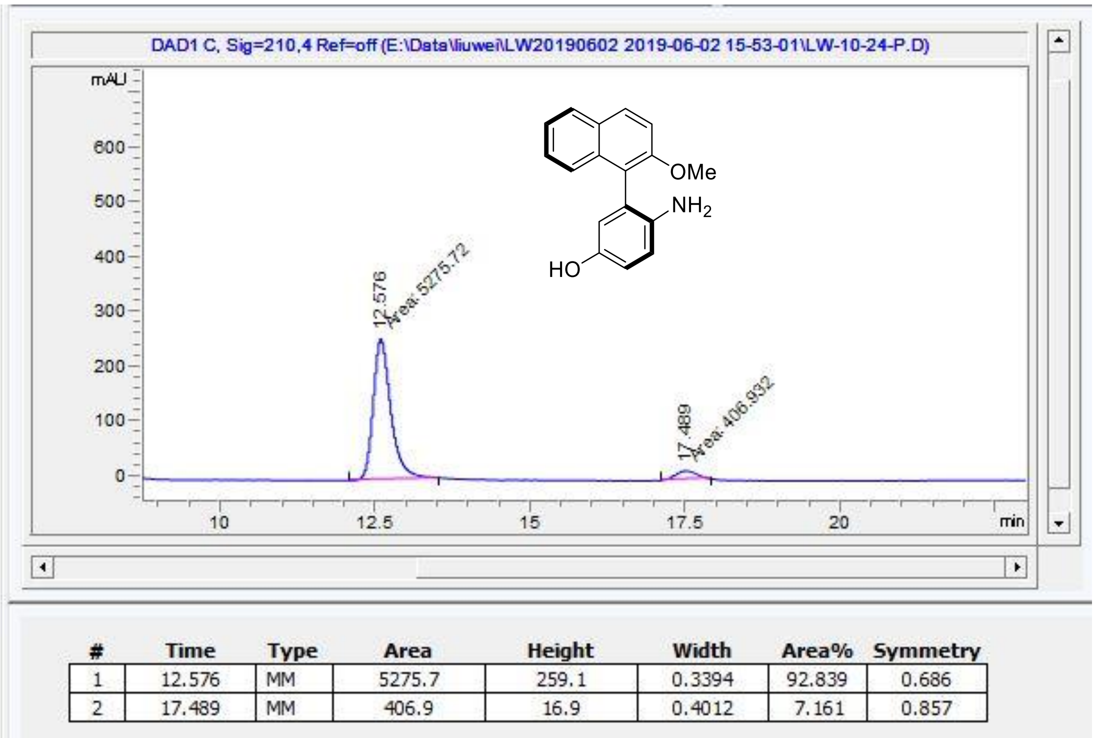

#	Time	Type	Area	Height	Width	Area%	Symmetry
1	12.576	MM	5275.7	259.1	0.3394	92.839	0.686
2	17.489	MM	406.9	16.9	0.4012	7.161	0.857

Figure S90. Full HPLC spectrum of **10a**, related to **Scheme 6**.

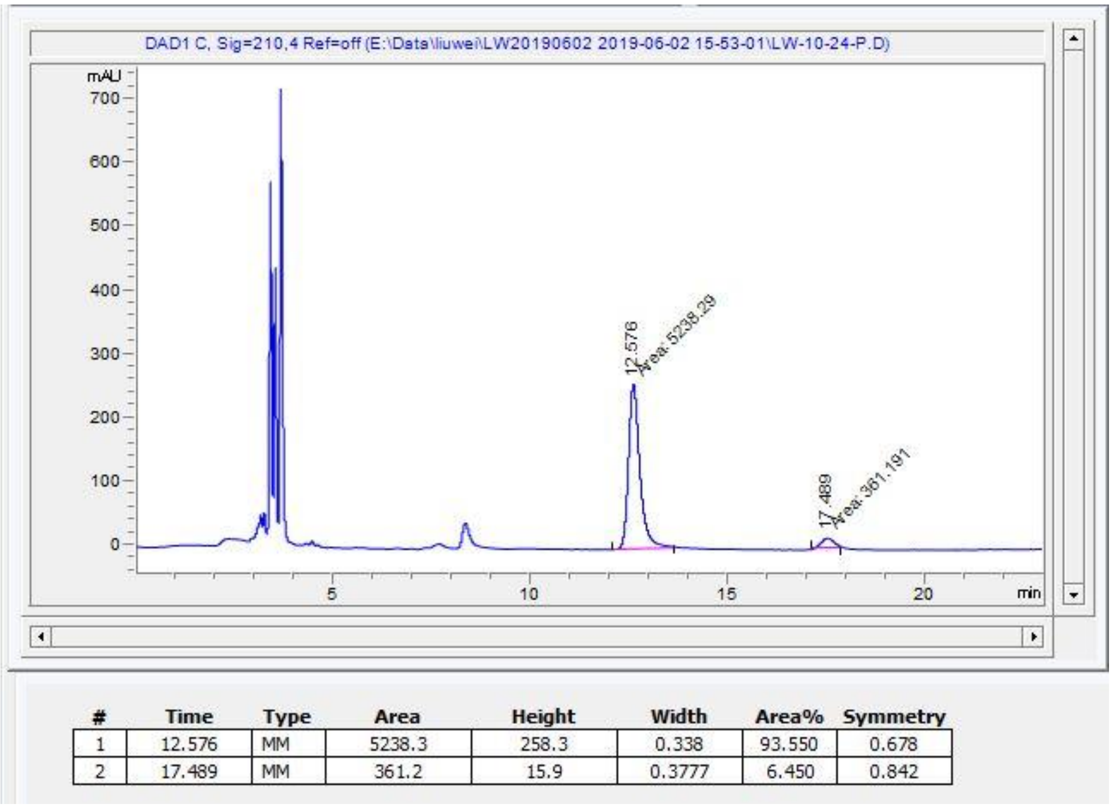

#	Time	Type	Area	Height	Width	Area%	Symmetry
1	12.576	MM	5238.3	258.3	0.338	93.550	0.678
2	17.489	MM	361.2	15.9	0.3777	6.450	0.842

Figure S91. HPLC spectrum of racemic-**11n**, related to **Scheme 6**.

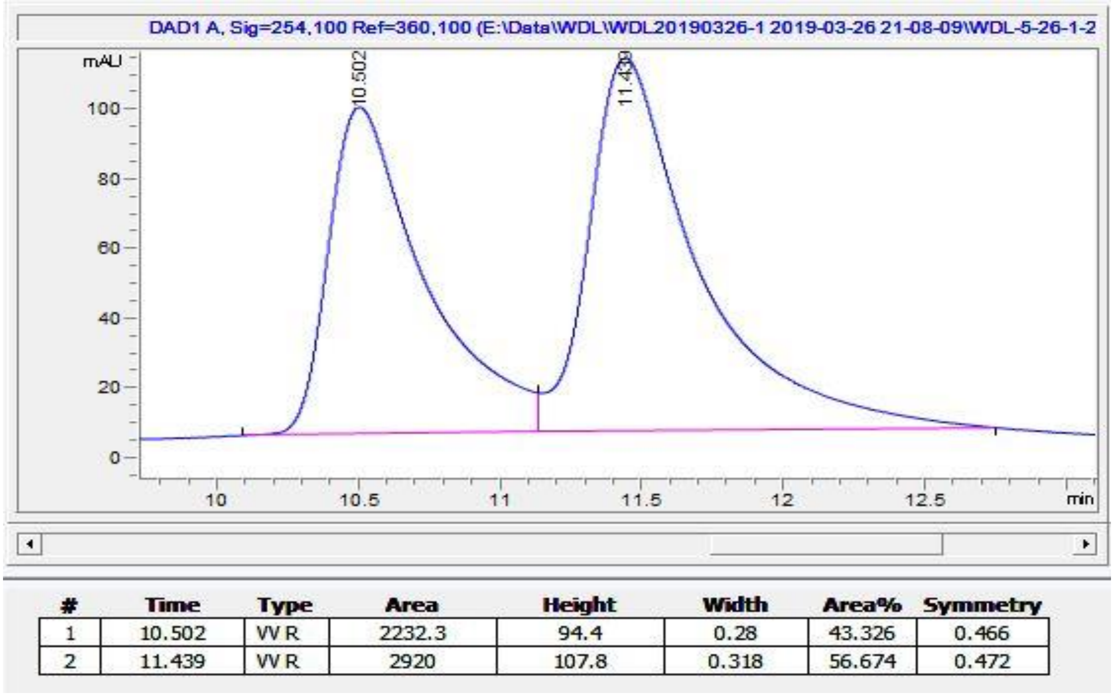

#	Time	Type	Area	Height	Width	Area%	Symmetry
1	10.502	VV R	2232.3	94.4	0.28	43.326	0.466
2	11.439	VV R	2920	107.8	0.318	56.674	0.472

Figure S92. HPLC spectrum of **11n**, related to **Scheme 6**.

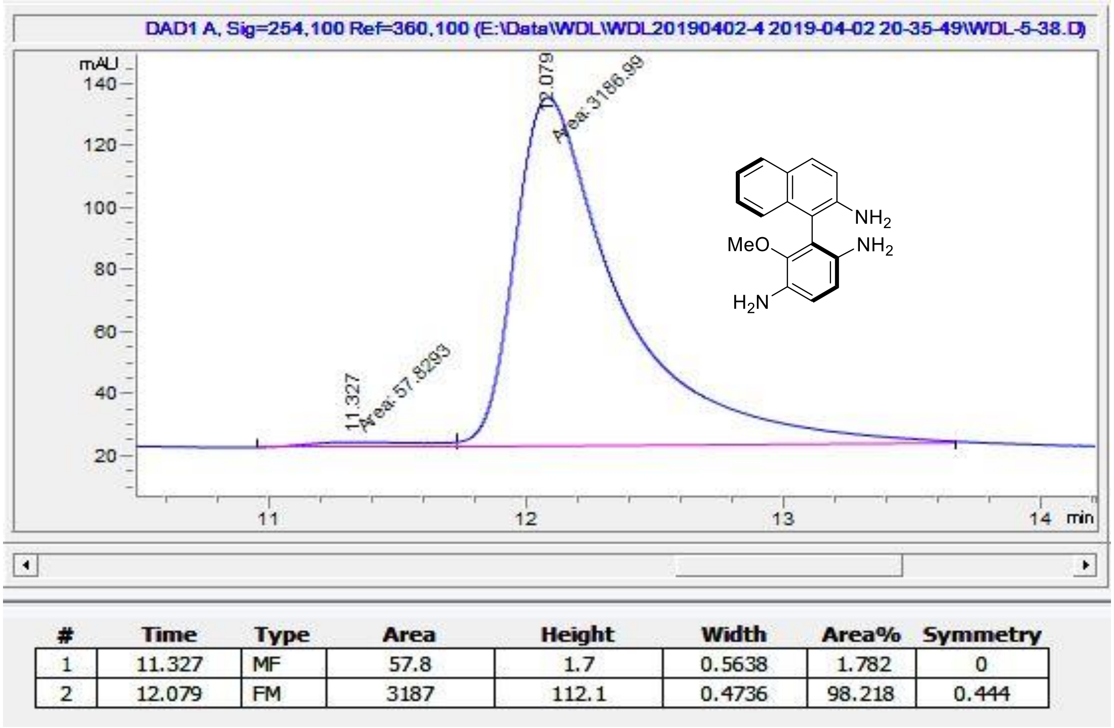

#	Time	Type	Area	Height	Width	Area%	Symmetry
1	11.327	MF	57.8	1.7	0.5638	1.782	0
2	12.079	FM	3187	112.1	0.4736	98.218	0.444

Figure S93. Full HPLC spectrum of **8a**, related to **Scheme 6**.

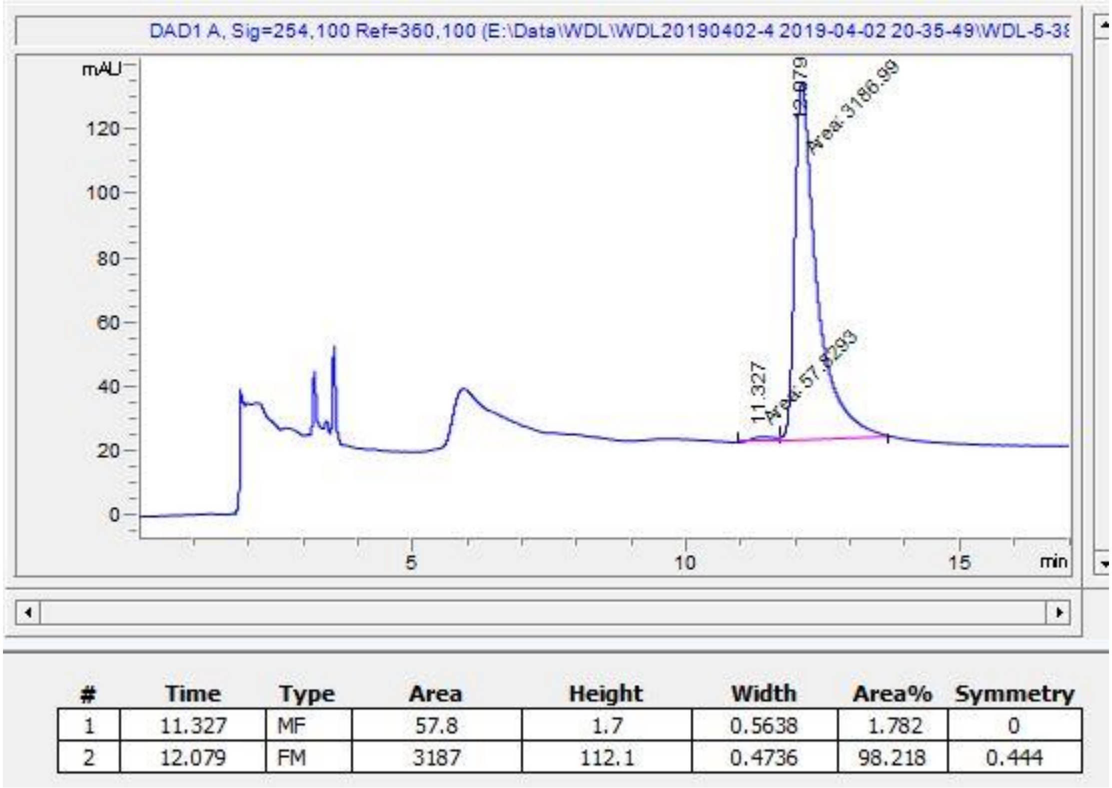

#	Time	Type	Area	Height	Width	Area%	Symmetry
1	11.327	MF	57.8	1.7	0.5638	1.782	0
2	12.079	FM	3187	112.1	0.4736	98.218	0.444

Figure S94. HPLC spectrum of racemic-**12a**, related to **Scheme 6**.

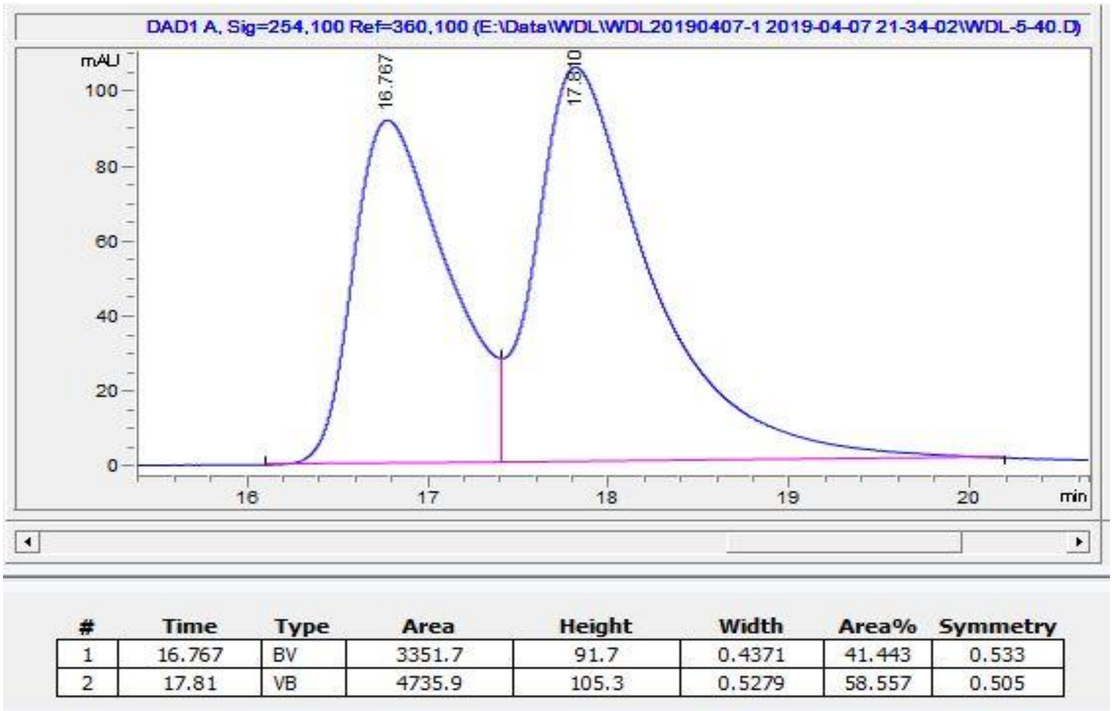

#	Time	Type	Area	Height	Width	Area%	Symmetry
1	16.767	BV	3351.7	91.7	0.4371	41.443	0.533
2	17.81	VB	4735.9	105.3	0.5279	58.557	0.505

Figure S95. HPLC spectrum of **12a**, related to **Scheme 6**.

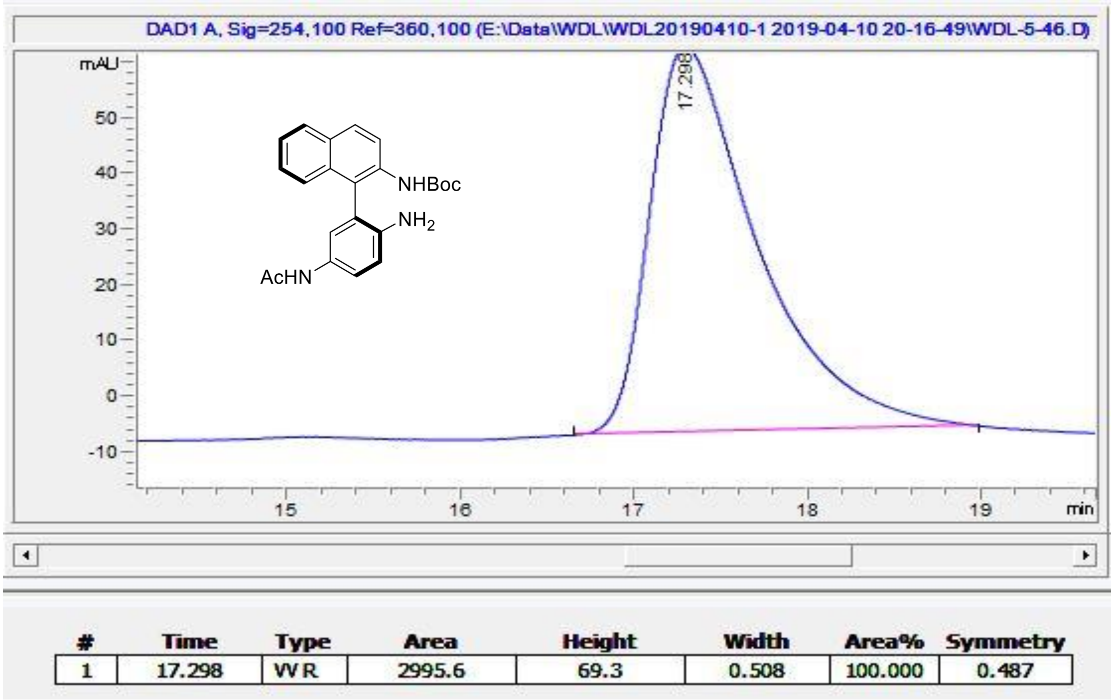

#	Time	Type	Area	Height	Width	Area%	Symmetry
1	17.298	VV R	2995.6	69.3	0.508	100.000	0.487

Figure S96. Full HPLC spectrum of **12a**, related to **Scheme 6**.

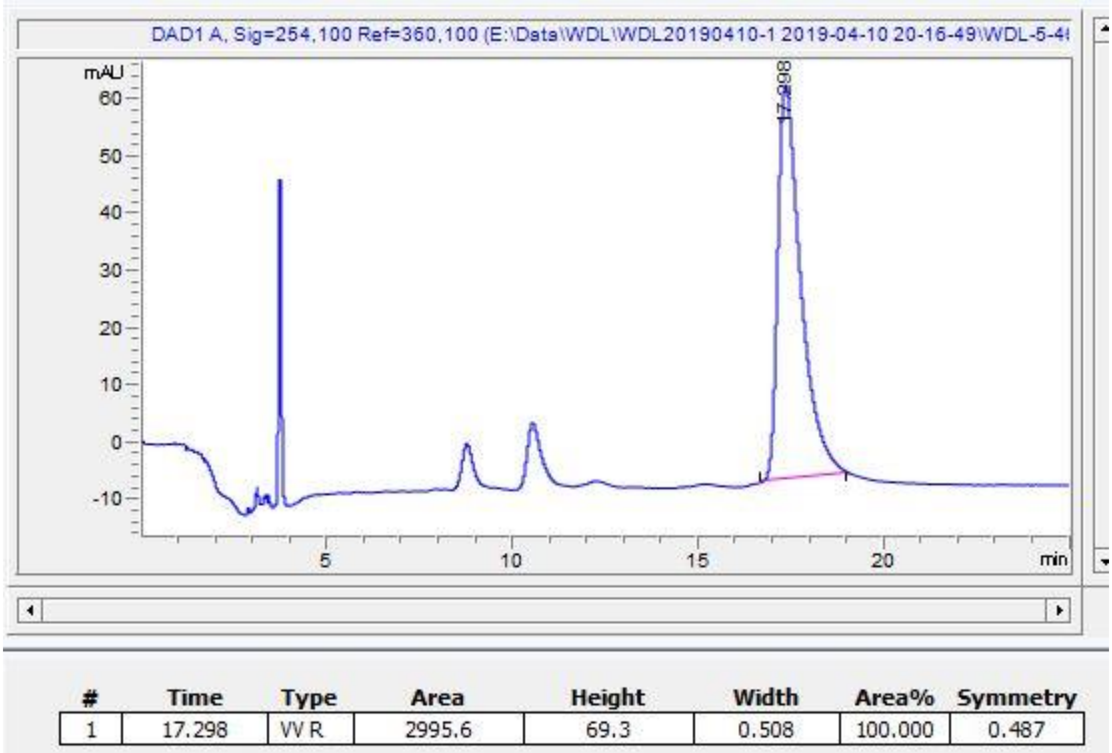

#	Time	Type	Area	Height	Width	Area%	Symmetry
1	17.298	VV R	2995.6	69.3	0.508	100.000	0.487

Figure S97. HPLC spectrum of racemic-**13a**, related to **Scheme 6**.

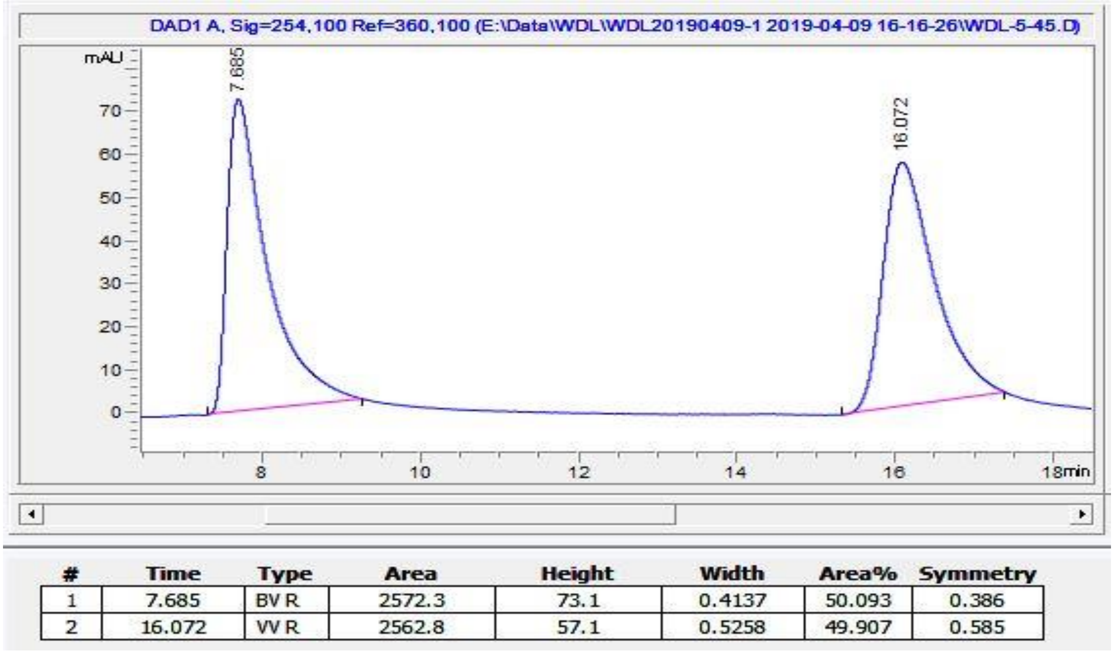

#	Time	Type	Area	Height	Width	Area%	Symmetry
1	7.685	BV R	2572.3	73.1	0.4137	50.093	0.386
2	16.072	VV R	2562.8	57.1	0.5258	49.907	0.585

Figure S98. HPLC spectrum of **13a**, related to **Scheme 6**.

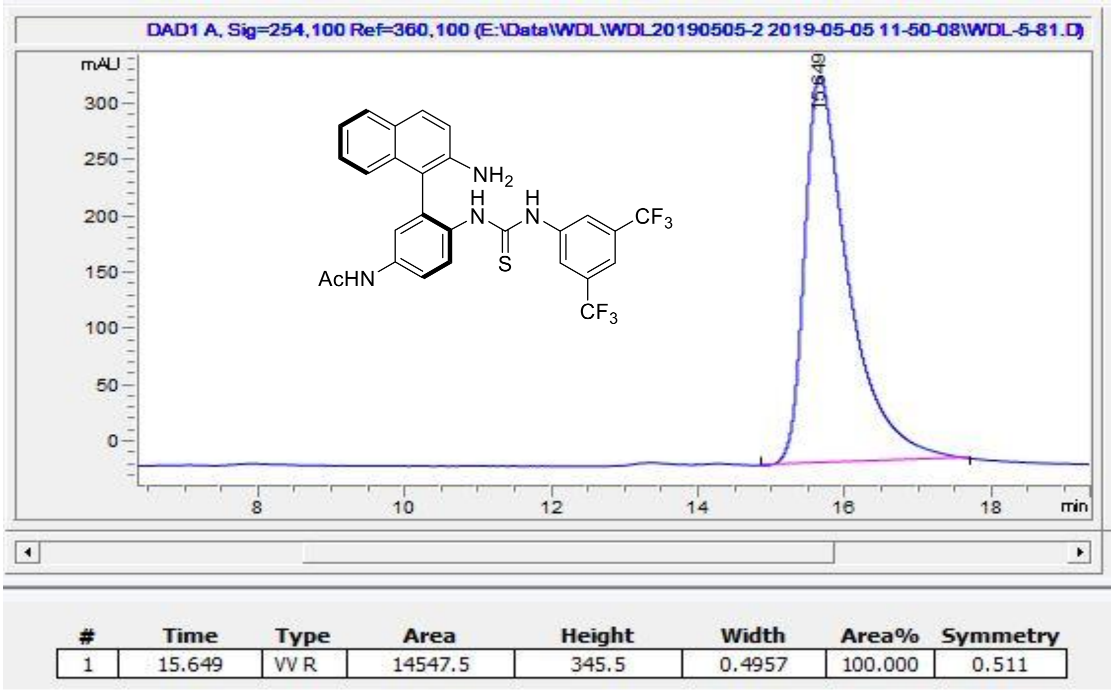

#	Time	Type	Area	Height	Width	Area%	Symmetry
1	15.649	VV R	14547.5	345.5	0.4957	100.000	0.511

Figure S99. Full HPLC spectrum of **13a**, related to **Scheme 6**.

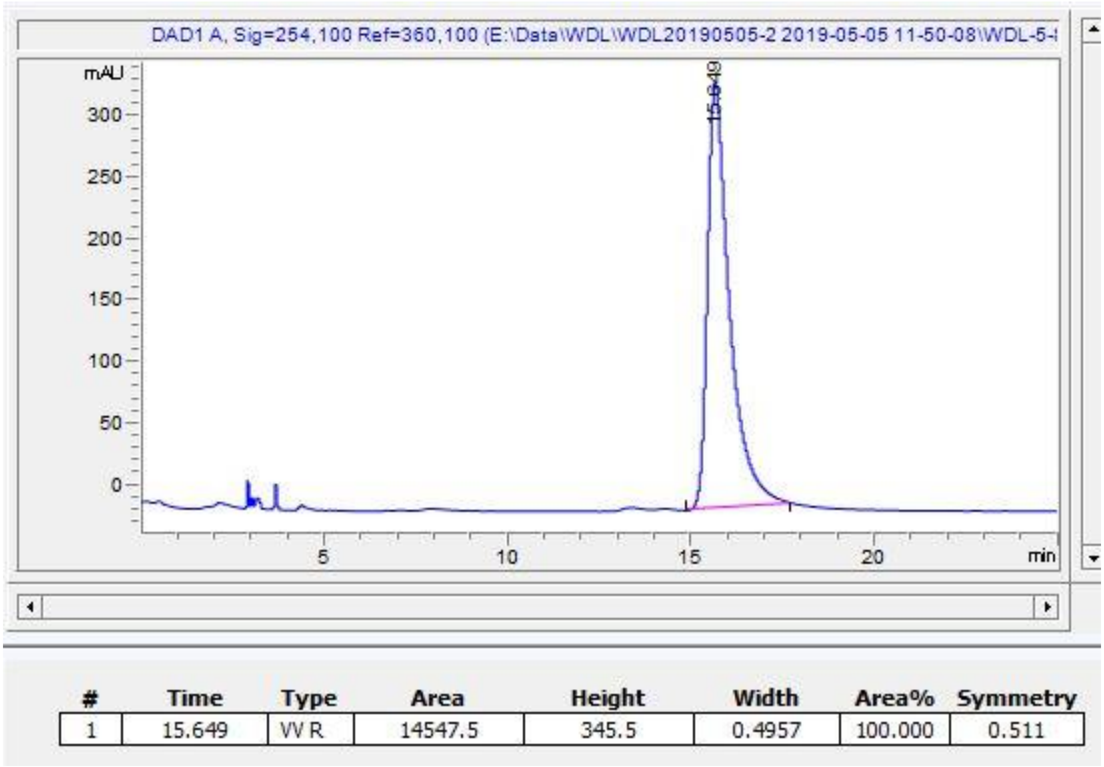

#	Time	Type	Area	Height	Width	Area%	Symmetry
1	15.649	VV R	14547.5	345.5	0.4957	100.000	0.511

Figure S100. HPLC spectrum of racemic-**16**, related to **Scheme 6**.

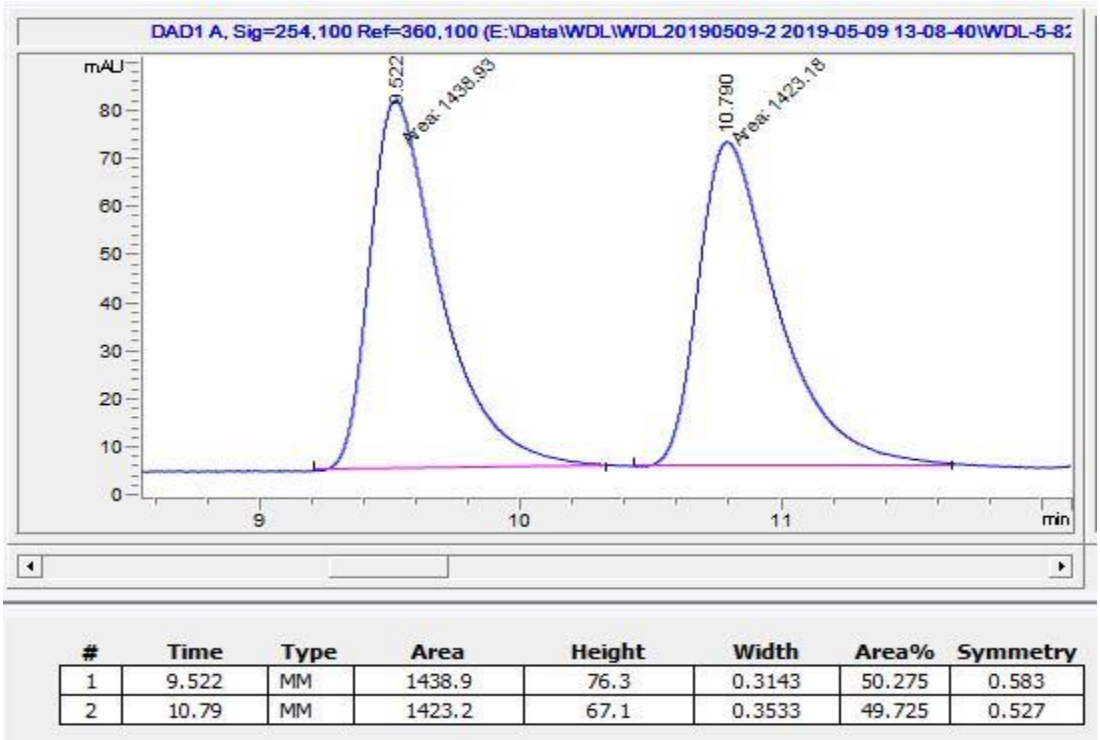

#	Time	Type	Area	Height	Width	Area%	Symmetry
1	9.522	MM	1438.9	76.3	0.3143	50.275	0.583
2	10.79	MM	1423.2	67.1	0.3533	49.725	0.527

Figure S101. HPLC spectrum of **16**, related to **Scheme 6**.

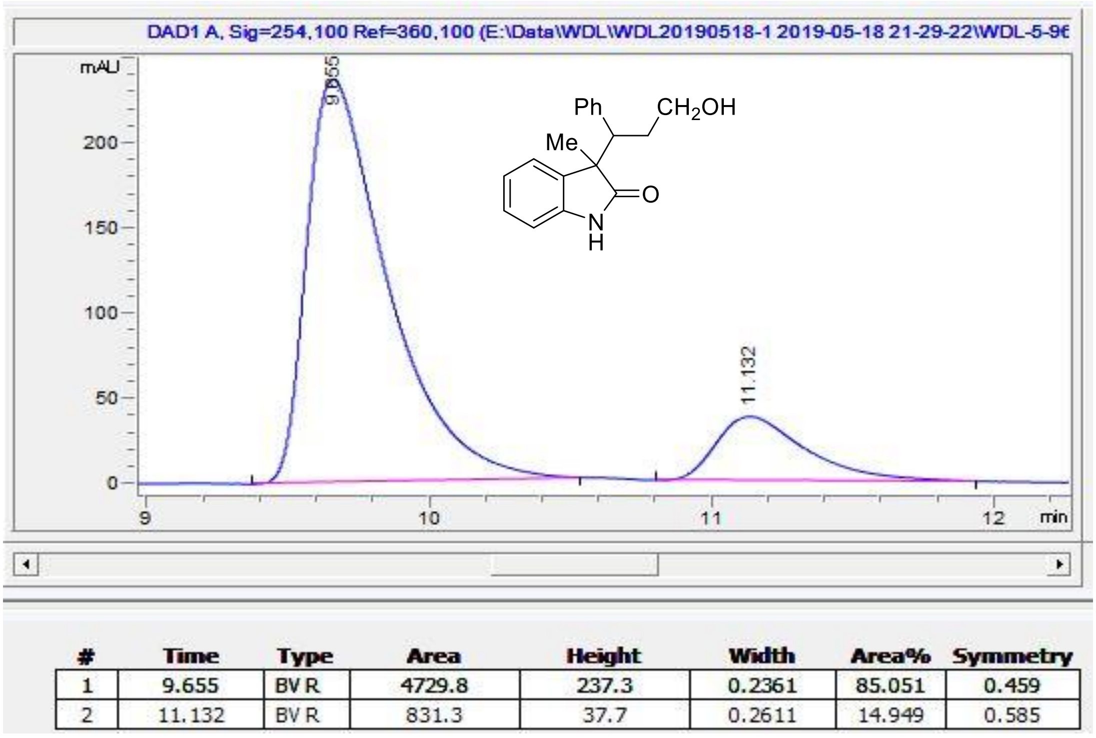

DAD1 A, Sig=254,100 Ref=360,100 (E:\Data\WDL\WDL20190518-1 2019-05-18 21-29-22\WDL-5-9

#	Time	Type	Area	Height	Width	Area%	Symmetry
1	9.655	BV R	4729.8	237.3	0.2361	85.051	0.459
2	11.132	BV R	831.3	37.7	0.2611	14.949	0.585

Figure S102. Full HPLC spectrum of **16**, related to **Scheme 6**.

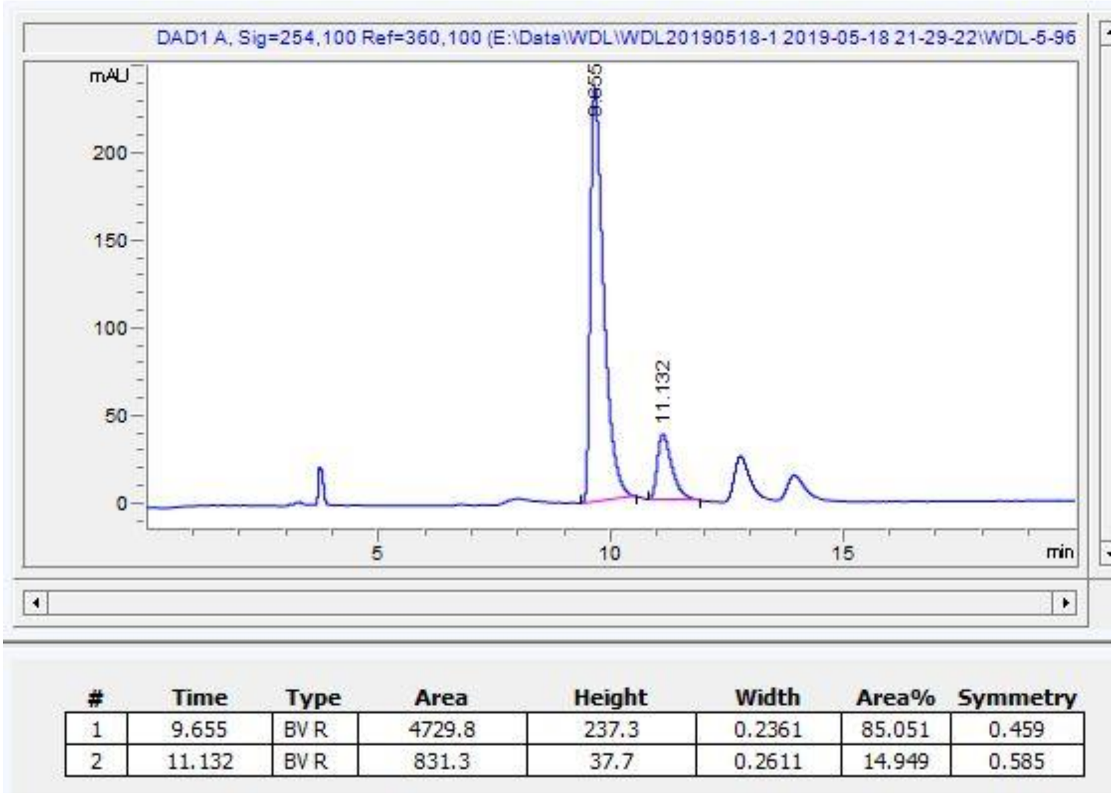

DAD1 A, Sig=254,100 Ref=360,100 (E:\Data\WDL\WDL20190518-1 2019-05-18 21-29-22\WDL-5-96

#	Time	Type	Area	Height	Width	Area%	Symmetry
1	9.655	BV R	4729.8	237.3	0.2361	85.051	0.459
2	11.132	BV R	831.3	37.7	0.2611	14.949	0.585

Supplemental Figures for NMR spectrums:

Figure S103. ^{1}H NMR spectrum of substrate **1a**, related to **Table 1**.

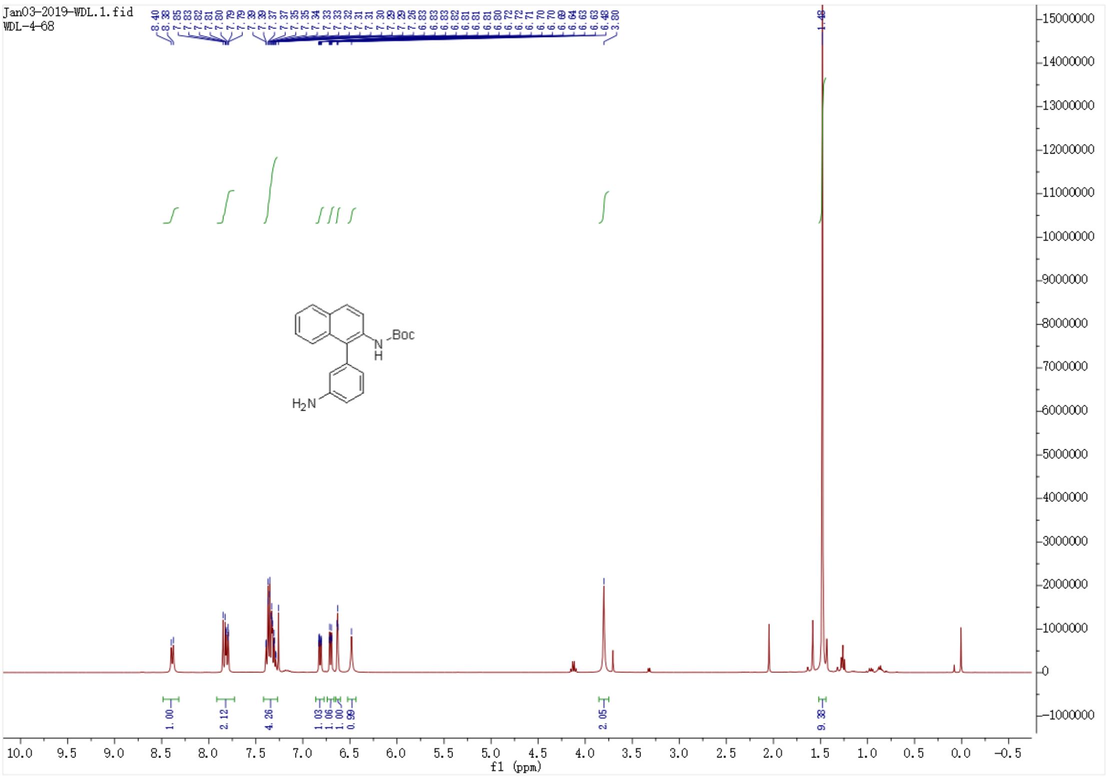

Figure S104. ^{13}C NMR spectrum of substrate **1a**, related to **Table 1**.

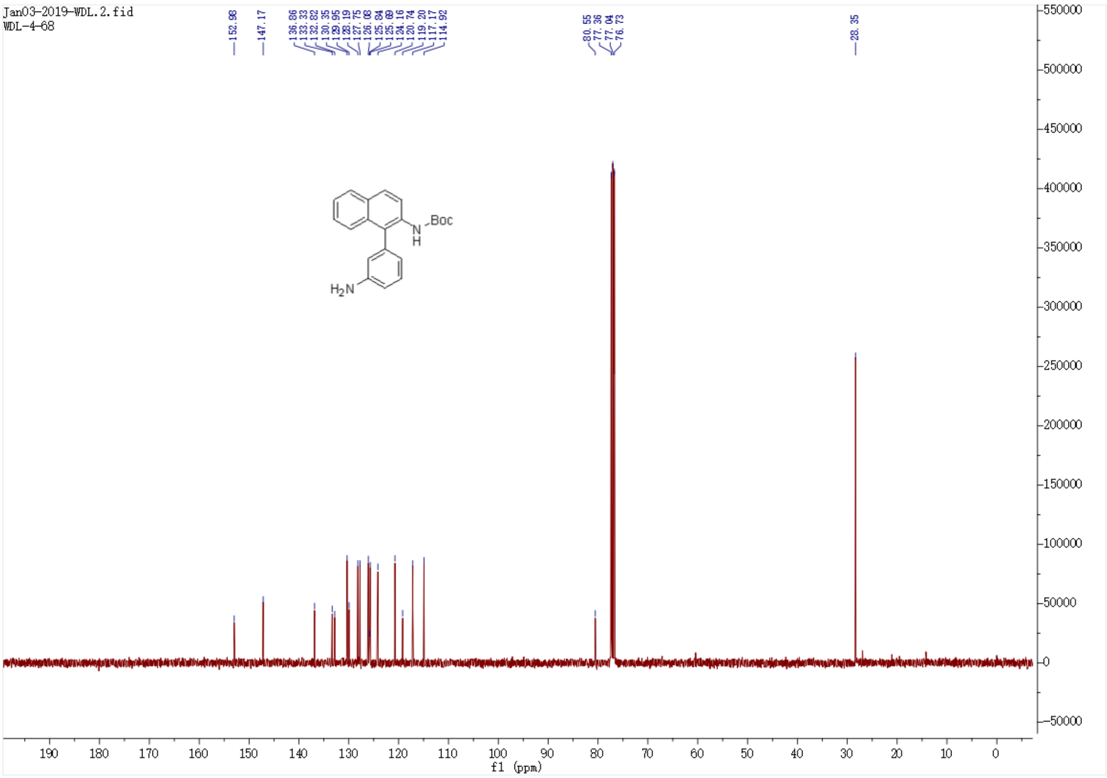

Figure S105. ^{1}H NMR spectrum of substrate **1b**, related to **Scheme 2**.

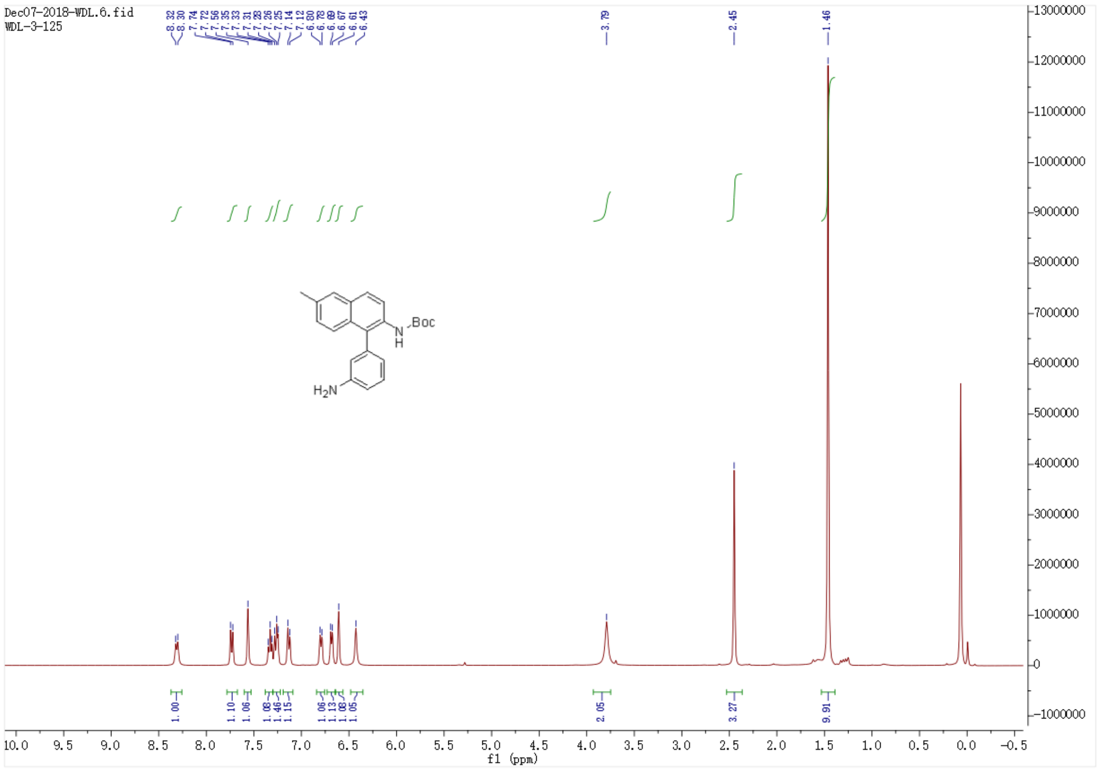

Figure S106. ^{13}C NMR spectrum of substrate **1b**, related to **Scheme 2**.

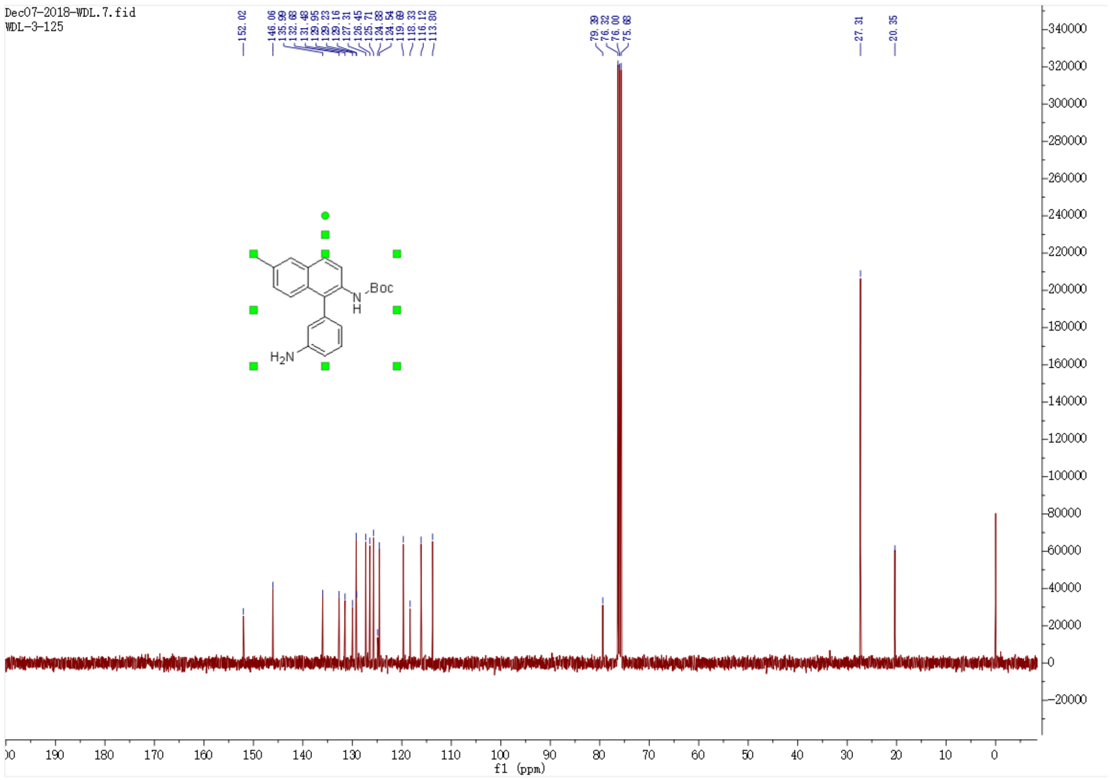

Figure S107. ^{1}H NMR spectrum of substrate **1c**, related to **Scheme 2**.

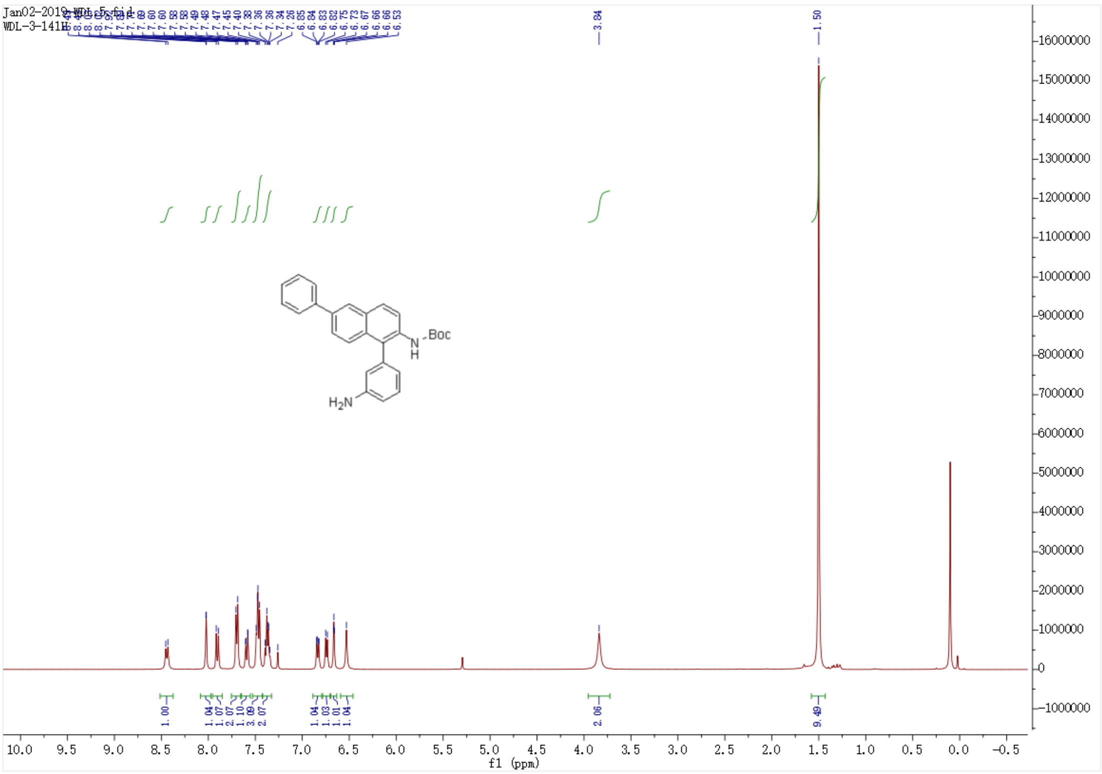

Figure S108. ^{13}C NMR spectrum of substrate **1c**, related to **Scheme 2**.

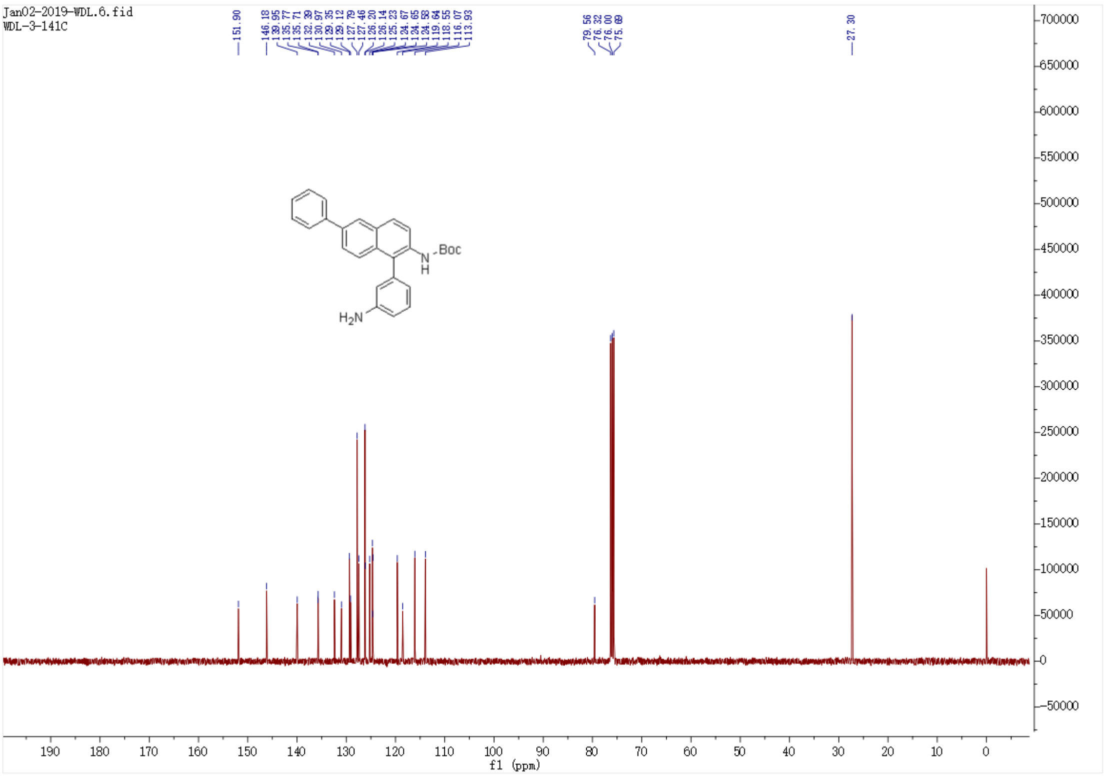

Figure S109. ^{1}H NMR spectrum of substrate **1d**, related to **Scheme 2**.

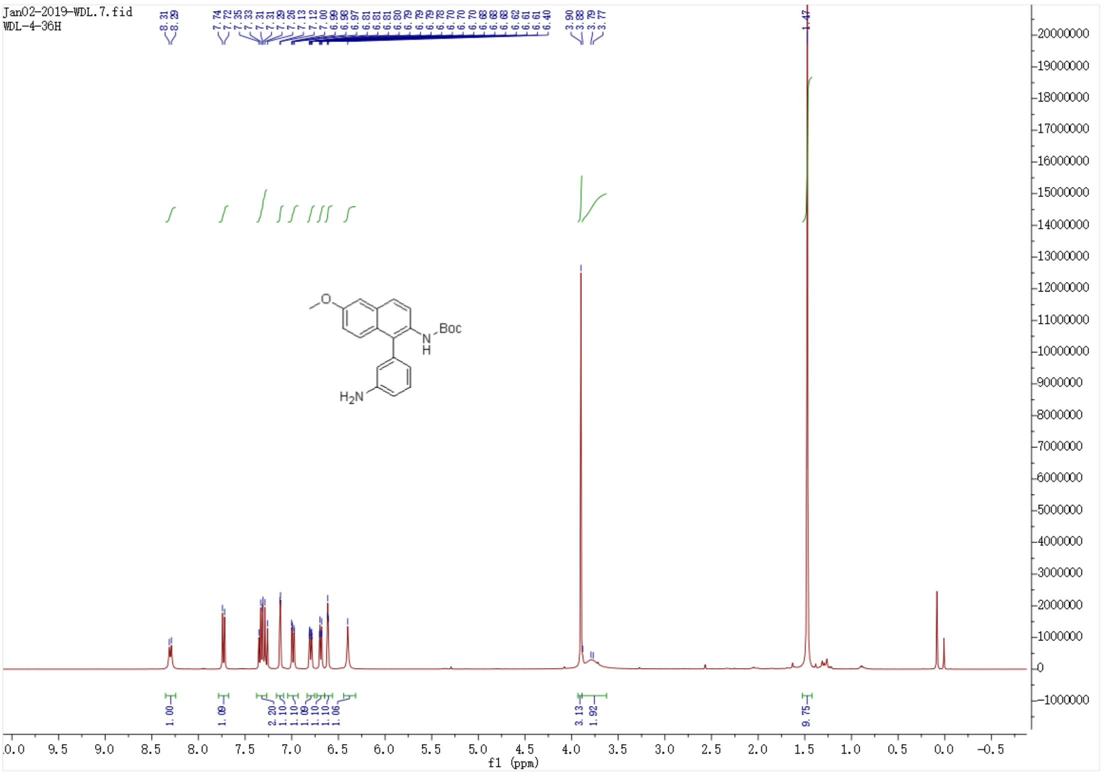

Figure S110. ^{13}C NMR spectrum of substrate **1d**, related to **Scheme 2**.

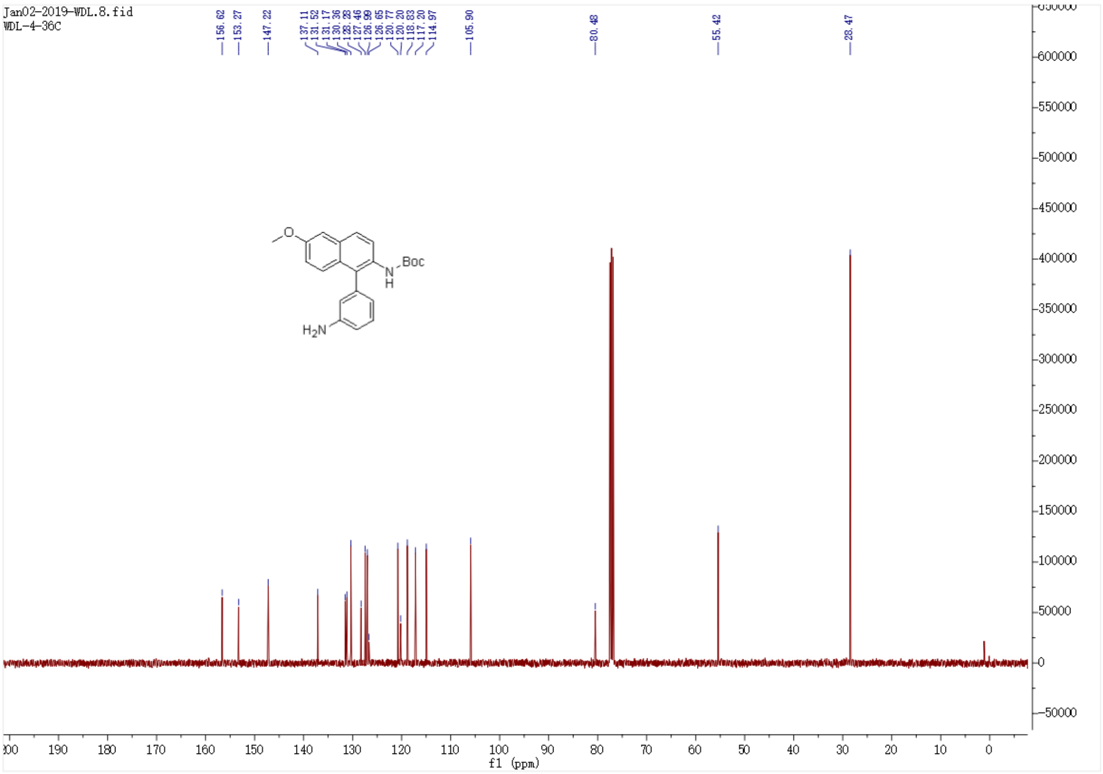

Figure S111. ^{1}H NMR spectrum of substrate **1e**, related to **Scheme 2**.

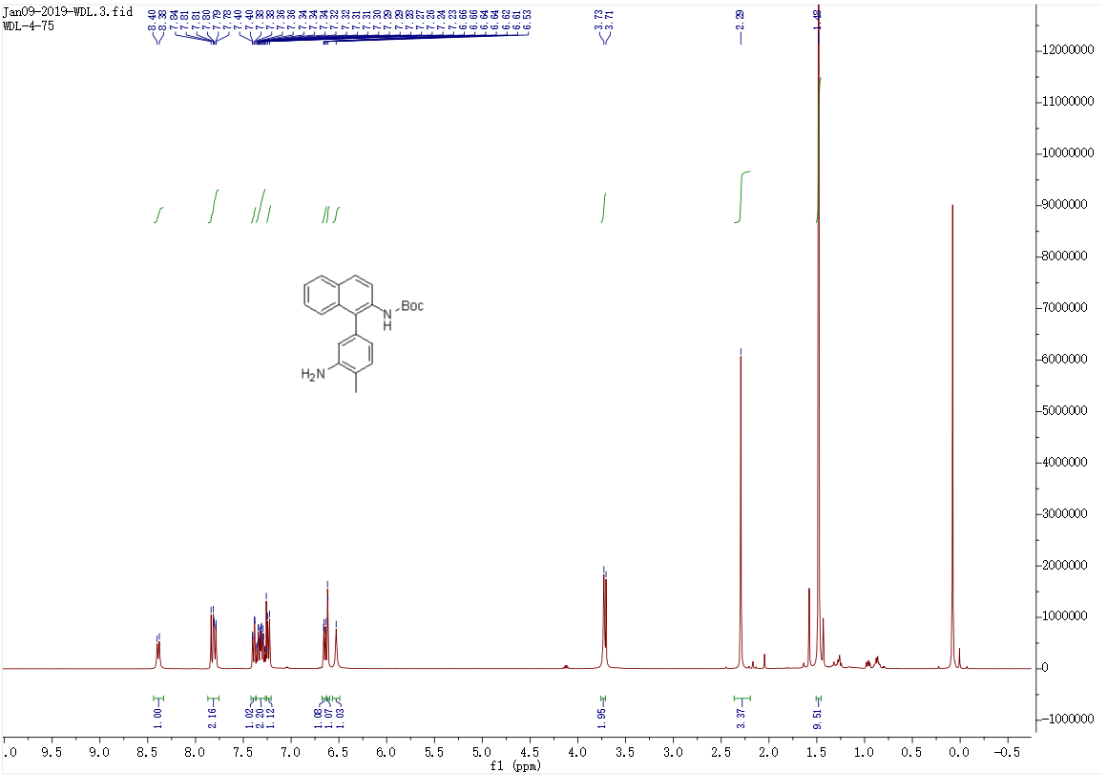

Figure S112. ^{13}C NMR spectrum of substrate **1e**, related to **Scheme 2**.

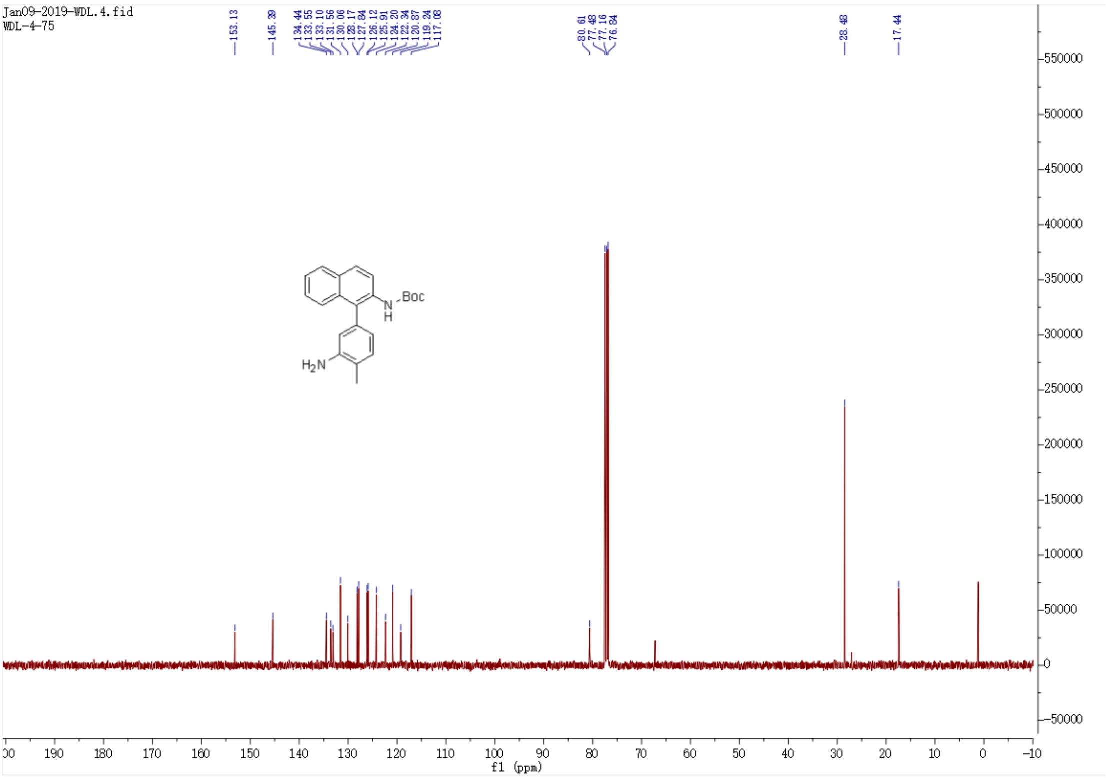

Figure S113. ^{1}H NMR spectrum of substrate **1f**, related to **Scheme 2**.

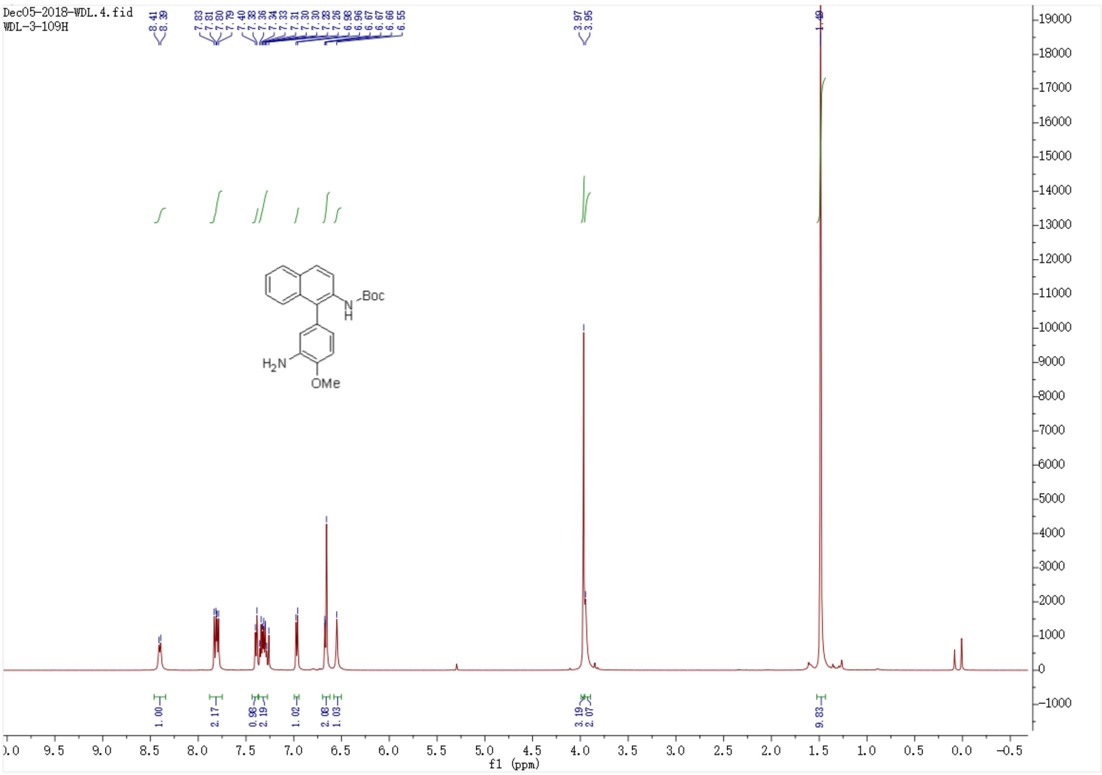

Figure S114. ^{13}C NMR spectrum of substrate **1f**, related to **Scheme 2**.

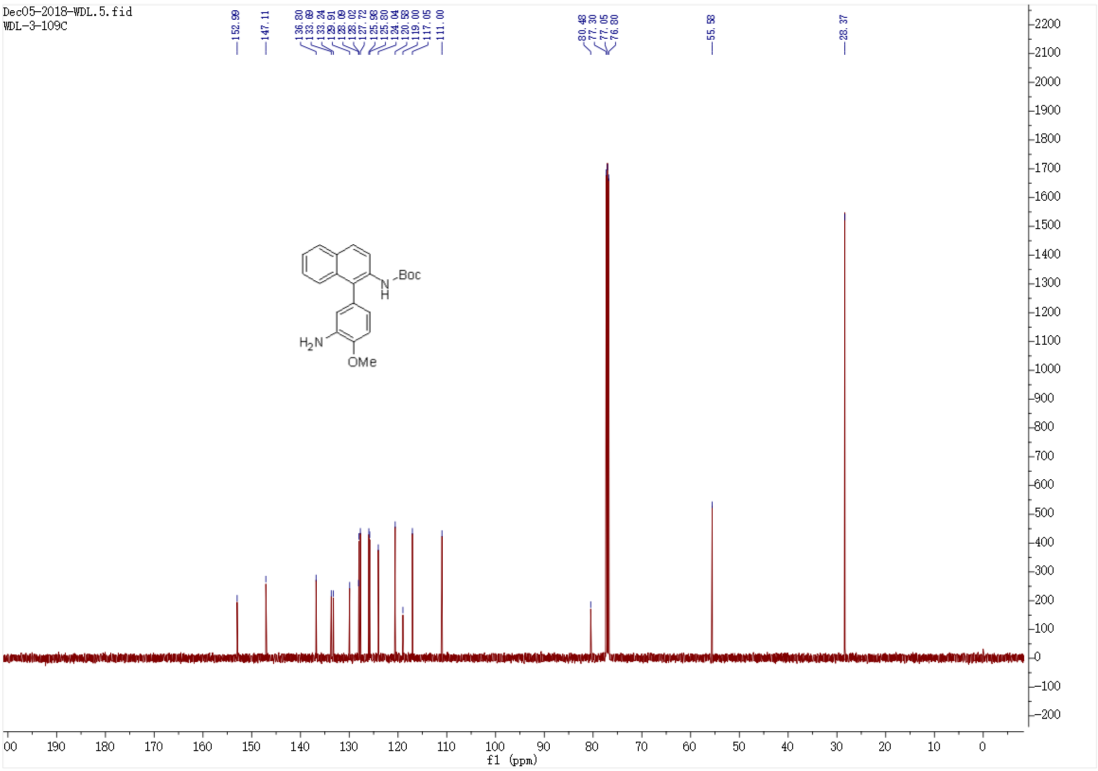

Figure S115. ^{1}H NMR spectrum of substrate **1g**, related to **Scheme 2**.

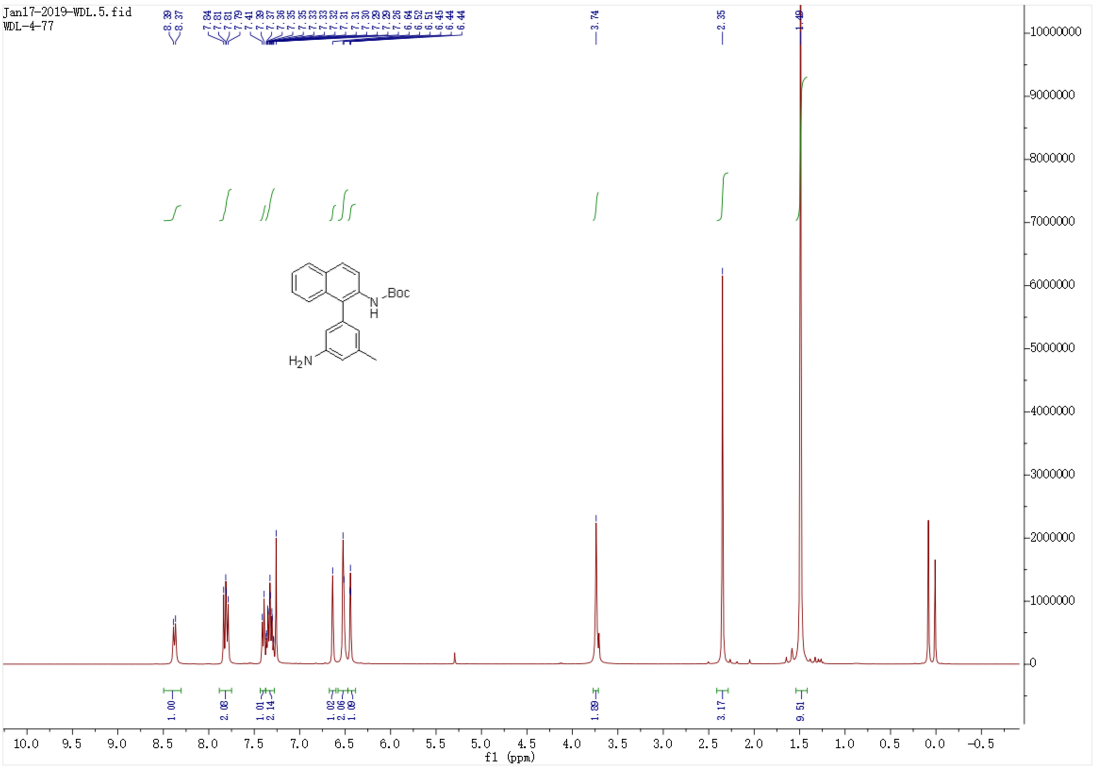

Figure S116. ^{13}C NMR spectrum of substrate **1g**, related to **Scheme 2**.

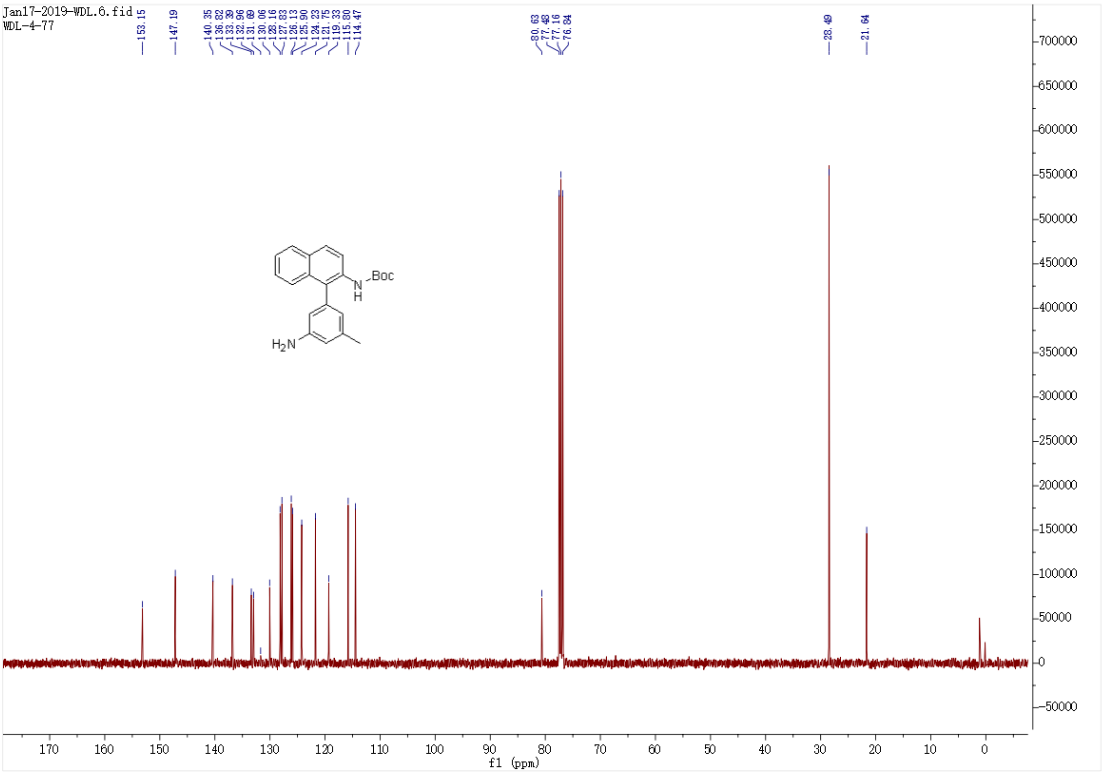

Figure S117. ^{1}H NMR spectrum of substrate **1h**, related to **Scheme 2**.

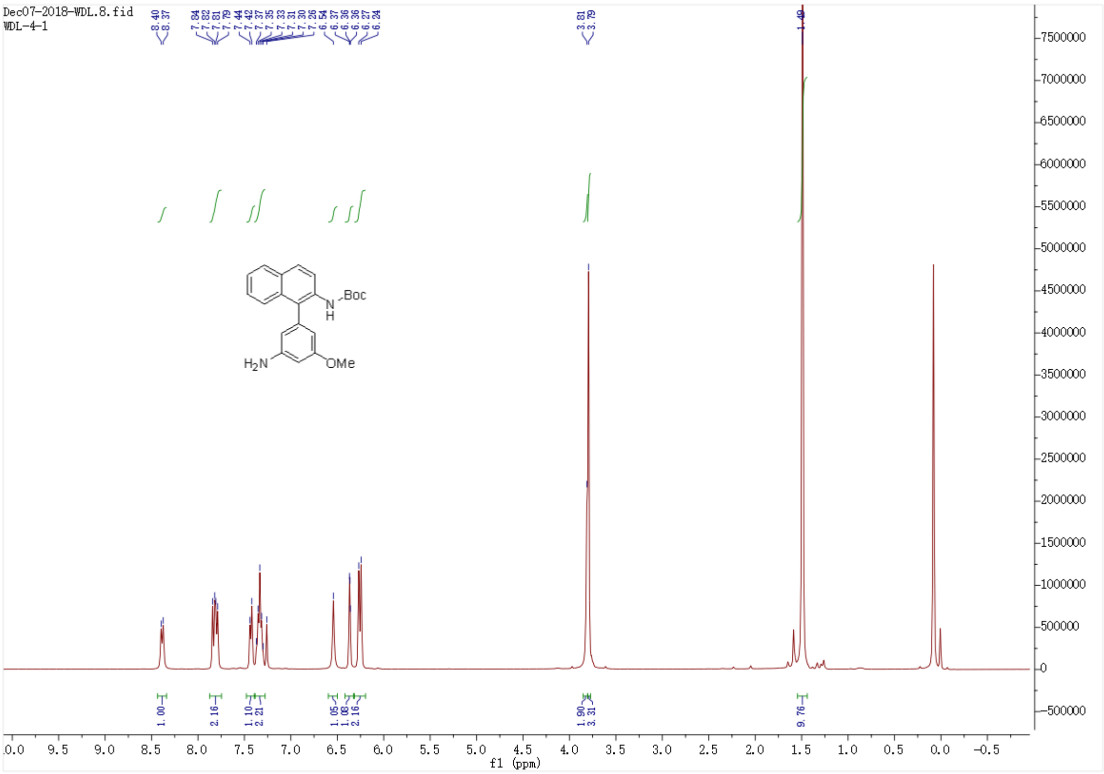

Figure S118. ^{13}C NMR spectrum of substrate **1h**, related to **Scheme 2**.

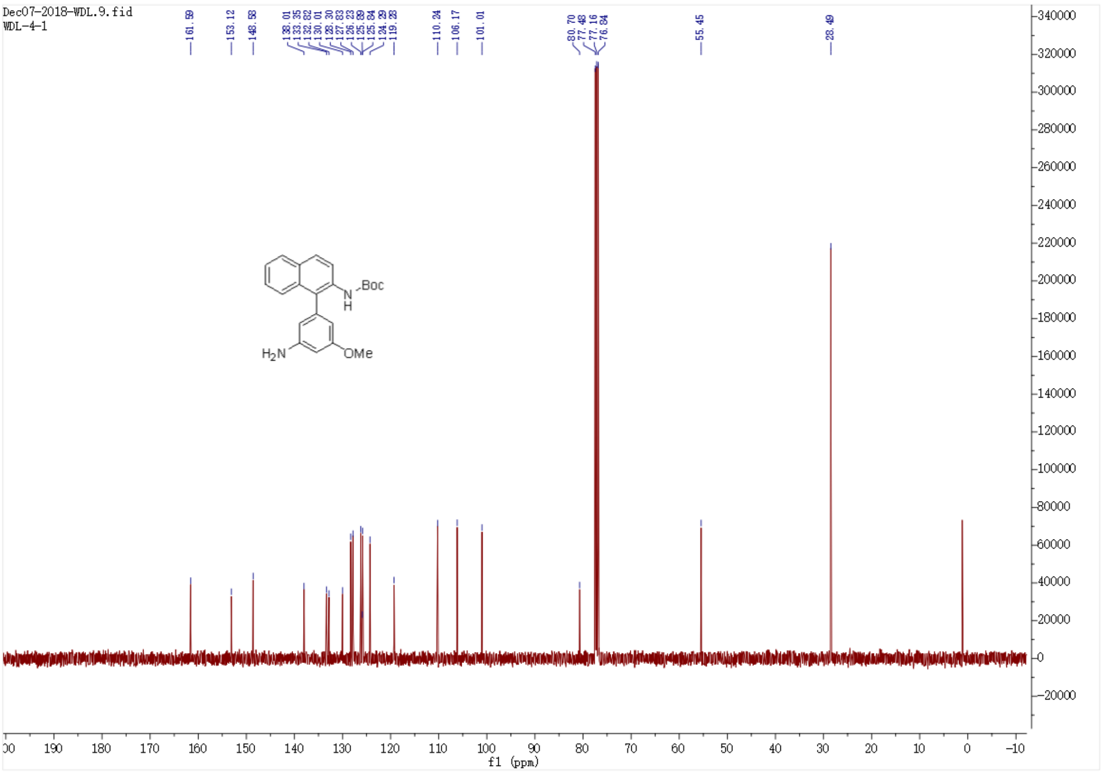

Figure S119. ^{1}H NMR spectrum of substrate **1i**, related to **Scheme 2**.

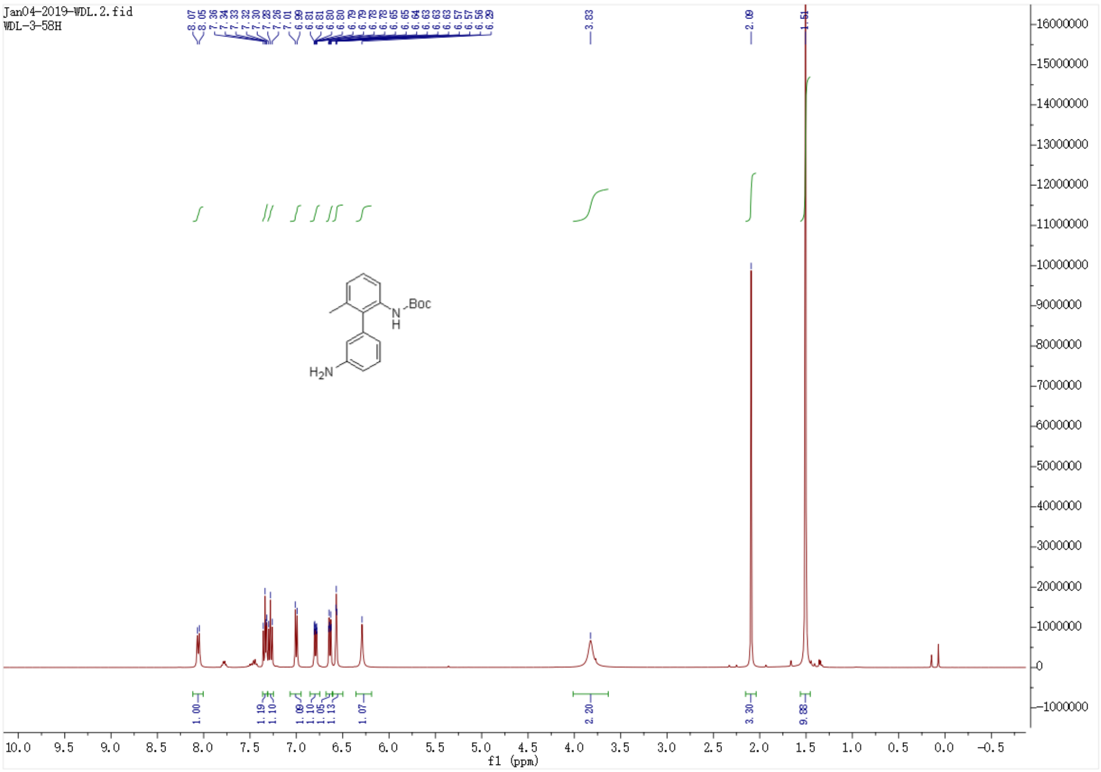

Figure S120. ^{13}C NMR spectrum of substrate **1i**, related to **Scheme 2**.

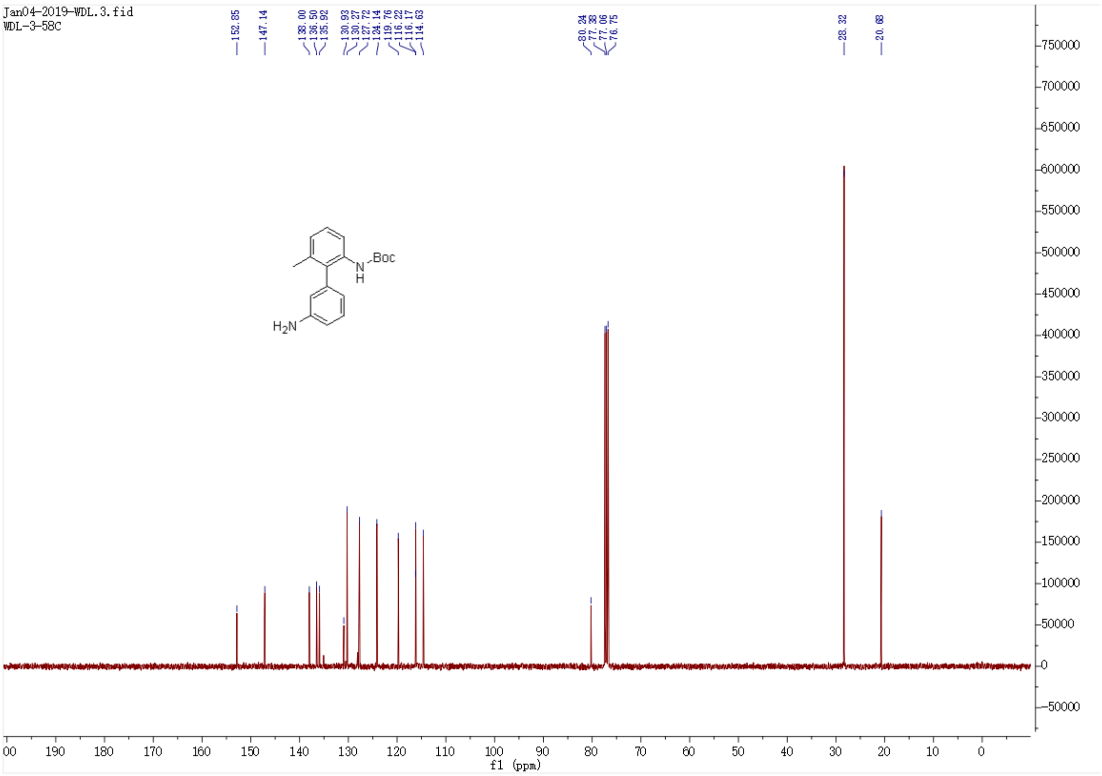

Figure S121. ^{1}H NMR spectrum of substrate **1j**, related to **Scheme 2**.

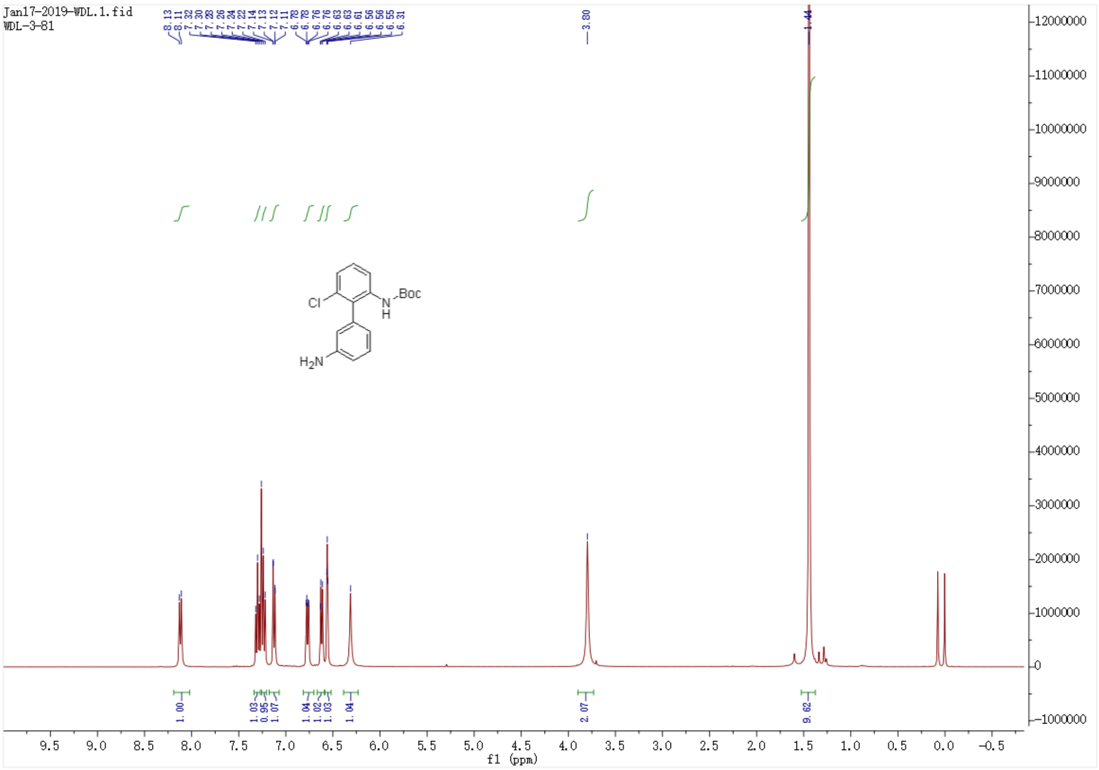

Figure S122. ^{13}C NMR spectrum of substrate **1j**, related to **Scheme 2**.

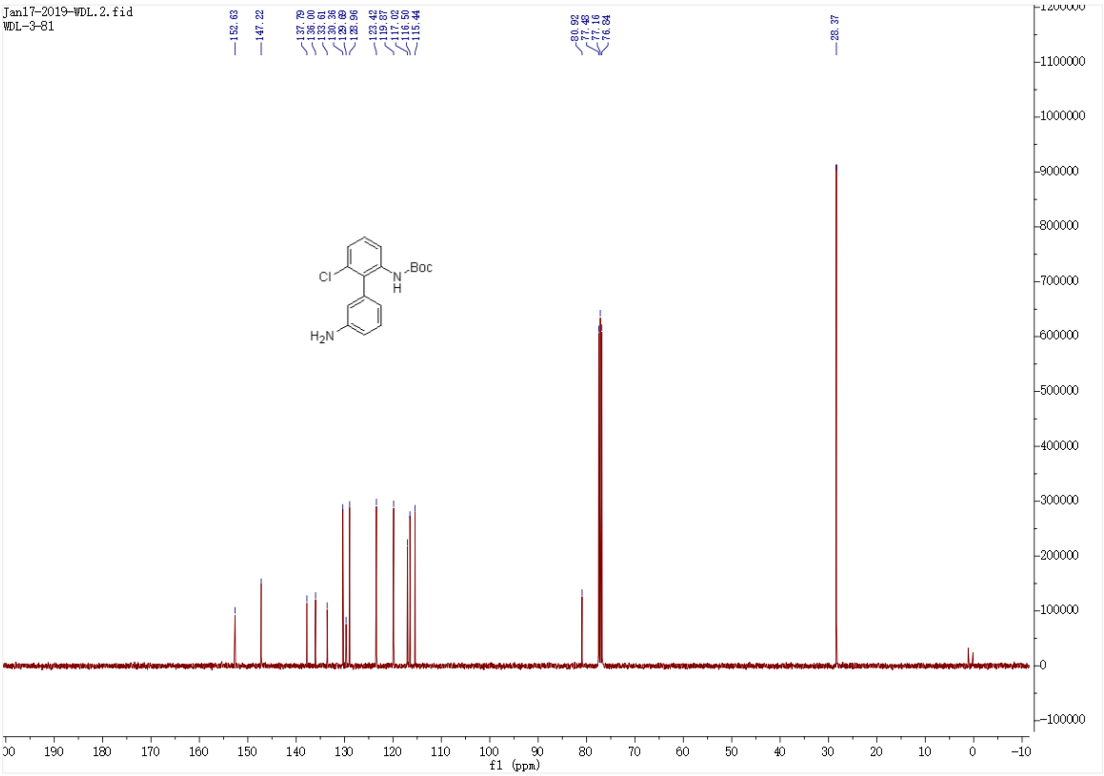

Figure S123. ^{1}H NMR spectrum of substrate **1k**, related to **Scheme 2**.

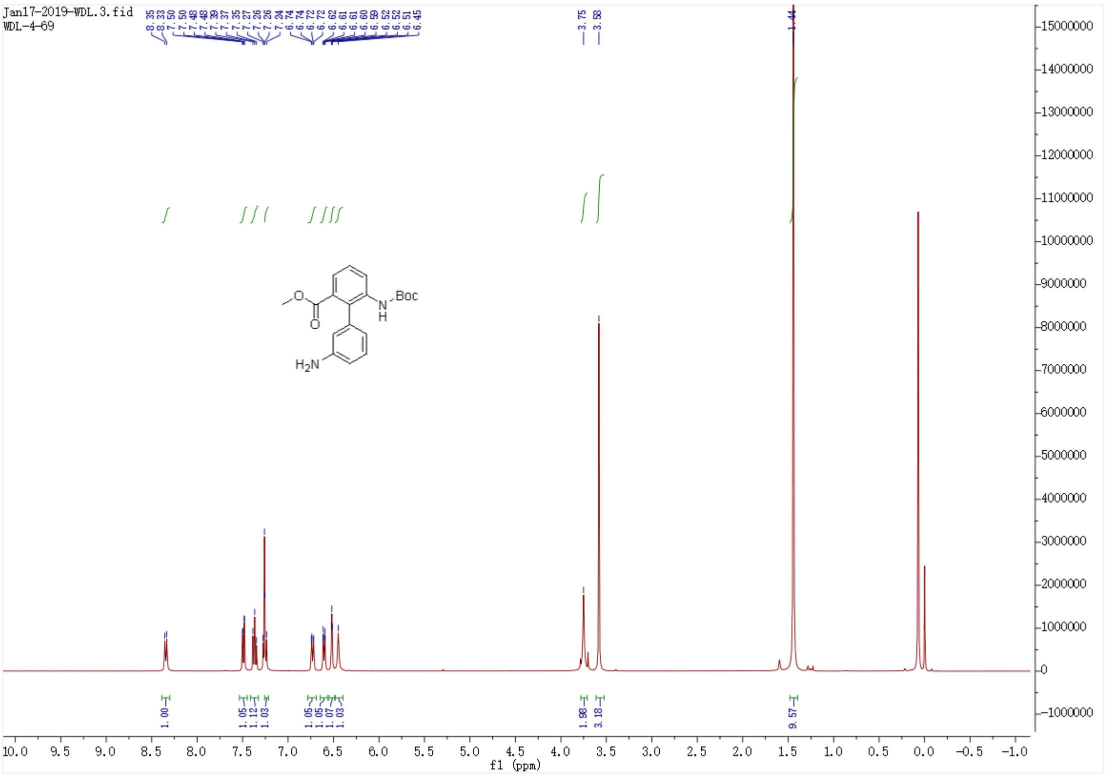

Figure S124. ^{13}C NMR spectrum of substrate **1k**, related to **Scheme 2**.

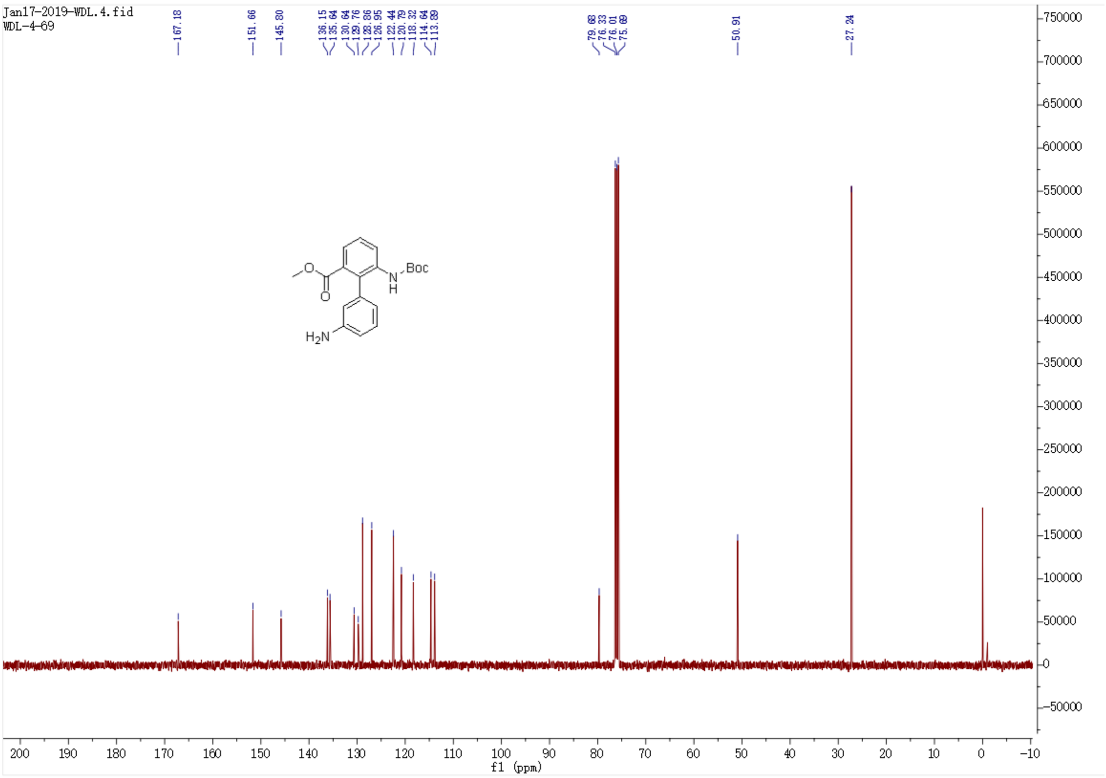

Figure S125. ^{1}H NMR spectrum of substrate **1l**, related to **Scheme 2**.

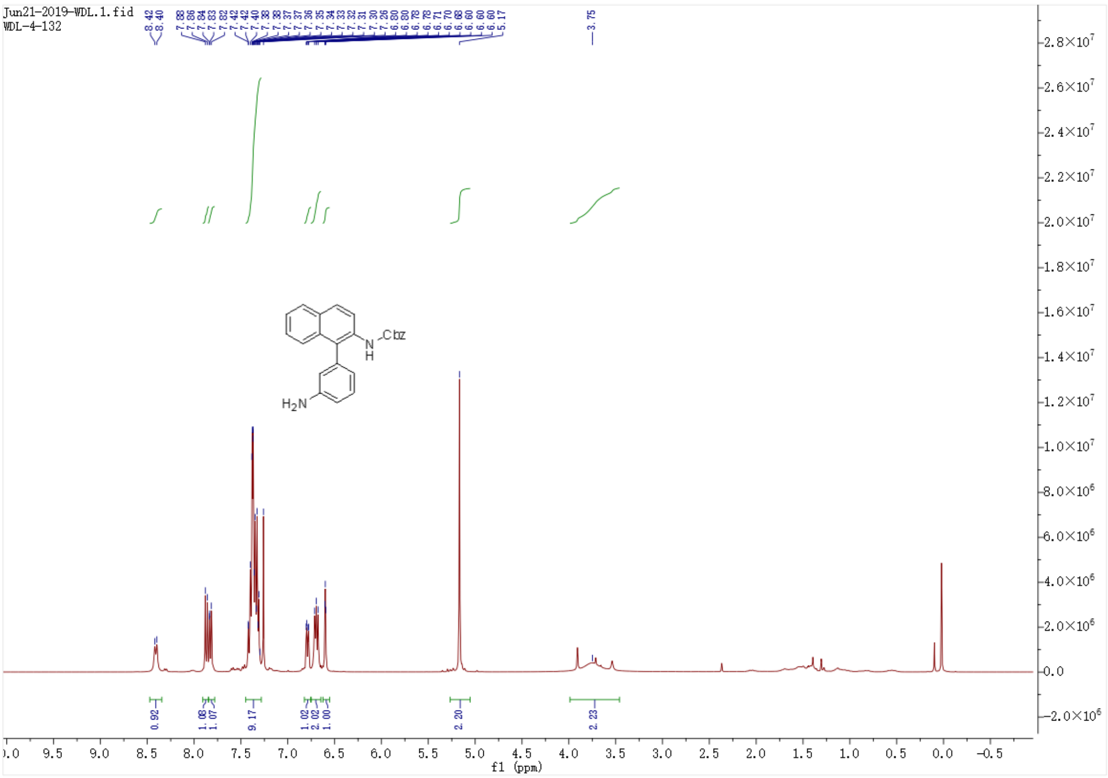

Figure S126. ^{13}C NMR spectrum of substrate **1l**, related to **Scheme 2**.

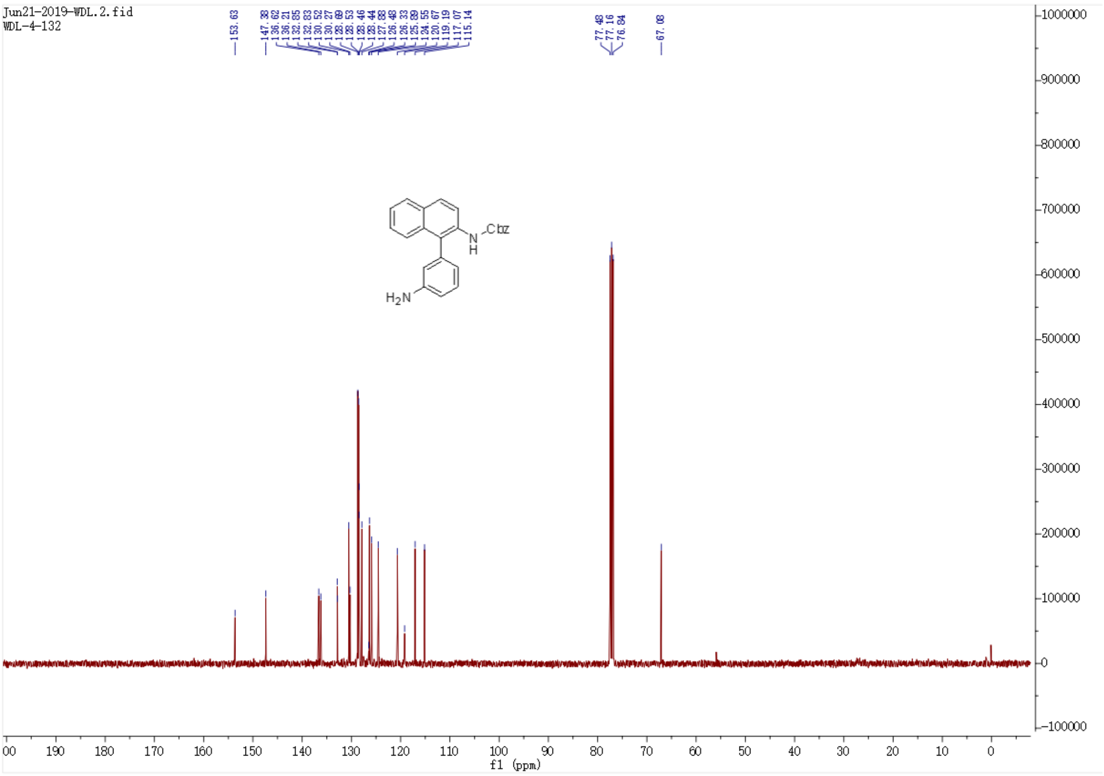

Figure S127. ^{1}H NMR spectrum of substrate **1m**, related to **Scheme 3.**.

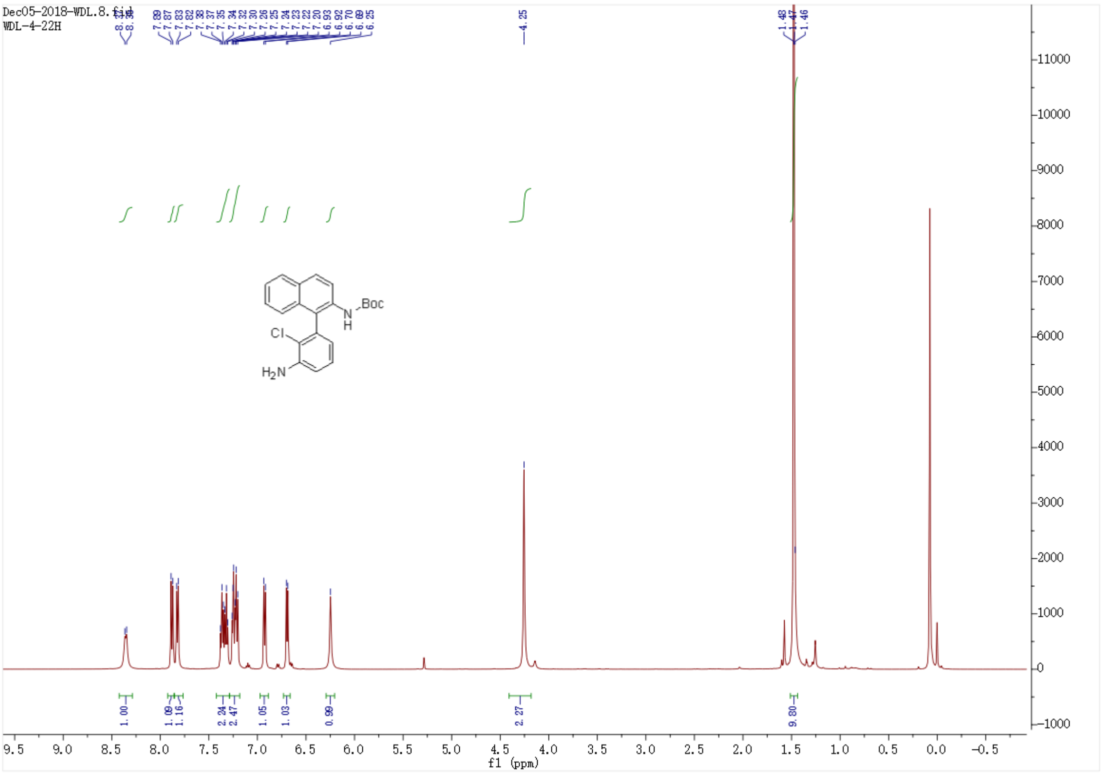

Figure S128. ^{13}C NMR spectrum of substrate **1m**, related to **Scheme 3.**.

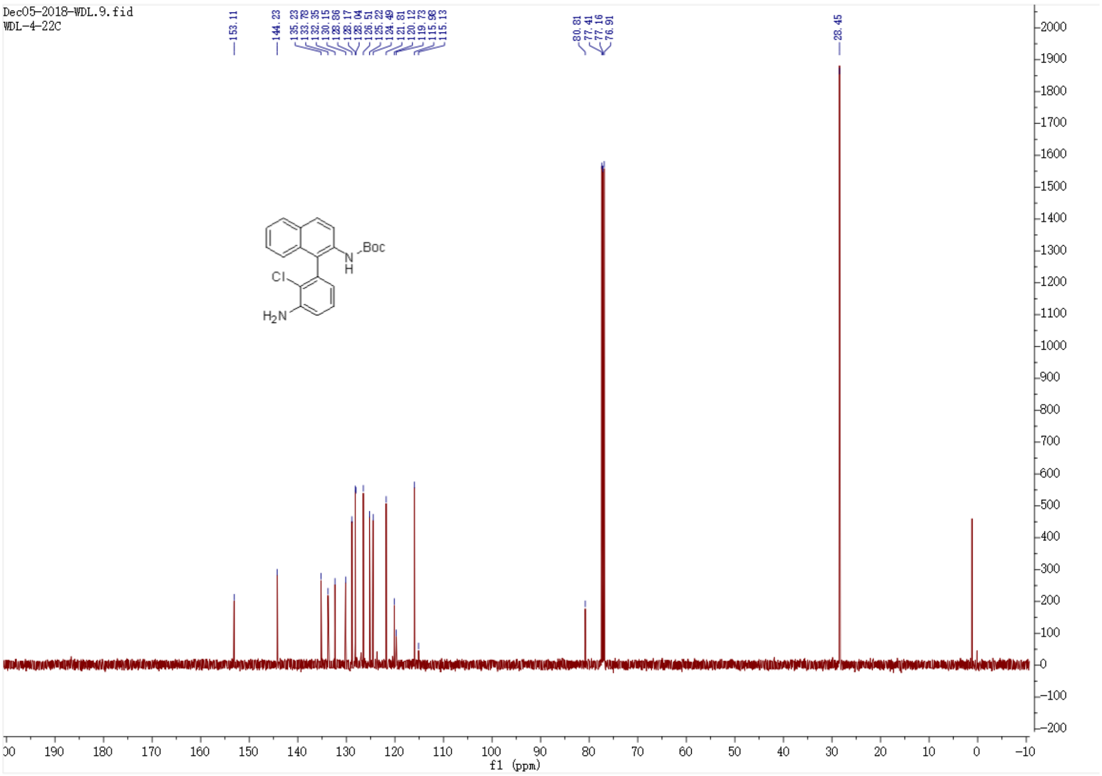

Figure S129. ^{1}H NMR spectrum of substrate **1n**, related to **Scheme 3.**.

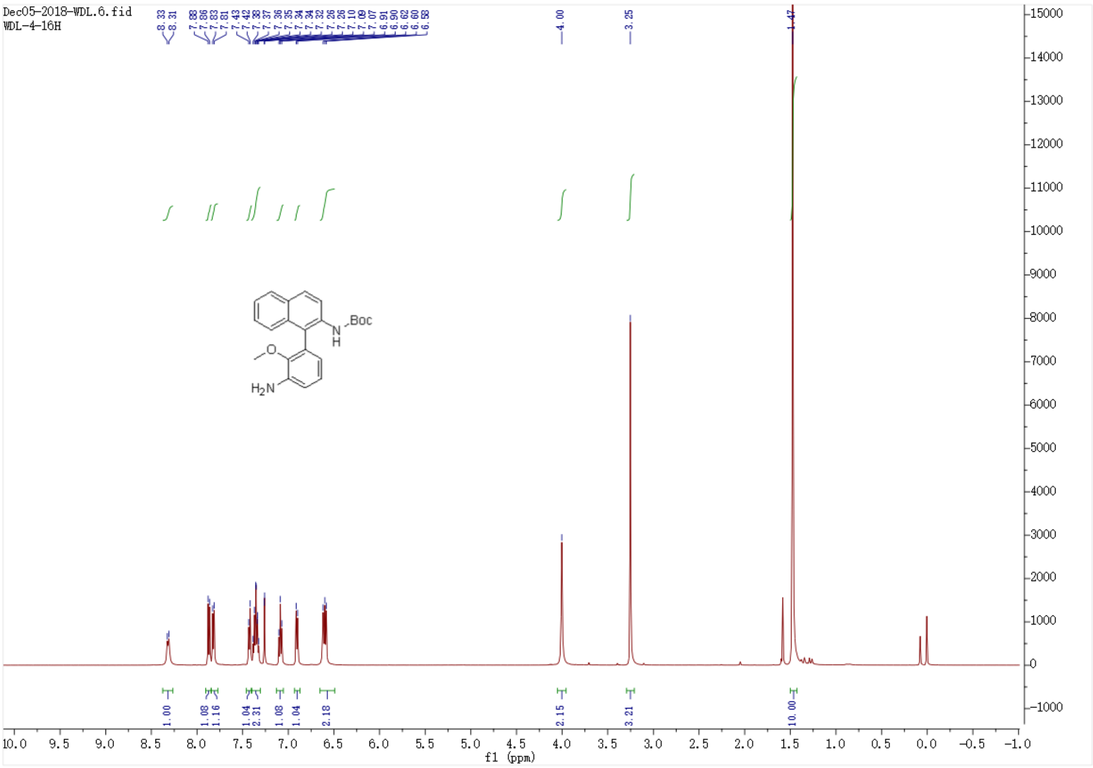

Figure S130. ^{13}C NMR spectrum of substrate **1n**, related to **Scheme 3.**.

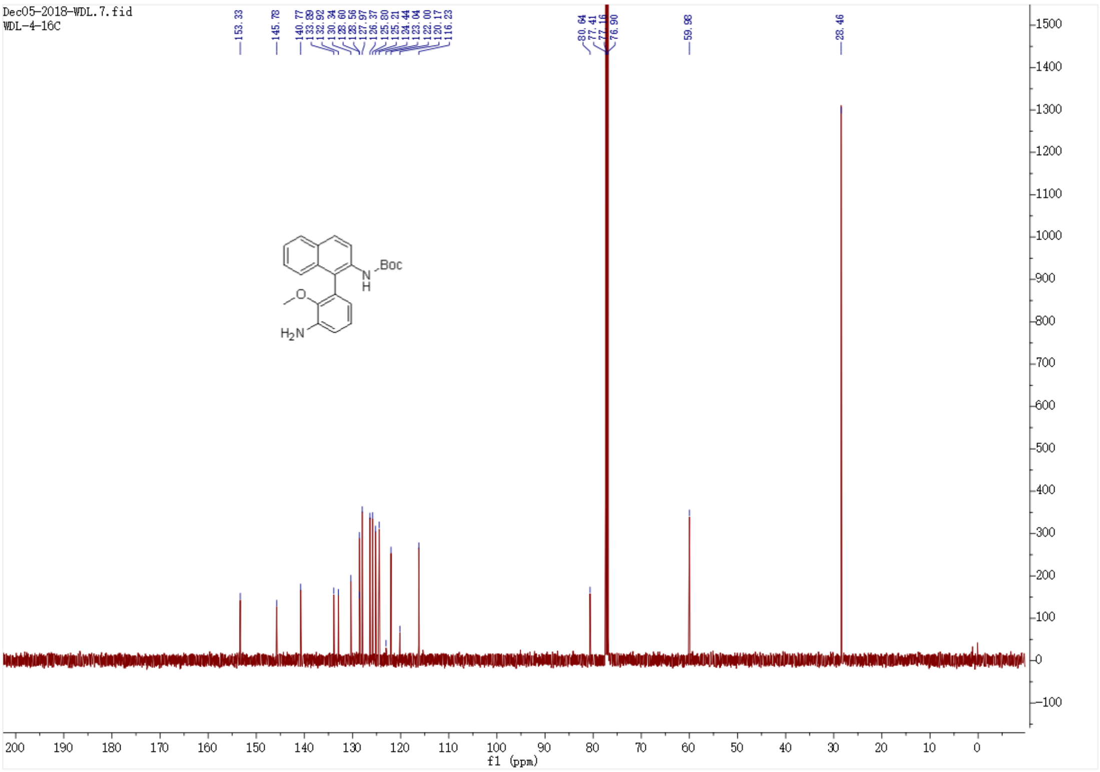

Figure S131. ^{1}H NMR spectrum of substrate **1o**, related to **Scheme 3.**.

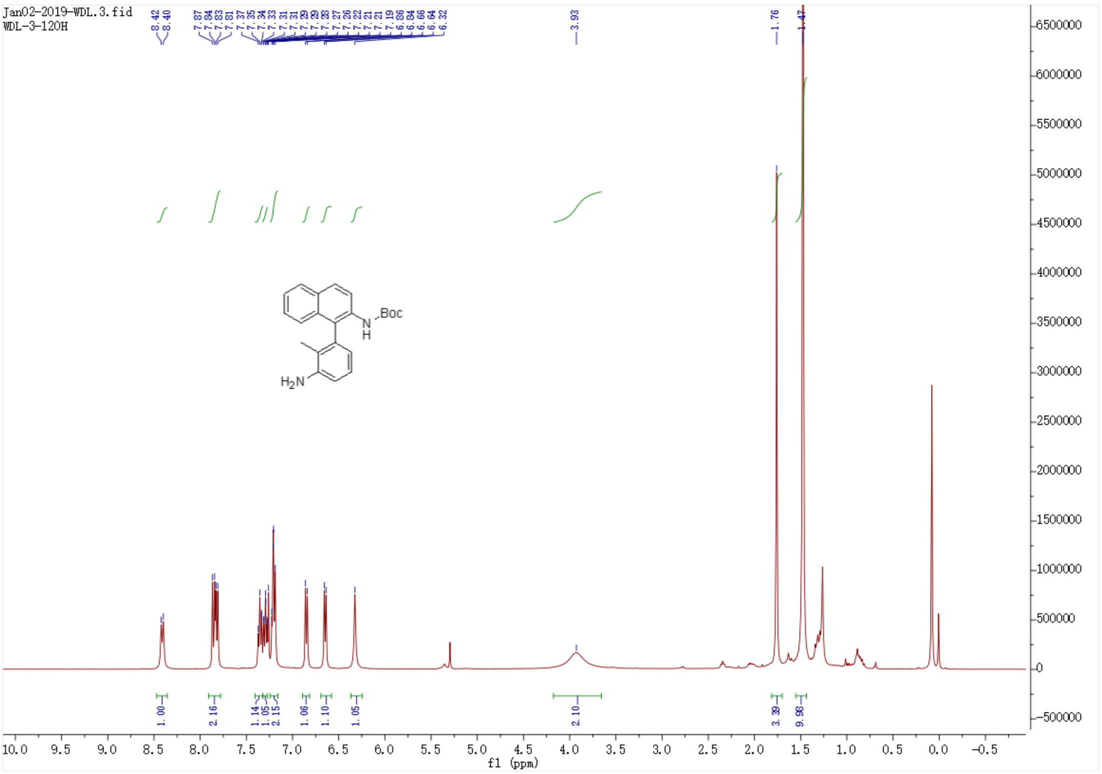

Figure S132. ^{13}C NMR spectrum of substrate **1o**, related to **Scheme 3.**.

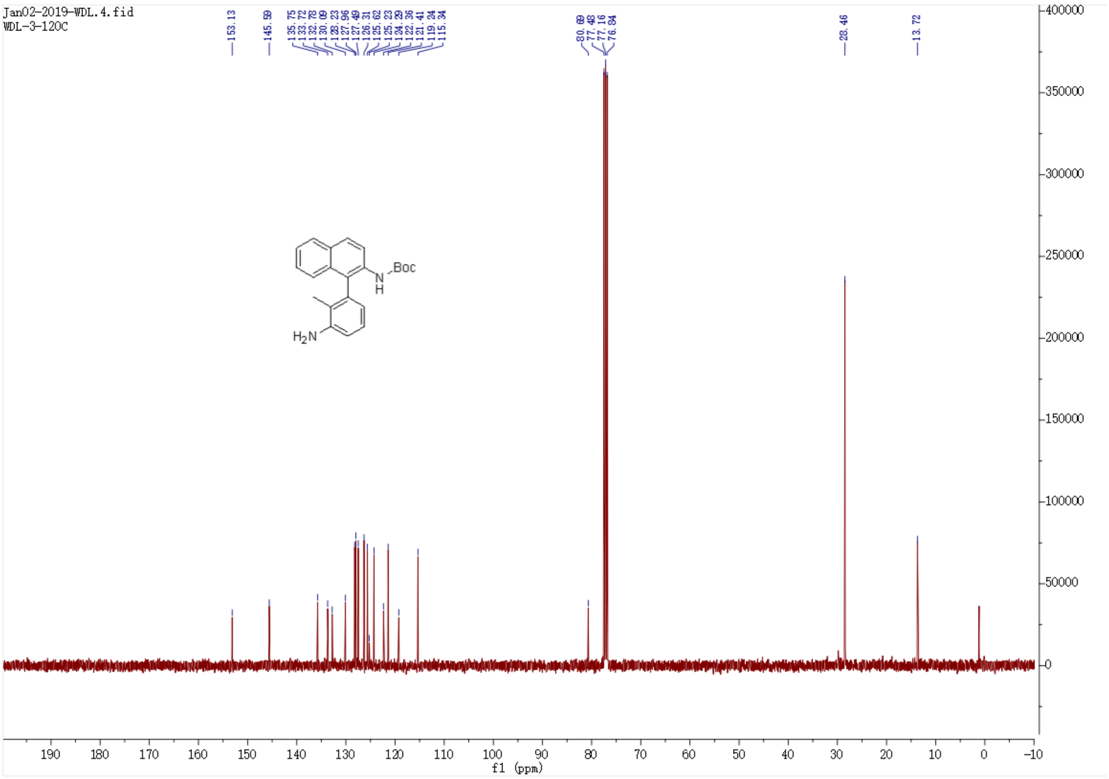

Figure S133. ^{1}H NMR spectrum of substrate **1p**, related to **Scheme 3.**.

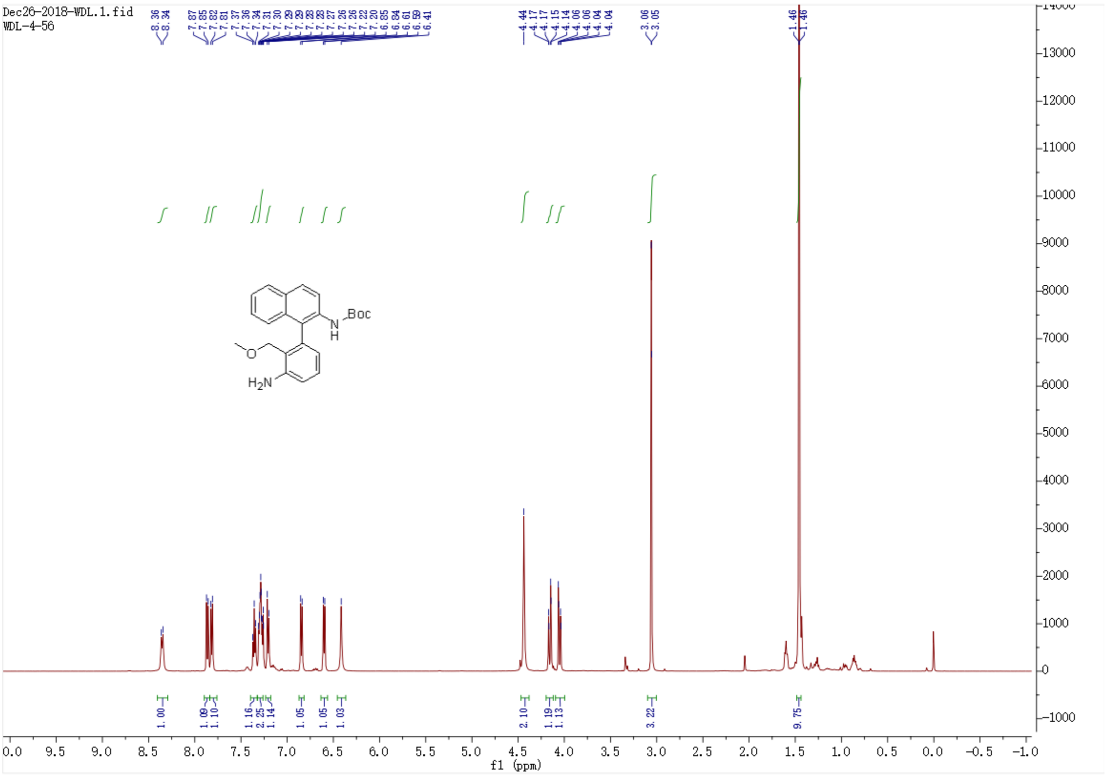

Figure S134. ^{13}C NMR spectrum of substrate **1p**, related to **Scheme 3.**.

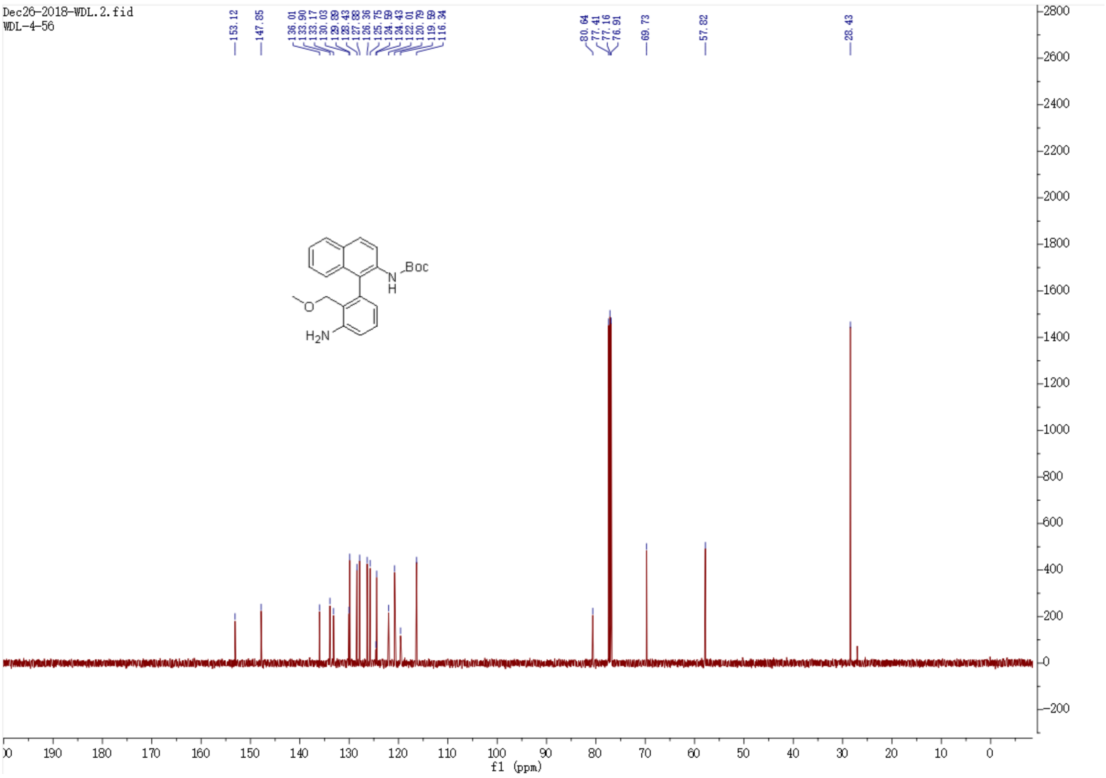

Figure S135. ^{1}H NMR spectrum of product **3a** at **room temperature**, related to **Table 1**.

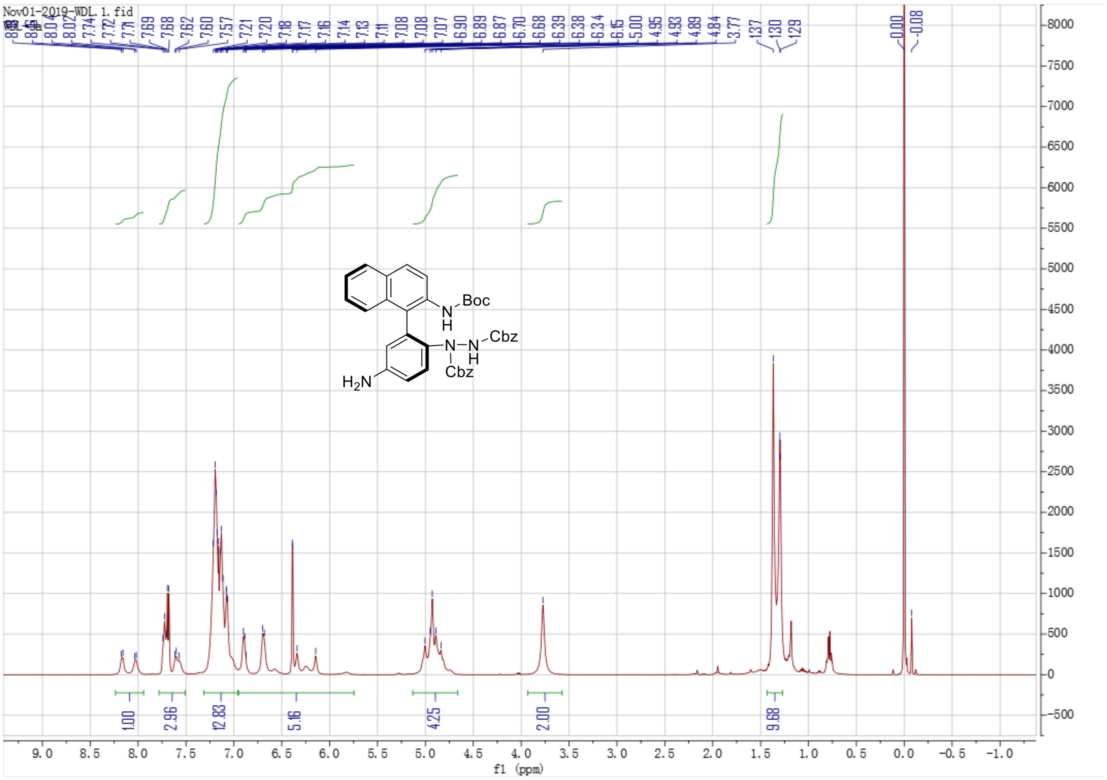

Figure S136. ^{13}C NMR spectrum of product **3a** at **room temperature**, related to **Table 1**.

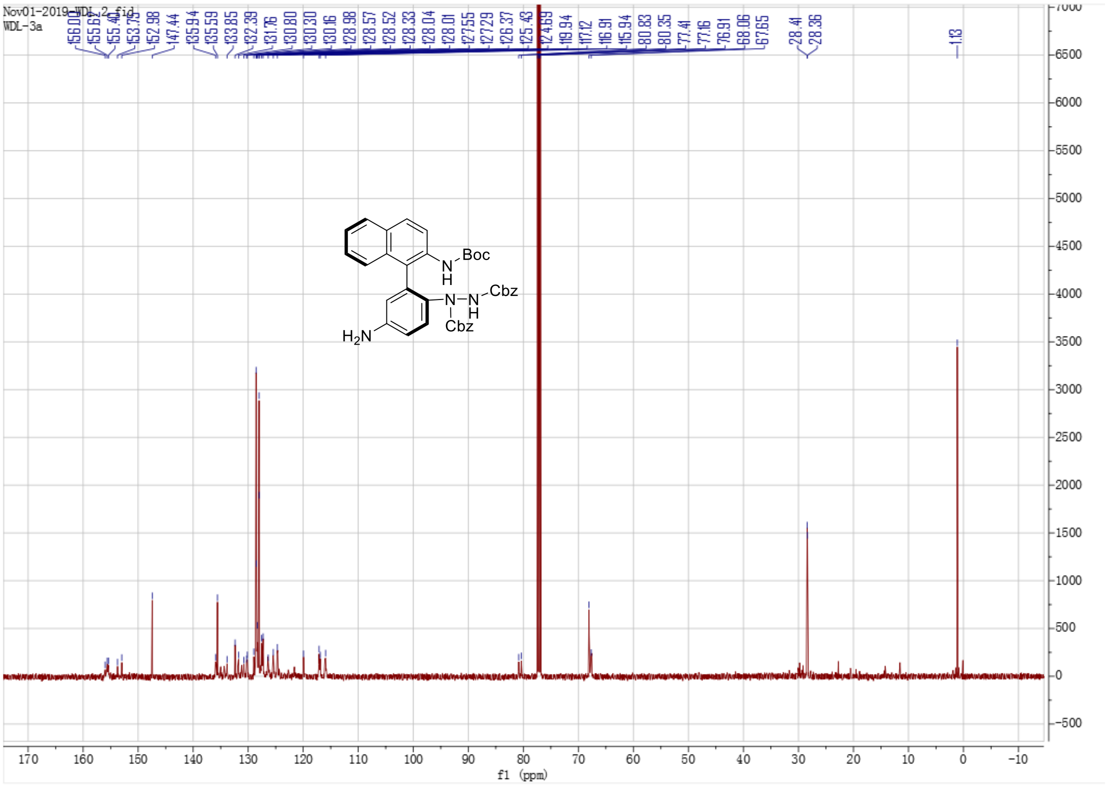

Figure S137. ^{1}H NMR spectrum of product **3a** at **45 °C**, related to **Table 1**.

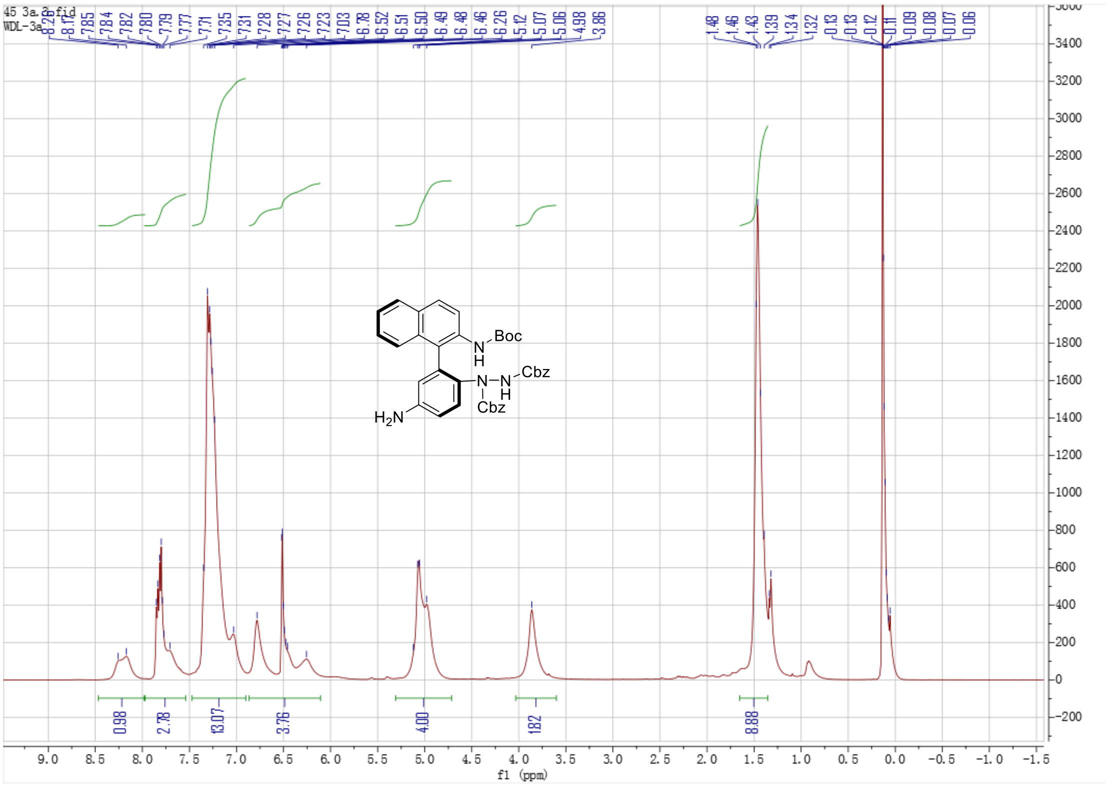

Figure S138. ^{13}C NMR spectrum of product **3a** at **45** °C, related to **Table 1**.

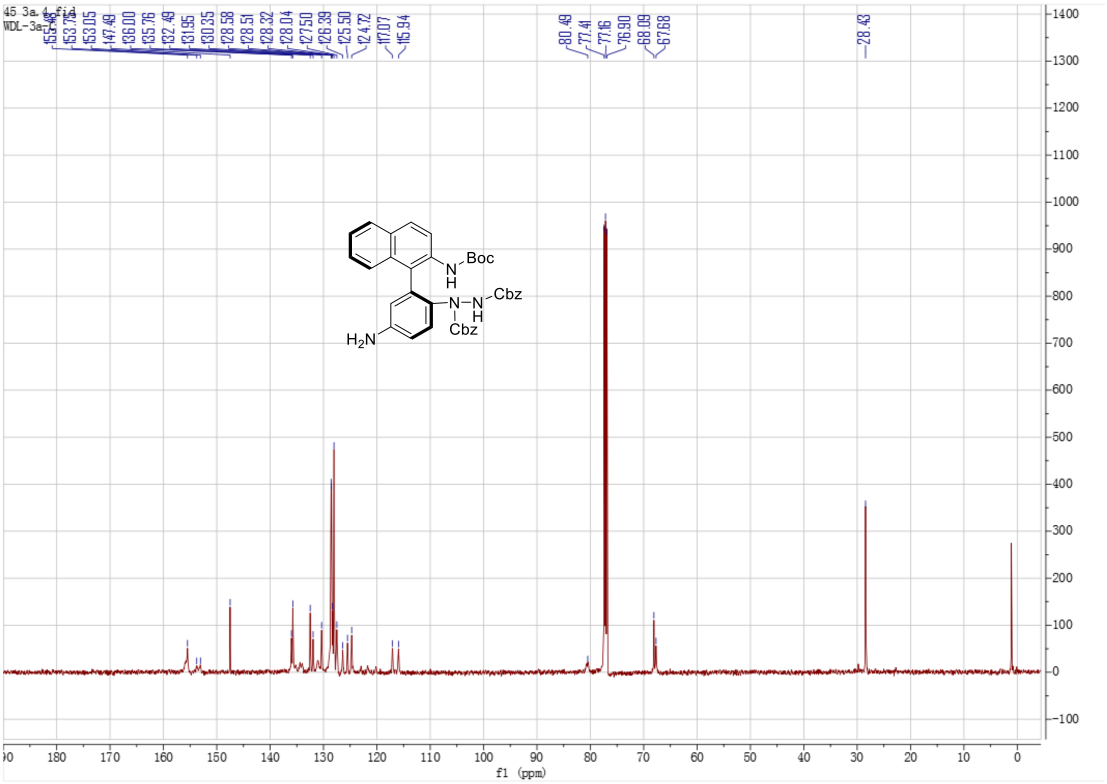

Figure S139. ^{1}H NMR spectrum of product **3a** at **-50 ^{o}C**, related to **Table 1**.

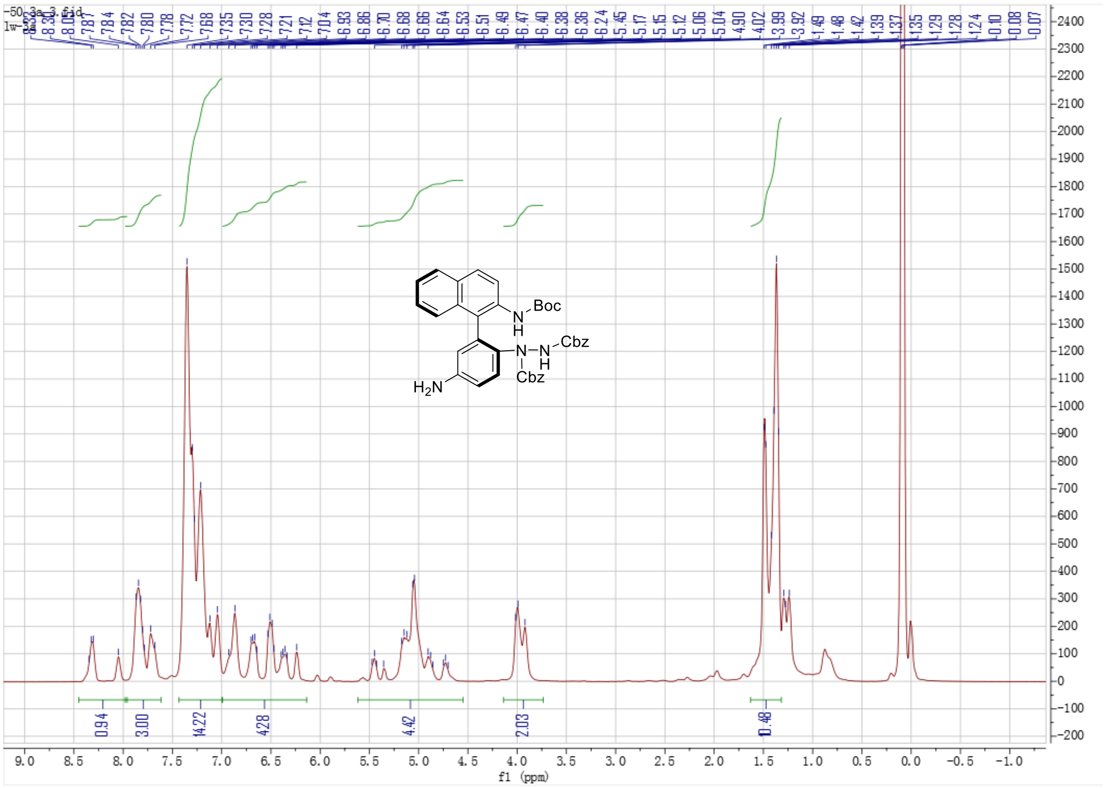

Figure S140. ^{13}C NMR spectrum of product **3a** at **-50** ^{o}C, related to **Table 1**.

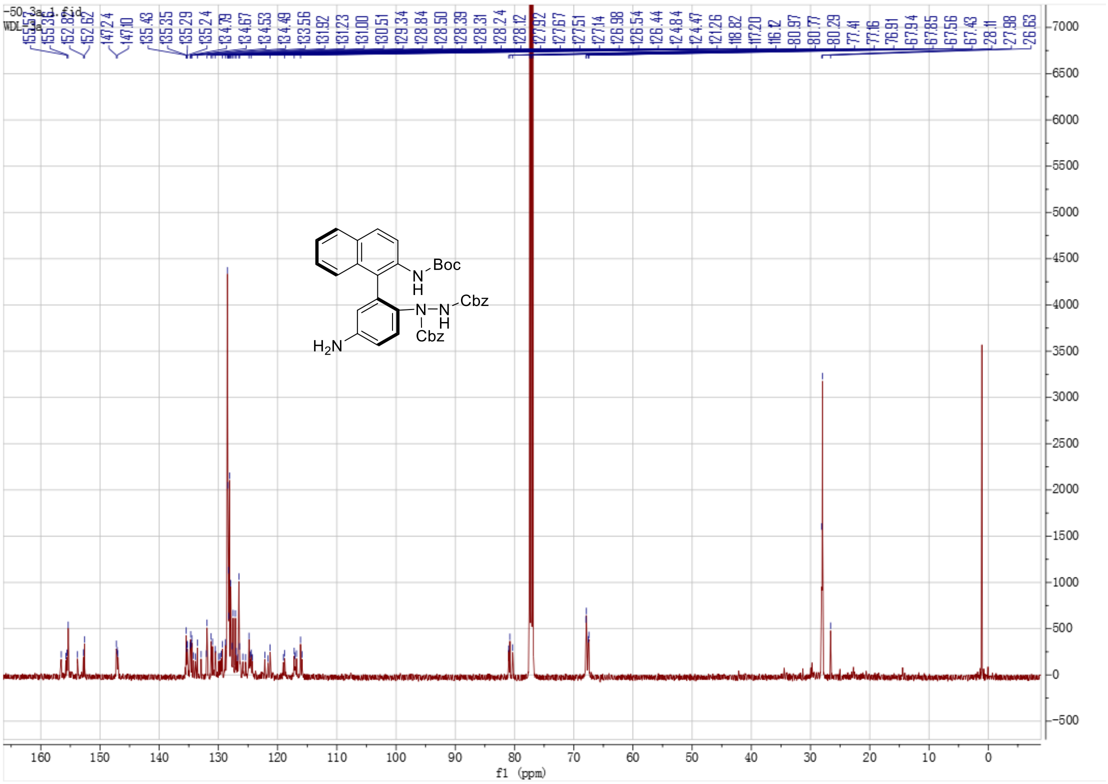

Figure S141. ^{1}H NMR spectrum of product **3b**, related to **Scheme 2**.

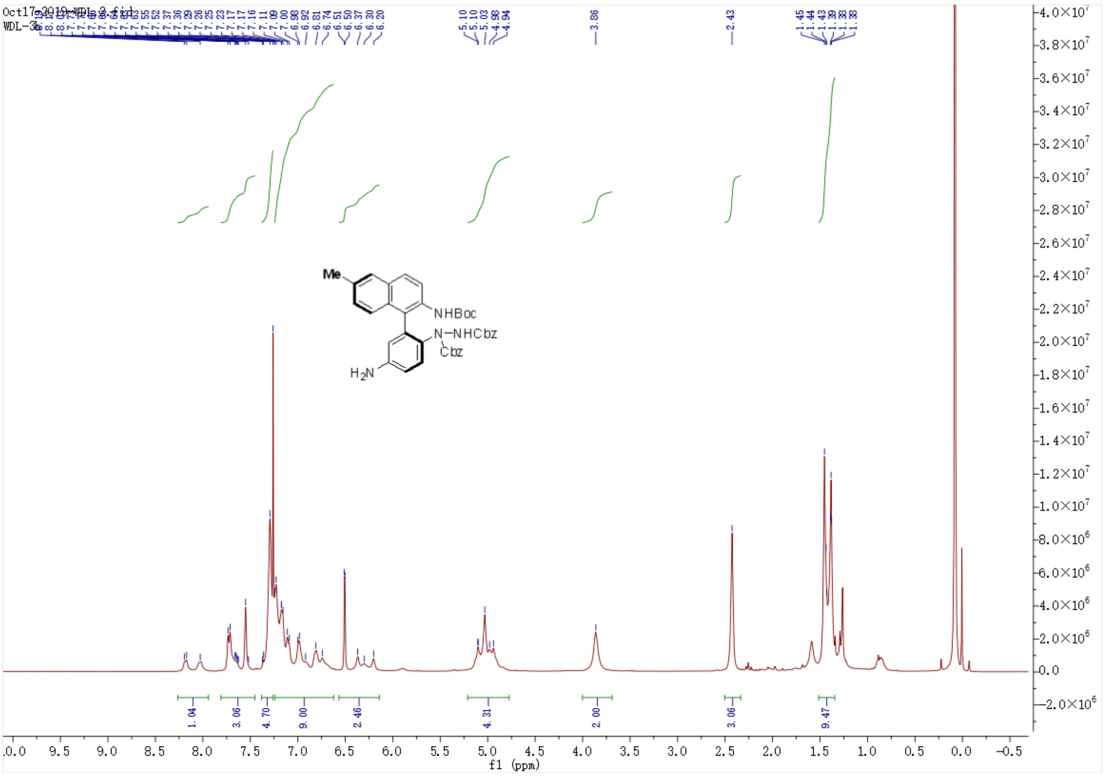

Figure S142. ^{13}C NMR spectrum of product **3b**, related to **Scheme 2**.

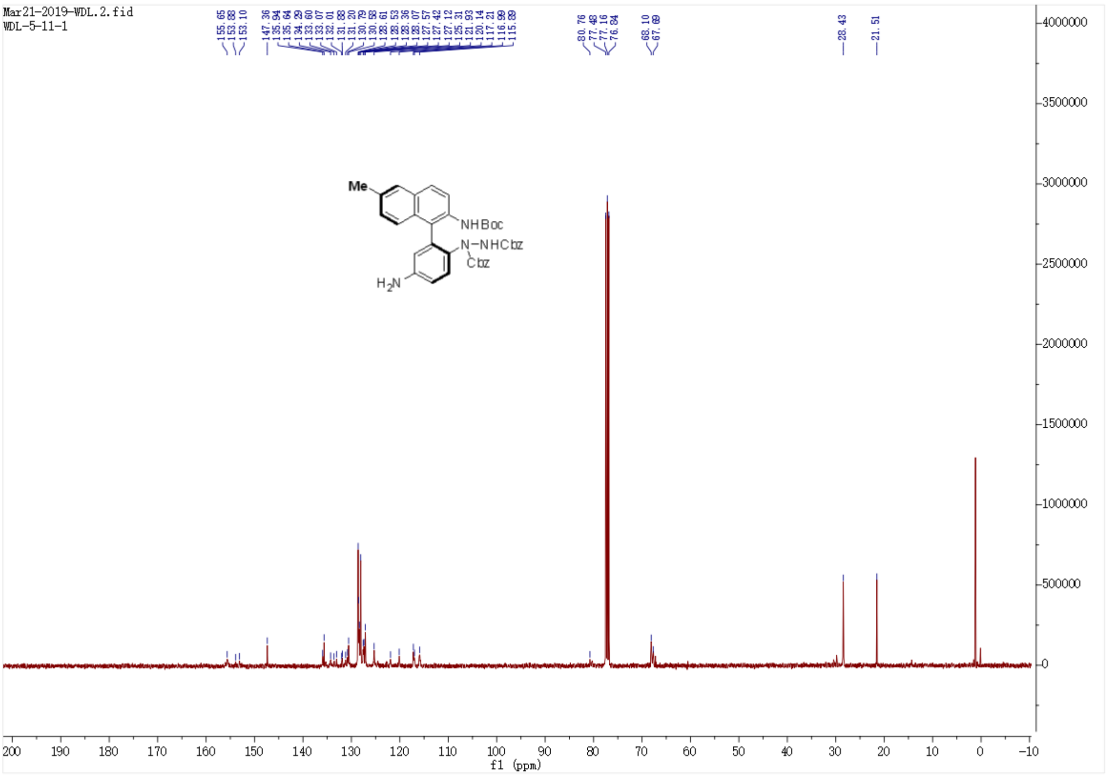

Figure S143. ^{1}H NMR spectrum of product **3c**, related to **Scheme 2**.

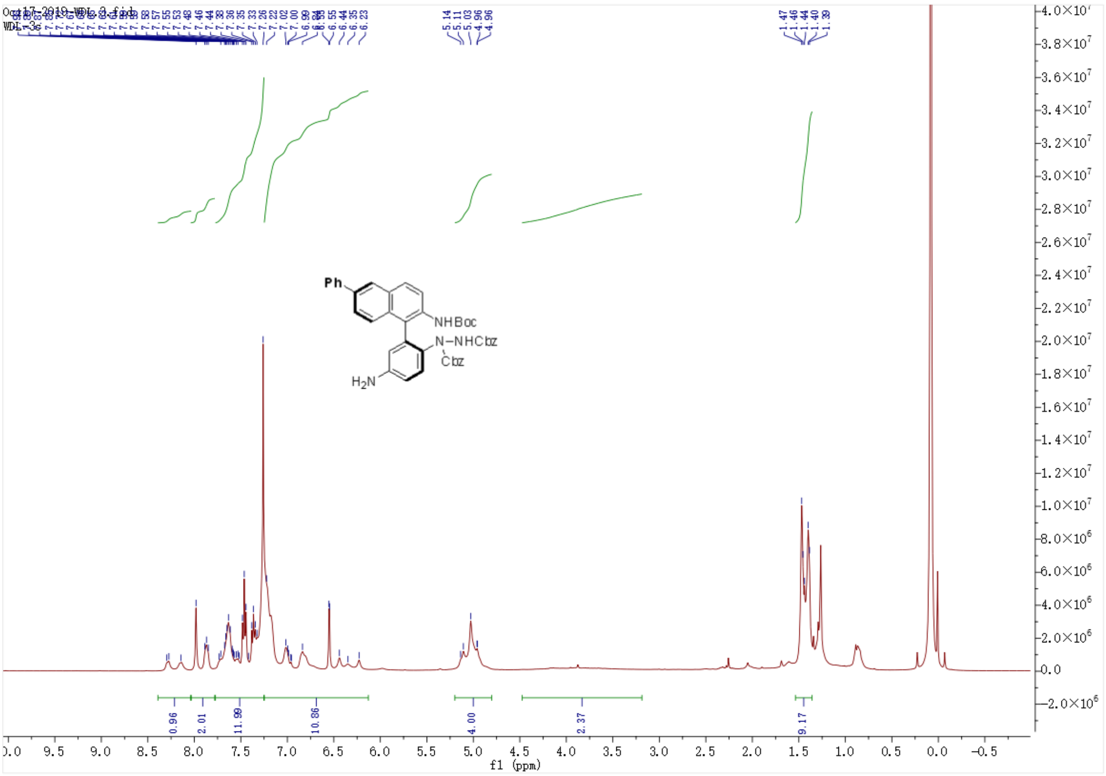

Figure S144. ^{13}C NMR spectrum of product **3c**, related to **Scheme 2**.

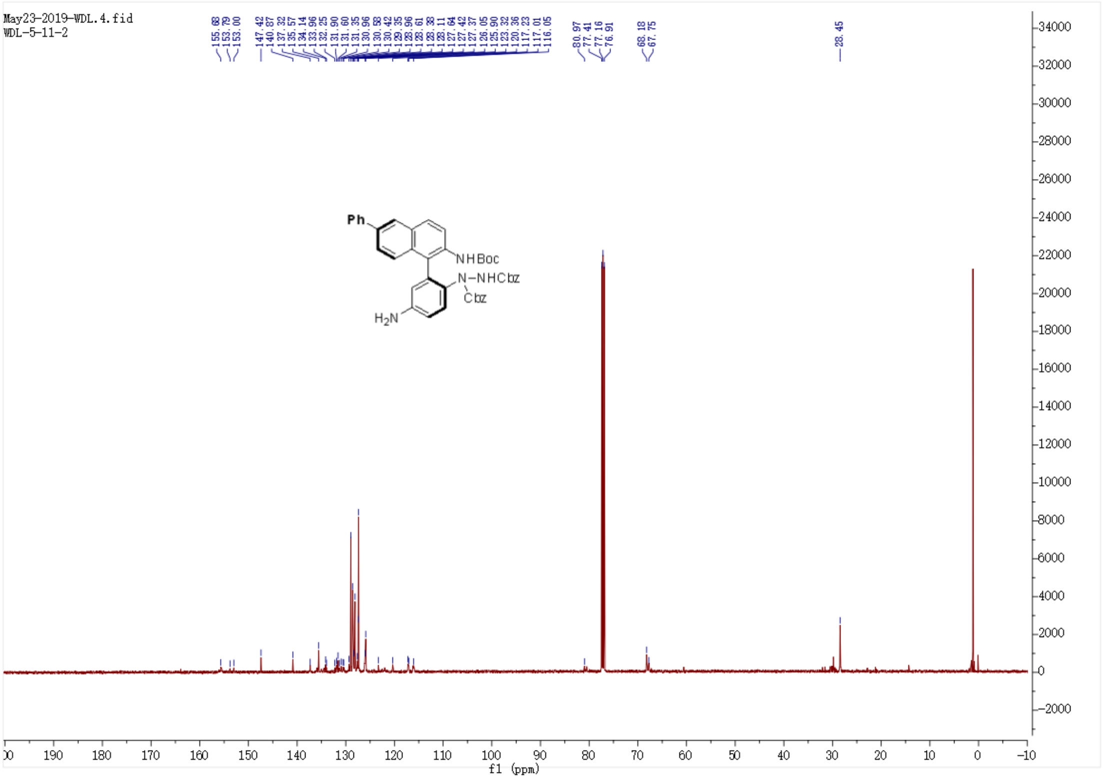

Figure S145. ^{1}H NMR spectrum of product **3d**, related to **Scheme 2**.

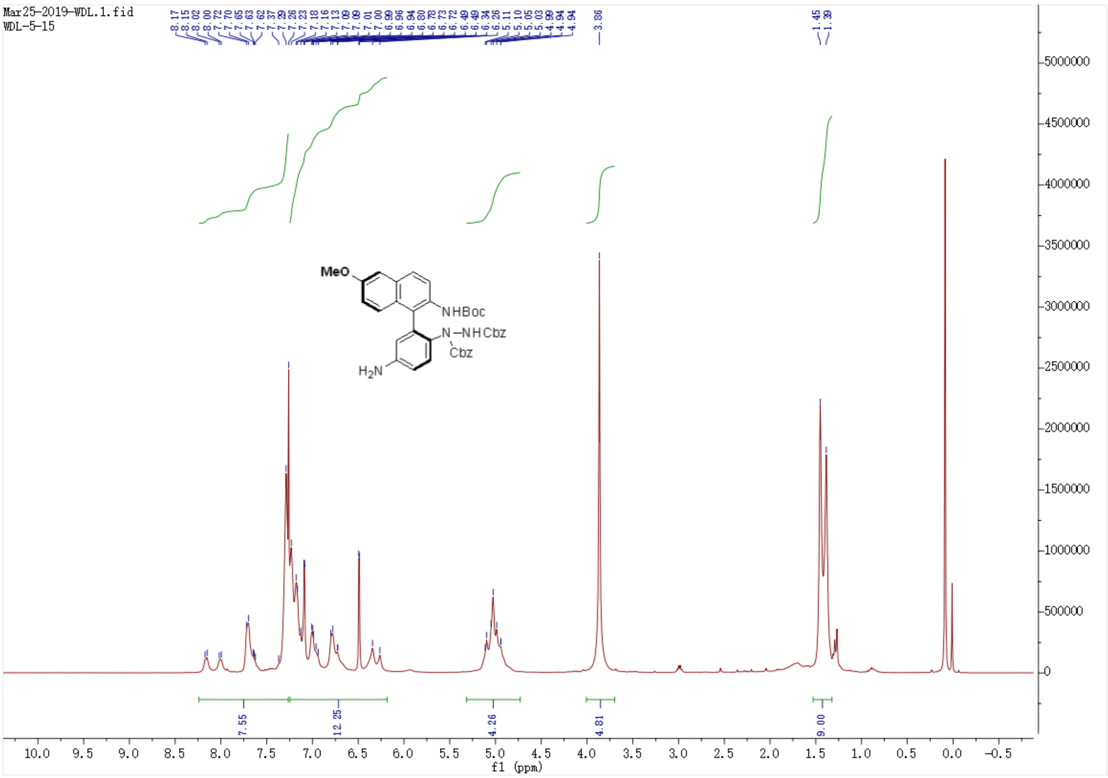

Figure S146. ^{13}C NMR spectrum of product **3d**, related to **Scheme 2**.

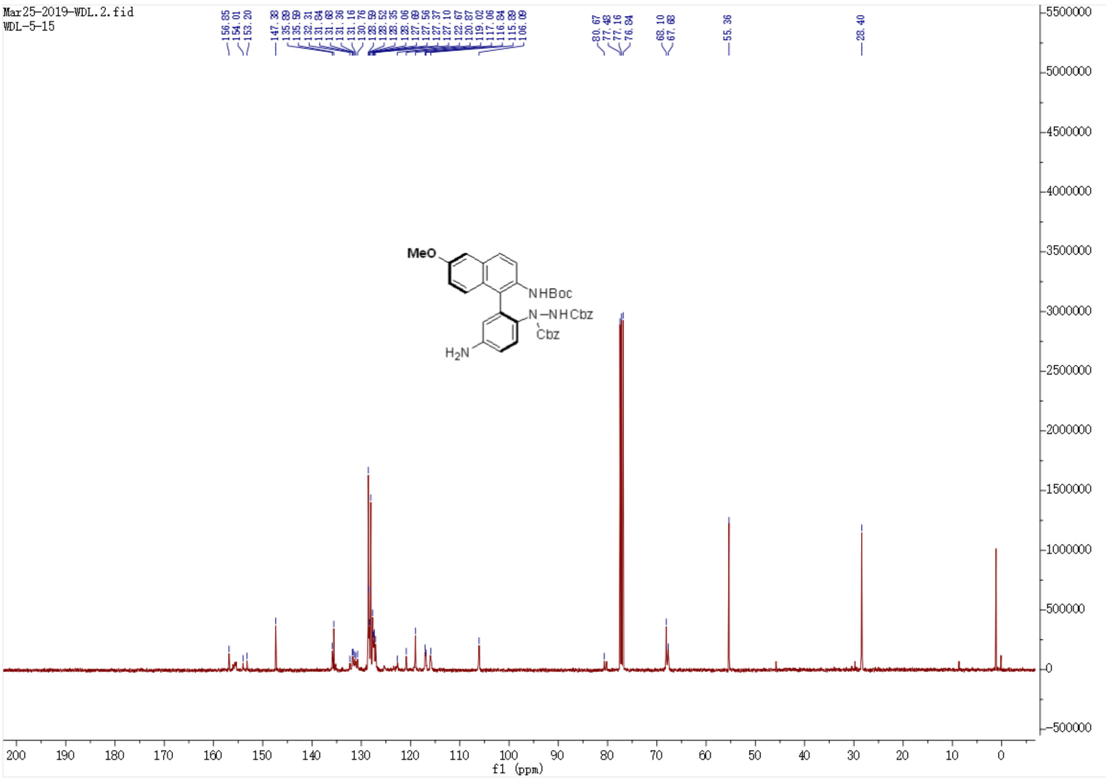

Figure S147. ^{1}H NMR spectrum of product **3e**, related to **Scheme 2**.

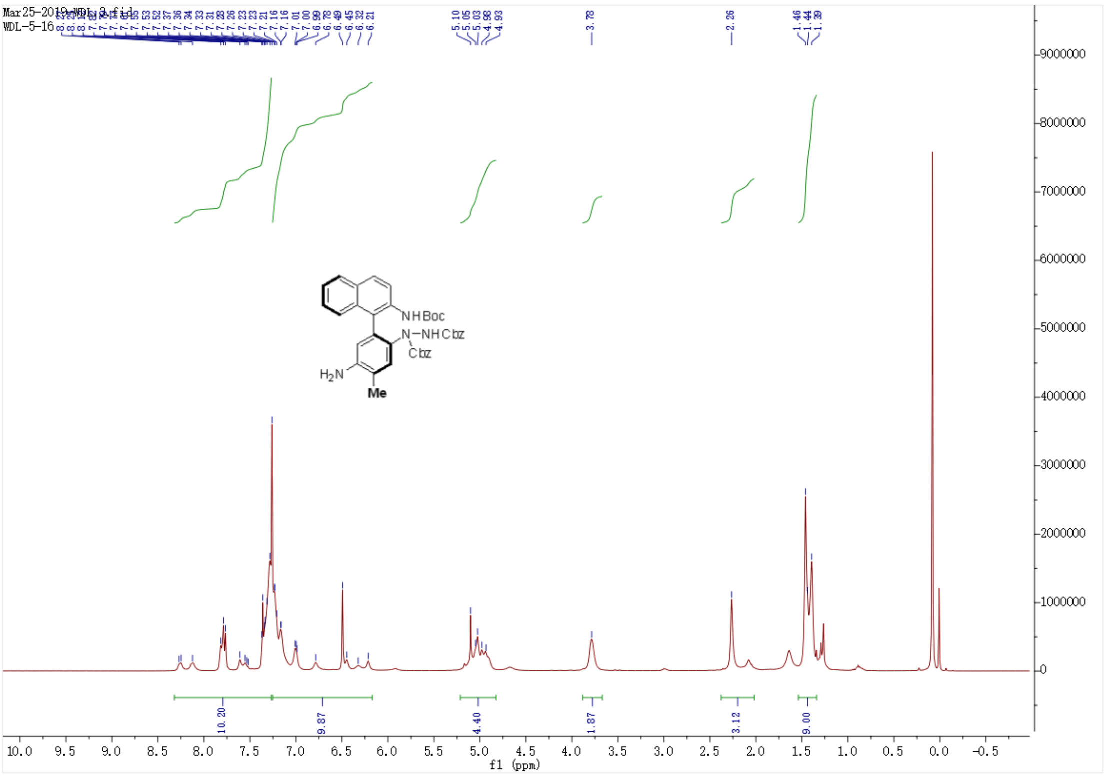

Figure S148. ^{13}C NMR spectrum of product **3e**, related to **Scheme 2**.

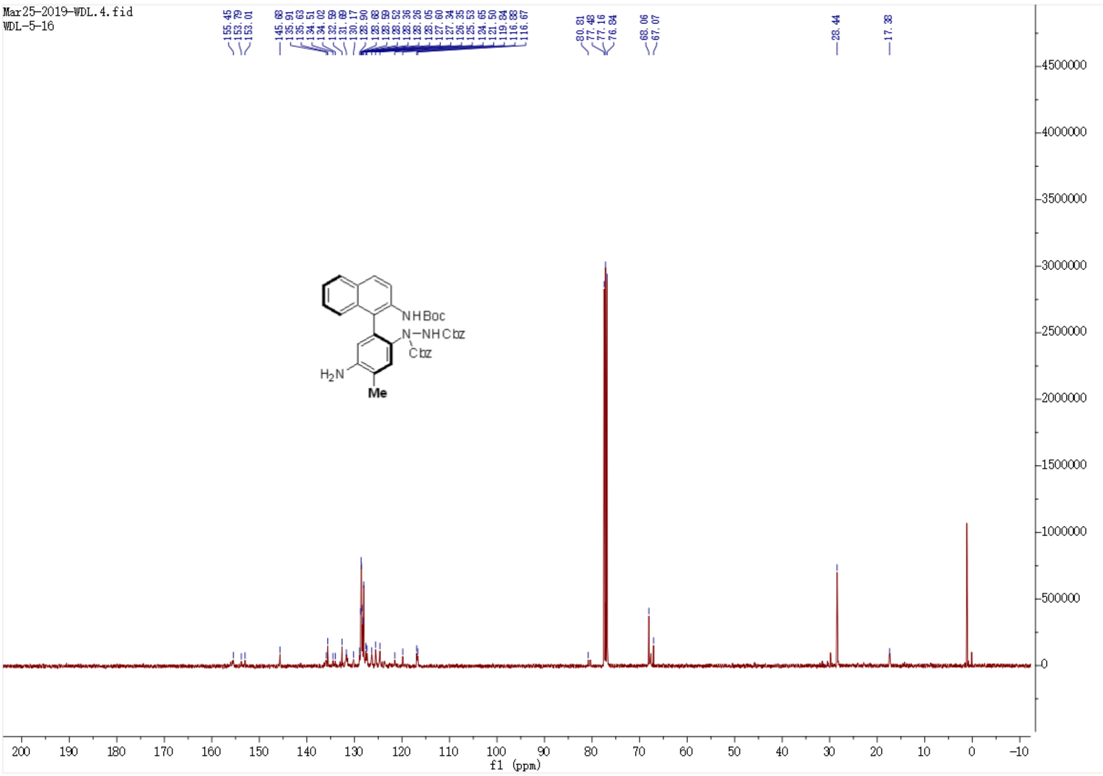

Figure S149. ^{1}H NMR spectrum of product **3f**, related to **Scheme 2**.

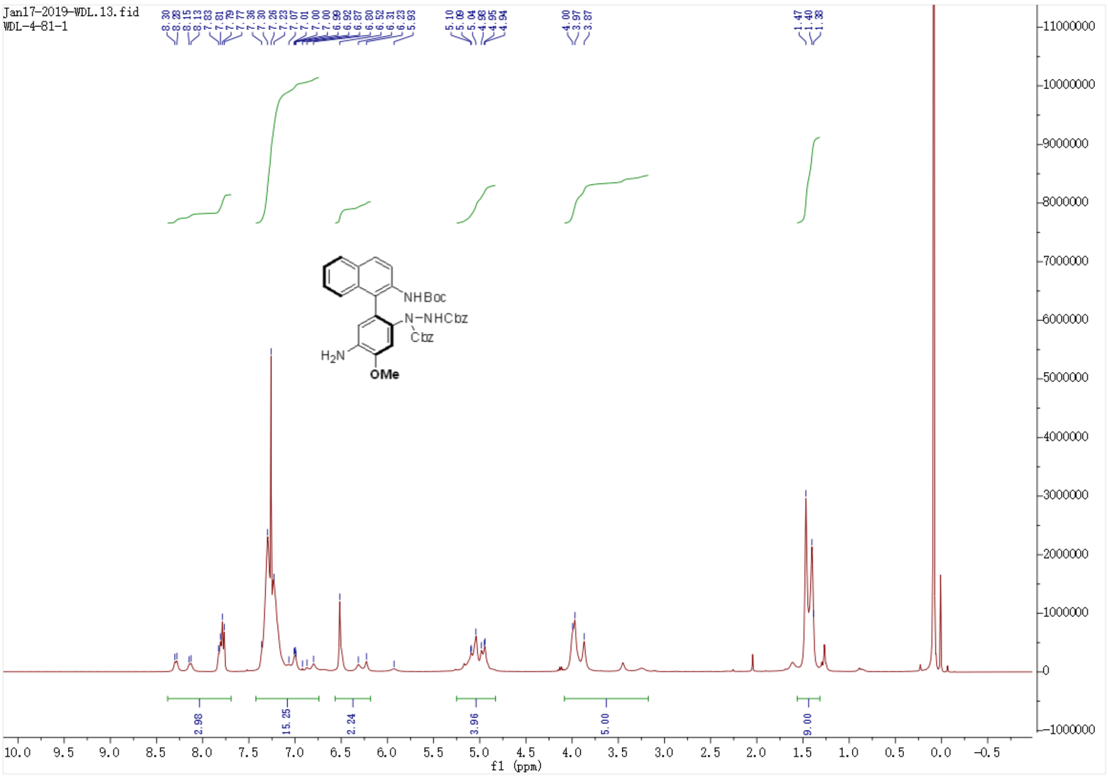

Figure S150. ^{13}C NMR spectrum of product **3f**, related to **Scheme 2**.

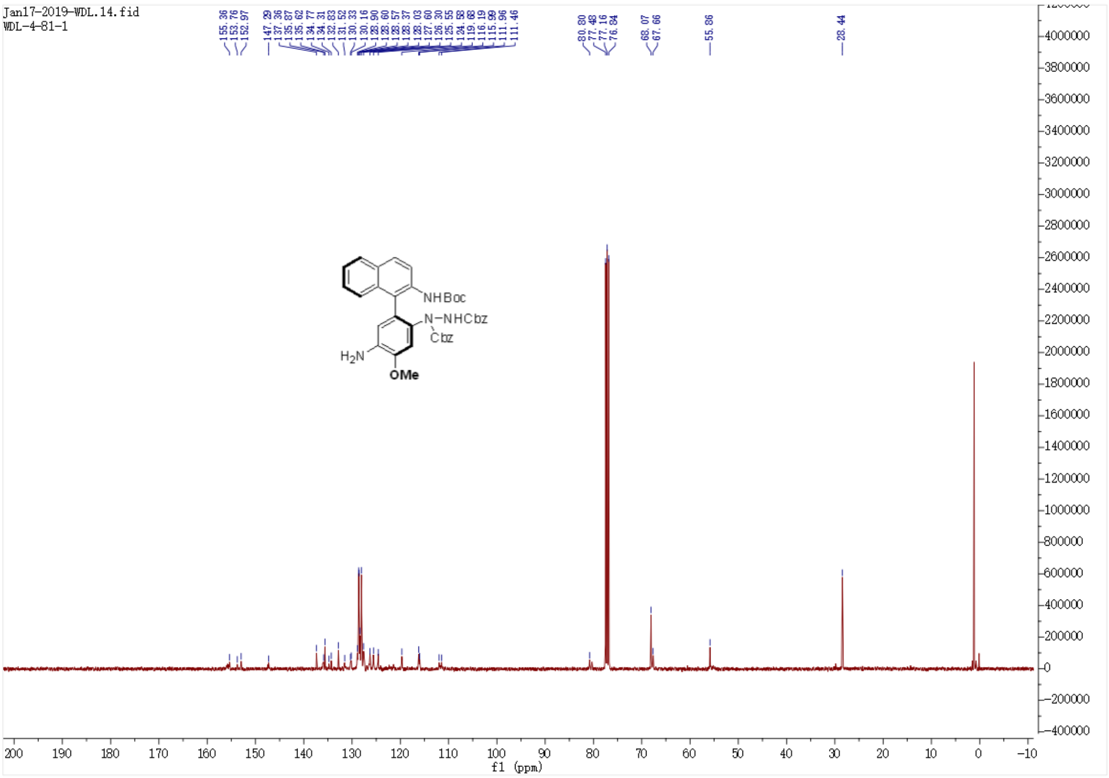

Figure S151. ^{1}H NMR spectrum of product **3g**, related to **Scheme 2**.

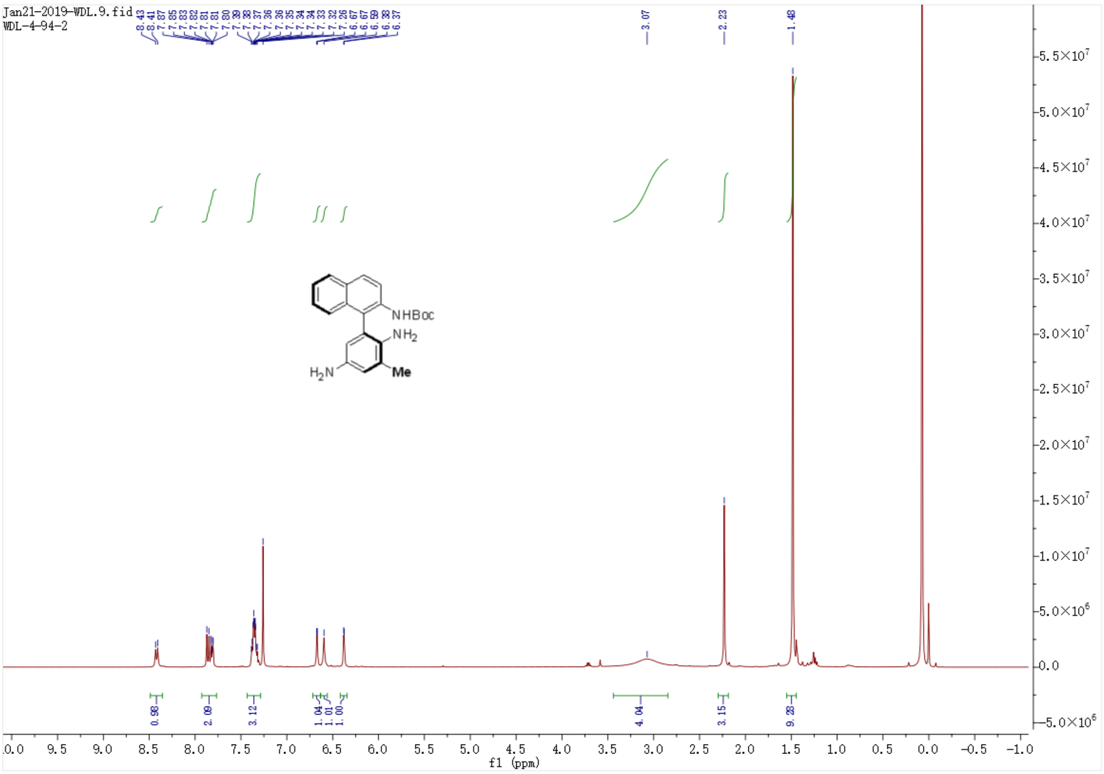

Figure S152. ^{13}C NMR spectrum of product **3g**, related to **Scheme 2**.

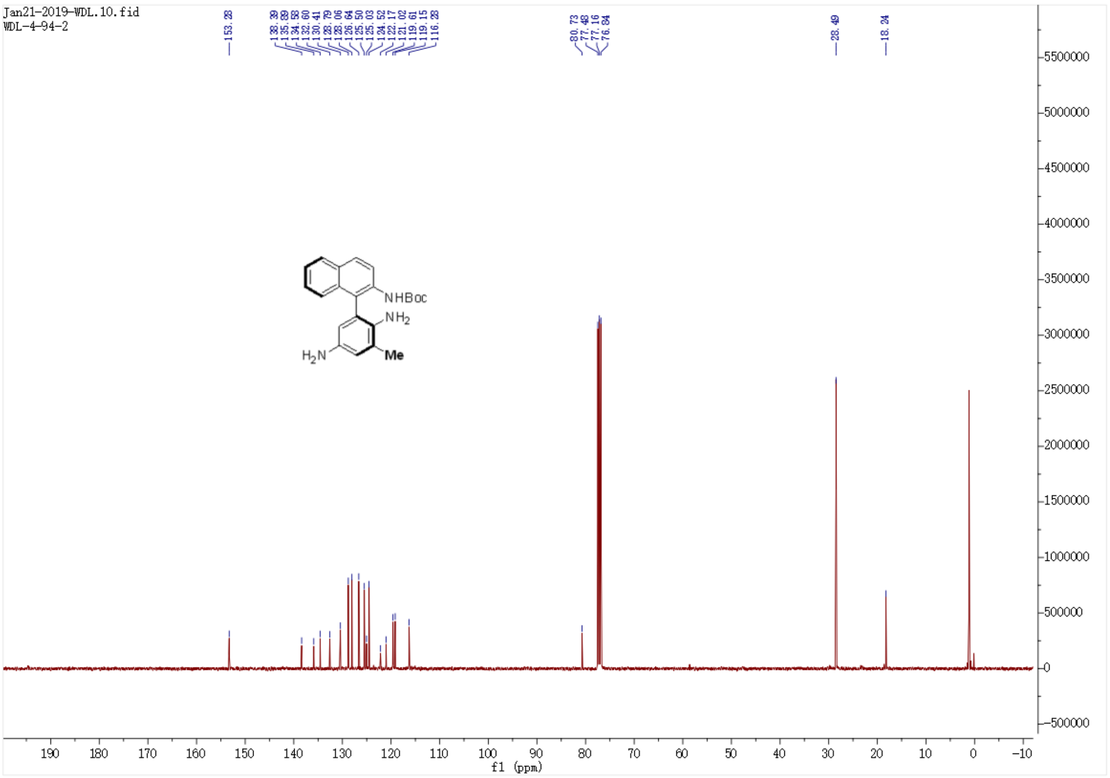

Figure S153. ^{1}H NMR spectrum of product **3h**, related to **Scheme 2**.

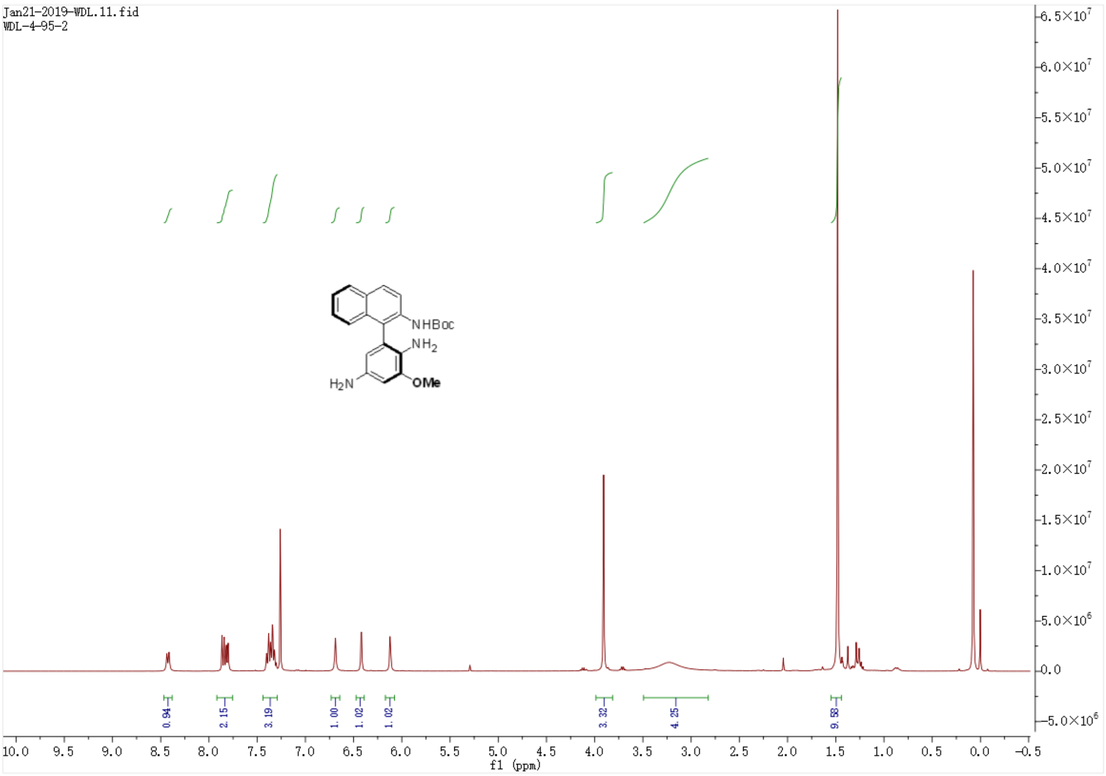

Figure S154. ^{13}C NMR spectrum of product **3h**, related to **Scheme 2**.

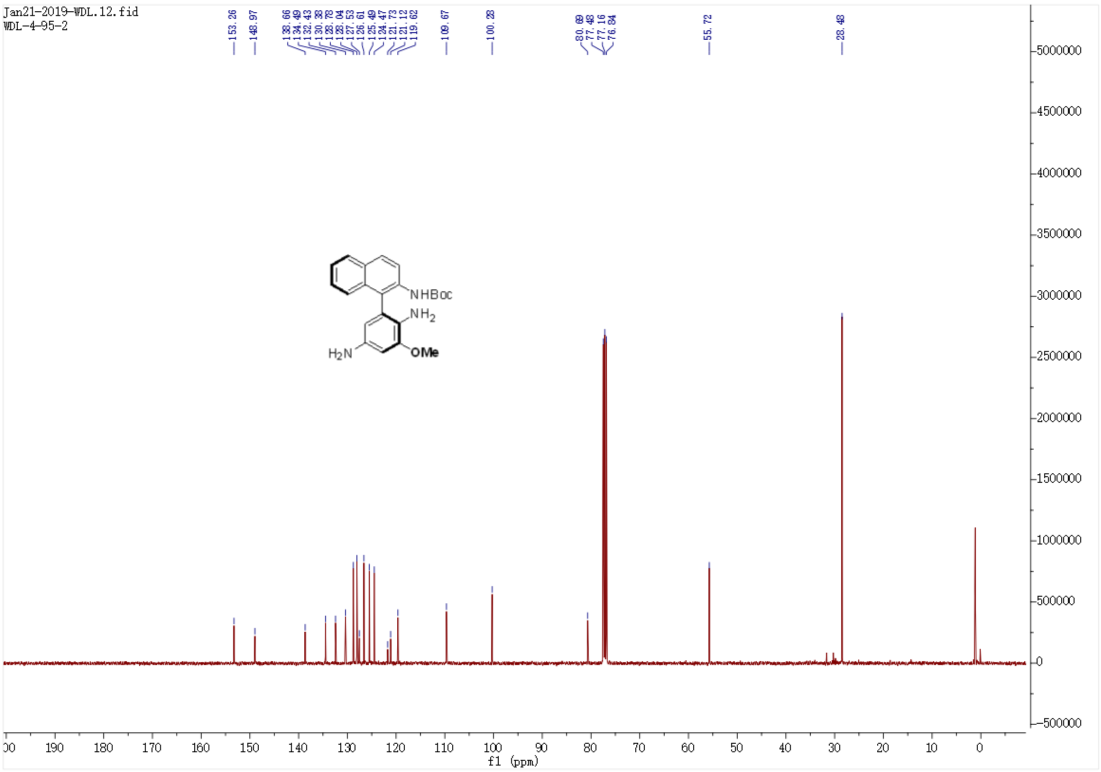

Figure S155. ^{1}H NMR spectrum of product **3i**, related to **Scheme 2**.

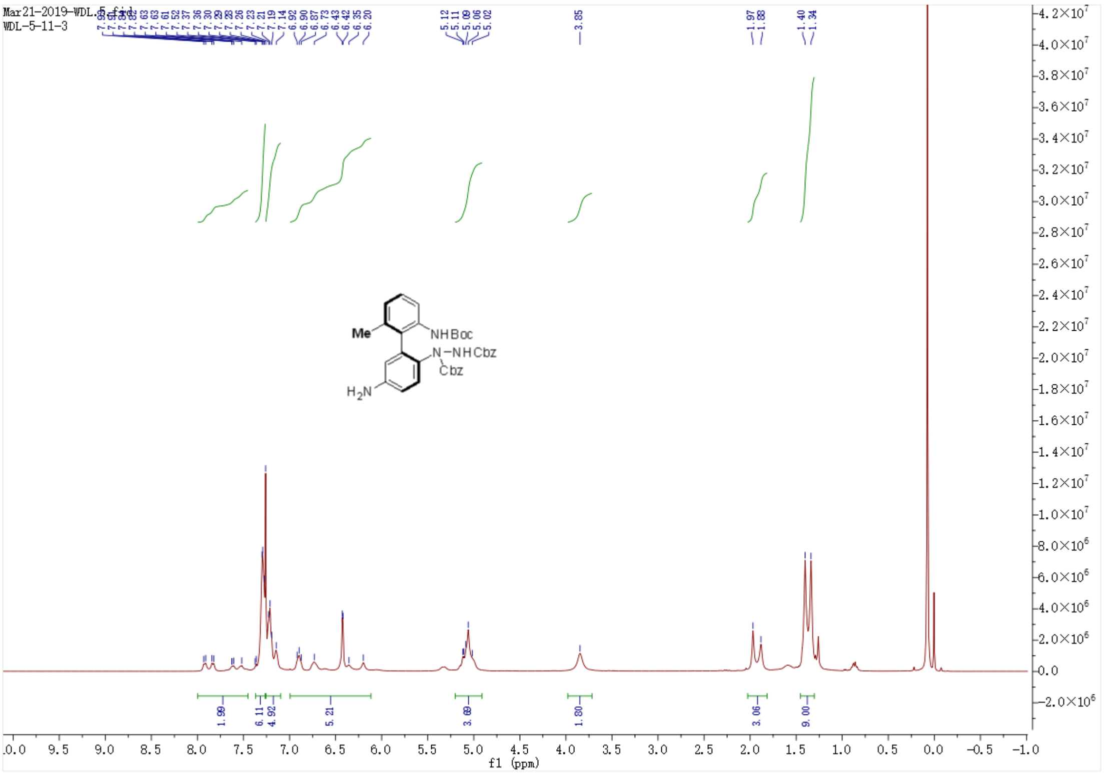

Figure S156. ^{13}C NMR spectrum of product **3i**, related to **Scheme 2**.

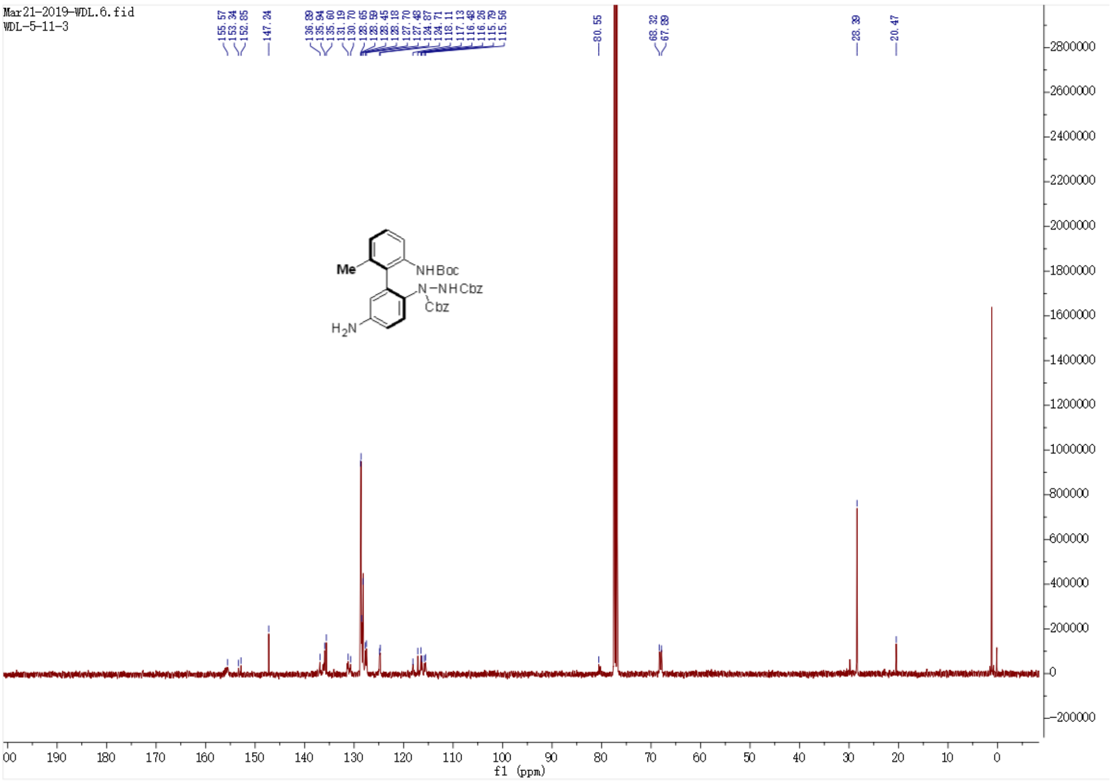

Figure S157. ^{1}H NMR spectrum of product **3j**, related to **Scheme 2**.

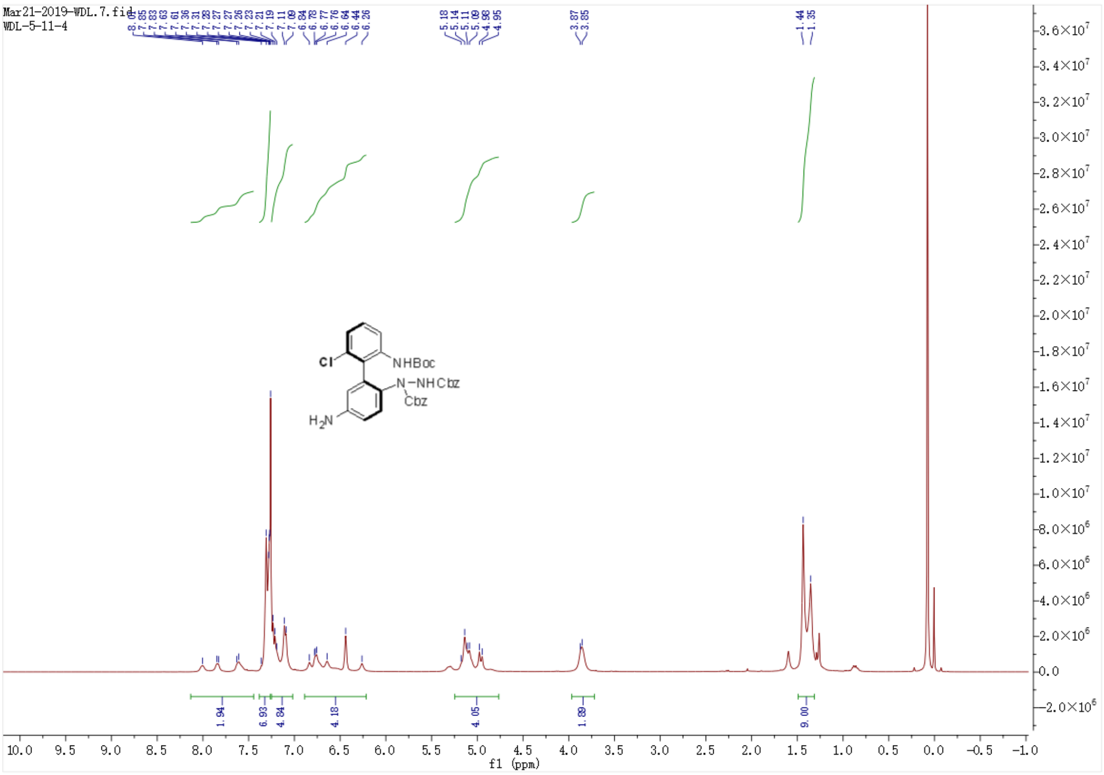

Figure S158. ^{13}C NMR spectrum of product **3j**, related to **Scheme 2**.

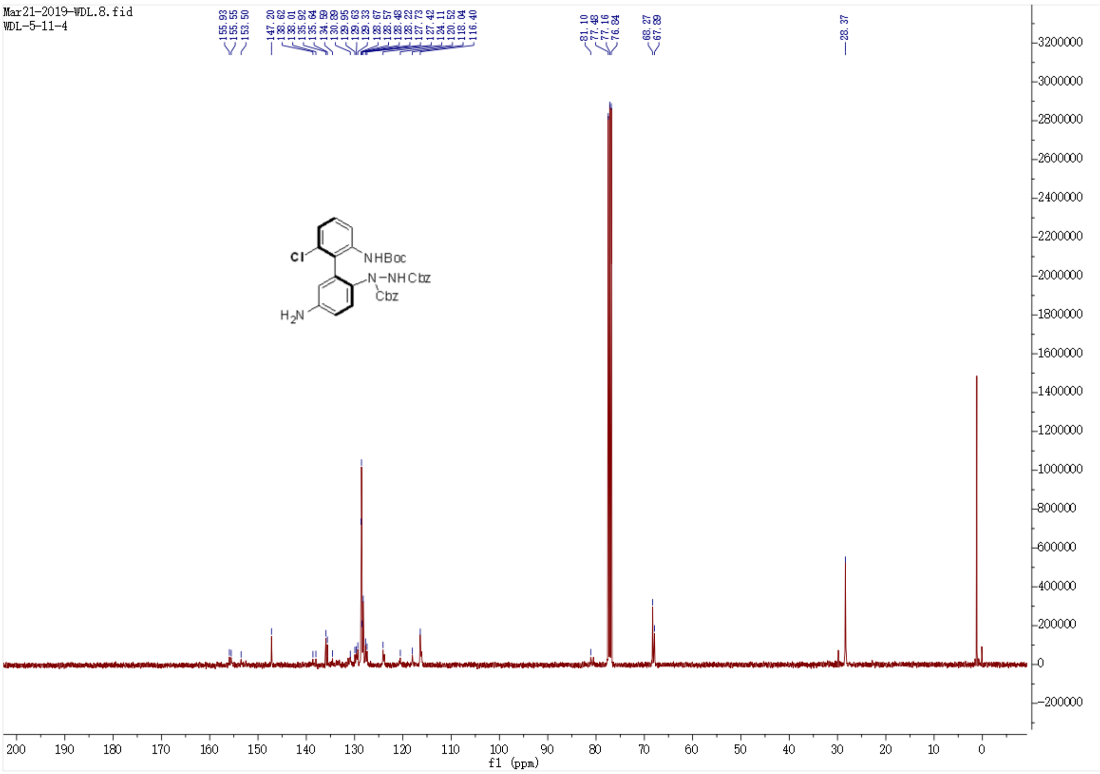

Figure S159. ^{1}H NMR spectrum of product **3k**, related to **Scheme 2**.

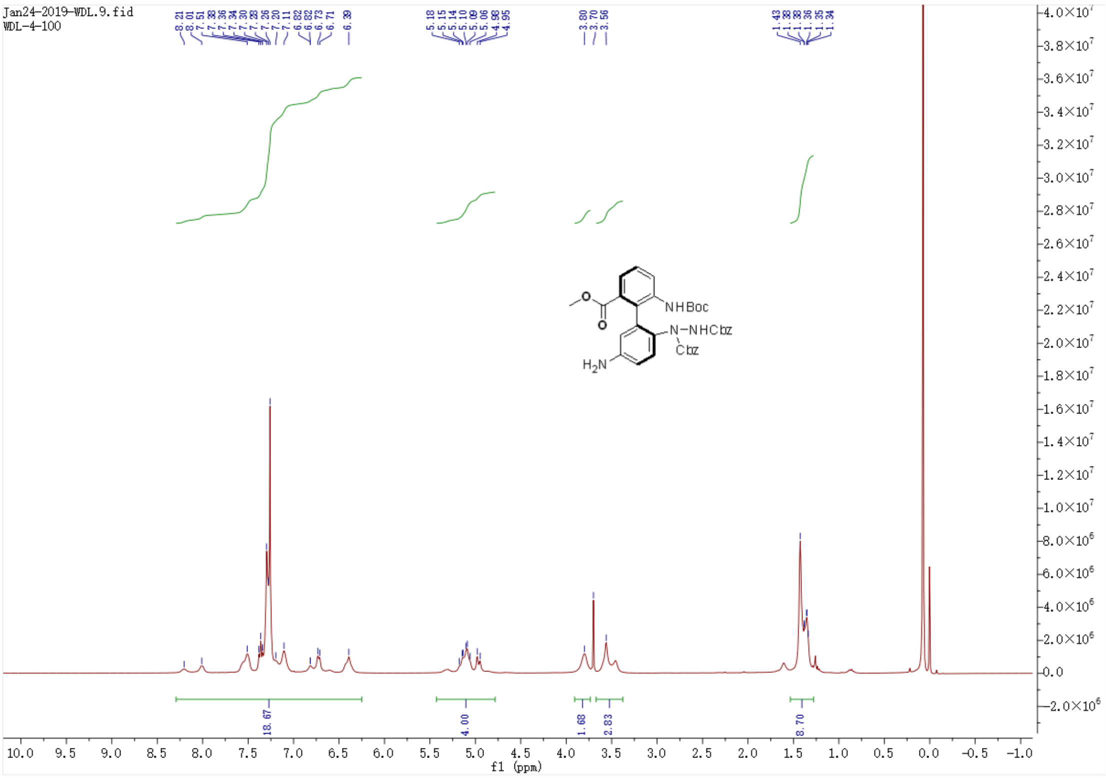

Figure S160. ^{13}C NMR spectrum of product **3k**, related to **Scheme 2**.

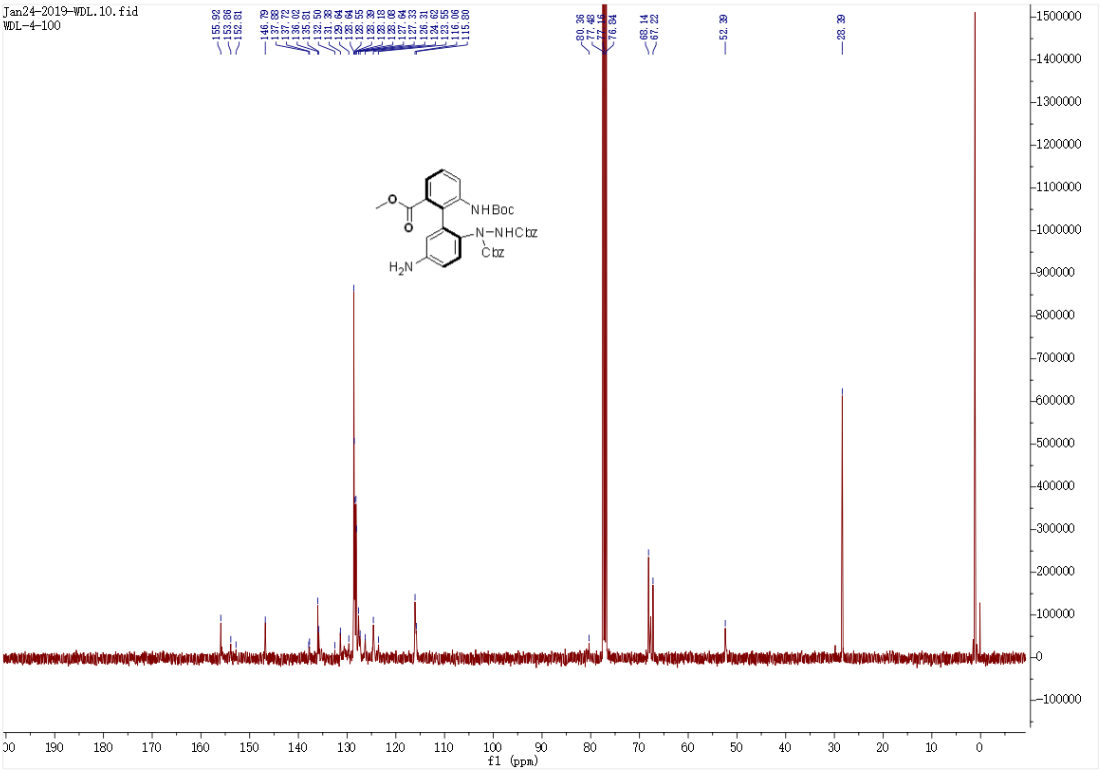

Figure S161. ^{1}H NMR spectrum of product **3l**, related to **Scheme 2**.

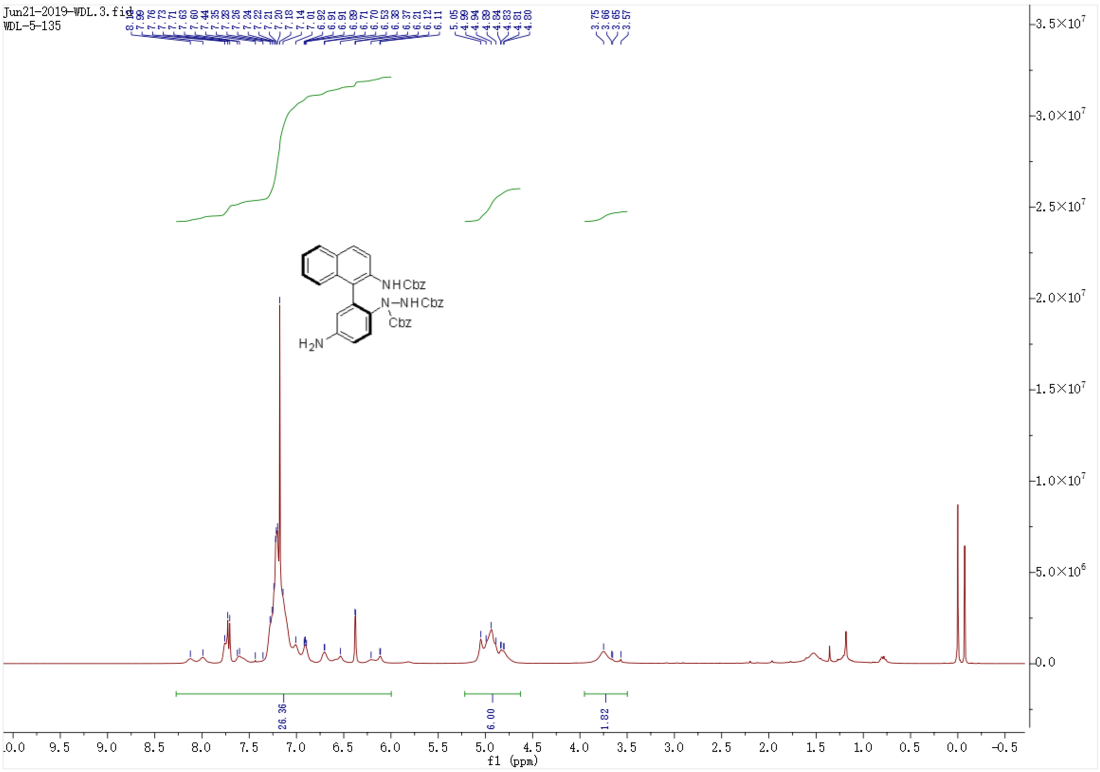

Figure S162. ^{13}C NMR spectrum of product **3l**, related to **Scheme 2**.

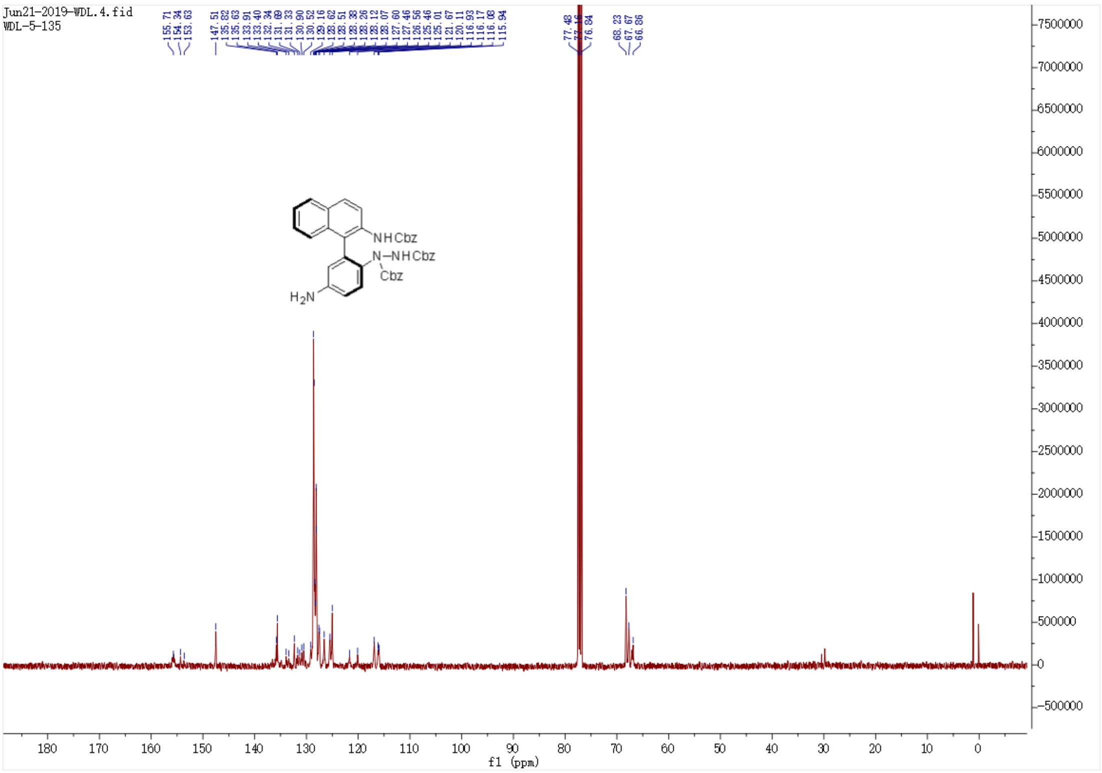

Figure S163. ^{1}H NMR spectrum of product **3m**, related to **Scheme 3.**.

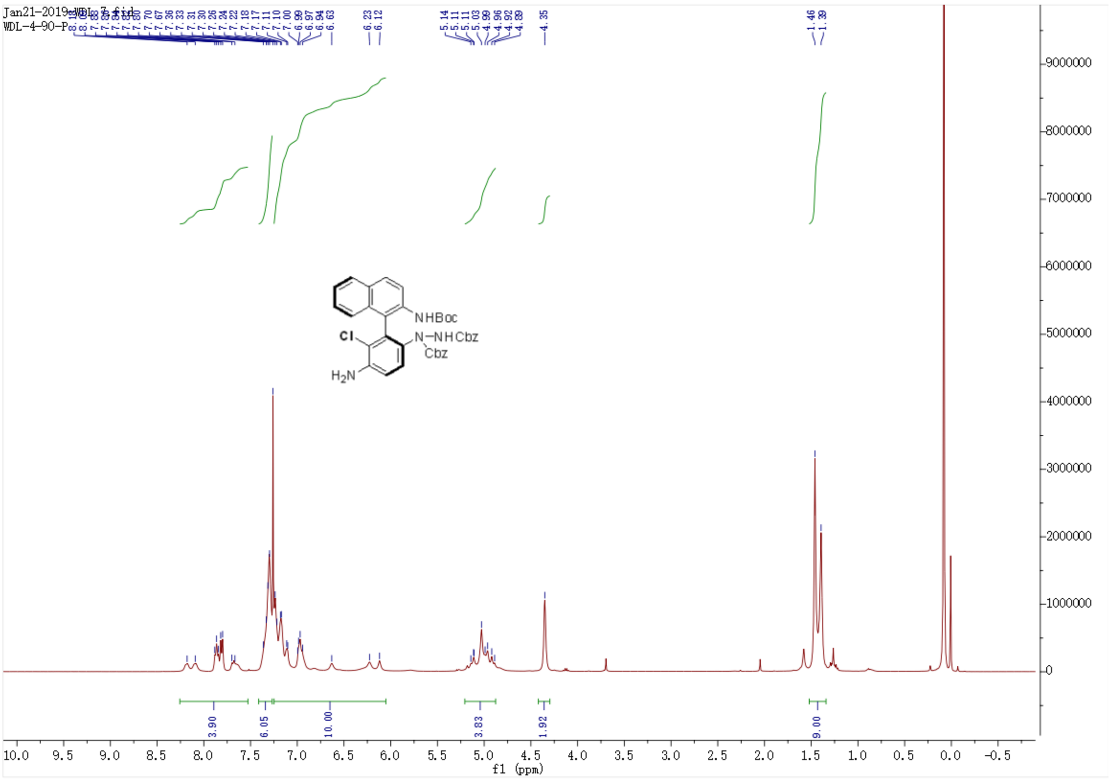

Figure S164. ^{13}C NMR spectrum of product **3m**, related to **Scheme 3.**.

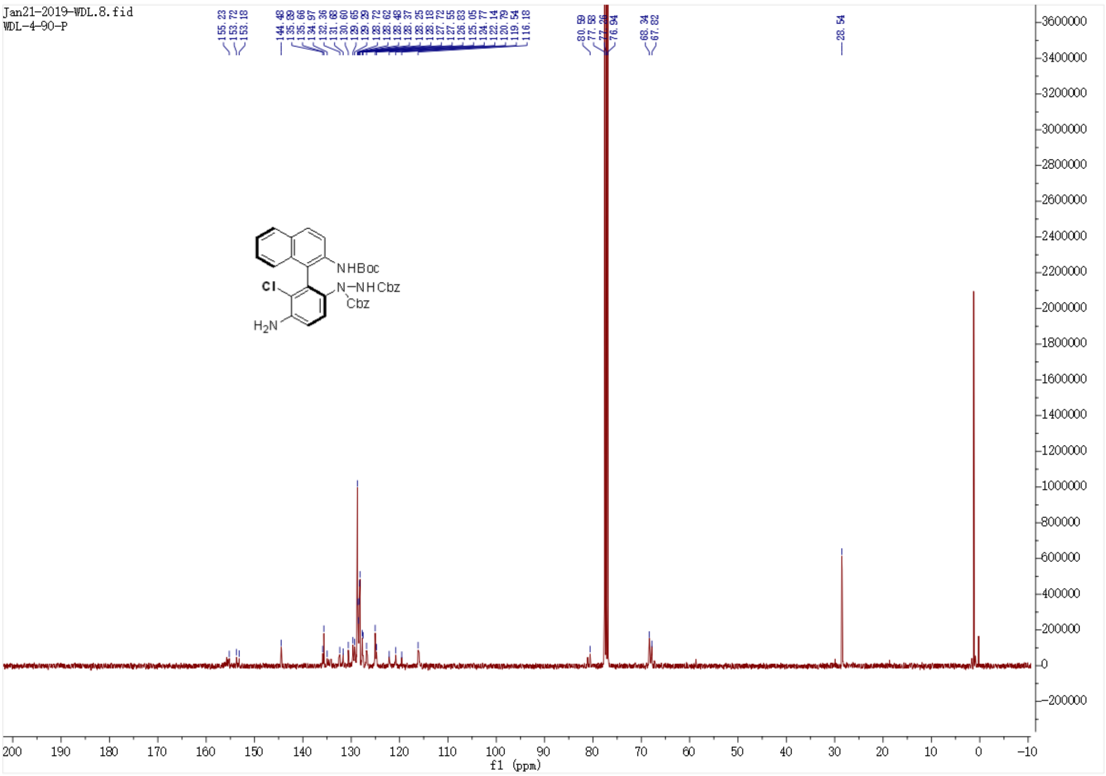

Figure S165. ^{1}H NMR spectrum of product **3n**, related to **Scheme 3.**

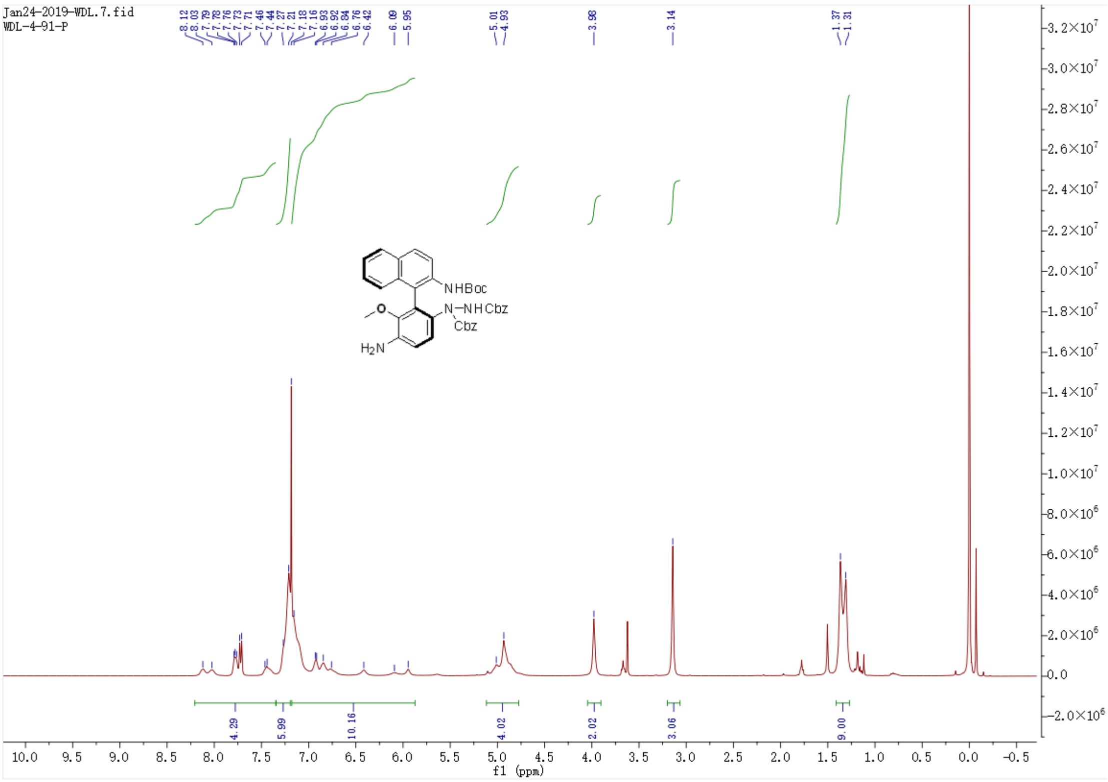

Figure S166. ^{13}C NMR spectrum of product **3n**, related to **Scheme 3.**

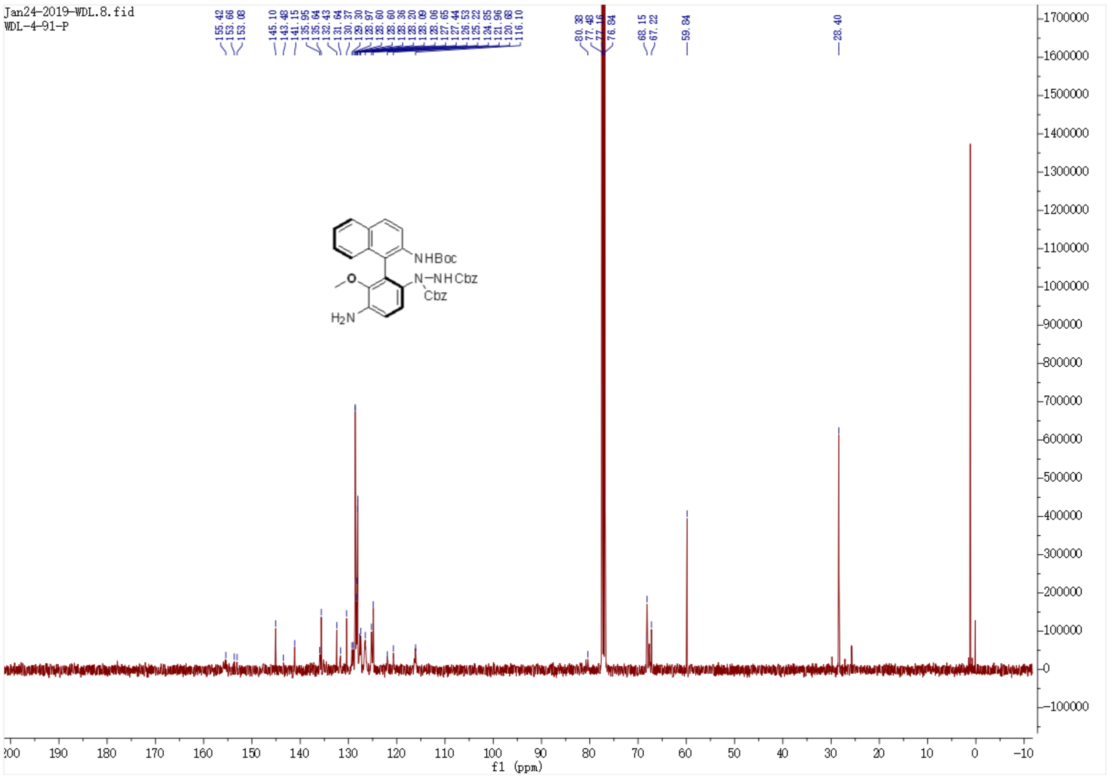

Figure S167. ^{1}H NMR spectrum of product **3o**, related to **Scheme 3.**

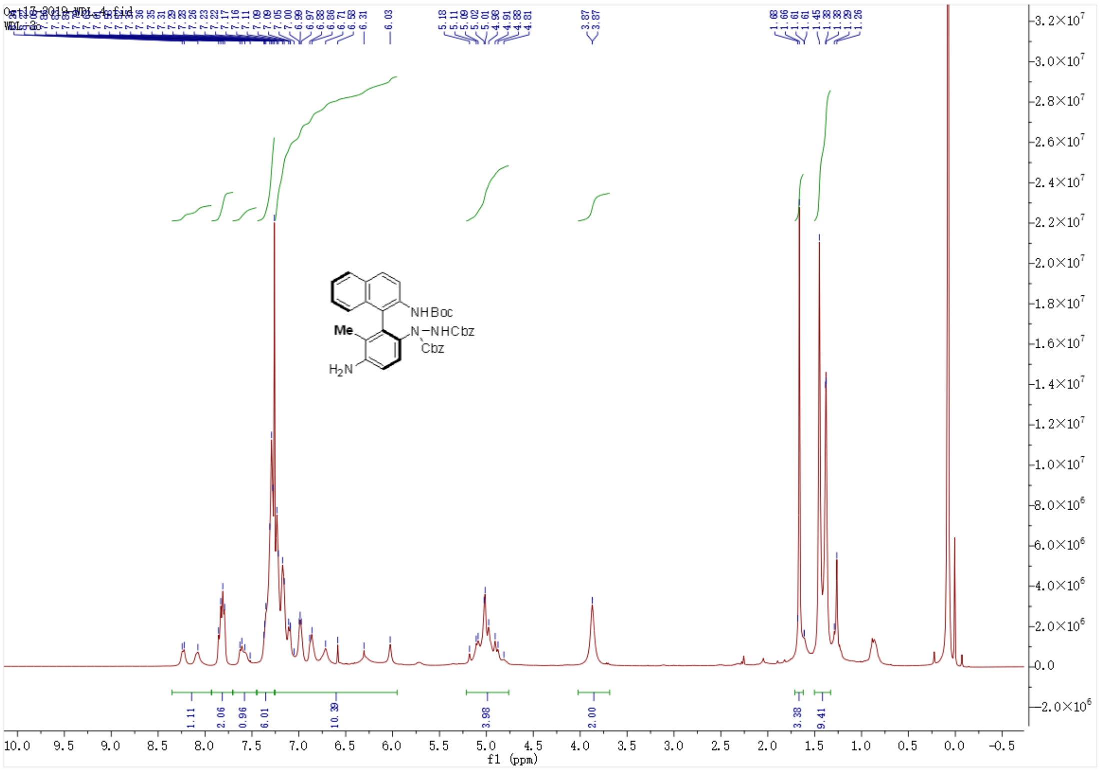

Figure S168. ^{13}C NMR spectrum of product **3o**, related to **Scheme 3.**

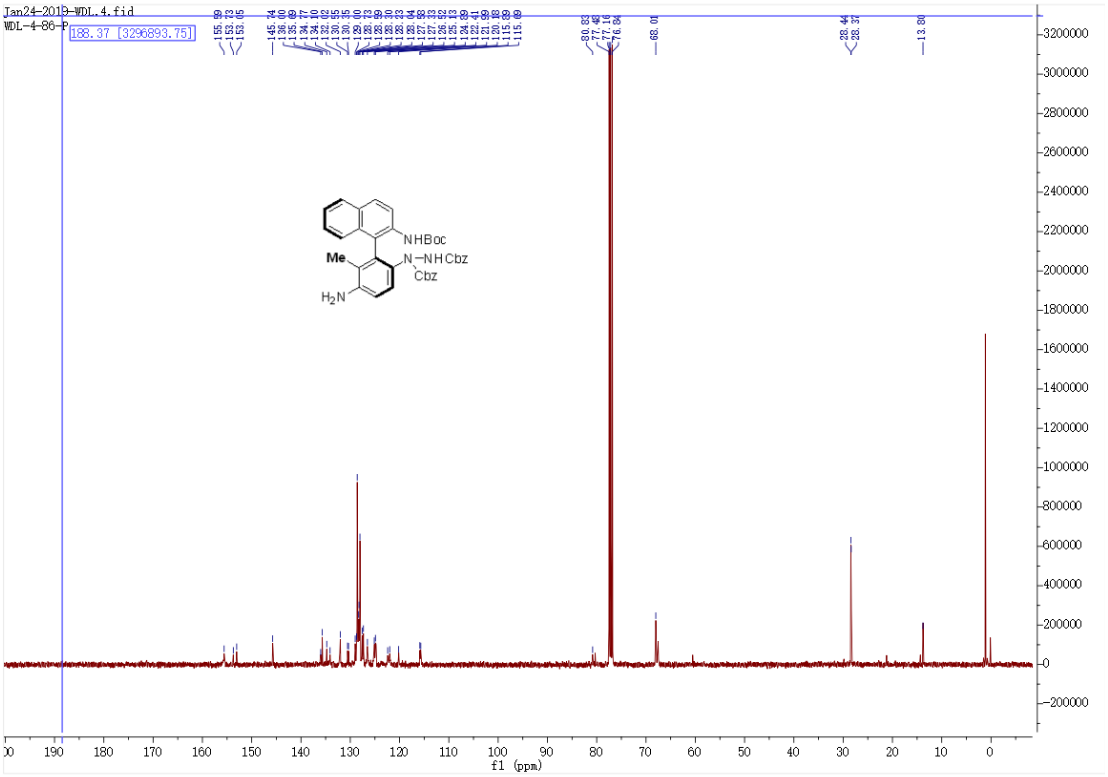

Figure S169. ^{1}H NMR spectrum of product **3p**, related to **Scheme 3.**

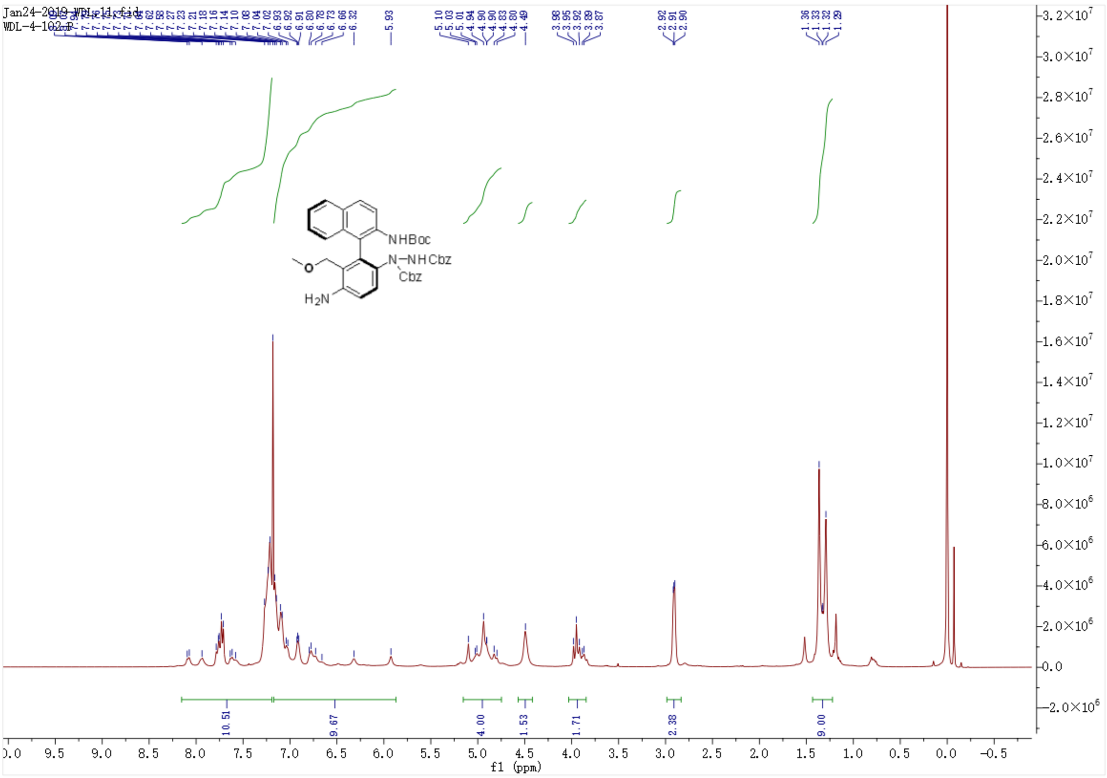

Figure S170. ^{13}C NMR spectrum of product **3p**, related to **Scheme 3.**

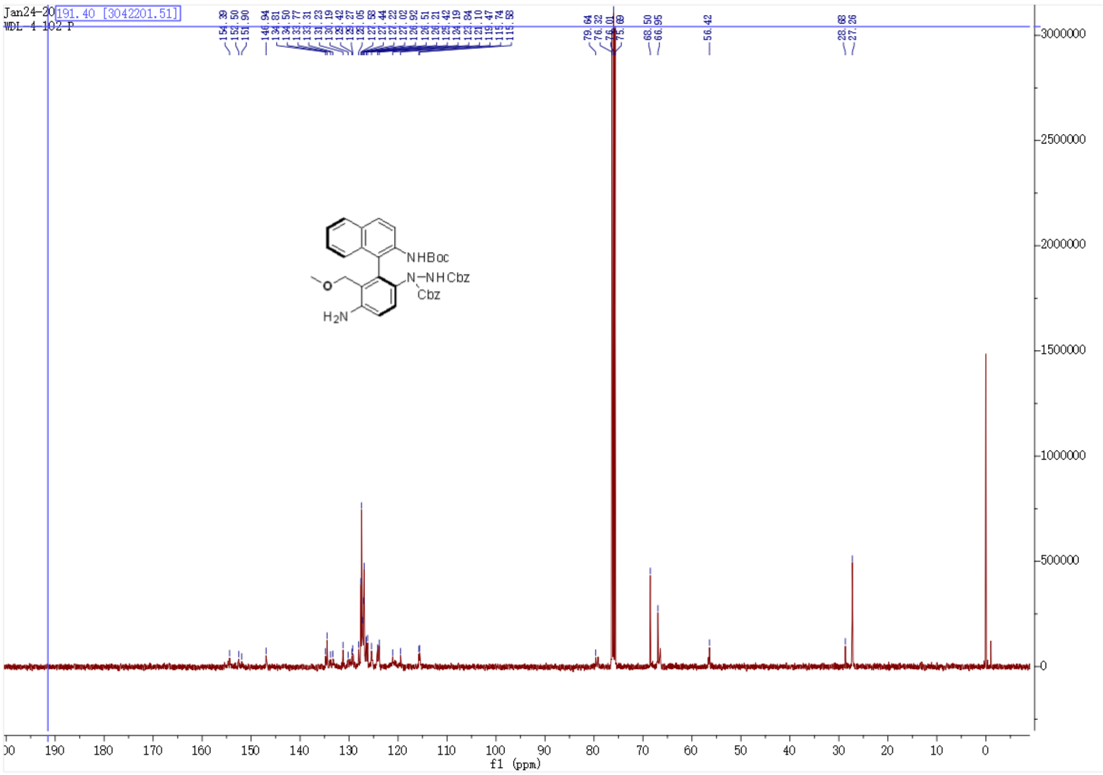

Figure S171. ^{1}H NMR spectrum of product **4a**, related to **Table 1**.

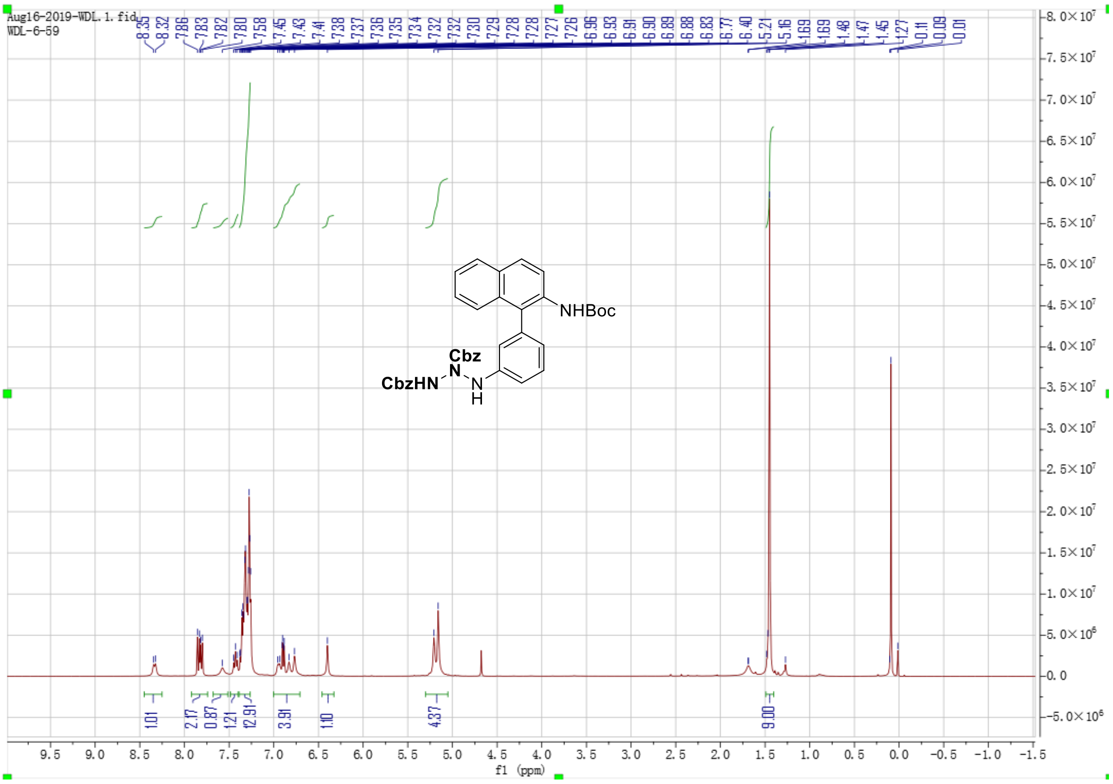

Figure S172. ^{13}C NMR spectrum of product **4a**, related to **Table 1**.

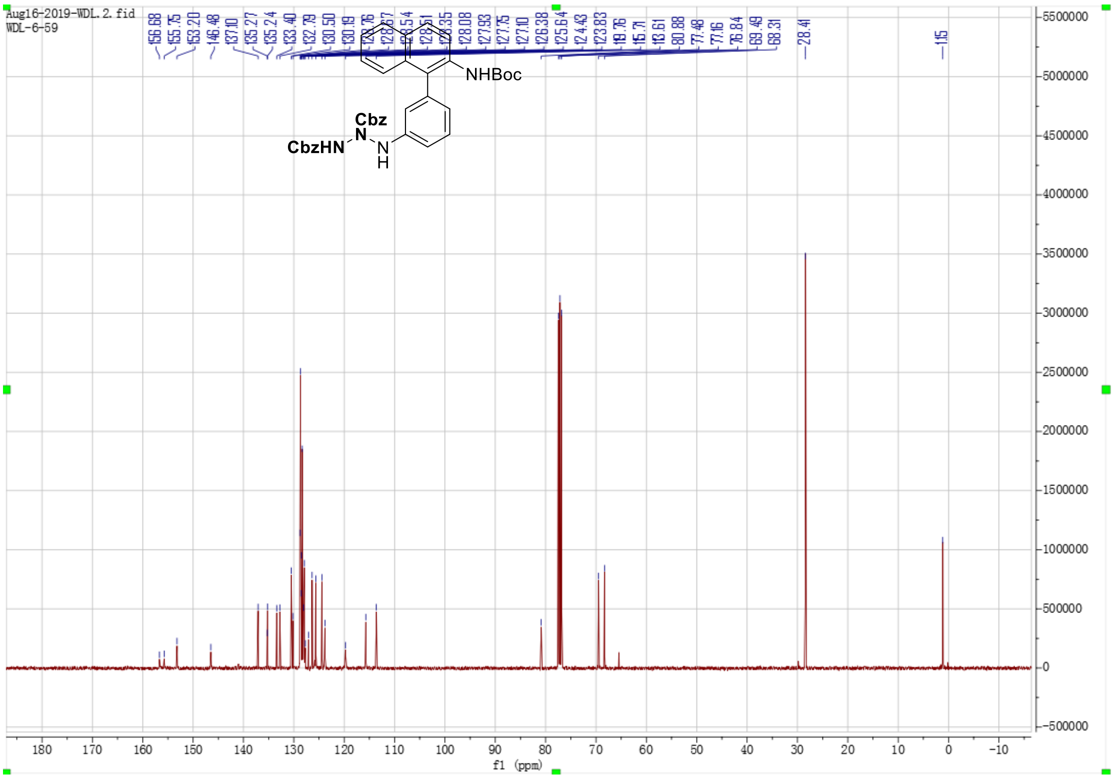

Figure S173. ^{1}H NMR spectrum of substrate **6a**, related to **Scheme 4**.

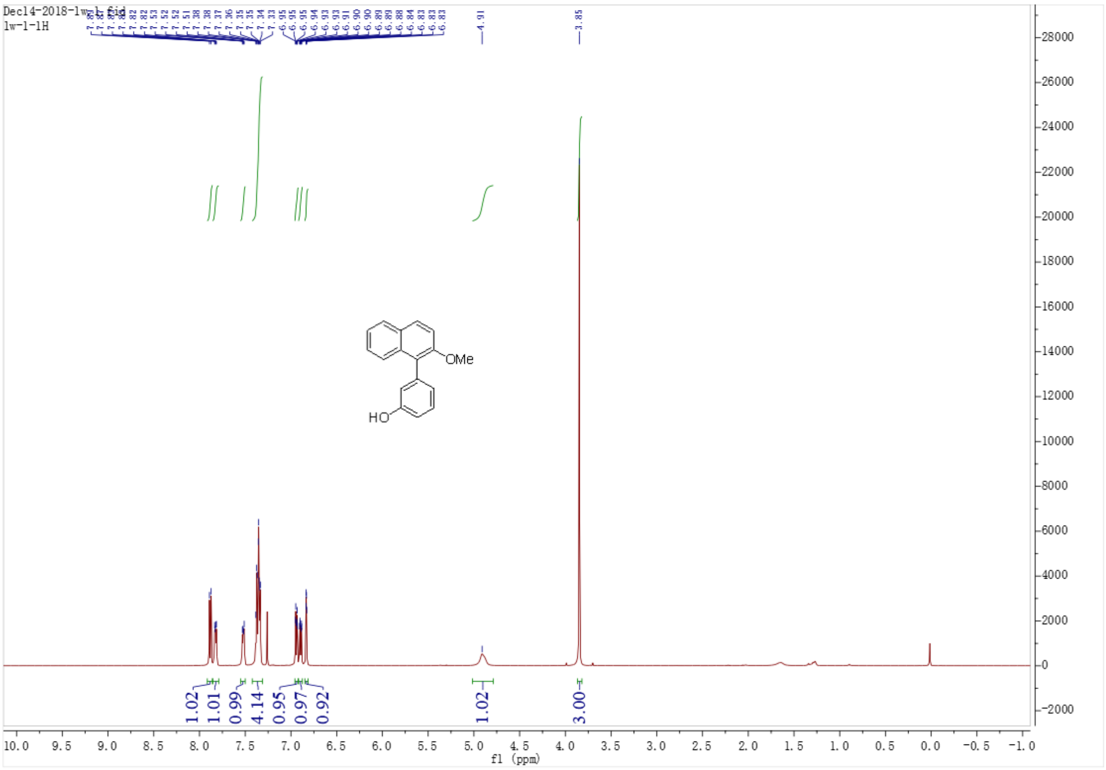

Figure S174. ^{13}C NMR spectrum of substrate **6a**, related to **Scheme 4**.

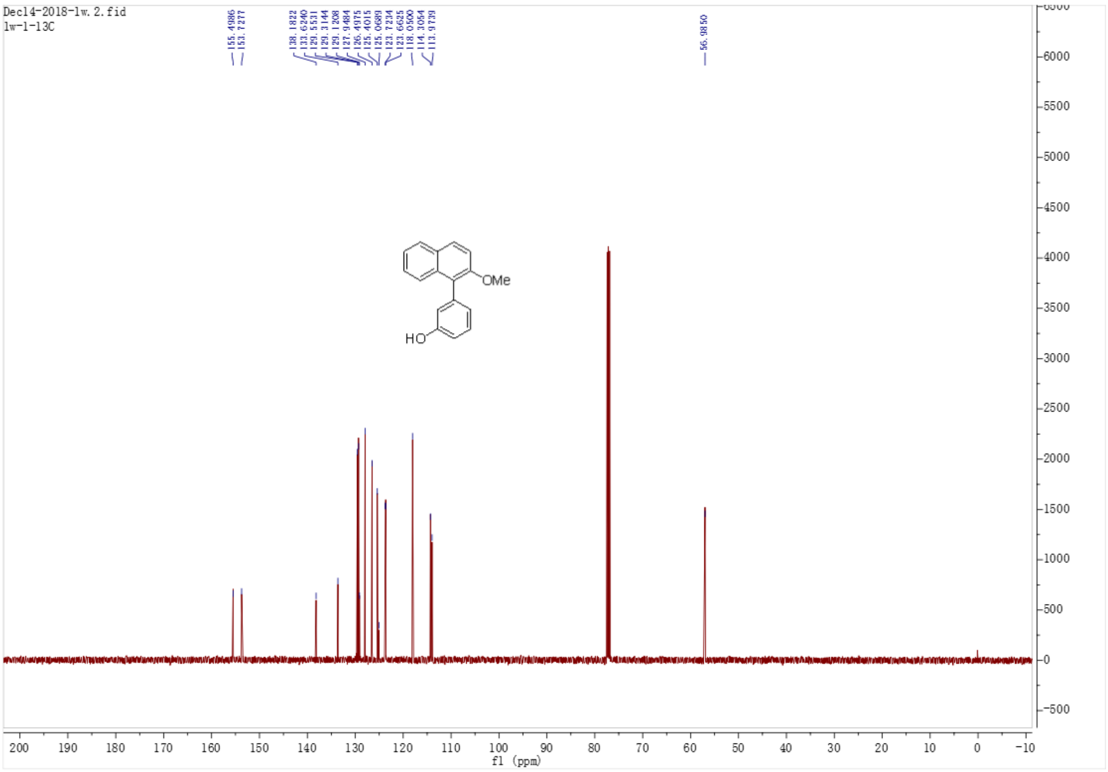

Figure S175. ^{1}H NMR spectrum of substrate **6b**, related to **Scheme 4**.

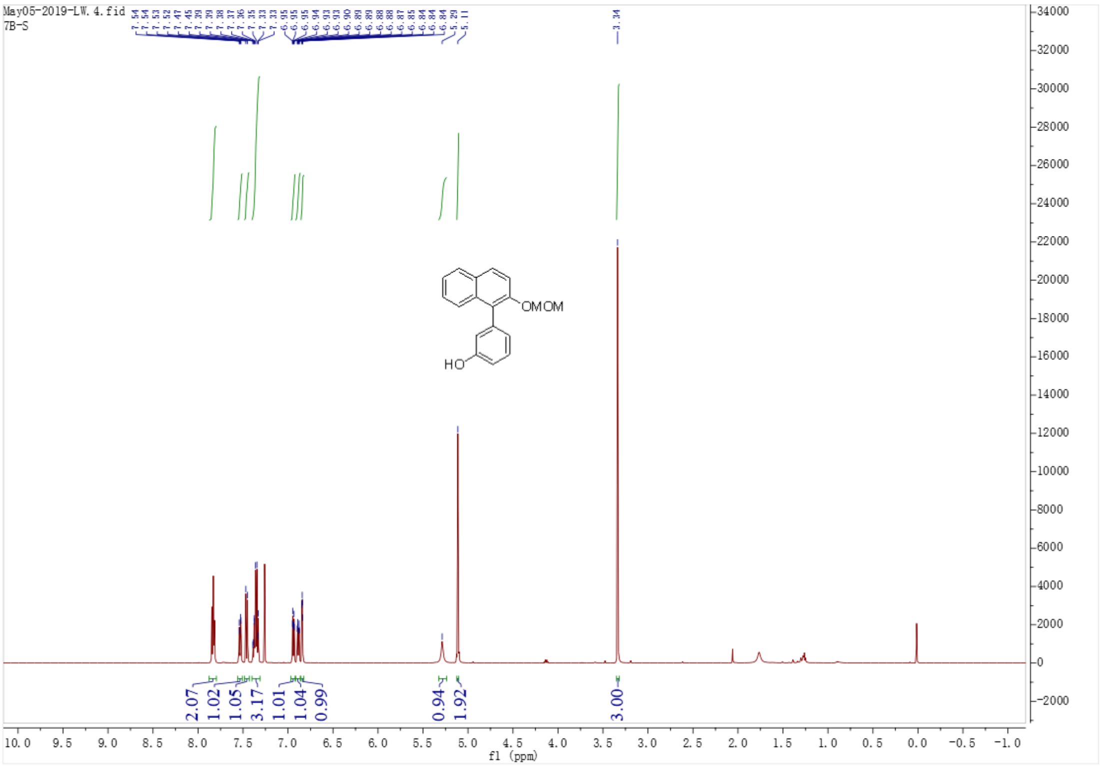

Figure S176. ^{13}C NMR spectrum of substrate **6b**, related to **Scheme 4**.

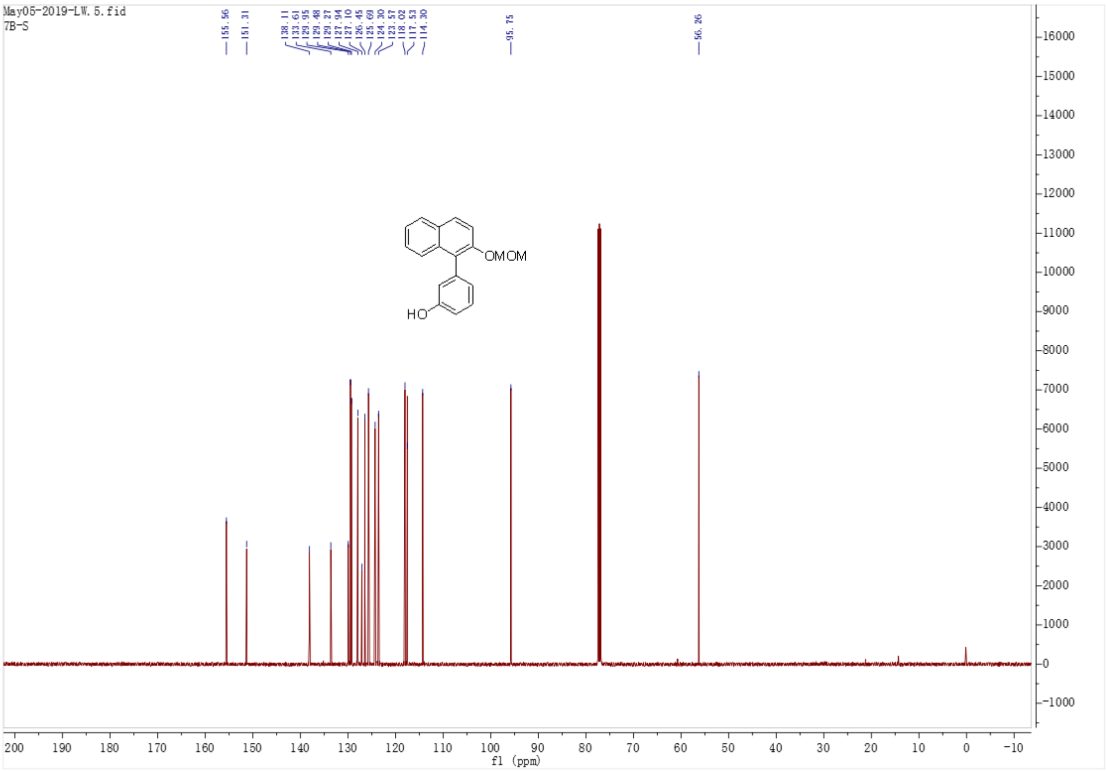

Figure S177. ^{1}H NMR spectrum of substrate **6c**, related to **Scheme 4**.

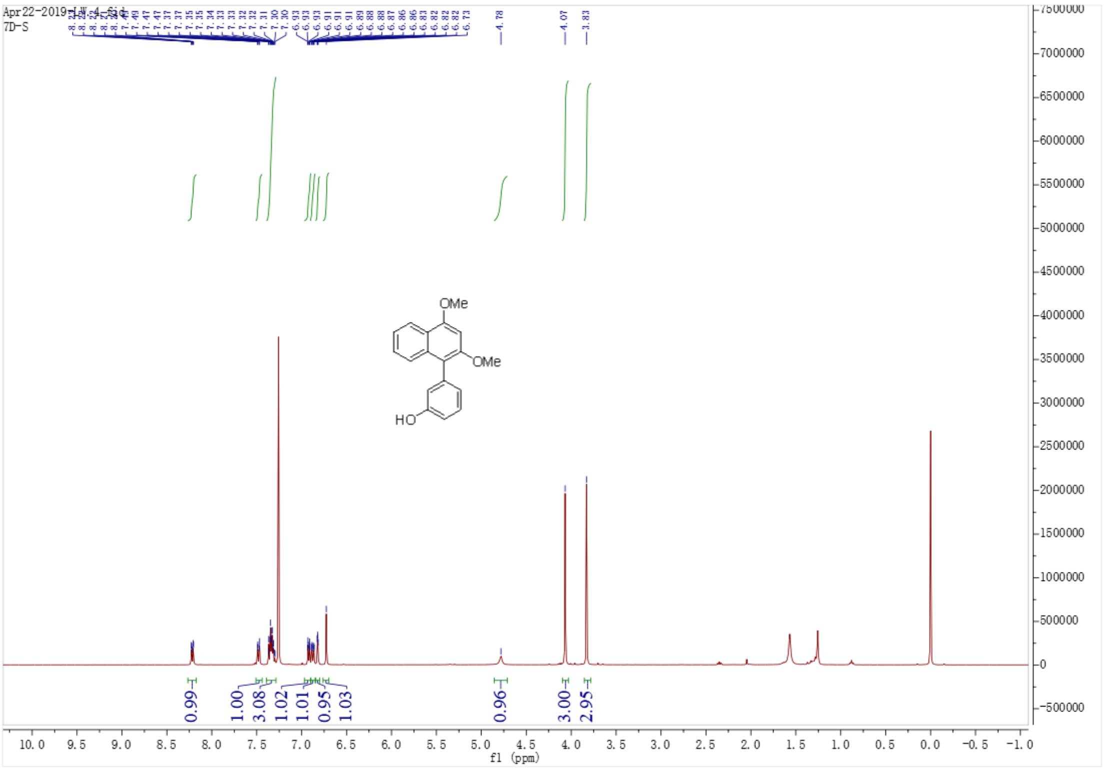

Figure S178. ^{13}C NMR spectrum of substrate **6c**, related to **Scheme 4**.

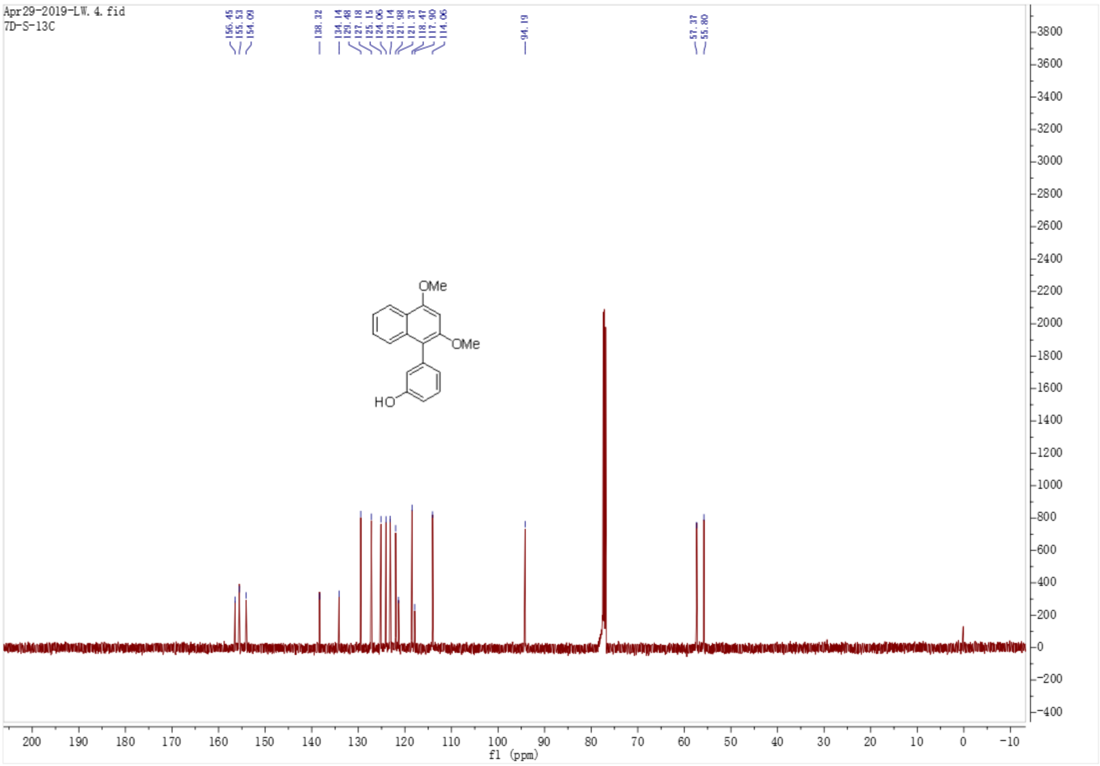

Figure S179. ^{1}H NMR spectrum of substrate **6d**, related to **Scheme 4**.

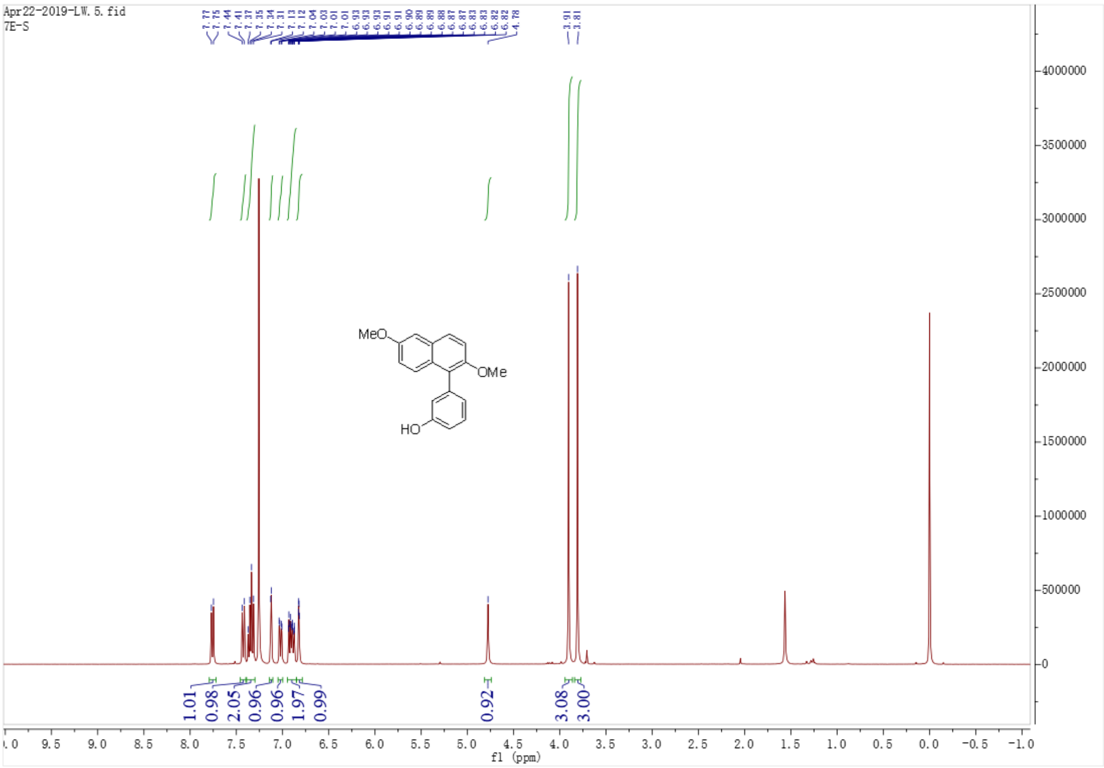

Figure S180. ^{13}C NMR spectrum of substrate **6d**, related to **Scheme 4**.

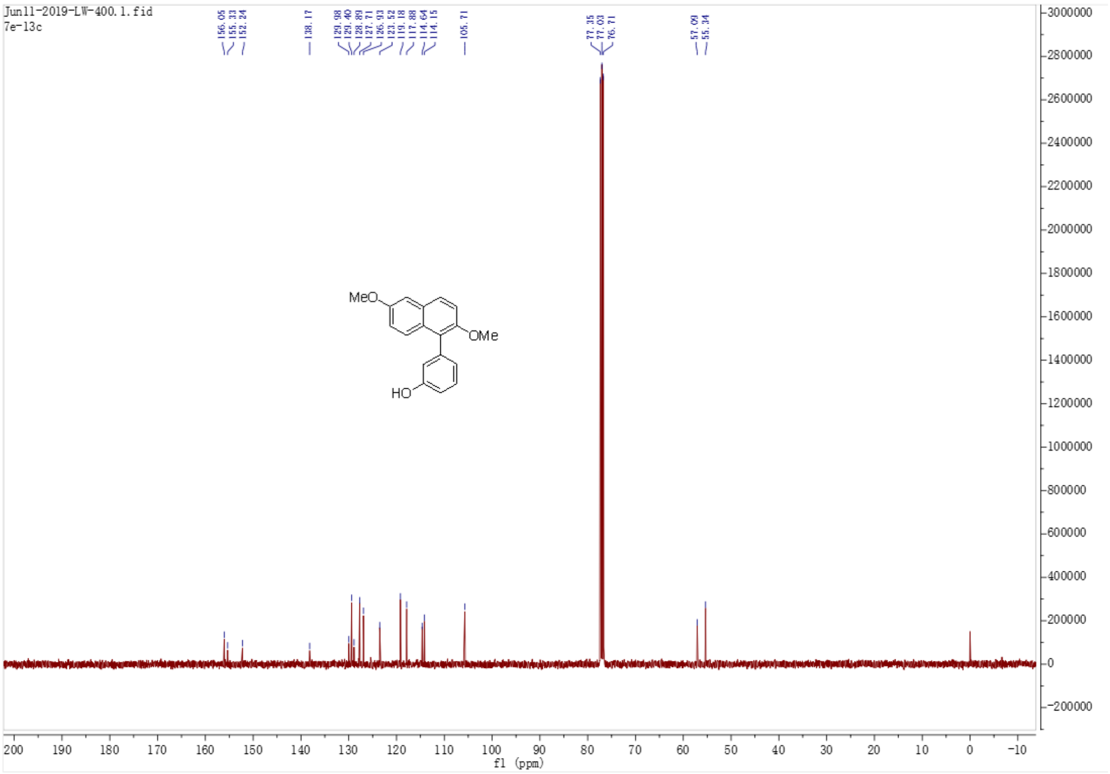

Figure S181. ^{1}H NMR spectrum of substrate **6e**, related to **Scheme 4**.

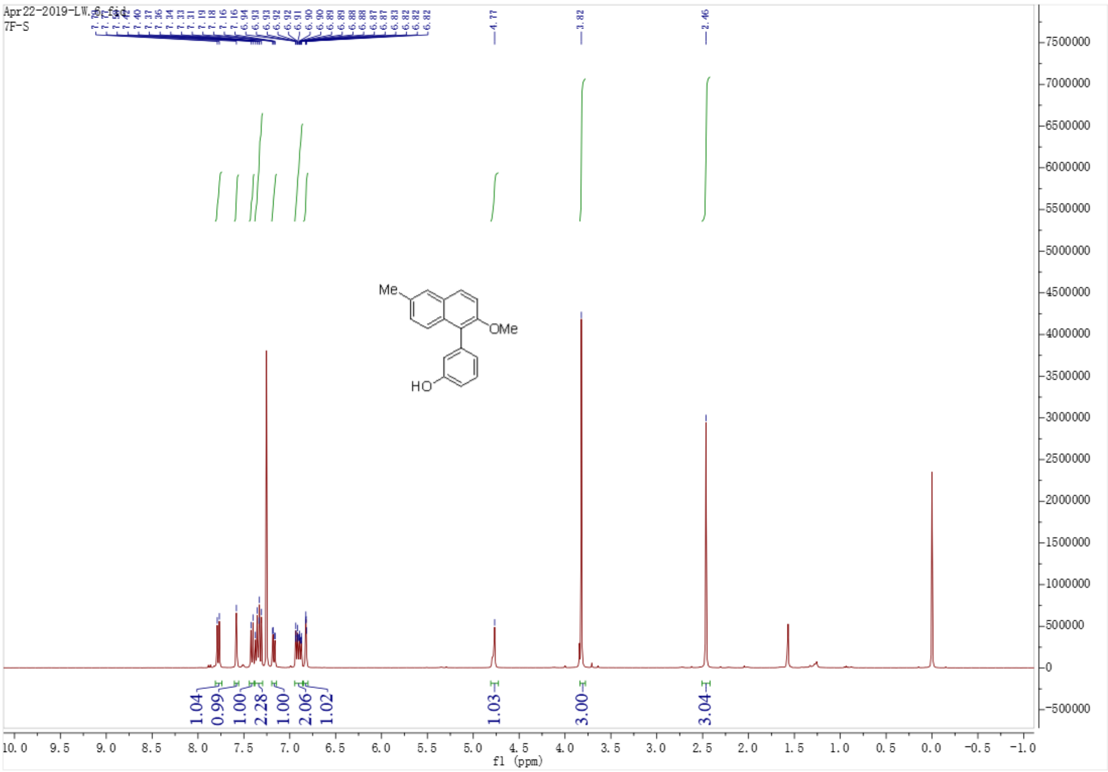

Figure S182. ^{13}C NMR spectrum of substrate **6e**, related to **Scheme 4**.

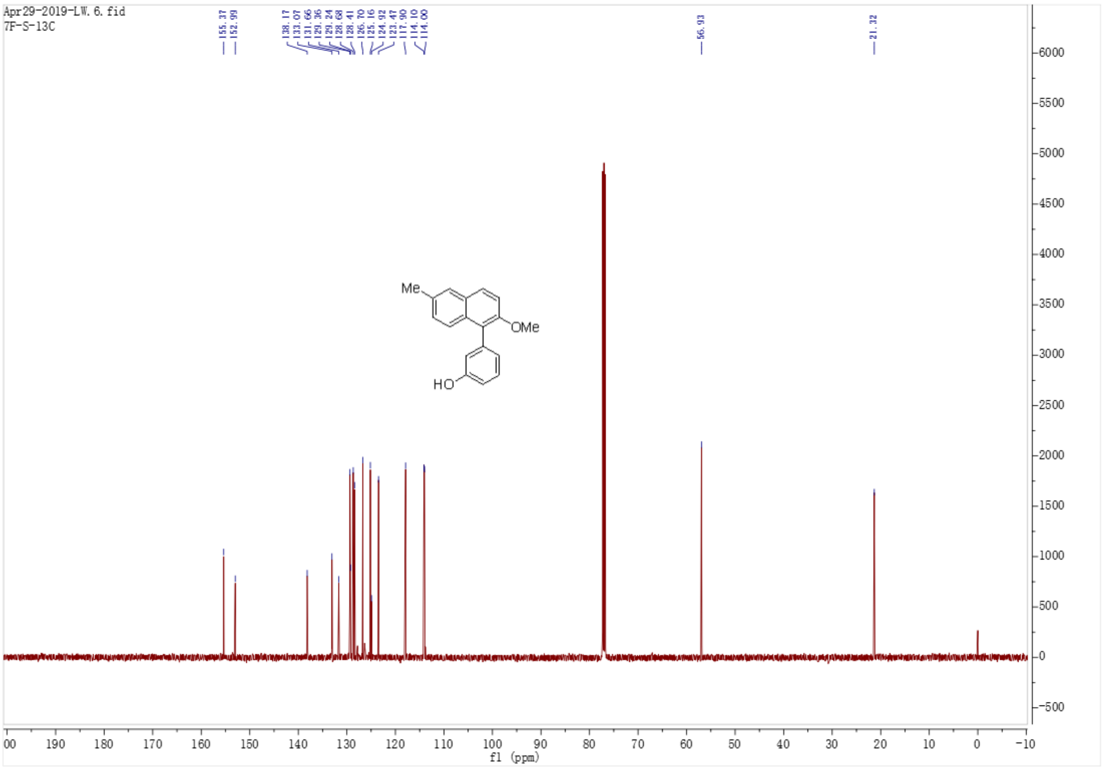

Figure S183. ^{1}H NMR spectrum of substrate **6f**, related to **Scheme 4**.

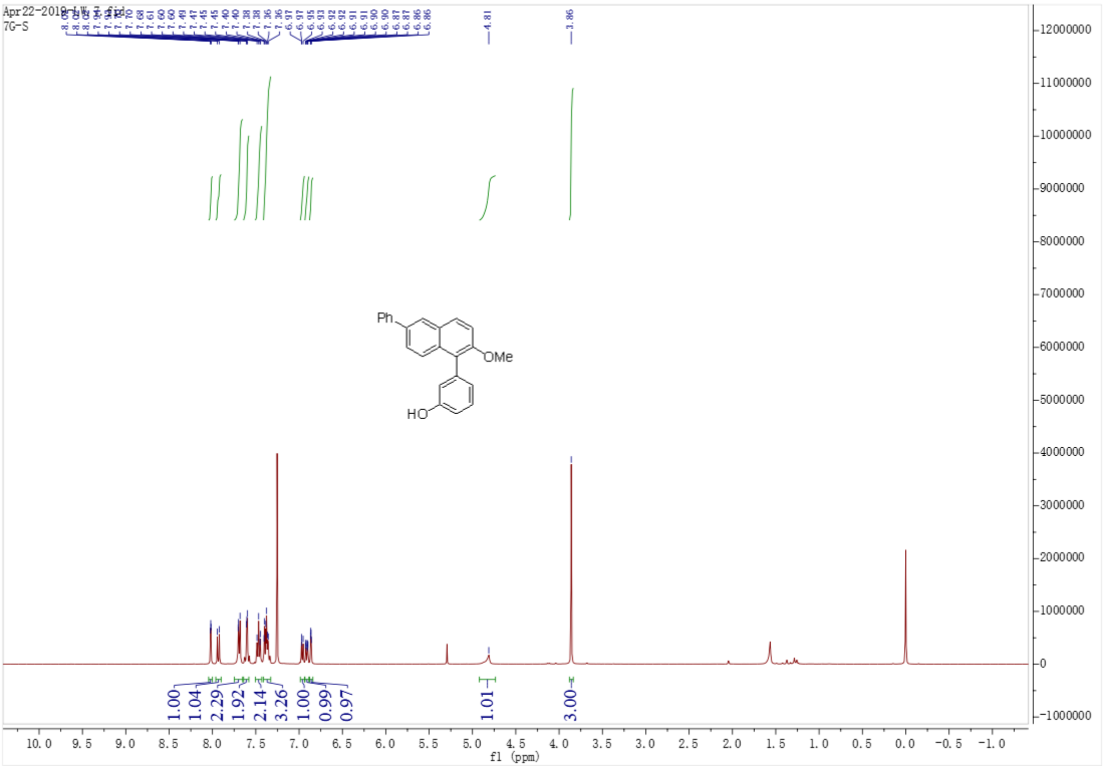

Figure S184. ^{13}C NMR spectrum of substrate **6f**, related to **Scheme 4**.

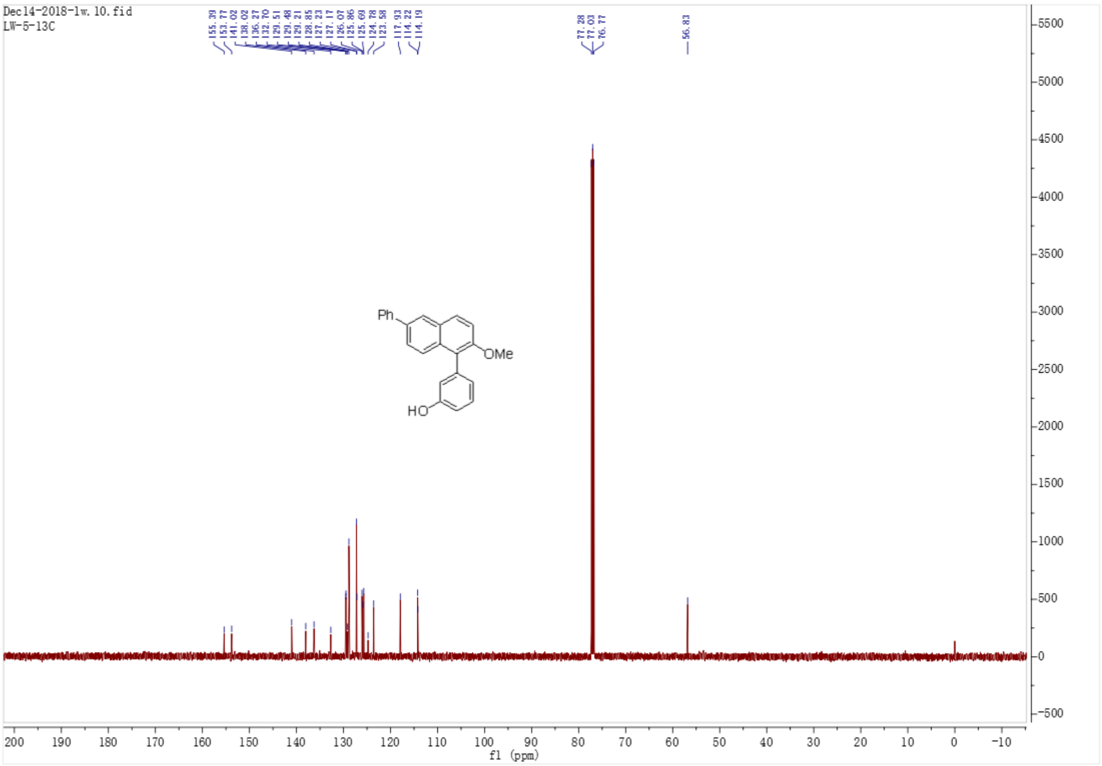

Figure S185. ^{1}H NMR spectrum of substrate **6g**, related to **Scheme 4**.

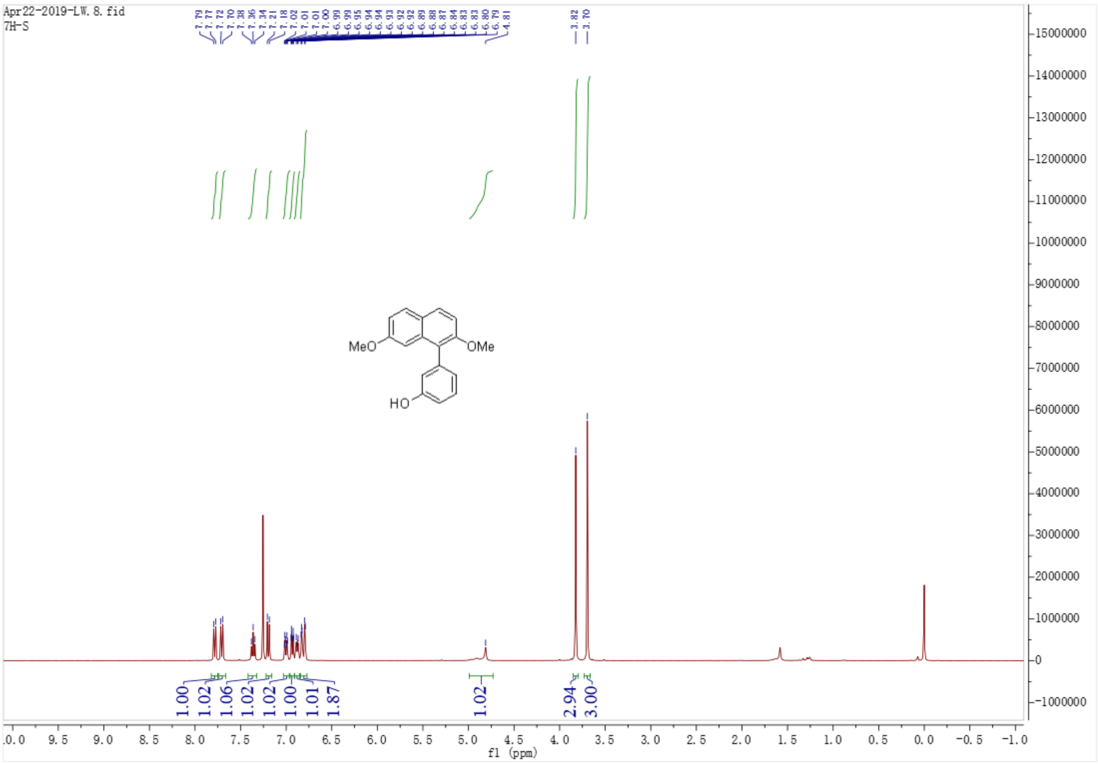

Figure S186. ^{13}C NMR spectrum of substrate **6g**, related to **Scheme 4**.

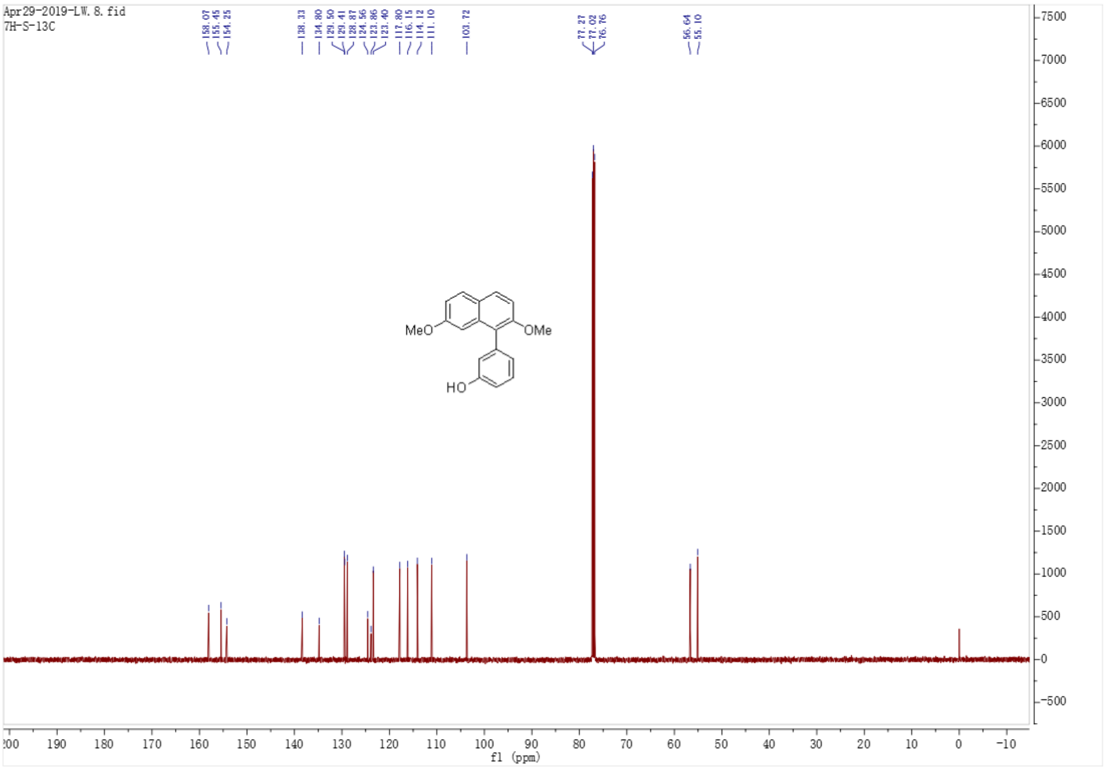

Figure S187. ^{1}H NMR spectrum of product **7a**, related to **Scheme 4**.

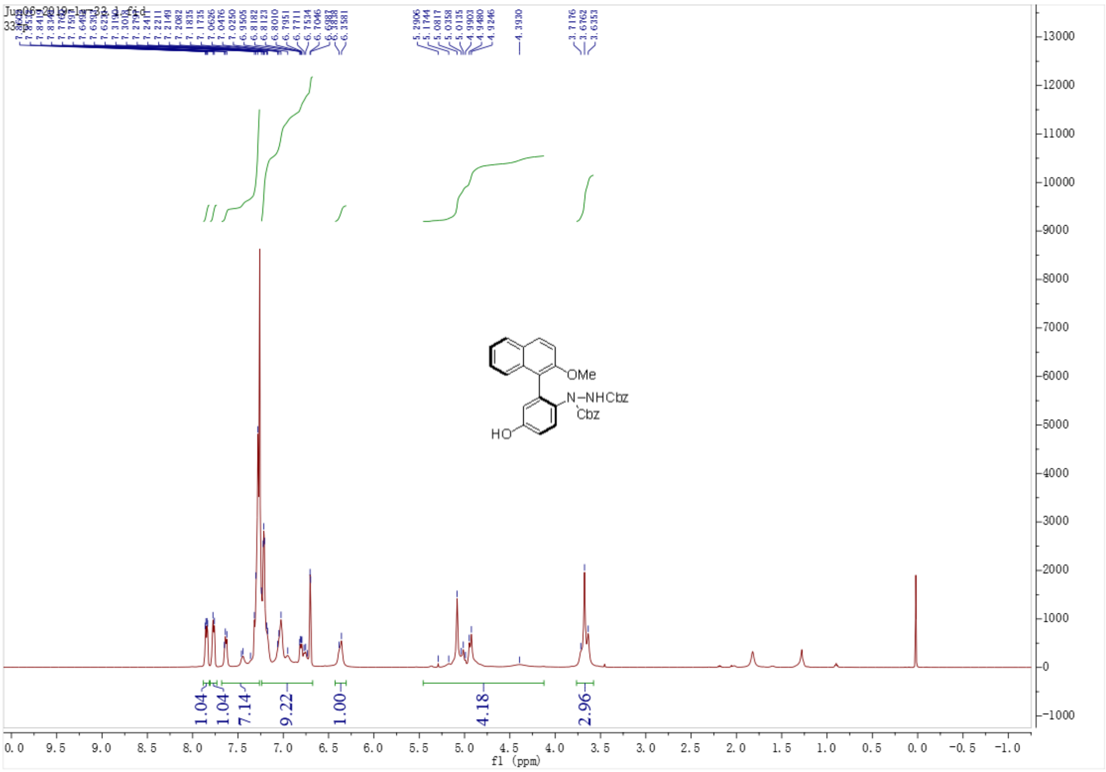

Figure S188. ^{13}C NMR spectrum of product **7a**, related to **Scheme 4**.

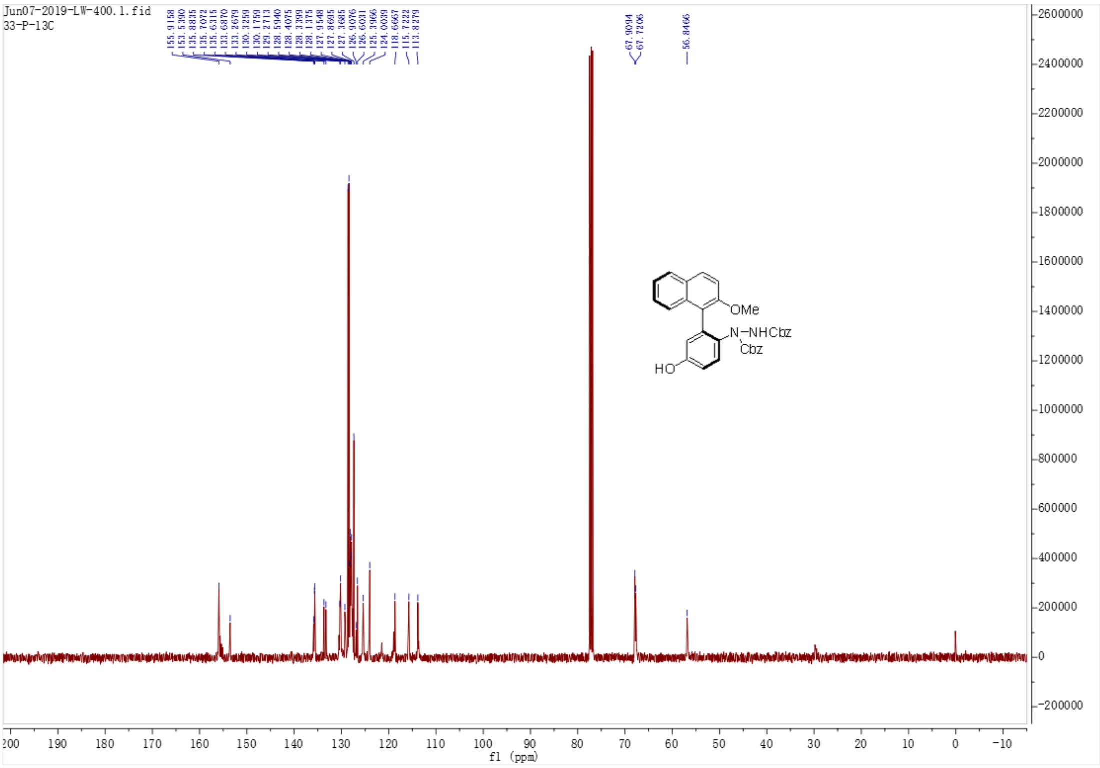

Figure S189. ^{1}H NMR spectrum of product **7b**, related to **Scheme 4**.

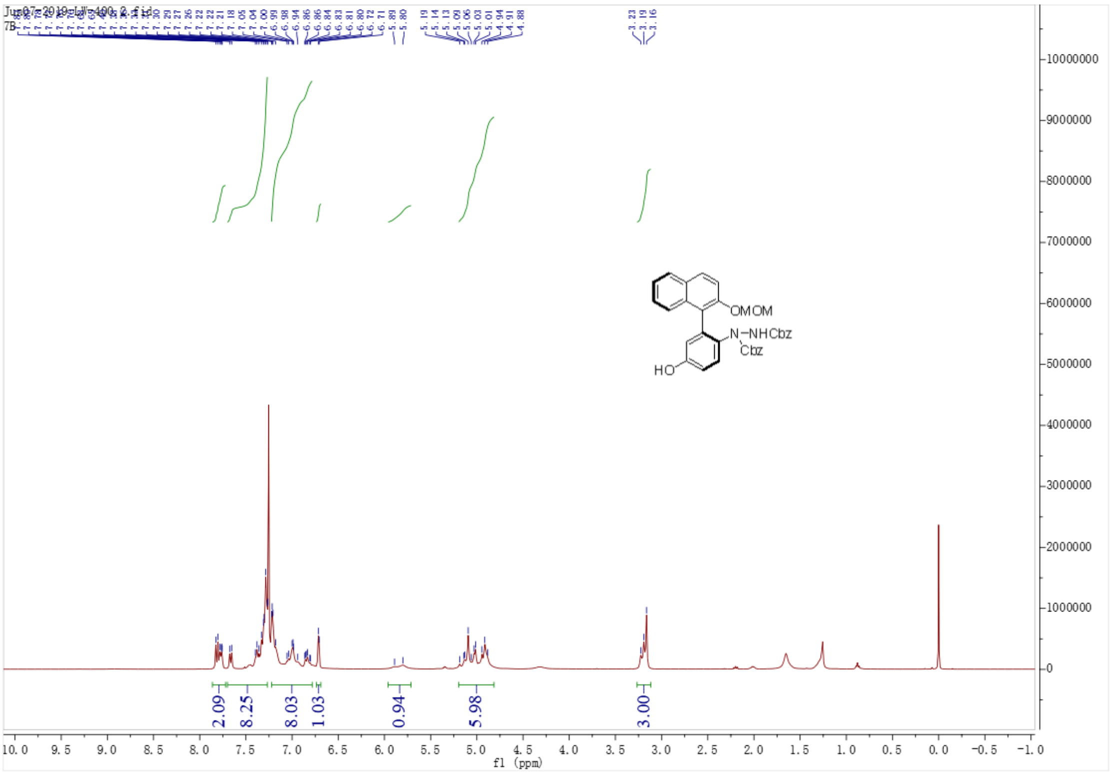

Figure S190. ^{13}C NMR spectrum of product **7b**, related to **Scheme 4**.

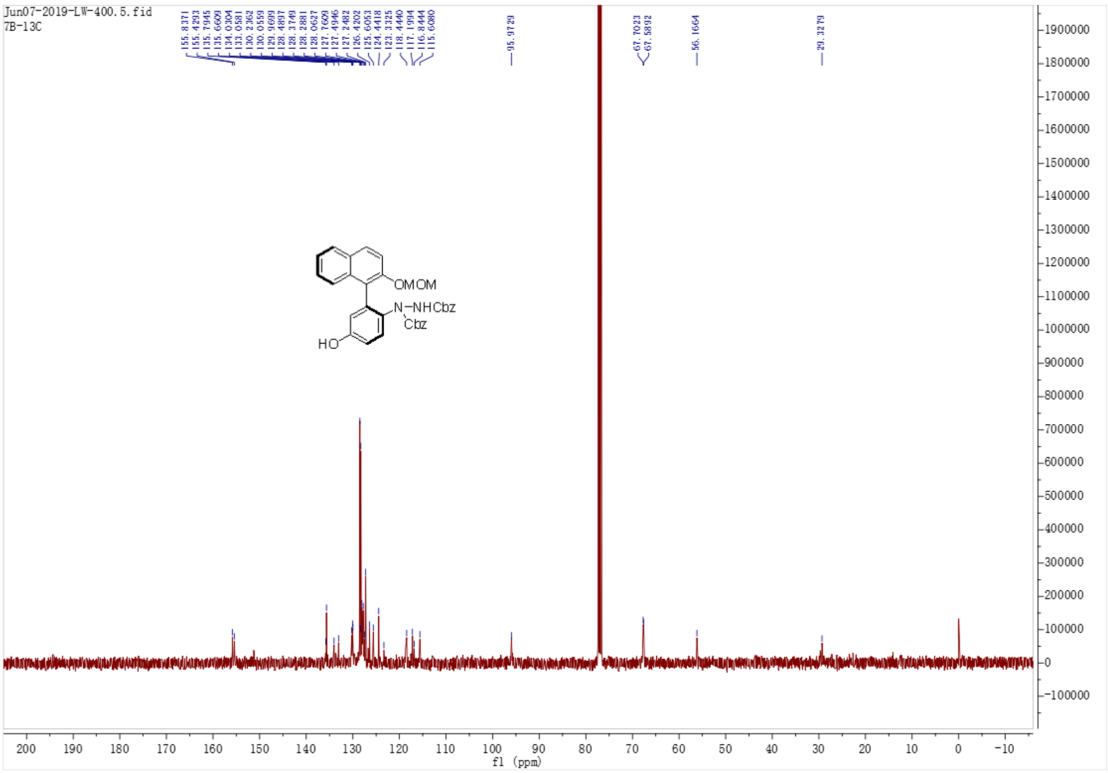

Figure S191. ^{1}H NMR spectrum of product **7c**, related to **Scheme 4**.

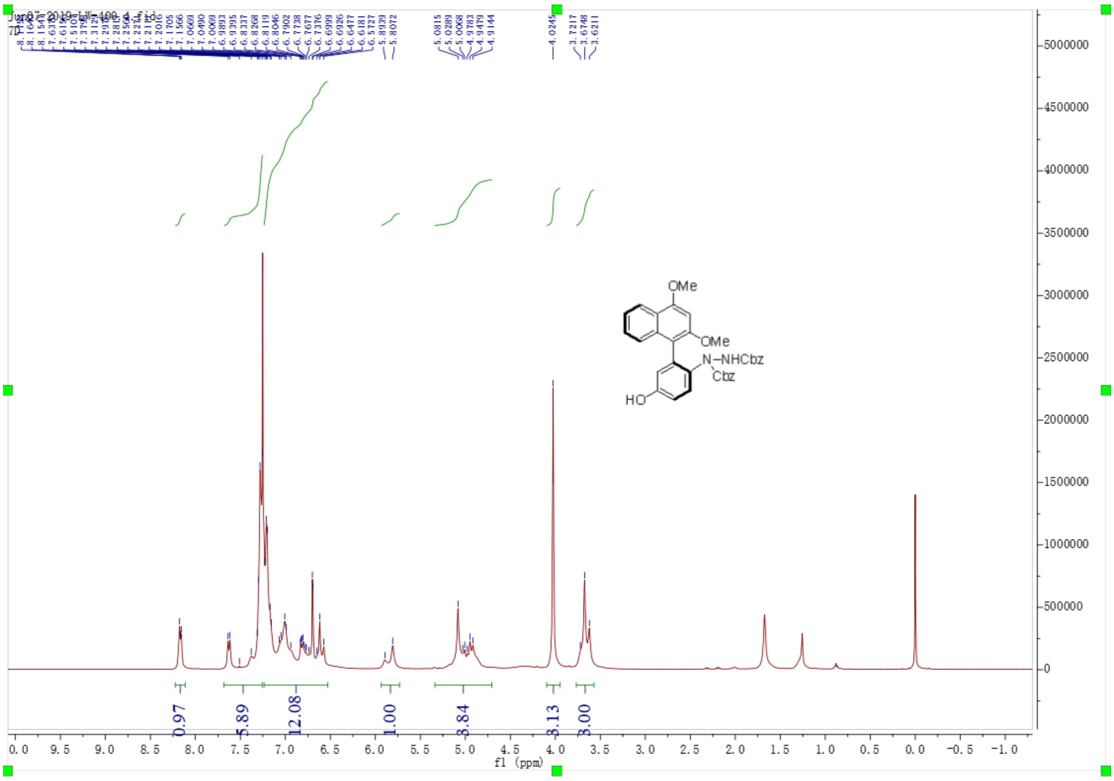

Figure S192. ^{13}C NMR spectrum of product **7c**, related to **Scheme 4**.

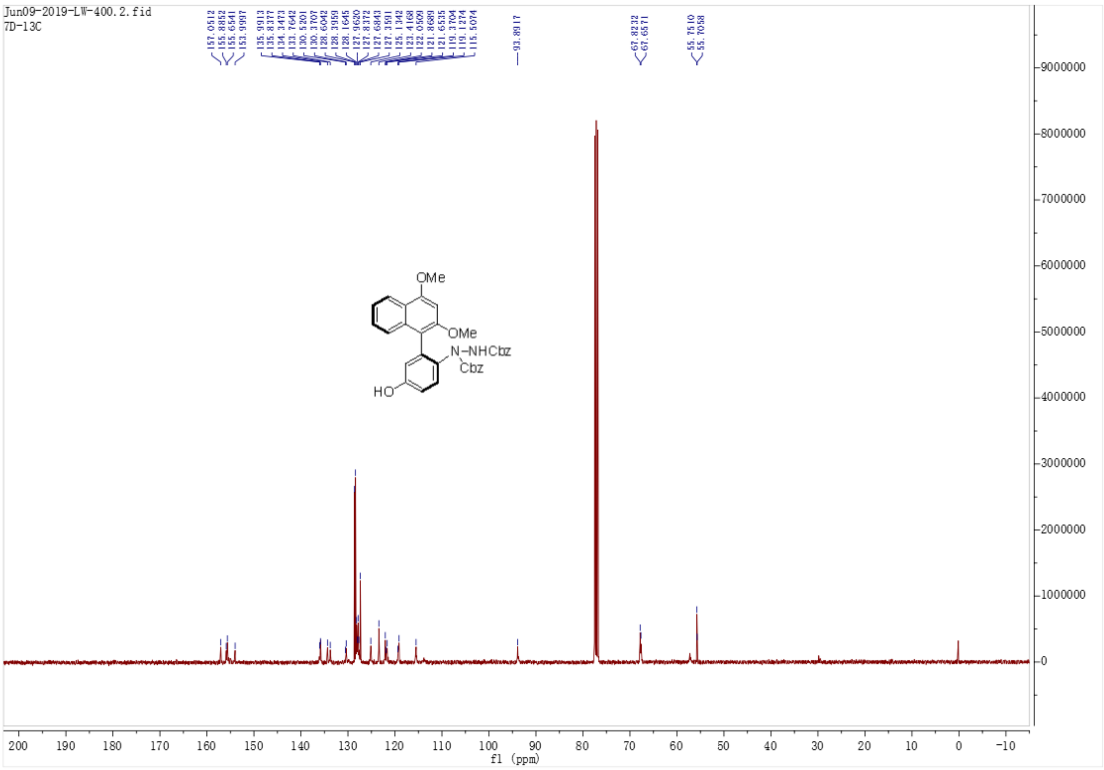

Figure S193. ^{1}H NMR spectrum of product **7d**, related to **Scheme 4**.

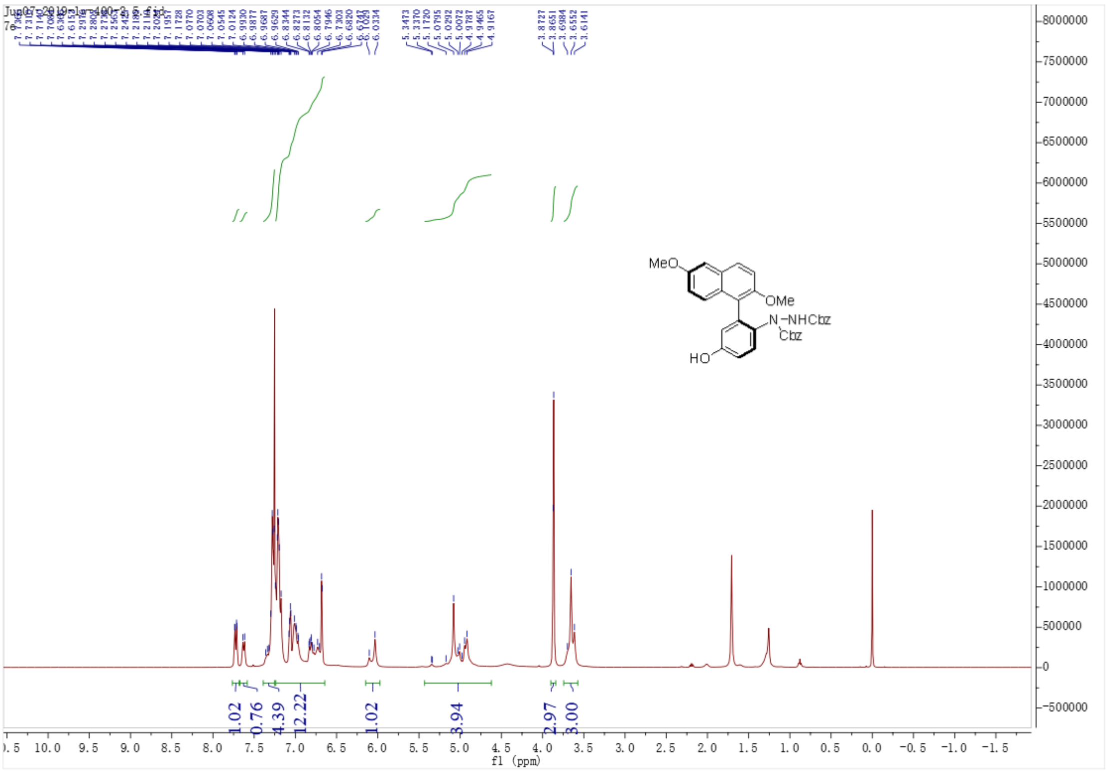

Figure S194. ^{13}C NMR spectrum of product **7d**, related to **Scheme 4**.

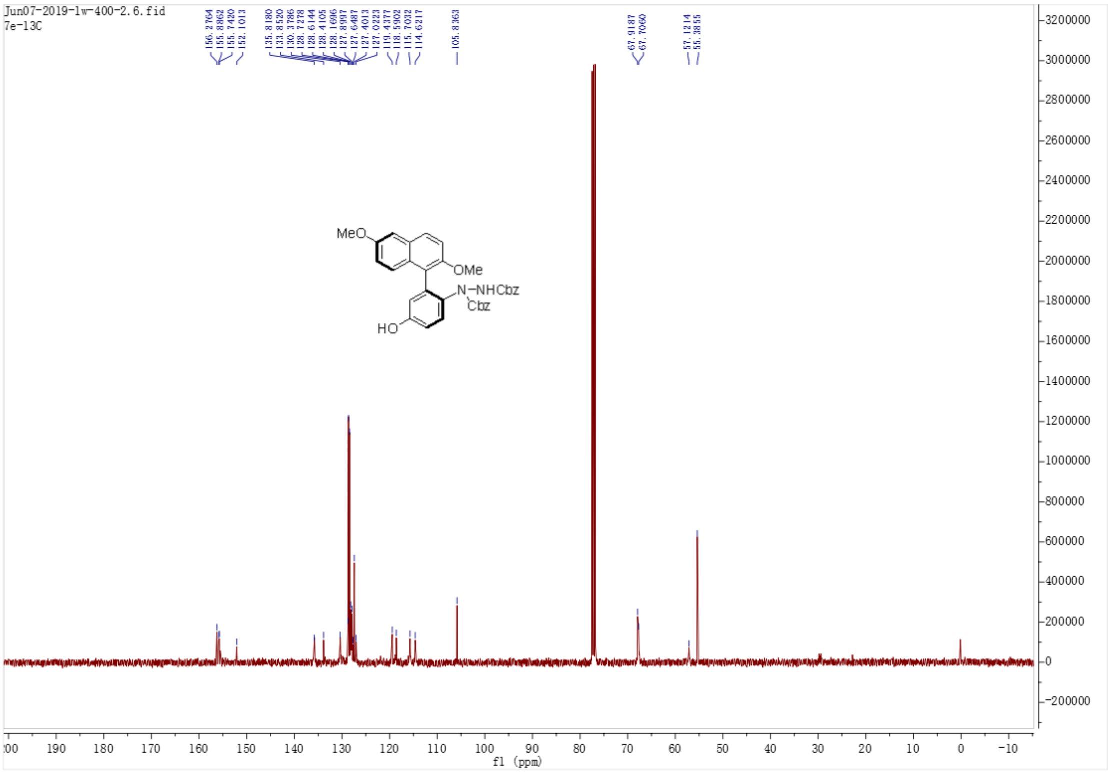

Figure S195. ^{1}H NMR spectrum of product **7e**, related to **Scheme 4**.

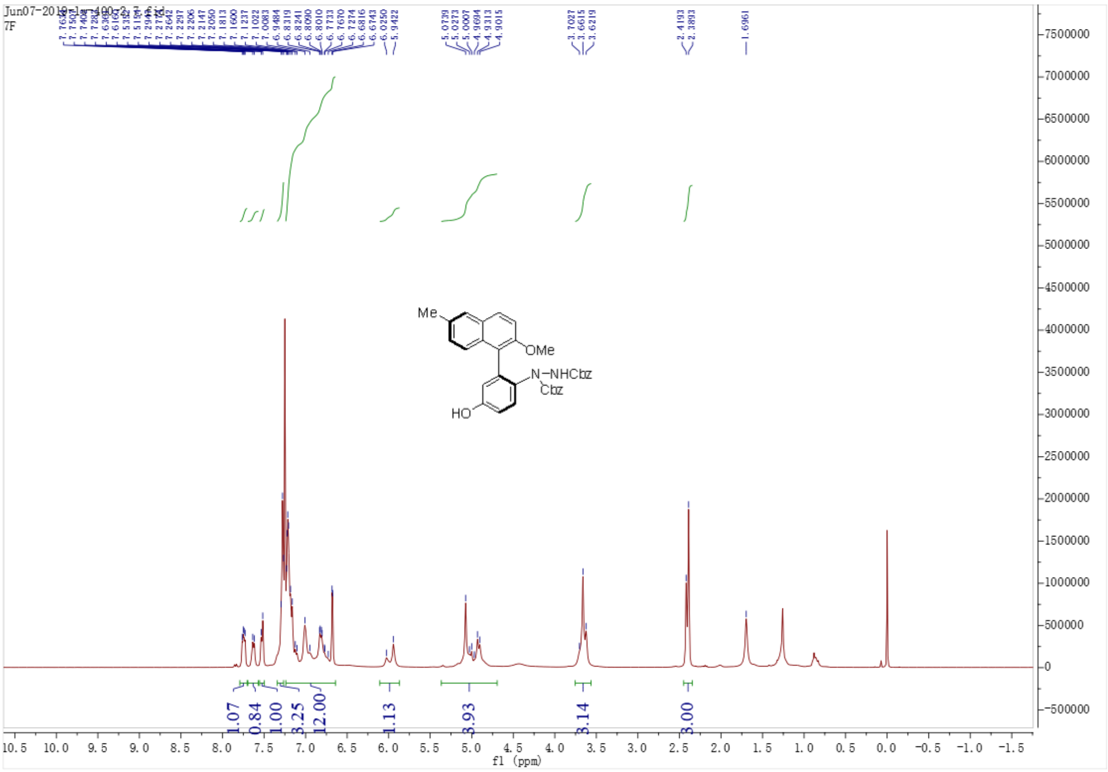

Figure S196. ^{13}C NMR spectrum of product **7e**, related to **Scheme 4**.

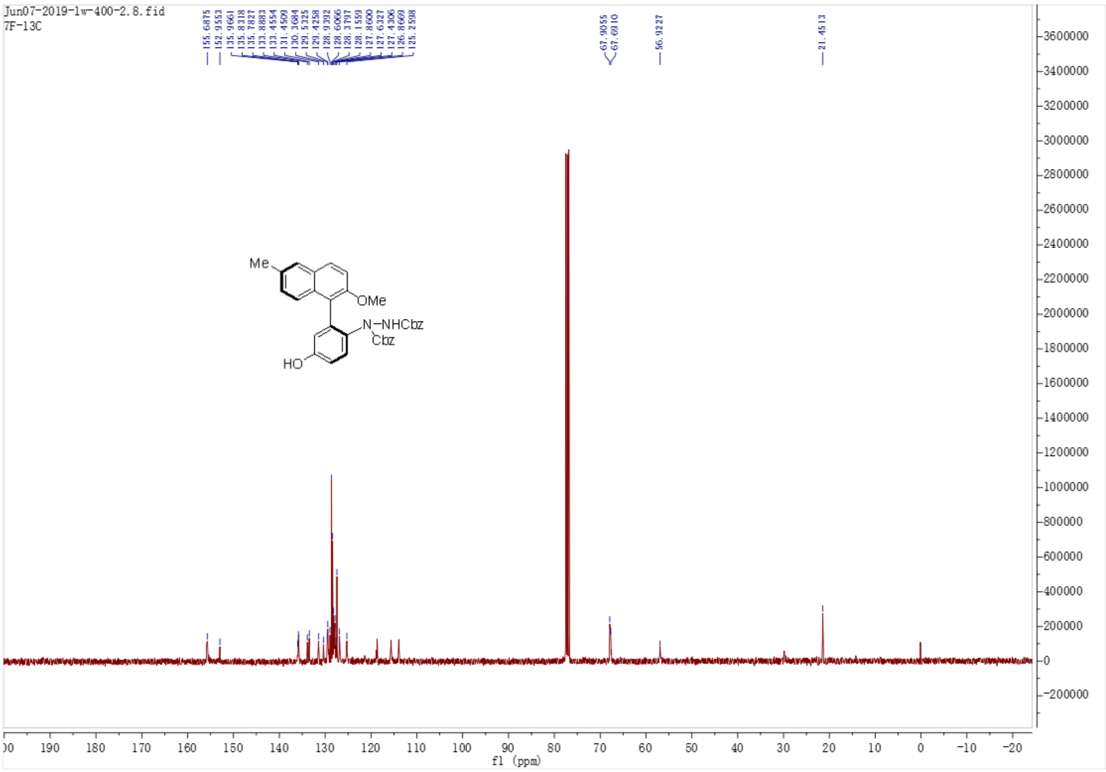

Figure S197. ^{1}H NMR spectrum of product **7f**, related to **Scheme 4**.

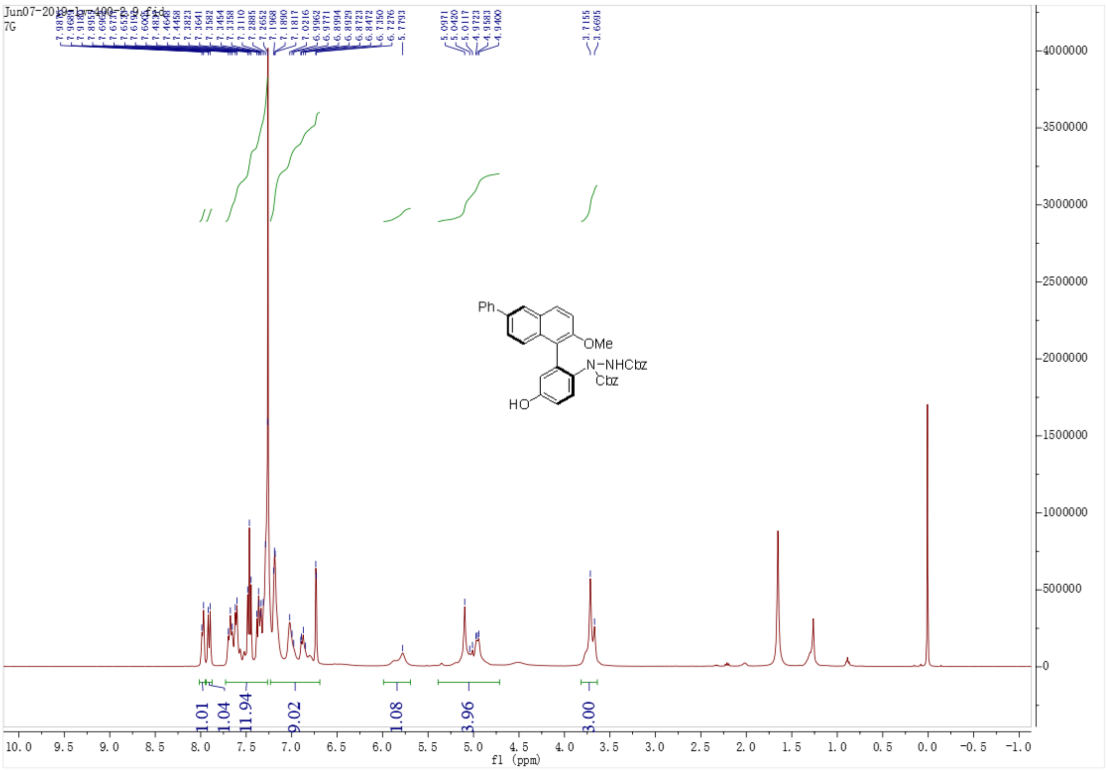

Figure S198. ^{13}C NMR spectrum of product **7f**, related to **Scheme 4**.

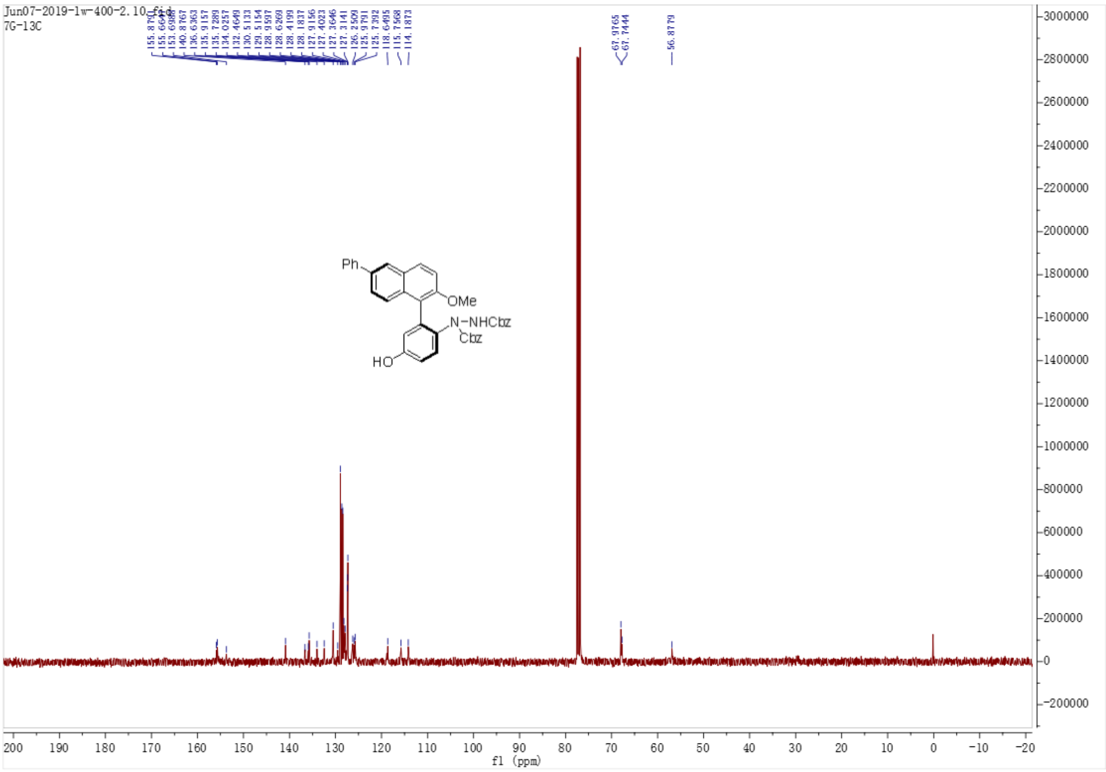

Figure S199. ^{1}H NMR spectrum of product **7g**, related to **Scheme 4**.

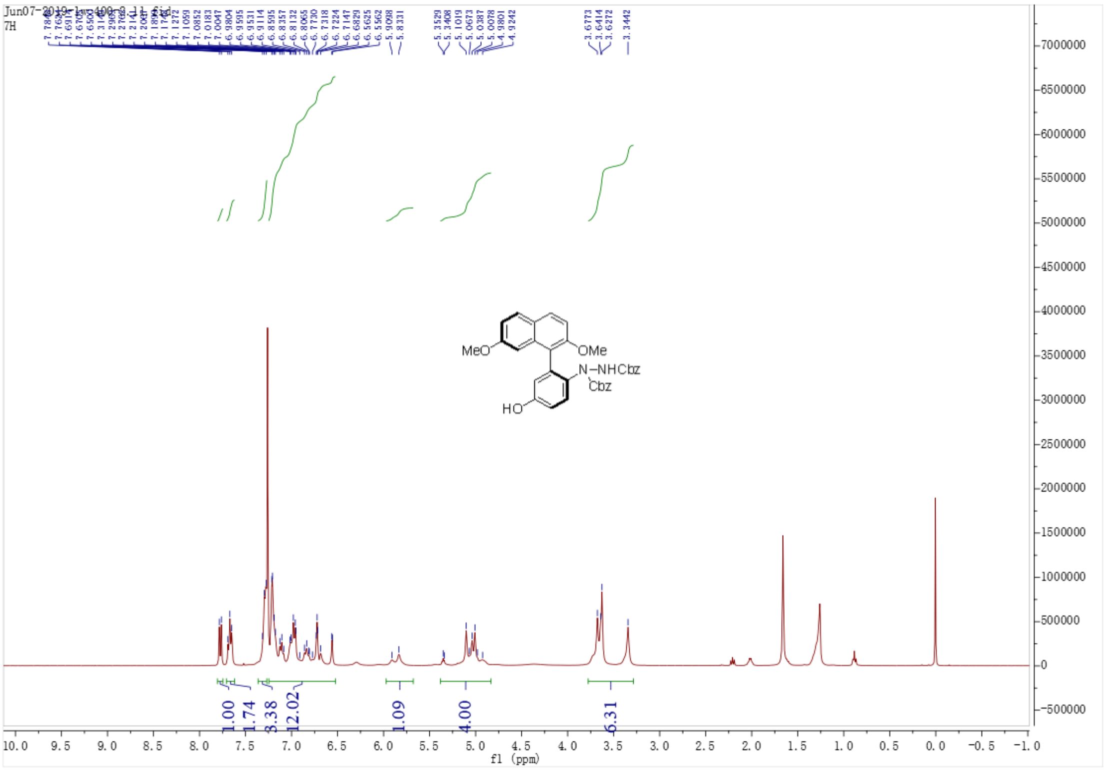

Figure S200. ^{13}C NMR spectrum of product **7g**, related to **Scheme 4**.

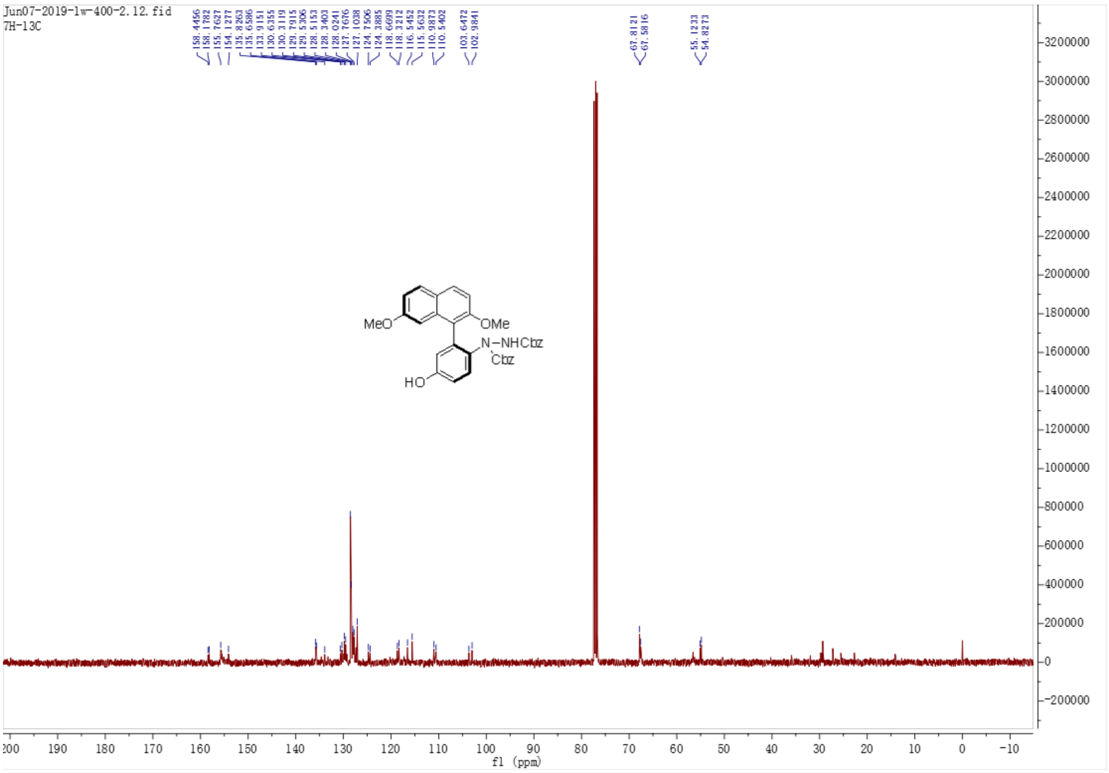

Figure S201. ^{1}H NMR spectrum of product **8a**, related to **Scheme 6**.

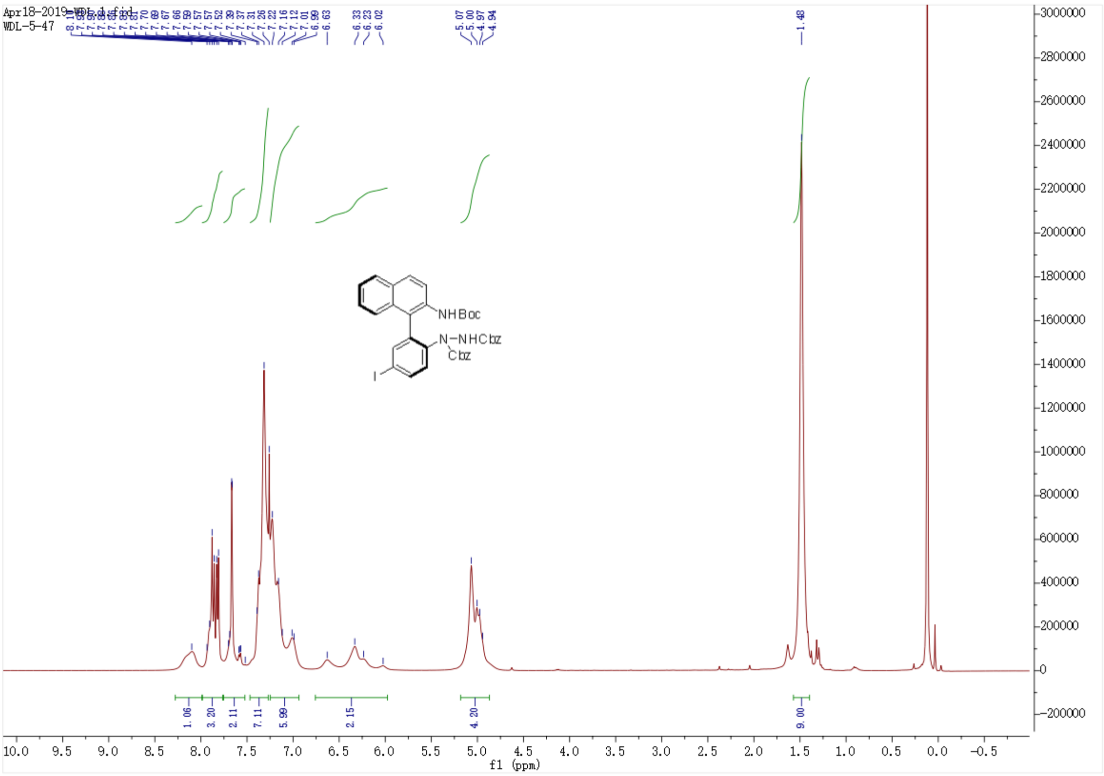

Figure S202. ^{13}C NMR spectrum of product **8a**, related to **Scheme 6**.

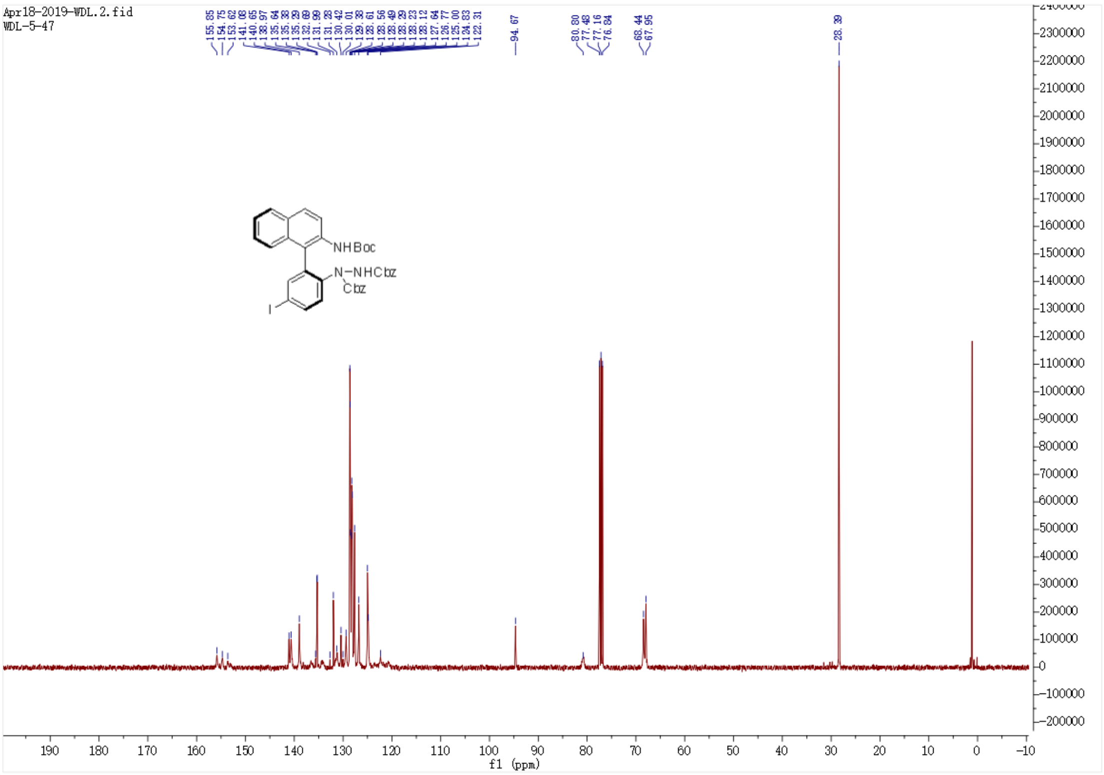

Figure S203. ^{1}H NMR spectrum of product **9a**, related to **Scheme 6**.

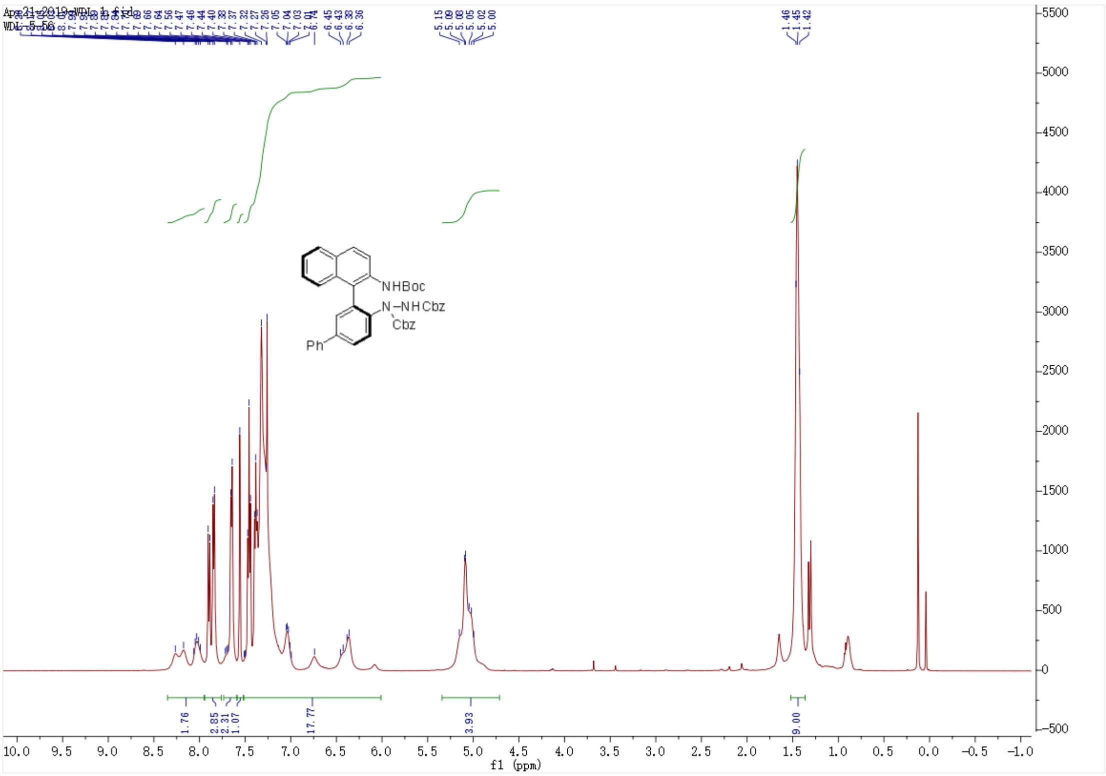

Figure S204. ^{13}C NMR spectrum of product **9a**, related to **Scheme 6**.

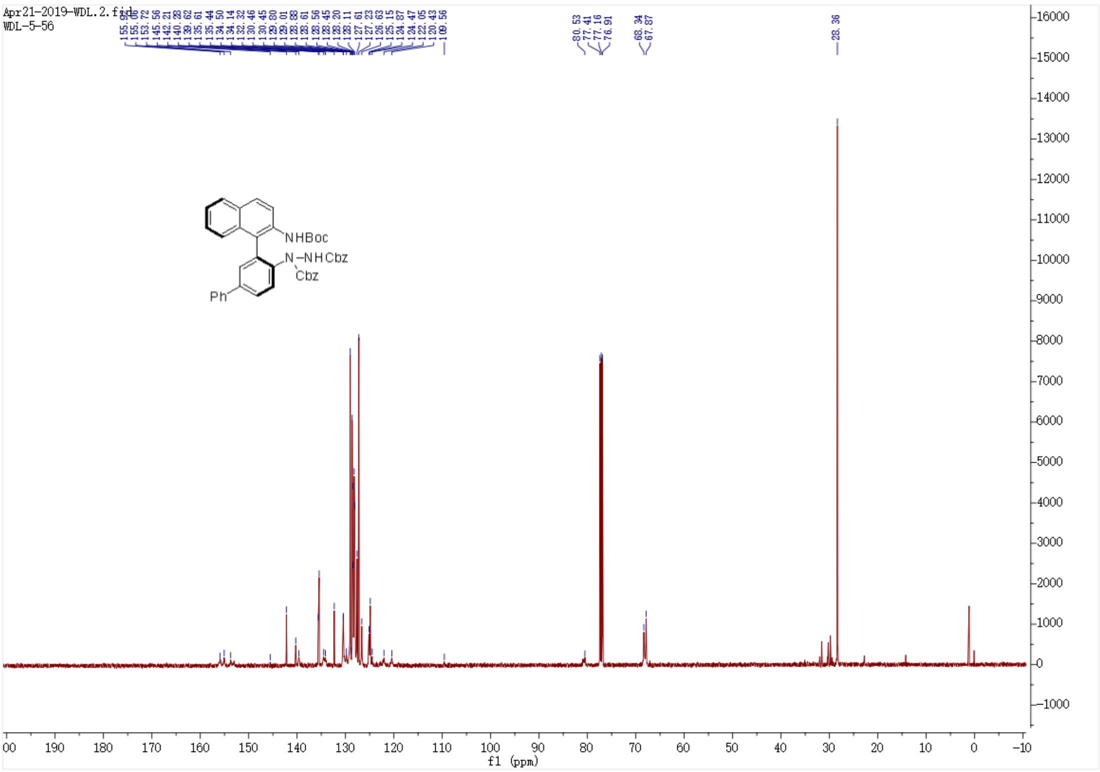

Figure S205. ^{1}H NMR spectrum of product **10a**, related to **Scheme 6**.

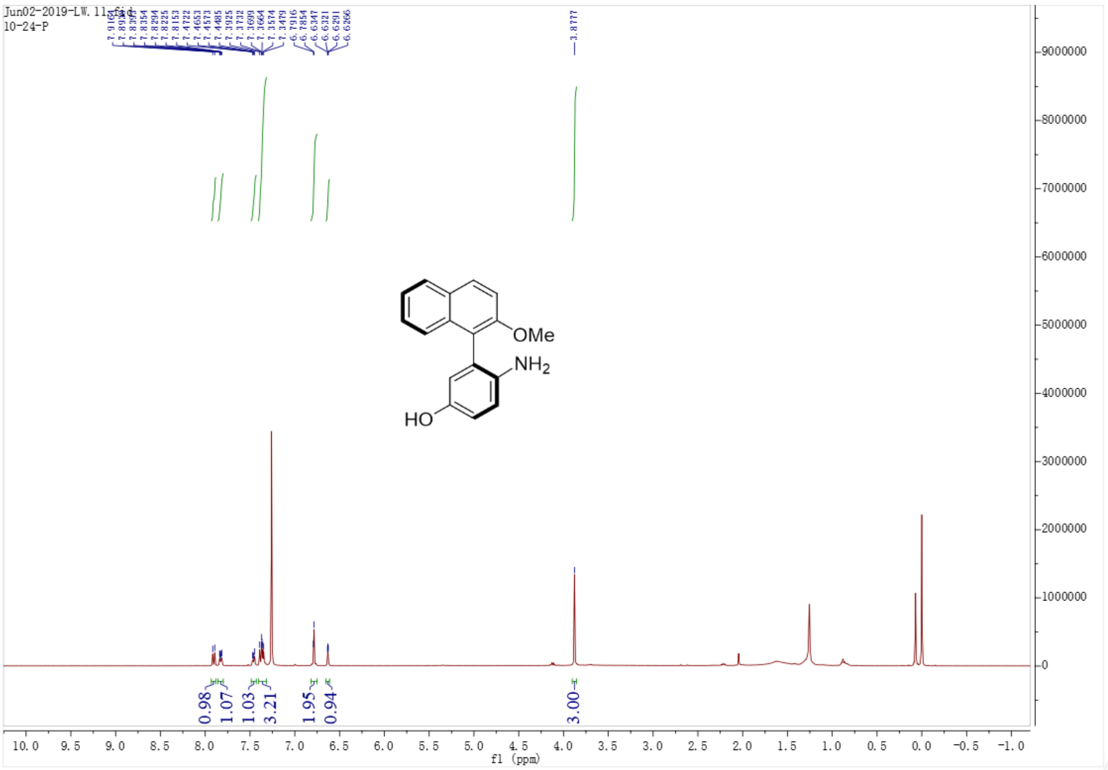

Figure S206. ^{13}C NMR spectrum of product **10a**, related to **Scheme 6**.

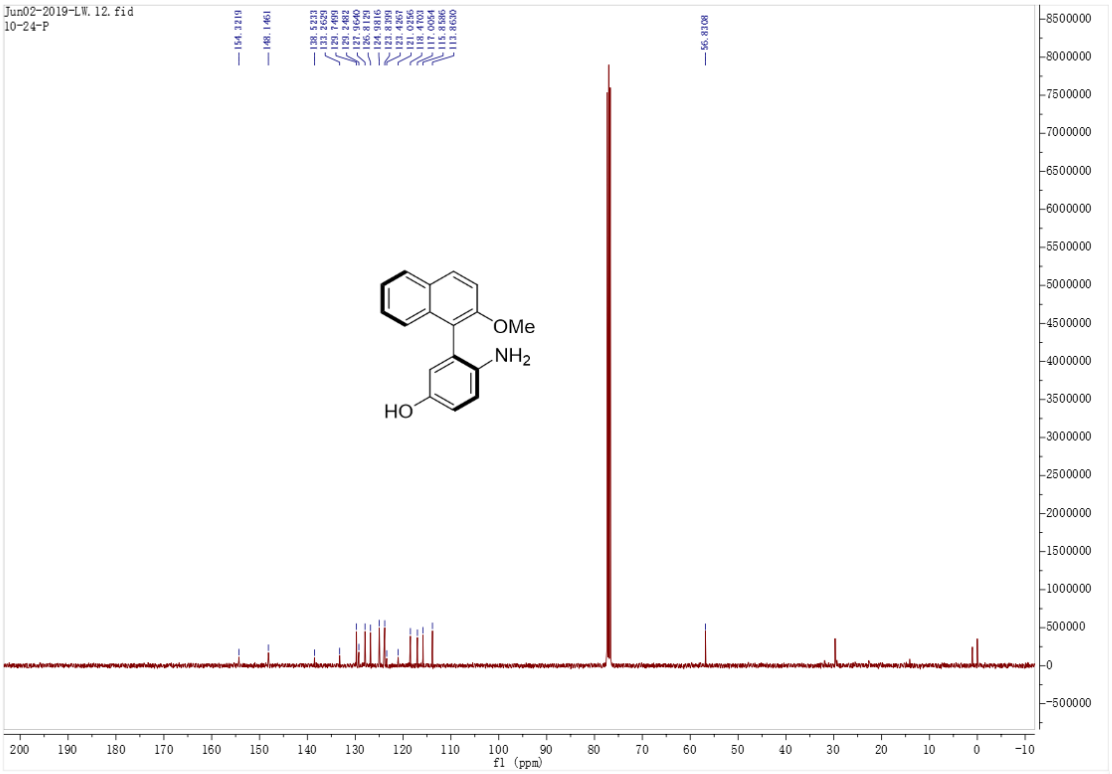

Figure S207. ^{1}H NMR spectrum of product **11n**, related to **Scheme 6**.

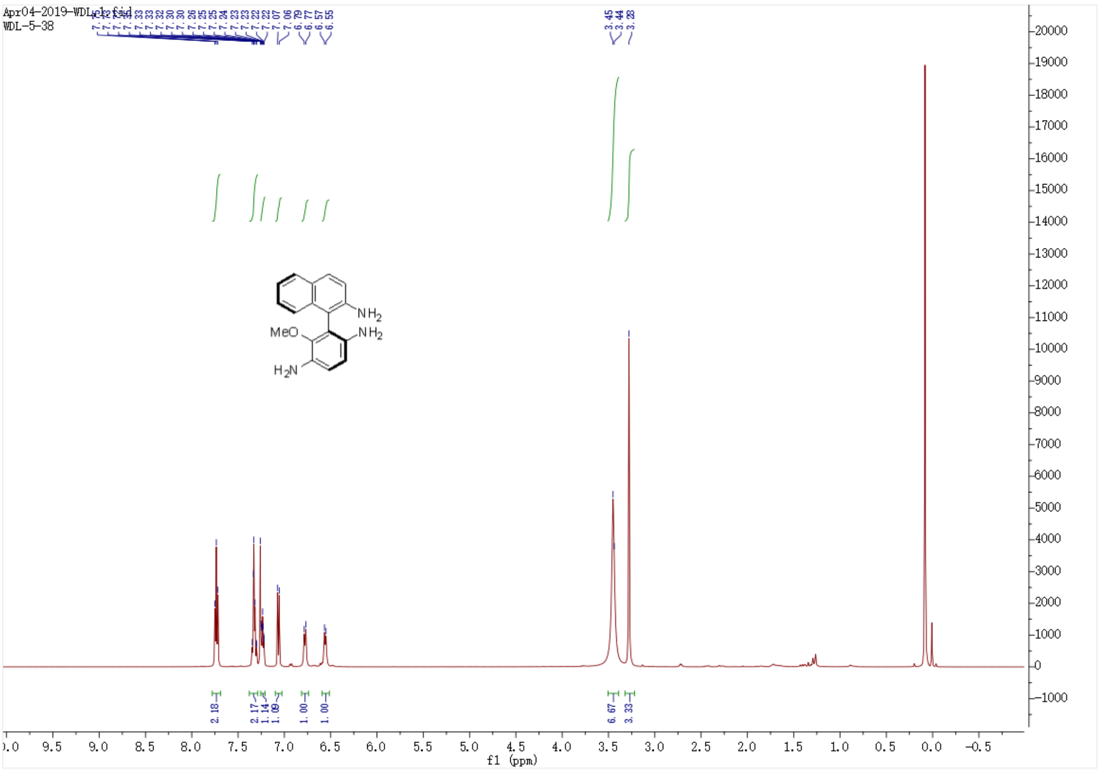

Figure S208. ^{13}C NMR spectrum of product **11n**, related to **Scheme 6**.

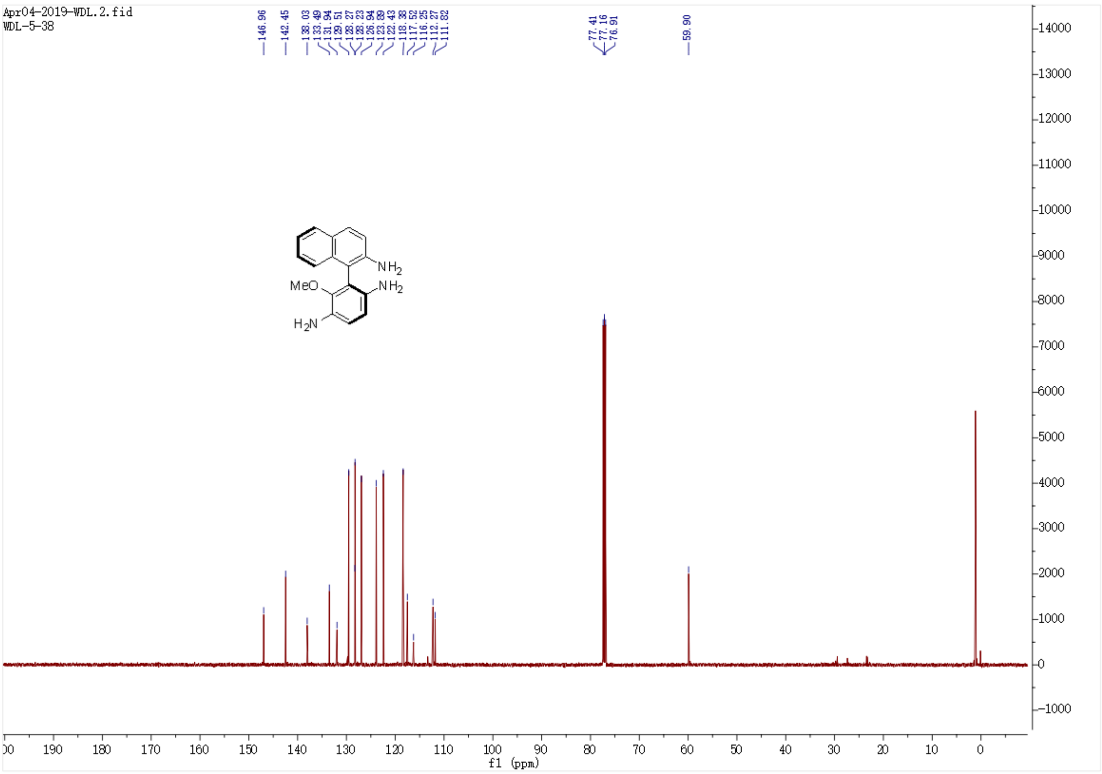

Figure S209. ^{1}H NMR spectrum of product **12a**, related to **Scheme 6**.

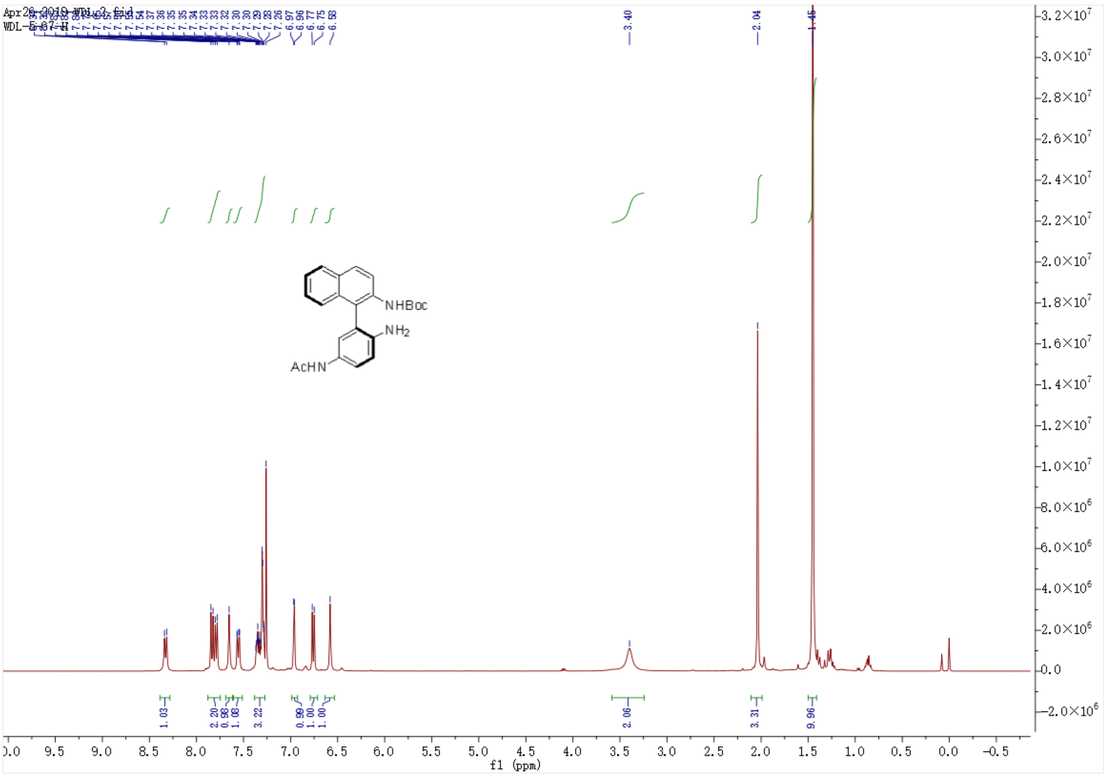

Figure S210. ^{13}C NMR spectrum of product **12a**, related to **Scheme 6**.

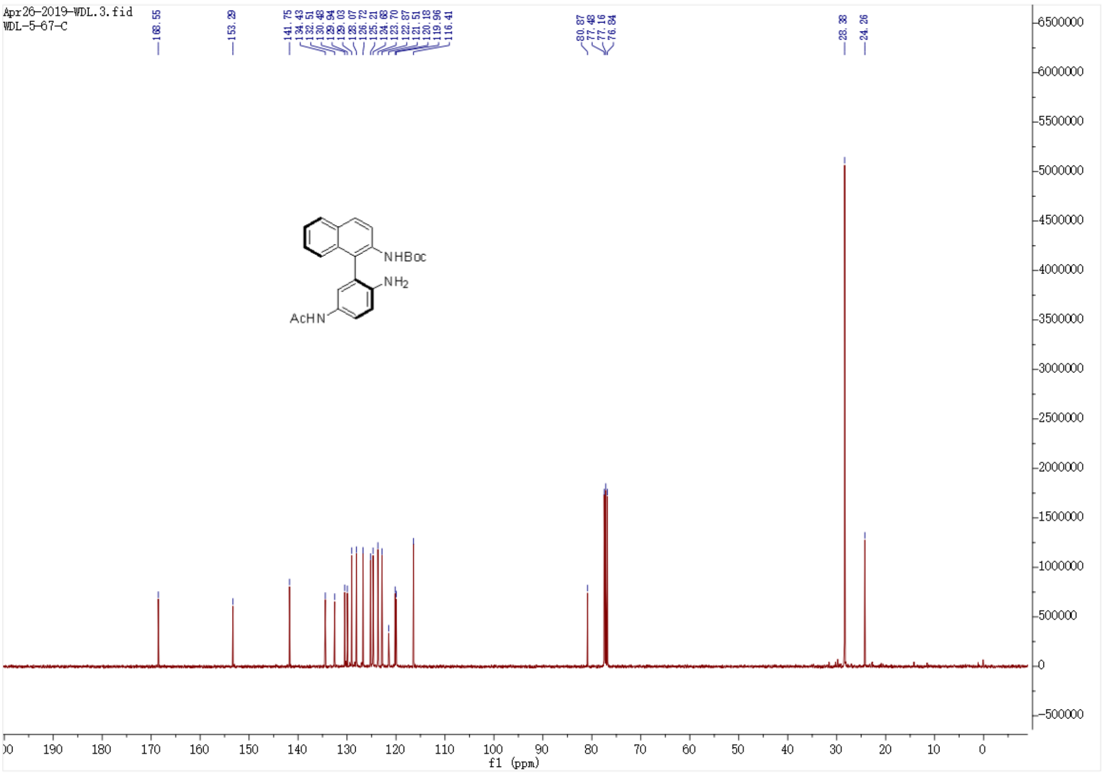

Figure S211. ^{1}H NMR spectrum of product **13a**, related to **Scheme 6**.

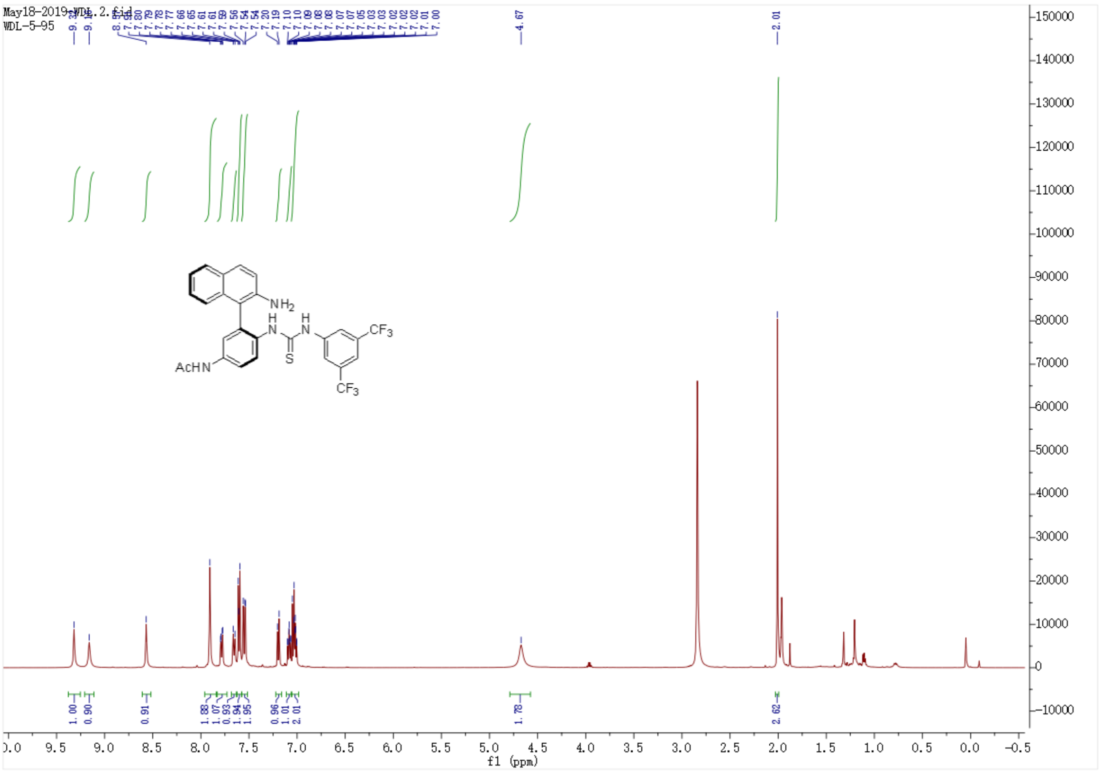

Figure S212. ^{13}C NMR spectrum of product **13a**, related to **Scheme 6**.

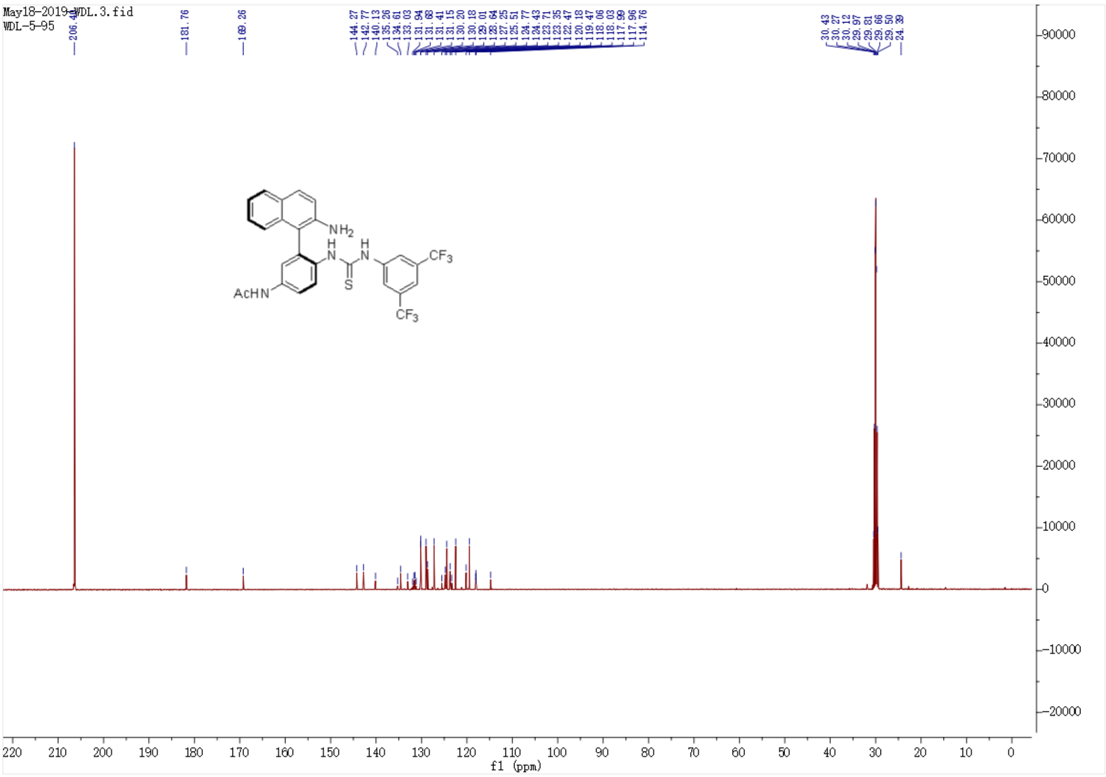

Figure S213. ^{1}H NMR spectrum of product **16**, related to **Scheme 6**.

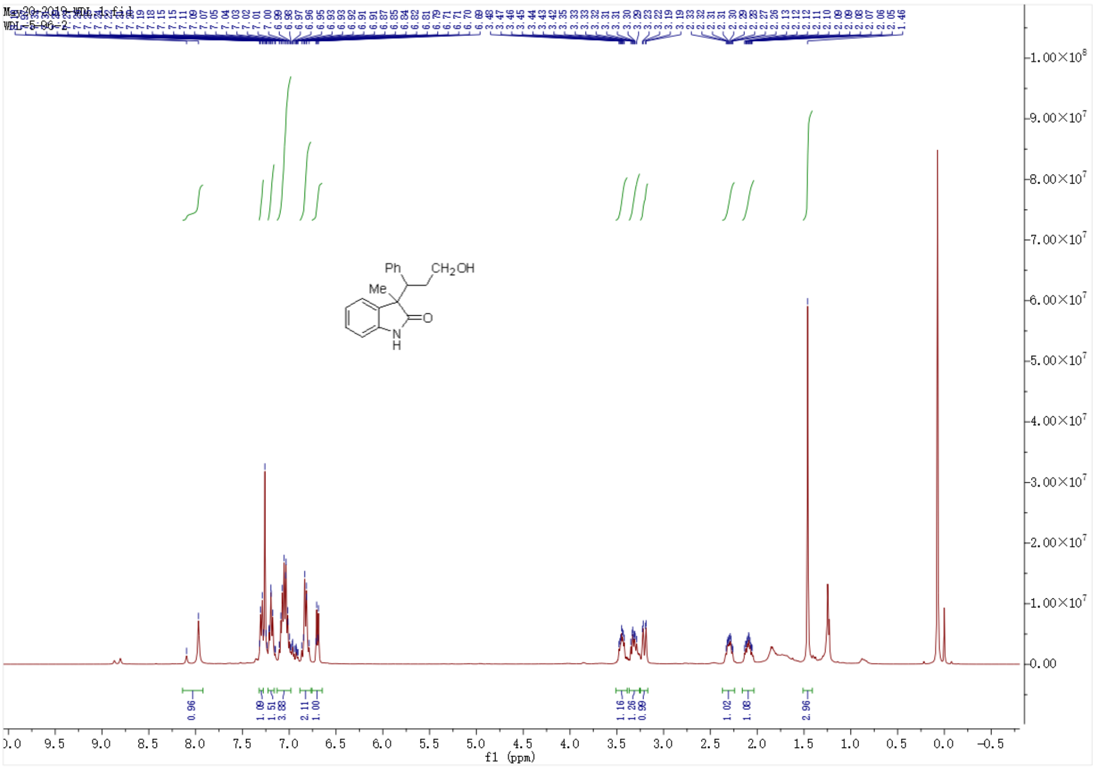

Supplemental figures and tables for X-Ray structures

Figure S214. X-ray structure of **3g**, related to **Scheme 2**

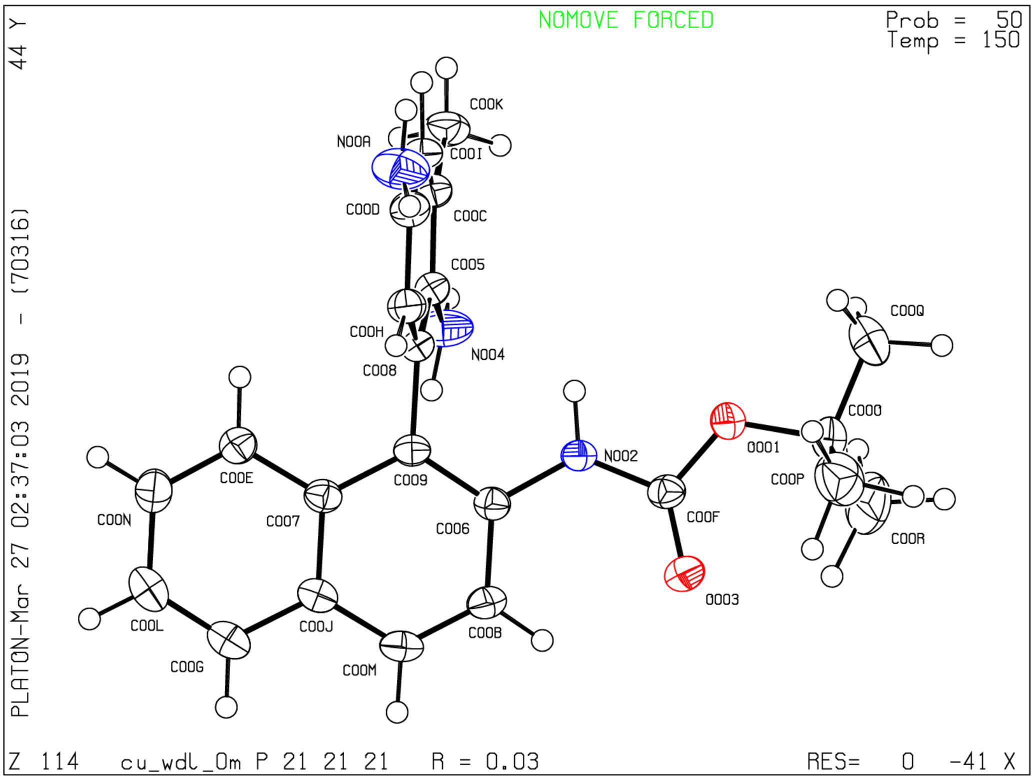

Table S2: Crystal data for **3g**, related to **Scheme 2**.

Identification code	
Empirical formula	$C_{22}H_{27}N_3O_2$
Formula weight	365.46
Temperature / K	150.0
Crystal system	Orthorhombic
Space group	$P2_12_12_1$
a / Å, b / Å, c / Å	8.4379(2), 10.5541(3), 22.3081(6)
α/°, β/°, γ/°	90, 90, 90
Volume / Å^3	1986.64(9)
Z	4
ρcalc / mg mm^{-3}	1.222
μ / mm^{-1}	0.629
F(000)	784.0
Crystal size / mm^3	0.2 × 0.15 × 0.1
Theta range for data collection	11.21 to 148.884°
Index ranges	$-8 \leq h \leq 10$, $-13 \leq k \leq 13$, $-26 \leq l \leq 27$
Reflections collected	16588
Independent reflections	4017[R(int) = 0.0214,R(sigma)=0.0187]
Data/restraints/parameters	4017/0/250
Goodness-of-fit on F^2	1.071
Final R indexes [I>2σ (I)]	R_1 = 0.0398, wR_2 = 0.1107
Final R indexes [all data]	R_1 = 0.0405, wR_2 = 0.1115
Largest diff. peak/hole / e Å^{-3}	0.31/-0.29

Figure S215. X-ray structure of (S)-**1m**, related to **Scheme 3.**.

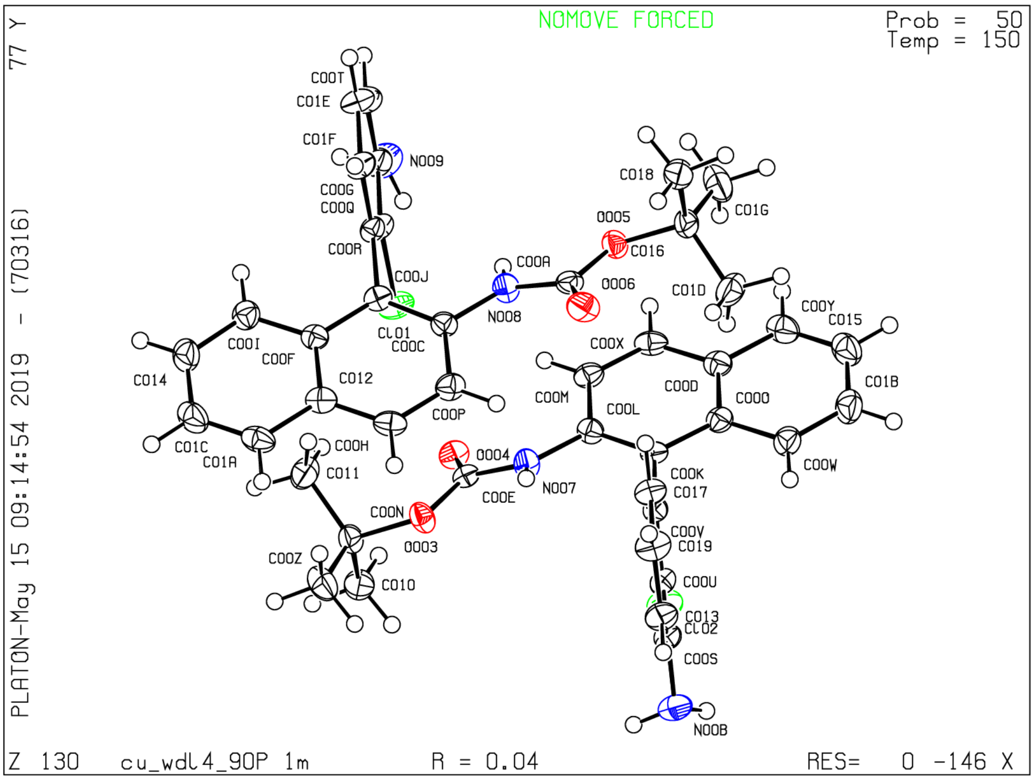

Table S3: Crystal data for (S)-**1m**, related to **Scheme 3.**

Identification code	
Empirical formula	$C_{21}H_{21}ClN_2O_2$
Formula weight	368.85
Temperature / K	150.01
Crystal system	Triclinic
Space group	P1
a / Å, b / Å, c / Å	8.1592(3),10.4448(4),12.8750(5)
α/°, β/°, γ/°	69.108(2),89.972(2),67.392(2)
Volume / $Å^3$	934.37(6)
Z	2
ρcalc / mg mm^{-3}	1.311
μ / mm^{-1}	1.947
F(000)	388.0
Crystal size / mm^3	0.2 × 0.15 × 0.1
Theta range for data collection	9.856 to 144.234°
Index ranges	$-9 \le h \le 8$, $-12 \le k \le 12$, $-15 \le l \le 15$
Reflections collected	30818
Independent reflections	6979[R(int) = 0.0652,R(sigma)=0.0639]
Data/restraints/parameters	6979/3/477
Goodness-of-fit on F^2	1.050
Final R indexes [I>2σ (I)]	$R_1 = 0.0400$, $wR_2 = 0.1036$
Final R indexes [all data]	$R_1 = 0.0422$, $wR_2 = 0.1061$
Largest diff. peak/hole / e $Å^{-3}$	0.33/-0.36

Figure S216. X-ray structure of **7c**, related to **Scheme 4**.

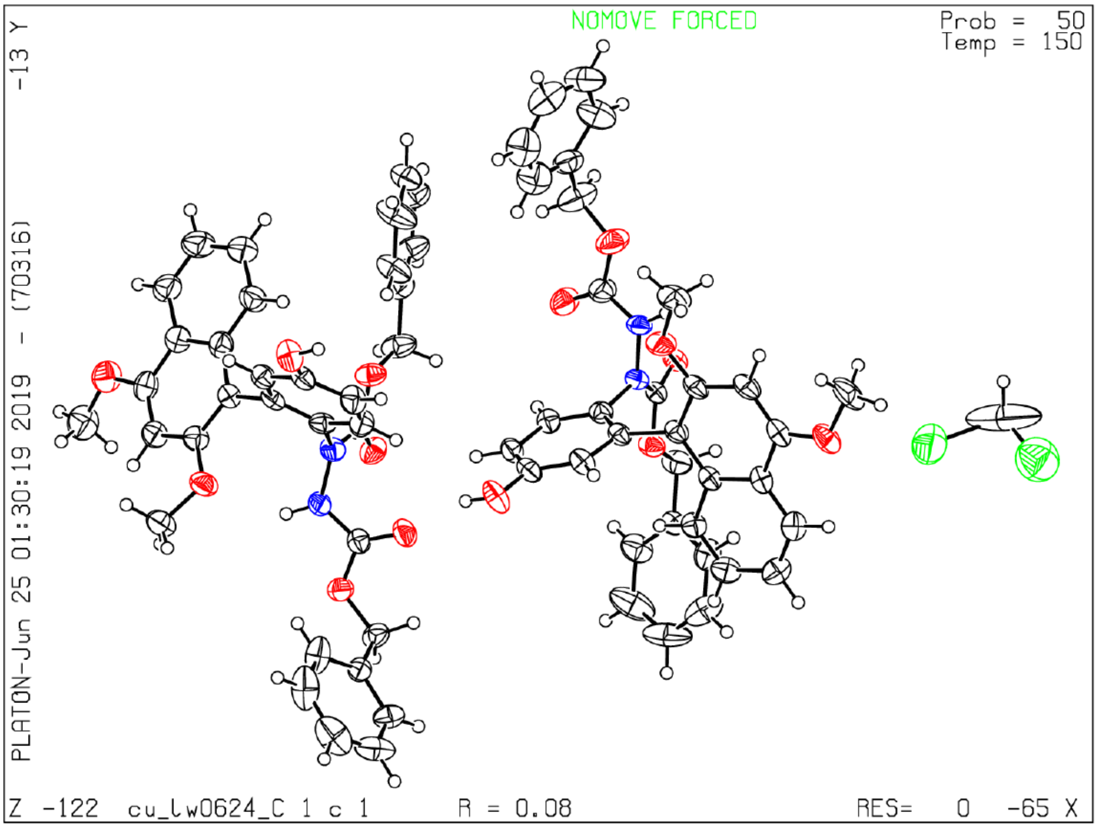

Table S4: Crystal data for **7c**, related to **Scheme 4**.

Identification code	
Empirical formula	$C_{69}H_{62}Cl_2N_4O_{14}$
Formula weight	1242.12
Temperature / K	150.0
Crystal system	Monoclinic
Space group	Cc
a / Å, b / Å, c / Å	30.4852(9),10.4675(3),19.5605(6)
α/°, β/°, γ/°	90, 96.8720(10), 90
Volume / Å^3	6197.0(3)
Z	4
ρcalc / mg mm^{-3}	1.331
μ / mm^{-1}	1.528
F(000)	2600.0
Crystal size / mm^3	0.2 × 0.15 × 0.1
Theta range for data collection	8.938 to 158.802°
Index ranges	$-38 \le h \le 38$, $-13 \le k \le 13$, $-24 \le l \le 20$
Reflections collected	63322
Independent reflections	11465[R(int) = 0.0749,R(sigma)=0.0644]
Data/restraints/parameters	11465/2/808
Goodness-of-fit on F^2	1.086
Final R indexes [I>2σ (I)]	R_1 = 0.0799, wR_2 = 0.2268
Final R indexes [all data]	R_1 = 0.0854, wR_2 = 0.2334
Largest diff. peak/hole / e Å^{-3}	0.61/-0.54

Transparent Methods

General Information:

Unless otherwise noted, all commercial reagents were used without further purification. Dichloromethane, toluene, ether, THF were purified by passage through an activated alumina column under argon. Thin-layer chromatography (TLC) analysis of reaction mixtures were performed using Huanghai silica gel HSGF254 TLC plates, and visualized under UV or by staining with ceric ammonium molybdate or potassium permanganate. Flash column chromatography was carried out on Huanghai Silica Gel HHGJ-300, 300-400 mesh. Nuclear magnetic resonance (NMR) spectra were recorded using Bruker Avance III HD spectrometer (FT, 400 MHz for ^{1}H, 101 MHz for ^{13}C). ^{1}H and ^{13}C chemical shifts are reported in ppm downfield of tetramethylsilane and referenced to residual solvent peak ($CHCl_3$; δH = 7.26 and δC = 77.16, CD_3OD, δH = 3.31 and δC = 49.00, $(CD_3)_2CO$, δH = 2.05 and δC = 29.84). Multiplicities are reported using the following abbreviations: s = singlet, d = doublet, t = triplet, q = quartet, m = multiplet, br = broad resonance. FT-IR spectras were recorded on PerkinElmer Frontier FT-IR Spectrometer, and absorption frequencies are reported in reciprocal centimeters (cm^{-1}). Mass spectral data were obtained from the Agilent Technologies 6230 TOF LC/MS spectrometer in electrospray ionization (ESI^+) mode. Optical rotations were measured with an Autopol V Plus/VI digital polarimeter. X-Ray structure analyses were performed using a Bruker D8 Venture X-ray single crystal diffractometer. Enantiomeric excesses were determined on an Agilent 1260 Chiral HPLC using IA, IB, IC columns under the detective wavelength of 254 nm. The racemic products were synthesized by using (±)-A5 or (±)-A6 as catalyst.

Synthesis of substrates:

Scheme S1, Synthesis of 1-bromo-2-naphthylamine **S2**, related to **Scheme 2**.

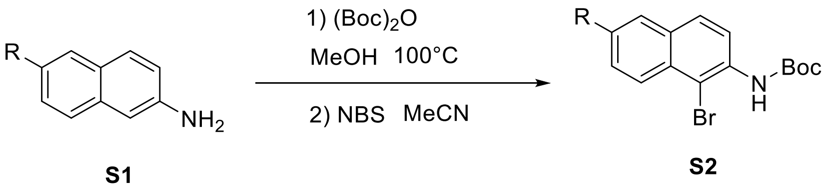

General procedure for synthesis S2: Substituted naphthalene **S1** (3.5 mmol) was dissolved in dry MeOH (10 mL) in a pressure vessel, which was followed by adding $(Boc)_2O$ (0.96 mL, 4.2 mmol). After stirring at 100 ℃ overnight, the reaction mixture was concentrated under vacuum to give a residue, which was then dissolved in MeCN (8ml) and was added NBS (668 mg, 3.7 mmol) portion-wise at 0 ℃. After stirring for 2 h at this temperature, the reaction mixture was quenched with H_2O (10 mL) and the aqueous layer was extracted with EtOAc for 3 times. The combined organic layers were dried over Na_2SO_4 and concentrated under vacuum to give a residue, which was purified with flash column chromatography to give the product **S2**.

tert-butyl (1-bromo-6-methylnaphthalen-2-yl)carbamate (**S2a**)

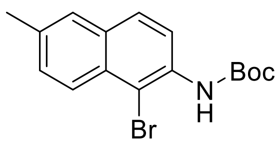

This reaction was performed on 3.7 mmol scale of **S1**. Purification by flash column chromatography (petroleum ether/EtOAc = 20: 1) gave the product **S2a** (1.1 g, 89%).
^{1}H NMR (500 MHz, Chloroform-*d*) δ 8.30 (d, *J* = 9.1 Hz, 1H), 8.03 (d, *J* = 8.7 Hz, 1H), 7.70 (d, *J* = 9.0 Hz, 1H), 7.55 (s, 1H), 7.38 (dd, *J* = 8.7, 1.8 Hz, 1H), 7.26 (d, *J* = 2.9 Hz, 1H), 2.50 (s, 3H), 1.57 (s, 9H). ^{13}C NMR (126 MHz, $CDCl_3$) δ 153.0, 135.0, 134.3, 131.4, 130.7, 130.2, 127.9, 127.4, 126.6, 120.0, 110.5, 81.5, 28.7, 21.6. IR (cm^{-1}): *ƒ* = 3401, 2974, 1719, 1489, 1458, 1224, 1147, 1069, 809. m/z HRMS (ESI) found $[M+H]^+$ 336.0581, $C_{16}H_{19}BrNO_2^+$ requires 336.0594.

tert-butyl (1-bromo-6-phenylnaphthalen-2-yl)carbamate (**S2b**)

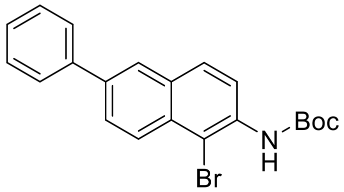

This reaction was performed on 2.05 mmol scale of **S1**. Purification by flash column chromatography (petroleum ether/EtOAc = 20: 1) gave the product **S2b** (1.1 g, 89%).

^{1}H NMR (500 MHz, Chloroform-*d*) δ 8.40 (d, *J* = 9.0 Hz, 1H), 8.20 (d, *J* = 8.8 Hz, 1H), 7.99 (d, *J* = 1.9 Hz, 1H), 7.91 – 7.79 (m, 2H), 7.76 – 7.66 (m, 2H), 7.49 (t, *J* = 7.8 Hz, 2H), 7.43 – 7.36 (m, 1H), 7.35 (s, 1H), 1.59 (s, 9H). ^{13}C NMR (126 MHz, $CDCl_3$) δ 152.9, 140.7, 138.0, 135.2, 131.6, 131.5, 129.3, 128.9, 127.8, 127.6, 127.58, 127.3, 126.2, 120.3, 110.1, 81.6, 28.7. IR (cm^{-1}): *ƒ* = 3403, 2980, 1723, 1518, 1223, 1153, 767, 695. m/z HRMS (ESI) found $[M+H]^+$ 398.0740, $C_{21}H_{21}BrNO_2^+$ requires 398.0750.

Scheme S2, Synthesis of biaryl anilines and phenols, related to **Scheme 2** and **Scheme 4**.

Method A for synthesis of substrate 1:

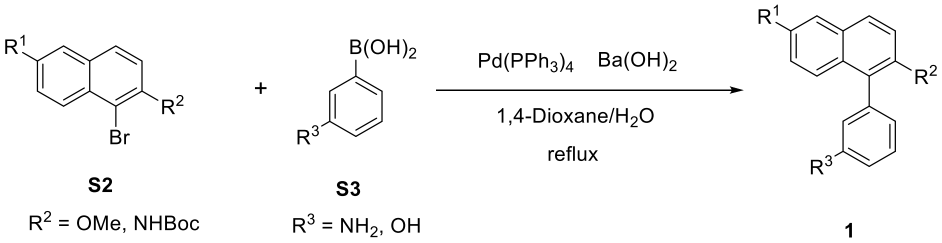

General procedure of method A for synthesis of substrate 1: A mixture of **S2** (400 mg, 1.25 mmol), arylboronic acid **S3** (1.87 mmol), tetrakis(triphenylphosphine) palladium(72 mg, 0.06mmol) and $Ba(OH)_2$ (639 mg, 3.74 mmol) were dissolved in 1,4-dioxane (24 mL) and H_2O (8mL). The mixture was purged with N_2 for 3 times and then heated to reflux overnight. The reaction mixture was then cooled to room temperature and filtered through celite to give the filtrate, which was extracted with EtOAc for 3 times. The combined organic layer was dried over Na_2SO_4 and concentrated under vacuum to give a residue, which was purified by flash column chromatography to give the product **1.**

Scheme S3. Synthesis of biaryl anilines, related to **Scheme 2**.

Method B for synthesis of substrate 1:

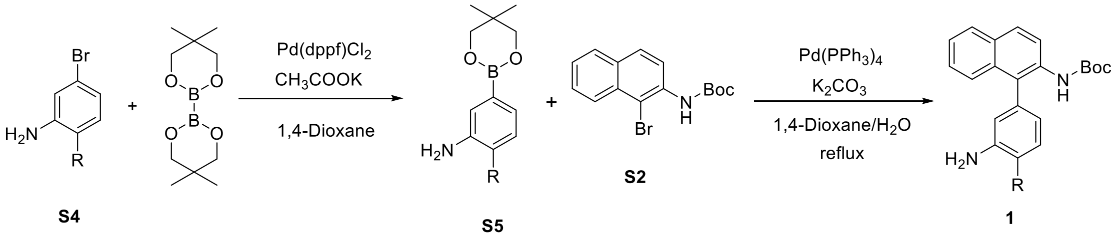

General procedure of method B for synthesis 1:

Step 1: A mixture of **S4** (2.9 mmol), 2,2,2',2'-tetramethyl-5,5'-bi(1,3,5-dioxaborinane) (688 mg, 3.05 mmol), and potassium acetate (568 mg, 5.8 mmol) were dissolved in dioxane (8 ml). The mixture was purged with N_2 for 3 times, which was followed by adding $PdC1_2$(dppf)-DCM (57 mg, 0.07 mmol). After refluxing for 3 h, the reaction mixture was cooled to room temperature and filtered through celite. The combined filtrates were concentrated under vacuum to afford a residue, which was purified by flash column chromatography to give the product **S5** for the next step.

Step 2: A mixture of tert-butyl (1-bromonaphthalen-2-yl)carbamate (**S2**, 321mg, 1mmol), **S5** (1.3mmol), tetrakis(triphenylphosphine) palladium (46.2 mg, 0.04mmol) and K_2CO_3 (331mg, 2.4mmol) were dissolved in 1,4-dioxane (10 mL) and H_2O (5mL). The mixture was purged with N_2 for 3 times, and then heated to reflux overnight. The reaction mixture was then cooled to room temperature and filtered through celite to give the filtrate, which was extracted with EtOAc for 3 times. The combined organic layers were dried over Na_2SO_4 and concentrated under vacuum to give a residue, which was purified by flash column chromatography to give the product **1.**

tert-butyl (1-(3-aminophenyl)naphthalen-2-yl)carbamate (**1a**)

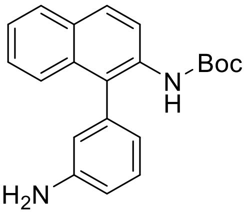

This reaction was performed on 0.47 mmol scale of **S2** according to **method A**. Purification by flash column chromatography (petroleum ether/EtOAc = 9: 1) gave the product **1a** (155 mg, 99%).

^{1}H NMR (400 MHz, Chloroform-*d*) δ 8.39 (d, *J* = 9.1 Hz, 1H), 7.84 (d, *J* = 9.1 Hz, 1H), 7.84 – 7.77 (m, 1H), 7.42 – 7.28 (m, 4H), 6.82 (ddd, *J* = 8.0, 2.4, 1.0 Hz, 1H), 6.71 (dt, *J* = 7.5, 1.3 Hz, 1H), 6.63 (t, *J* = 2.0 Hz, 1H), 6.48 (s, 1H), 3.80 (s, 2H), 1.48 (s, 9H). ^{13}C NMR (101 MHz, $CDCl_3$) δ 153.3, 147.5, 137.2, 133.7, 133.1, 130.7, 130.3, 128.5, 128.1, 126.4, 126.2, 126.0, 124.5, 121.1, 119.5, 117.5, 115.2, 80.9, 28.7. IR (cm^{-1}): *ƒ* = 3467, 3409, 3364, 2979, 1703, 1490, 1236, 1152, 828, 751. m/z HRMS (ESI) found $[M+H]^+$ 335.1750, $C_{21}H_{23}N_2O_2^+$ requires 335.1754.

tert-butyl (1-(3-aminophenyl)-6-methylnaphthalen-2-yl)carbamate (**1b**)

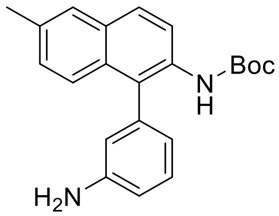

This reaction was performed on 0.6 mmol scale of **S2** according to **method A**. Purification by flash column chromatography (petroleum ether/EtOAc = 9: 1) gave the product **1b** (204 mg, 98%).

^{1}H NMR (400 MHz, Chloroform-*d*) δ 8.31 (d, *J* = 9.0 Hz, 1H), 7.73 (d, *J* = 9.1 Hz, 1H), 7.56 (s, 1H), 7.33 (t, *J* = 7.8 Hz, 1H), 7.30 – 7.22 (t, 1H), 7.13 (d, *J* = 8.6 Hz, 1H), 6.79 (d, *J* = 8.0 Hz, 1H), 6.68 (d, *J* = 7.5 Hz, 1H), 6.61 (s, 1H), 6.43 (s, 1H), 3.79 (s, 2H), 2.45 (s, 3H), 1.46 (s, 9H). ^{13}C NMR (101 MHz, $CDCl_3$) δ 153.4, 147.4, 137.4, 134.0, 132.8, 131.3, 130.6, 130.5, 128.7, 127.8, 127.1, 126.3, 125.9, 121.2, 119.7, 117.5, 115.2, 80.8, 28.7, 21.7. IR (cm^{-1}): *ƒ* = 3472, 3409, 3380, 2973, 1717, 1701, 1495, 1151, 816. m/z HRMS (ESI) found $[M+H]^+$ 349.1906, $C_{22}H_{25}N_2O_2^+$ requires 349.1911.

tert-butyl (1-(3-aminophenyl)-6-phenylnaphthalen-2-yl)carbamate (**1c**)

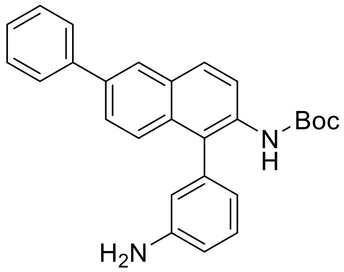

This reaction was performed on 0.63 mmol scale of **S2** according to **methodA**. Purification by flash column chromatography (petroleum ether/EtOAc = 9: 1) gave the product **1c** (247 mg, 96%).

^{1}H NMR (400 MHz, Chloroform-*d*) δ 8.44 (d, *J* = 9.1 Hz, 1H), 8.02 (d, *J* = 2.0 Hz, 1H), 7.90 (d, *J* = 9.1 Hz, 1H), 7.70 (d, *J* = 7.6 Hz, 2H), 7.59 (dd, *J* = 8.9, 2.0 Hz, 1H), 7.47 (dd, *J* = 8.5, 6.0 Hz, 3H), 7.42 – 7.31 (m, 2H), 6.83 (dd, *J* = 8.0, 2.4 Hz, 1H), 6.74 (d, *J* = 7.5 Hz, 1H), 6.66 (t, *J* = 2.0 Hz, 1H), 6.53 (s, 1H), 3.84 (s, 2H), 1.50 (s, 9H). ^{13}C NMR (101 MHz, $CDCl_3$) δ 153.3, 147.5, 141.3, 137.1, 137.1, 133.8, 132.3, 130.7, 130.4, 129.2, 128.8, 127.6, 127.5, 126.6, 126.0, 126.0, 125.9, 121.0, 119.9, 117.4, 115.3, 80.9, 28.7. IR (cm^{-1}): *ƒ* = 3461, 3414, 3373, 2981, 1714, 1596, 1490, 1230, 1151, 760, 695. m/z HRMS (ESI) found $[M+H]^+$ 411.2058, $C_{27}H_{27}N_2O_2^+$ requires 411.2067.

tert-butyl (1-(3-aminophenyl)-6-methoxynaphthalen-2-yl)carbamate (**1d)**

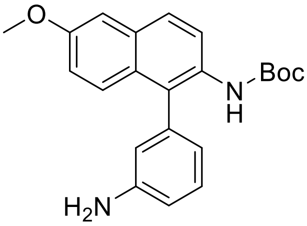

This reaction was performed on 0.32 mmol scale of **S2** according to **method A**. Purification by flash column chromatography (petroleum ether/EtOAc = 9: 1) gave the product **1d** (78 mg, 67%).

^{1}H NMR (400 MHz, Chloroform-*d*) δ 8.30 (d, *J* = 9.1 Hz, 1H), 7.73 (d, *J* = 9.0 Hz, 1H), 7.40 – 7.27 (m, 2H), 7.12 (d, *J* = 2.7 Hz, 1H), 6.99 (dd, *J* = 9.2, 2.7 Hz, 1H), 6.80 (ddd, *J* = 8.1, 2.4, 1.0 Hz, 1H), 6.69 (dt, *J* = 7.4, 1.3 Hz, 1H), 6.61 (t, *J* = 2.0 Hz, 1H), 6.40 (s, 1H), 3.90 (s, 3H), 3.86 – 3.60 (m, 2H), 1.47 (s, 9H). ^{13}C NMR (101 MHz, $CDCl_3$) δ 156.8, 153.5, 147.4, 137.3, 131.7, 131.4, 130.6, 128.5, 127.7, 127.2, 126.9, 121.0, 120.4, 119.0, 117.4, 115.2, 106.1, 80.7, 55.6, 28.7. IR (cm^{-1}): *ƒ* = 3475, 3409, 3371, 2975, 1700, 1599, 1467, 1234, 1152, 853. m/z HRMS (ESI) found $[M+H]^+$ 365.1852, $C_{22}H_{25}N_2O_3^+$ requires 365.1860.

tert-butyl (1-(3-amino-4-methylphenyl)naphthalen-2-yl)carbamate (**1e**)

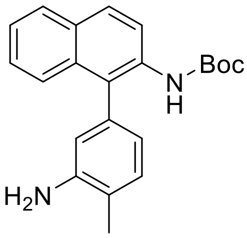

This reaction was performed on 0.94 mmol scale of **S5** according to **method B**. Purification by flash column chromatography (petroleum ether/EtOAc = 9: 1) gave the product **1e** (274 mg, 99%).

^{1}H NMR (400 MHz, Chloroform-*d*) δ 8.39 (d, *J* = 9.1 Hz, 1H), 7.88 – 7.74 (m, 2H), 7.38 (td, *J* = 8.5, 1.5 Hz, 1H), 7.35 – 7.27 (m, 2H), 7.23 (d, *J* = 7.5 Hz, 1H), 6.65 (dd, *J* = 7.4, 1.7 Hz, 1H), 6.62 (d, *J* = 1.6 Hz, 1H), 6.53 (s, 1H), 3.73 (s, 2H), 2.29 (s, 3H), 1.48 (s, 9H). ^{13}C NMR (101 MHz, $CDCl_3$) δ 153.1, 145.4, 134.4, 133.5, 133.1, 131.6, 130.1, 128.2, 127.8, 126.1, 125.9, 124.2, 122.3, 120.9, 119.2, 117.1, 80.6, 28.5, 17.4. 17.6. IR (cm^{-1}): *ƒ* = 3475, 3413, 3366, 3010, 1717, 1700, 1490, 1235, 1156, 825, 746. m/z HRMS (ESI) found [M+H]$^+$ 349.1902, $C_{22}H_{25}N_2O_2^+$ requires 349.1911.

tert-butyl (1-(3-amino-4-methoxyphenyl)naphthalen-2-yl)carbamate (**1f**)

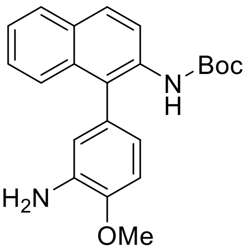

This reaction was performed on 0.67 mmol scale of **S5** according to **method B**. Purification by flash column chromatography (petroleum ether/EtOAc = 9: 1) gave the product **1f** (202 mg, 88%).

^{1}H NMR (500 MHz, Chloroform-*d*) δ 8.40 (d, *J* = 9.1 Hz, 1H), 7.81 (dd, *J* = 14.2, 8.5 Hz, 2H), 7.39 (d, *J* = 8.3 Hz, 1H), 7.37 – 7.27 (m, 2H), 6.97 (d, *J* = 7.9 Hz, 1H), 6.67 (d, *J* = 9.0 Hz, 2H), 6.55 (s, 1H), 3.97 (s, 3H), 3.95 (s, 2H), 1.49 (s, 9H). ^{13}C NMR (126 MHz, $CDCl_3$) δ 153.3, 147.4, 137.1, 134.0, 133.6, 130.2, 128.4, 128.3, 128.0, 126.3, 126.1, 126.0, 124.4, 120.9, 119.3, 117.4, 111.3, 80.8, 55.9, 28.7. IR (cm^{-1}): *ƒ* = 3468, 3395, 3373, 2988, 1698, 1500, 1227, 1155, 1027, 823. m/z HRMS (ESI) found [M+H]$^+$ 365.1855, $C_{22}H_{25}N_2O_3^+$ requires 365.1860.

tert-butyl (1-(3-amino-5-methylphenyl)naphthalen-2-yl)carbamate (**1g**)

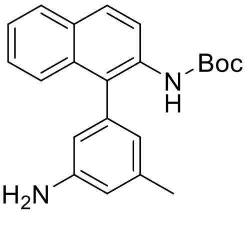

This reaction was performed on 0.91 mmol scale of **S5** according to **method B**. Purification by flash column chromatography (petroleum ether/EtOAc = 9: 1) gave the product **1g** (198 mg, 75%).

^{1}H NMR (400 MHz, Chloroform-*d*) δ 8.38 (d, *J* = 9.1 Hz, 1H), 7.81 (dd, *J* = 11.3, 8.4 Hz, 2H), 7.40 (d, *J* = 8.1 Hz, 1H), 7.38 – 7.28 (m, 2H), 6.64 (s, 1H), 6.52 (d, *J* = 4.0 Hz, 2H), 6.44 (t, *J* = 1.8 Hz, 1H), 3.74 (s, 2H), 2.35 (s, 3H), 1.49 (s, 9H). ^{13}C NMR (101 MHz, CDCl$_3$) δ 153.2, 147.2, 140.4, 136.8, 133.4, 133.0, 131.7, 130.1, 128.2, 127.8, 126.1, 125.9, 124.2, 121.7, 119.3, 115.8, 114.5, 80.6, 28.5, 21.6. IR (cm^{-1}): ƒ = 3463, 3405, 3375, 2974, 1731, 1595, 1499, 1249, 1145, 821, 747. m/z HRMS (ESI) found [M+H]$^+$ 349.1901, $C_{22}H_{25}N_2O_2^+$ requires 349.1911.

tert-butyl (1-(3-amino-5-methoxyphenyl)naphthalen-2-yl)carbamate (**1h**)

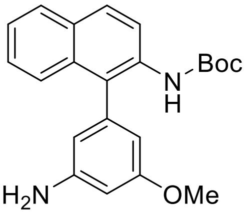

This reaction was performed on 0.63 mmol scale of **S5** according to **method B**. Purification by flash column chromatography (petroleum ether/EtOAc = 9: 1) gave the product **1h** (227 mg, 99%).

^{1}H NMR (400 MHz, Chloroform-*d*) δ 8.39 (d, *J* = 9.0 Hz, 1H), 7.81 (dd, *J* = 13.2, 8.5 Hz, 2H), 7.43 (d, *J* = 8.1 Hz, 1H), 7.33 (t, *J* = 7.7 Hz, 2H), 6.54 (s, 1H), 6.37 (d, *J* = 2.1 Hz, 1H), 6.26 (d, *J* = 10.1 Hz, 2H), 3.81 (s, 2H), 3.79 (s, 3H), 1.49 (s, 9H). ^{13}C NMR (101 MHz, CDCl$_3$) δ 161.8, 153.3, 148.8, 138.2, 133.6, 133.0, 130.2, 128.5, 128.0, 126.4, 126.1, 126.0, 124.5, 119.5, 110.4, 106.4, 101.2, 80.9, 55.7, 28.7. IR (cm^{-1}): ƒ = 3470, 3380, 2976, 1721, 1499, 1229, 1198, 1151, 1072, 814. m/z HRMS (ESI) found [M+H]$^+$ 365.1854, $C_{22}H_{25}N_2O_3^+$ requires 365.1860.

tert-butyl (3'-amino-6-methyl-[1,1'-biphenyl]-2-yl)carbamate (**1i**)

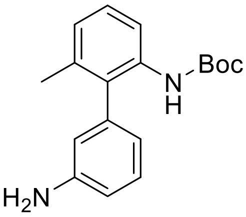

This reaction was performed on 2.42 mmol scale of **S2** according to **method A**. Purification by flash column chromatography (petroleum ether/EtOAc = 9: 1) gave the product **1i** (500 mg, 69%).

^{1}H NMR (400 MHz, Chloroform-*d*) δ 8.06 (d, *J* = 8.3 Hz, 1H), 7.37 – 7.31 (m, 1H), 7.28 (t, *J* = 7.9 Hz, 1H), 7.00 (d, *J* = 7.5 Hz, 1H), 6.79 (ddd, *J* = 8.0, 2.5, 1.0 Hz, 1H), 6.64 (dt, *J* = 7.5, 1.3 Hz, 1H), 6.57 (t, *J* = 2.0 Hz, 1H), 6.29 (s, 1H), 3.83 (s, 2H), 2.09 (s, 3H), 1.51 (s, 9H). ^{13}C NMR (101 MHz, CDCl$_3$) δ 153.2, 147.4, 138.3, 136.8, 136.2, 131.2, 130.6, 128.0, 124.4, 120.1, 116.5, 116.5, 114.9, 80.5, 28.6, 21.0. IR (cm^{-1}): *ƒ* = 3441, 3419, 3353, 2985, 1704, 1507, 1233, 1154, 758. m/z HRMS (ESI) found $[M+H]^+$ 299.1746, $C_{18}H_{23}N_2O_2^+$ requires 299.1754.

tert-butyl (3'-amino-6-chloro-[1,1'-biphenyl]-2-yl)carbamate (**1j**)

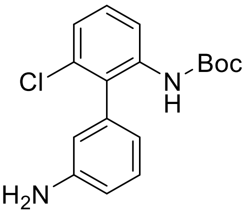

This reaction was performed on 0.7 mmol scale of **S2** according to **method A**. Purification by flash column chromatography (petroleum ether/EtOAc = 9: 1) gave the product **1j** (181 mg, 82%).

^{1}H NMR (400 MHz, Chloroform-*d*) δ 8.12 (d, *J* = 8.4 Hz, 1H), 7.30 (t, *J* = 7.8 Hz, 1H), 7.23 (d, *J* = 8.2 Hz, 1H), 7.16 – 7.06 (m, 1H), 6.77 (dd, *J* = 8.3, 2.4 Hz, 1H), 6.67 – 6.60 (m, 1H), 6.56 (t, *J* = 2.0 Hz, 1H), 6.31 (s, 1H), 3.80 (s, 2H), 1.44 (s, 9H). ^{13}C NMR (101 MHz, $CDCl_3$) δ 152.8, 147.4, 138.0, 136.2, 133.8, 130.6, 129.9, 129.2, 123.6, 120.1, 117.2, 116.7, 115.6, 81.1, 28.6. IR (cm^{-1}): *ƒ* = 3476, 3397, 3380, 2988, 1709, 1573, 1507, 1420, 1147, 846, 776. m/z HRMS (ESI) found $[M+H]^+$ 319.1198, $C_{17}H_{20}ClN_2O_2^+$ requires 319.1208.

methyl 3'-amino-6-((tert-butoxycarbonyl)amino)-[1,1'-biphenyl]-2-carboxylate (**1k**)

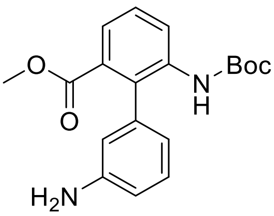

This reaction was performed on 0.7 mmol scale of **S2** according to **method A**. Purification by flash column chromatography (petroleum ether/EtOAc = 5: 1) gave the product **1k** (100 mg, 42%).

^{1}H NMR (400 MHz, Chloroform-*d*) δ 8.34 (d, *J* = 8.3 Hz, 1H), 7.49 (dd, *J* = 7.8, 1.2 Hz, 1H), 7.37 (t, *J* = 8.0 Hz, 1H), 7.31 – 7.15 (m, 1H), 6.73 (dd, *J* = 8.0, 2.4 Hz, 1H), 6.65 – 6.58 (m, 1H), 6.52 (t, *J* = 2.0 Hz, 1H), 6.45 (s, 1H), 3.75 (s, 2H), 3.58 (s, 3H), 1.44 (s, 9H). ^{13}C NMR (101 MHz, $CDCl_3$) δ 168.5, 153.0, 147.2, 137.5, 137.0, 132.0, 131.1, 130.2, 128.3, 123.8, 122.1, 119.7, 116.0, 115.2, 81.0, 52.3, 28.6. IR (cm^{-1}): *ƒ* = 3473, 3404, 3383, 2972, 1731, 1712, 1515, 1218, 1146, 986, 754. m/z HRMS (ESI) found $[M+H]^+$ 343.1640, $C_{19}H_{23}N_2O_4^+$ requires 343.1652.

benzyl (1-(3-aminophenyl)naphthalen-2-yl)carbamate (**1l**)

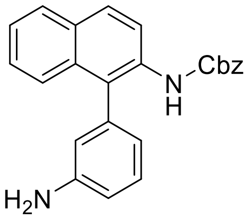

This reaction was performed on 0.85 mmol scale of **S2** according to **method A**. Purification by flash column chromatography (petroleum ether/EtOAc = 4: 1) gave the product **1l** (218 mg, 70%).

^{1}H NMR (400 MHz, Chloroform-*d*) δ 8.41 (d, *J* = 9.1 Hz, 1H), 7.87 (d, *J* = 9.1 Hz, 1H), 7.85 – 7.79 (m, 1H), 7.47 – 7.28 (m, 9H), 6.79 (dd, *J* = 8.1, 2.4 Hz, 1H), 6.74 – 6.67 (m, 2H), 6.60 (t, *J* = 1.9 Hz, 1H), 5.17 (s, 2H), 3.75 (s, 2H). ^{13}C NMR (101 MHz, $CDCl_3$) δ 153.6, 147.4, 136.6, 136.2, 132.8, 132.8, 130.5, 130.3, 128.7, 128.5, 128.5, 128.4, 127.9, 126.5, 126.3, 125.9, 124.5, 120.7, 119.2, 117.1, 115.1, 67.1. IR (cm^{-1}): *ƒ* = 3371, 3032, 2931, 1723, 1598, 1498, 1208, 1068, 743, 696. m/z HRMS (ESI) found $[M+H]^+$ 369.1603, $C_{24}H_{21}N_2O_2^+$ requires 369.1598.

tert-butyl (1-(3-amino-2-chlorophenyl)naphthalen-2-yl)carbamate (**1m**)

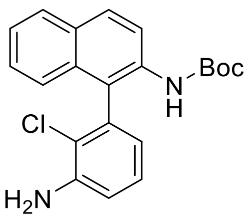

This reaction was performed on 0.9 mmol scale of **S5** according to **method B**. Purification by flash column chromatography (petroleum ether/EtOAc = 15: 1) gave the product **1m** (141 mg, 54%).

^{1}H NMR (500 MHz, Chloroform-*d*) δ 8.36 (d, *J* = 9.1 Hz, 1H), 7.88 (d, *J* = 9.1 Hz, 1H), 7.82 (d, *J* = 8.0 Hz, 1H), 7.34 (dt, *J* = 22.8, 7.1 Hz, 2H), 7.29 – 7.18 (m, 2H), 6.93 (d, *J* = 8.1 Hz, 1H), 6.69 (d, *J* = 7.4 Hz, 1H), 6.25 (s, 1H), 4.25 (s, 2H), 1.48 (d, *J* = 1.4 Hz, 9H). ^{13}C NMR (126 MHz, $CDCl_3$) δ 153.3, 144.4, 135.4, 134.0, 132.6, 130.4, 129.1, 128.4, 128.2, 126.7, 125.4, 124.7, 122.0, 120.3, 119.9, 116.2, 115.3, 81.0, 28.7. IR (cm^{-1}): *ƒ* = 3465, 3407, 3364, 2997, 2963, 1717, 1499, 1229, 1146, 816. m/z HRMS (ESI) found $[M+H]^+$ 369.1363, $C_{21}H_{22}ClN_2O_2^+$ requires 369.1364.

tert-butyl (1-(3-amino-2-methoxyphenyl)naphthalen-2-yl)carbamate (**1n**)

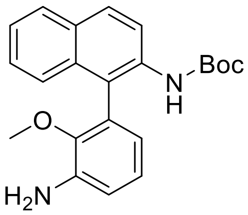

This reaction was performed on 0.85 mmol scale of **S5** according to **method B**. Purification by flash column chromatography (petroleum ether/EtOAc = 10: 1) gave the product **1n** (237 mg, 99%).

^{1}H NMR (500 MHz, Chloroform-*d*) δ 8.32 (d, *J* = 9.1 Hz, 1H), 7.87 (d, *J* = 9.0 Hz, 1H), 7.82 (d, *J* = 7.8 Hz, 1H), 7.43 (d, *J* = 8.1 Hz, 1H), 7.40 – 7.31 (m, 2H), 7.09 (t, *J* = 7.7 Hz, 1H), 6.91 (d, *J* = 7.9 Hz, 1H), 6.62 (s, 1H), 6.59 (d, *J* = 7.5 Hz, 1H), 4.00 (s, 2H), 3.25 (s, 3H), 1.47 (s, 9H). ^{13}C NMR (126 MHz, $CDCl_3$) δ 153.3, 145.8, 140.8, 133.9, 132.9, 130.3, 128.6, 128.6, 128.0, 126.4, 125.8, 125.2, 124.4, 123.0, 122.0, 120.2, 116.2, 80.6, 60.0, 28.5. IR (cm^{-1}): *ƒ* = 3411, 3366, 2977, 2932, 1717, 1497, 1470, 1221, 1153, 745. m/z HRMS (ESI) found $[M+H]^+$ 365.1854, $C_{22}H_{25}N_2O_3^+$ requires 365.1860.

tert-butyl (1-(3-amino-2-methylphenyl)naphthalen-2-yl)carbamate (**1o**)

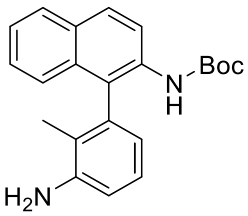

This reaction was performed on 0.66 mmol scale of **S5** according to **method B**. Purification by flash column chromatography (petroleum ether/EtOAc = 9: 1) gave the product **1o** (120 mg, 69%).

^{1}H NMR (400 MHz, Chloroform-*d*) δ 8.41 (d, *J* = 9.1 Hz, 1H), 7.84 (dd, *J* = 13.9, 8.5 Hz, 2H), 7.39 – 7.32 (m, 1H), 7.32 – 7.27 (m, 1H), 7.21 (dd, *J* = 8.6, 6.5 Hz, 2H), 6.85 (d, *J* = 7.9 Hz, 1H), 6.65 (d, *J* = 7.5 Hz, 1H), 6.32 (s, 1H), 3.93 (s, 2H), 1.76 (s, 3H), 1.47 (s, 9H). ^{13}C NMR (101 MHz, $CDCl_3$) δ 153.3, 145.8, 136.0, 133.9, 133.0, 130.3, 128.4, 128.2, 127.7, 126.5, 125.8, 125.4, 124.5, 122.6, 121.6, 119.4, 115.5, 80.9, 28.7, 13.9. IR (cm^{-1}): *ƒ* = 3470, 3399, 3373, 2978, 1712, 1496, 1228, 1157, 1066, 743. m/z HRMS (ESI) found $[M+H]^+$ 349.1902, $C_{22}H_{25}N_2O_2^+$ requires 349.1911.

tert-butyl (1-(3-amino-2-(methoxymethyl)phenyl)naphthalen-2-yl)carbamate (**1p**)

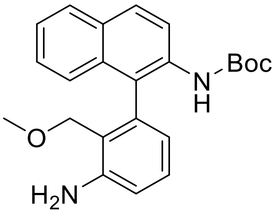

This reaction was performed on 1.37 mmol scale of **S5** according to **method B**. Purification by flash column chromatography (petroleum ether/EtOAc = 9: 1) gave the product **1p** (200 mg, 50%).

^{1}H NMR (500 MHz, Chloroform-*d*) δ 8.35 (d, *J* = 9.1 Hz, 1H), 7.86 (d, *J* = 9.0 Hz, 1H), 7.82 (d, *J* = 8.1 Hz, 1H), 7.36 (t, *J* = 7.5 Hz, 1H), 7.29 (td, *J* = 7.8, 5.1 Hz, 2H), 7.21 (d, *J* = 8.4 Hz, 1H), 6.85 (d, *J* = 7.9 Hz, 1H), 6.60 (d, *J* = 7.3 Hz, 1H), 6.41 (s, 1H), 4.44 (s, 2H), 4.23 – 4.10 (m, 1H), 4.10 – 3.99 (m, 1H), 3.06 (s, 3H), 1.46 (s, 9H). ^{13}C NMR (126 MHz, $CDCl_3$) δ 153.3, 148.1, 136.2, 134.1, 133.4, 130.2, 130.1, 128.6, 128.08, 126.6, 126.0, 124.8, 124.6, 122.2, 121.0, 119.8, 116.5, 80.8, 69.9, 58.0, 28.6. IR (cm^{-1}): *ƒ* = 3480, 3385, 2977, 2928, 1716, 1504, 1228, 1155, 1078, 740. m/z HRMS (ESI) found $[M+H]^+$ 379.2012, $C_{23}H_{27}N_2O_3^+$ requires 379.2016.

3-(2-methoxynaphthalen-1-yl)phenol (**6a)**

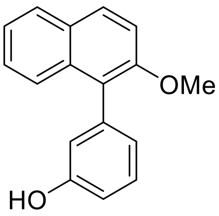

Yield = 98%. This reaction was performed on 3.0 mmol according to **Method A**. Purification by flash column chromatography (petroleum ether/EtOAc = 4: 1) gave the product **6a** (782 mg, 98%) as white solid.

^{1}H NMR (500 MHz, Chloroform-*d*) δ 7.88 (d, *J* = 9.0 Hz, 1H), 7.82 (dd, *J* = 6.3, 3.2 Hz, 1H), 7.52 (dd, *J* = 6.3, 3.5 Hz, 1H), 7.40 – 7.32 (m, 4H), 6.94 (dt, *J* = 7.5, 1.2 Hz, 1H), 6.89 (dt, *J* = 8.1, 1.6 Hz, 1H), 6.83 (dd, *J* = 2.6, 1.4 Hz, 1H), 4.91 (s, 1H), 3.85 (s, 3H). ^{13}C NMR (126 MHz, $CDCl_3$) δ 155.5, 153.7, 138.2, 133.6, 129.6, 129.3, 129.1, 127.9, 126.5, 125.4, 125.1, 123.7, 123.6, 118.1, 114.3, 113.9, 57.0. IR (cm-1): *ƒ* = 3471, 1577, 1510, 1467, 1334, 1296, 1260, 1247, 1176, 1064, 886, 786, 741, 716, 683. m/z HRMS (ESI) found $[M+H]^+$ 251.1057, $C_{17}H_{15}O_2^+$ requires 251.1067.

Scheme S4. Synthesis of biaryl phenol, related to **Scheme 4**.

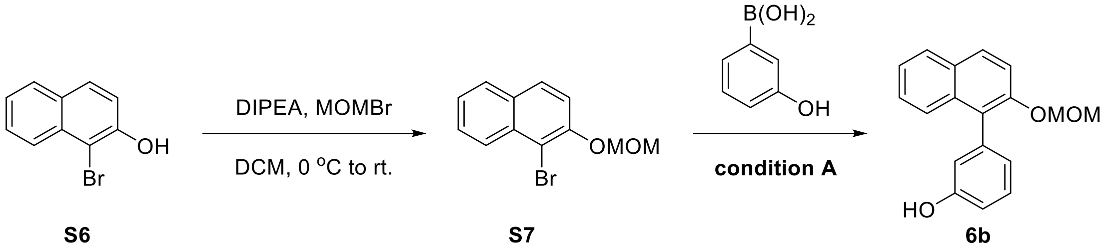

3-(2-(methoxymethoxy)naphthalen-1-yl)phenol (**6b**)

Compound **S7** was synthesized according to the procedure reported by Katsuk and co-workers (Oguma and Katsuki, 2012).

Substrate **6b** was synthesized according to the general procedure of **Method A**. This reaction was performed on 3.0 mmol scale, and purification by flash column chromatography (petroleum ether/EtOAc = 3: 1) afforded the product **6b** (826 mg, 98%) as white solid.

^{1}H NMR (500 MHz, Chloroform-*d*) δ 7.53 (dd, *J* = 7.7, 1.8 Hz, 1H), 7.46 (d, *J* = 9.0 Hz, 1H), 7.40 – 7.31 (m, 3H), 6.94 (dt, *J* = 7.5, 1.2 Hz, 1H), 6.89 (dt, *J* = 8.3, 1.7 Hz, 1H), 6.84 (dd, *J* = 2.6, 1.5 Hz, 1H), 5.29 (s, 1H), 5.11 (s, 2H), 3.34 (s, 3H). ^{13}C NMR (126 MHz, $CDCl_3$) δ 155.5, 151.3, 138.1, 133.6, 129.9, 129.5, 129.3, 127.9, 127.1, 126.4, 125.7, 124.3, 123.6, 118.0, 117.5, 114.3, 95.7, 56.3. IR (cm-1): *ƒ* = 3487, 3415, 3150, 2944, 1590, 1504, 1239, 1143, 1040, 1017, 810, 746, 686. m/z HRMS (ESI) found $[M+H]^+$ 281.1173, $C_{18}H_{17}O_3^+$ requires 281.1172.

3-(2,4-dimethoxynaphthalen-1-yl)phenol (**6c**)

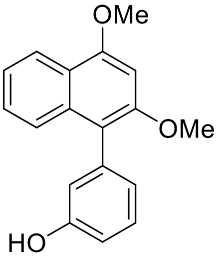

This reaction was performed on 2.34 mmol according to **Method A**. Purification by flash column chromatography (petroleum ether/EtOAc = 4: 1) afforded the product **6c** (450 mg, 69%) as white solid.

^{1}H NMR (400 MHz, Chloroform-*d*) δ 8.27 – 8.11 (m, 1H), 7.48 (dd, *J* = 7.6, 2.2 Hz, 1H), 7.39 – 7.29 (m, 3H), 6.92 (dt, *J* = 7.5, 1.2 Hz, 1H), 6.88 (dt, *J* = 8.2, 1.6 Hz, 1H), 6.82 (dd, *J* = 2.7, 1.4 Hz, 1H), 6.73 (s, 1H), 4.78 (s, 1H), 4.07 (s, 3H), 3.83 (s, 3H). ^{13}C NMR (126 MHz, $CDCl_3$) δ 156.4, 155.5, 154.1, 138.3, 134.1, 129.5, 127.2, 125.1, 124.1, 123.1, 121.9, 121.4, 118.5, 117.9, 114.1, 94.2, 57.4, 55.8. IR (cm-1): *ƒ* = 3529, 3420, 3183, 2917, 2848, 1589, 1447, 1344, 1202, 1104, 862, 768, 714. m/z HRMS (ESI) found $[M+H]^+$ 281.1164, $C_{18}H_{17}O_3^+$ requires 281.1172.

Scheme S5. Synthesis of biaryl phenol substrates, related to **Scheme 4**.

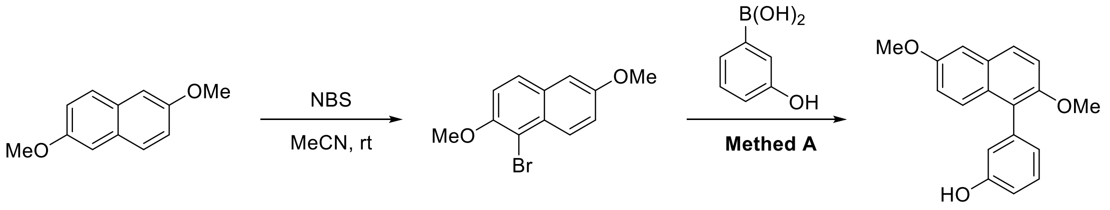

S8 **S9** **6d**

3-(2,6-dimethoxynaphthalen-1-yl)phenol (**6d**)

Compound **S9** was synthesized according to the procedure reported by Gu and co-workers (Pan et al., 2017).

Substrate **6d** was synthesized according to the general procedure of **Method A**. This reaction was performed on 1.09 mmol scale. Purification by flash column chromatography (petroleum ether/EtOAc = 20: 1) afforded the product **6d** (290 mg, 95%) as white solid.

^{1}H NMR (400 MHz, Chloroform-*d*) δ 7.76 (d, *J* = 9.0 Hz, 1H), 7.43 (d, *J* = 9.3 Hz, 1H), 7.39 – 7.29 (m, 2H), 7.12 (d, *J* = 2.7 Hz, 1H), 7.02 (dd, *J* = 9.3, 2.7 Hz, 1H), 6.96 – 6.86 (m, 2H), 6.84 – 6.80 (m, 1H), 4.78 (s, 1H), 3.91 (s, 3H), 3.81 (s, 3H). ^{13}C NMR (101 MHz, $CDCl_3$) δ 156.1, 155.3, 152.2, 138.2, 129.9, 129.4, 128.9, 127.7, 126.9, 123.5, 119.2, 117.9, 114.6, 114.2, 105.7, 57.1, 55.3. IR (cm-1): ƒ = 3481, 2935, 2838, 1576, 1458, 1339, 1250, 1179, 1111, 1065, 1025, 853, 798, 705, 668, 599. m/z HRMS (ESI) found $[M+H]^+$ 281.1162, $C_{18}H_{17}O_3^+$ requires 281.1172.

Scheme S6. Synthesis of biaryl phenol substrates, related to **Scheme 4**.

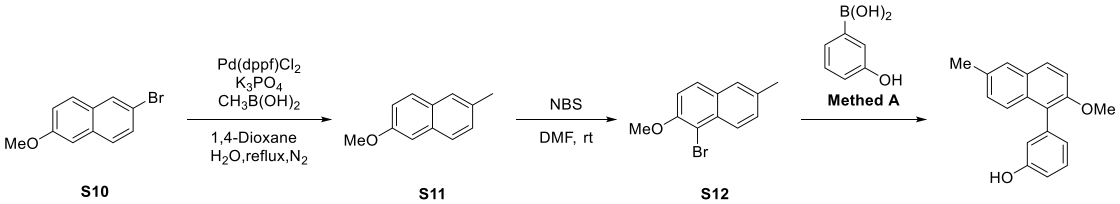

S10 **S11** **S12** **6e**

3-(2-methoxy-6-methylnaphthalen-1-yl)phenol (**6e**)

Compound **S11** was synthesized referenced to the procedure reported by Pappo and co-workers (Narute et al., 2016).

Compound **S12** was synthesized according to the procedure reported by Luan and co-workers (Zuo et al., 2017)

Substrate **6e** was synthesized according to the general procedure **Method A**. This reaction was performed on 3.75 mmol scale, and purification by flash column chromatography (petroleum ether/EtOAc = 20: 1) afforded the product **6e** (594 mg, 60%) as white solid.

^{1}H NMR (400 MHz, Chloroform-*d*) δ 7.78 (d, *J* = 9.0 Hz, 1H), 7.58 (s, 1H), 7.41 (d, *J* = 8.7 Hz, 1H), 7.38 – 7.30 (m, 2H), 7.17 (dd, *J* = 8.7, 1.8 Hz, 1H), 6.96 – 6.86 (m, 2H), 6.82 (dd, *J* = 2.6, 1.5 Hz, 1H), 4.77 (s, 1H), 3.82 (s, 3H), 2.46 (s, 3H). ^{13}C NMR (126 MHz, $CDCl_3$) δ 155.4, 152.9, 138.2, 133.1, 131.6, 129.4, 129.2, 128.7, 128.4, 126.7, 125.2, 124.9, 123.5, 117.9, 114.1, 114.0, 56.9, 21.3. IR (cm-1): ƒ = 3478, 3019, 2937, 2840, 1576, 1458, 1305, 1247, 1176, 1061, 1000, 929, 874, 815, 706, 673, 599. m/z HRMS (ESI) found $[M+H]^+$ 265.1215, $C_{18}H_{17}O_2^+$ requires 265.1223

Scheme S7. Synthesis of biaryl phenol substrates, related to **Scheme 4**.

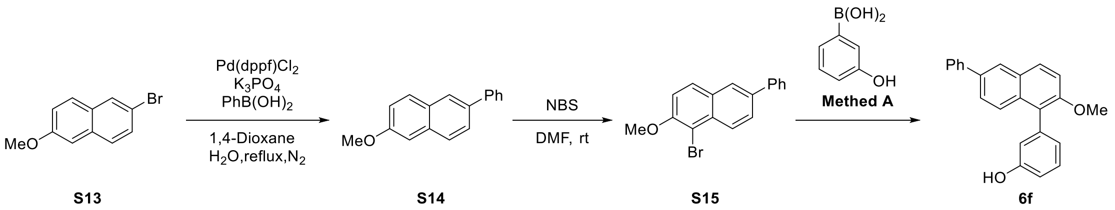

3-(2-methoxy-6-phenylnaphthalen-1-yl)phenol (**6f**)

Substrate **6f** was prepared by adopting the similar procedure for synthesizing **6e**. The Suzuki coupling of **S15** was carried out in 1.8 mmol scale, affording product **6f** (346 mg, 59%) as white solid.

^{1}H NMR (400 MHz, Chloroform-*d*) δ 8.04 – 7.97 (m, 1H), 7.93 (d, *J* = 9.0 Hz, 1H), 7.72 – 7.66 (m, 2H), 7.63 – 7.58 (m, 2H), 7.47 (t, *J* = 7.7 Hz, 2H), 7.38 (td, *J* = 7.9, 3.0 Hz, 3H), 7.00 – 6.95 (m, 1H), 6.94 – 6.89 (m, 1H), 6.86 (dd, *J* = 2.6, 1.4 Hz, 1H), 4.81 (s, 1H), 3.86 (s, 3H). ^{13}C NMR (126 MHz, $CDCl_3$) δ 155.4, 153.7, 141.0, 138.0, 136.2, 132.7, 129.5, 129.4, 129.2, 128.8, 127.2, 127.2, 126.1, 125.8, 125.7, 124.7, 123.5, 117.9, 114.2, 114.2, 56.8. IR (cm-1): ƒ = 3472, 2945, 1580, 1490, 1248, 1177, 1061, 903, 884, 757, 695. m/z HRMS (ESI) found $[M+H]^+$ 327.1369, $C_{23}H_{19}O_2^+$ requires 327.1380

3-(2,7-dimethoxynaphthalen-1-yl)phenol (**6g**)

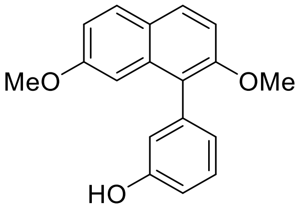

This reaction was performed on 1.8 mmol according to **Method A**. Purification by flash column chromatography (petroleum ether/EtOAc = 5: 1) afforded the product **6g** (488 mg, 97%) as white solid.

^{1}H NMR (400 MHz, Chloroform-*d*) δ 7.78 (d, *J* = 8.9 Hz, 1H), 7.71 (d, *J* = 8.9 Hz, 1H), 7.36 (t, *J* = 7.9 Hz, 1H), 7.20 (d, *J* = 9.0 Hz, 1H), 7.00 (dt, *J* = 9.0, 2.2 Hz, 1H), 6.93 (dt, *J* = 7.6, 1.3 Hz, 1H), 6.88 (d, *J* = 8.3 Hz, 1H), 6.81 (dd, *J* = 13.9, 2.2 Hz, 2H), 4.81 (s, 1H), 3.82 (s, 3H), 3.70 (s, 3H). ^{13}C NMR (126 MHz, $CDCl_3$) δ 158.1, 155.4, 154.2, 138.3, 134.8, 129.5, 129.4, 128.8, 124.5, 123.8, 123.4, 117.8, 116.2, 114.1, 111.1, 103.7, 56.6, 55.1. IR (cm-1): ƒ = 3419, 2939, 1622, 1509, 1460, 1214, 1178, 1022, 827, 769, 706. m/z HRMS (ESI) found $[M+H]^+$ 281.1165, $C_{18}H_{17}O_3^+$ requires 281.1172.

Asymmetric synthesis of products:

Scheme S8. Asymmetric para-amination of biaryl aniline substrates, related to **Scheme 2**.

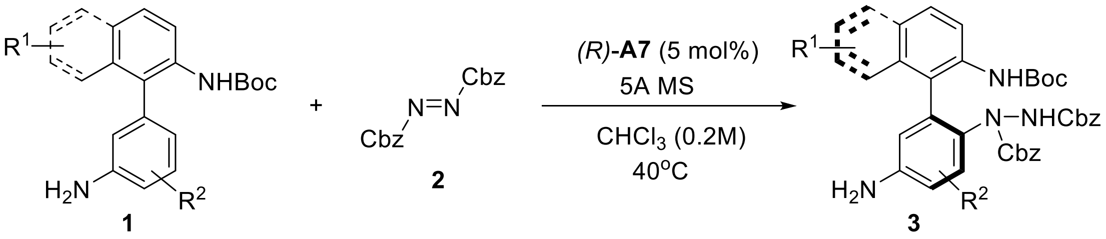

General procedure for the asymmetric synthesis of products 3a to 3p (expect **3g** and **3h):** To a solution of **1** (0.1 mmol), **2** (0.11 mmol) in $CHCl_3$ (0.5 mL) was added5 Å MS (30 mg) and (*R*)-**A7** (5mg 0.005 mmol). After stirring at 40 °C for 16 h, the reaction was filtered through celite and the filtrate were concentrated under vacuum to afford a residue, which was purified by flash column chromatography to give the product **3**.

Most of the NMR spectra of the products show rotamers and therefore doubling the signal set or line broadening. Conducting NMR experiment of 3a at 45 °C in $CDCl_3$ was attempted, which lead to some improvement of qualities of NMR spectra.

For product **3g** and **3h**, a further catalytic hydrogenation step was conducted. To the solution of the above residue in MeOH (2 mL) was added 10% Pd/C (20 mg). The reaction was purged with H_2 for 3 times and stirred under H_2 atmosphere overnight. Then the reaction mixture was filtered through celite and the filtrate was concentrated under vacuum to give a residue, which was purified by flash column chromatography to give the products **3g** and **3h**.

dibenzyl(S)-1-(4-amino-2-(2-((tert-butoxycarbonyl)amino)naphthalen-1-yl)phenyl)hydrazine-1, 2-dicarboxylate (**3a**)

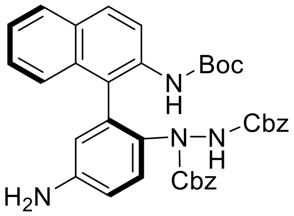

55mg, 87% yield. ^1H NMR (400 MHz, Chloroform-*d*) δ 8.36 – 7.95 (m, 1H), 7.92 – 7.57 (m, 3H), 7.27 (m, 6H), 7.15 – 6.07 (m, 11H), 5.04 (m, 4H), 3.86 (m, 2H), 1.53 – 1.34 (m, 9H). ^{13}C NMR (101 MHz, $CDCl_3$) δ 155.4, 153.8, 153.0, 147.4, 135.9, 135.6, 135.1, 134.4, 133.9, 132.4, 131.8, 131.2, 130.8, 130.2, 129.0, 128.6, 128.5, 128.4, 128.1, 127.6, 127.3, 126.4, 125.5, 124.7, 120.0, 117.2, 116.0, 80.9, 68.1, 67.7, 28.4. $[\alpha]_D^{25} = 25.40$ (c = 1.0, $CHCl_3$). IR (cm^{-1}): *ƒ* = 3369, 2962, 1715, 1497, 1223, 1153, 747, 695. m/z HRMS (ESI) found $[M+H]^+$ 633.2697, $C_{37}H_{37}N_4O_6^+$ requires 633.2708. HPLC: Chiralpak IA column, 75:25 hexanes/isopropanol, 1 ml/min; t_R = 13.6 min (major), 15.2 min (minor); 98% ee.

dibenzyl(S)-1-(4-amino-2-(2-((tert-butoxycarbonyl)amino)-6-methylnaphthalen-1-yl)phenyl)hydrazine-1,2-dicarboxylate (**3b**)

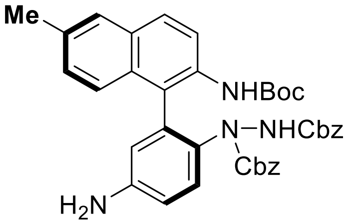

52 mg, 80% yield. ^1H NMR (400 MHz, Chloroform-*d*) δ 8.35 – 7.88 (m, 1H), 7.85 – 7.46 (m, 3H), 7.28 (m, 5H), 7.21 – 6.57 (m, 9H), 6.59 – 6.11 (m, 2H), 5.26 – 4.73 (m, 4H), 3.86 (s, 2H), 2.43 (s, 3H), 1.56 – 1.31 (m, 9H). ^{13}C NMR (101 MHz, $CDCl_3$) δ 155.7, 153.9, 153.1, 147.4, 135.9, 135.6, 134.3, 133.6, 133.1, 132.0, 131.9, 131.2, 130.8, 130.6, 128.6, 128.5, 128.4, 128.1, 127.6, 127.4, 127.1, 125.3, 121.9, 120.1, 117.2, 117.0, 115.9, 80.8, 68.1, 67.7, 28.4, 21.5. $[\alpha]_D^{25} = 28.80$ (c = 1.0, $CHCl_3$). IR (cm^{-1}): *ƒ* = 3368, 2966, 1715, 1497, 1225, 1153, 747, 695. m/z HRMS (ESI) found $[M+H]^+$ 647.2851, $C_{38}H_{39}N_4O_6^+$ requires 647.2864. HPLC: Chiralpak IA column, 75:25 hexanes/isopropanol, 1 ml/min; t_R = 13.7 min (minor), 16.3 min (major); 98% ee.

dibenzyl(S)-1-(4-amino-2-(2-((tert-butoxycarbonyl)amino)-6-phenylnaphthalen-1-yl)phenyl)hydrazine-1,2-dicarboxylate (**3c**)

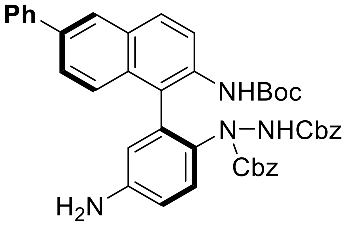

69 mg, 79% yield. ^1H NMR (400 MHz, Chloroform-*d*) δ 8.38 – 8.08 (m, 1H), 7.93 (m, 2H), 7.78 – 7.25 (m, 12H), 7.24 – 6.09 (m, 11H), 5.06 (m, 4H), 4.49 – 3.29 (m, 2H), 1.42 (m, 9H). ^{13}C NMR (126 MHz, $CDCl_3$) δ 155.7, 153.8, 153.0, 147.4, 140.9, 137.3, 135.6, 134.1, 134.0, 132.2, 131.9, 131.6, 131.4, 131.0, 130.6, 130.4, 129.3, 129.0, 128.6, 128.4, 128.1, 127.6, 127.4, 127.4, 126.0, 125.9, 123.3, 120.4, 117.2, 117.0, 116.1, 81.0, 68.2, 67.7, 28.5. $[\alpha]_D^{25} = 33.00$ (c = 1.0, $CHCl_3$). IR (cm^{-1}): *ƒ* = 3369, 2962, 1715, 1490, 1224, 1152, 748, 695. m/z HRMS (ESI) found $[M+H]^+$ 709.3004, $C_{43}H_{41}N_4O_6^+$ requires 709.3021. HPLC: Chiralpak IA column, 75:25 hexanes/isopropanol, 1 ml/min; t_R = 16.7 min (minor), 24.2 min (major); 98% ee.

dibenzyl(S)-1-(4-amino-2-(2-((tert-butoxycarbonyl)amino)-6-methoxynaphthalen-1-yl)phenyl)hydrazine-1,2-dicarboxylate (**3d**)

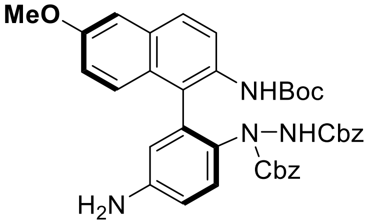

53 mg, 80% yield. ^1H NMR (400 MHz, Chloroform-*d*) δ 8.44 – 7.29 (m, 8H), 7.22 – 6.17 (m, 12H), 5.01 (m, 4H), 3.86 (s, 5H), 1.42 (m, 9H). ^{13}C NMR (101 MHz, $CDCl_3$) δ 156.9, 154.0, 153.2, 147.4, 135.9, 135.6, 132.3, 131.8, 131.7, 131.4, 131.2, 130.8, 128.6, 128.5, 128.4, 128.1, 127.7, 127.6, 127.4, 127.1, 122.7, 120.9, 119.0, 117.1, 116.8, 115.9, 106.1, 80.7, 68.1, 67.7, 55.4, 28.4. $[\alpha]_D^{25}$ = 36.55 (c = 2.0, $CHCl_3$). IR (cm^{-1}): *ƒ* = 3368, 2962, 2929, 1715, 1497, 1228, 1152, 1025, 749, 696. m/z HRMS (ESI) found $[M+H]^+$ 663.2802, $C_{38}H_{39}N_4O_7^+$ requires 663.2813. HPLC: Chiralpak IA column, 75:25 hexanes/isopropanol, 1 ml/min; t_R = 17.3 min (minor), 20.8 min (major); 98% ee.

dibenzyl(S)-1-(4-amino-2-(2-((tert-butoxycarbonyl)amino)naphthalen-1-yl)-5-methylphenyl)hydrazine-1,2-dicarboxylate (**3e**)

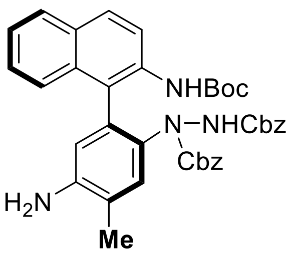

29 mg, 45% yield. ^1H NMR (400 MHz, Chloroform-*d*) δ 8.47 – 7.29 (m, 10H), 7.17 – 5.74 (m, 10H), 5.21 – 4.77 (m, 4H), 3.78 (s, 2H), 2.26 (s, 3H), 1.43 (m, 9H). ^{13}C NMR (101 MHz, $CDCl_3$) δ 155.4, 153.8, 153.0, 145.7, 135.9, 135.6, 134.5, 134.0, 132.6, 131.7, 130.2, 128.9, 128.7, 128.6, 128.5, 128.4, 128.3, 128.1, 127.6, 127.3, 126.4, 125.5, 124.6, 121.5, 119.8, 116.9, 116.7, 80.8, 68.1, 67.1, 28.4, 17.4. $[\alpha]_D^{25}$ = 25.60 (c = 1.0, $CHCl_3$). IR (cm^{-1}): *ƒ* = 3369, 2964, 2928, 1715, 1497, 1224, 1149, 1027, 783, 695. m/z HRMS (ESI) found $[M+H]^+$ 647.2844, $C_{38}H_{39}N_4O_6^+$ requires 647.2864. HPLC: Chiralpak IA column, 75:25 hexanes/isopropanol, 1 ml/min; t_R = 12.8 min (major), 14.2 min (minor); 93% ee.

dibenzyl(S)-1-(4-amino-2-(2-((tert-butoxycarbonyl)amino)naphthalen-1-yl)-5-methoxyphenyl)hydrazine-1,2-dicarboxylate (**3f**)

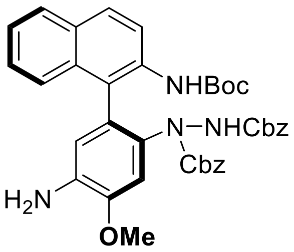

51 mg, 77% yield. ^{1}H NMR (400 MHz, Chloroform-*d*) δ 8.50 – 7.59 (m, 3H), 7.47 – 6.59 (m, 15H), 6.37 (m, 2H), 5.44 – 4.48 (m, 4H), 4.13 – 3.67 (m, 5H), 1.44 (m, 9H). ^{13}C NMR (101 MHz, $CDCl_3$) δ 155.4, 153.8, 153.0, 147.3, 137.4, 135.9, 135.6, 134.8, 134.3, 132.8, 131.5, 130.3, 130.2, 128.9, 128.6, 128.6, 128.4, 128.0, 127.6, 126.3, 125.6, 124.6, 119.7, 116.2, 116.0, 112.0, 111.5, 80.8, 68.1, 67.7, 55.9, 28.4. $[\alpha]_D^{25}$ = 28.10 (c = 1.0, $CHCl_3$). IR (cm^{-1}): *ƒ* = 3369, 2963, 1715, 1497, 1217, 1150, 1021, 745, 695. m/z HRMS (ESI) found $[M+H]^+$ 663.2792, $C_{38}H_{39}N_4O_7^+$ requires 663.2813. HPLC: Chiralpak IA column, 75:25 hexanes/isopropanol, 1 ml/min; t_R = 10.8 min (major), 12.1 min (minor); 99% ee.

tert-butyl (S)-(1-(2,5-diamino-3-methylphenyl)naphthalen-2-yl)carbamate (**3g**)

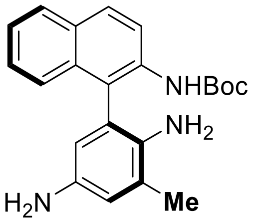

20mg, 56% yield for two steps. ^{1}H NMR (400 MHz, Chloroform-*d*) δ 8.42 (d, *J* = 9.1 Hz, 1H), 7.96 – 7.72 (m, 2H), 7.42 – 7.29 (m, 3H), 6.67 (d, *J* = 2.6 Hz, 1H), 6.59 (s, 1H), 6.38 (d, *J* = 2.6 Hz, 1H), 3.07 (s, 4H), 2.23 (s, 3H), 1.48 (s, 9H). ^{13}C NMR (101 MHz, $CDCl_3$) δ 153.5, 138.6, 136.1, 134.8, 132.8, 130.6, 129.0, 128.3, 126.8, 125.7, 125.2, 124.7, 122.4, 121.2, 119.8, 119.4, 116.5, 80.9, 28.7, 18.4. $[\alpha]_D^{25}$ = 7.80 (c = 1.0, $CHCl_3$). IR (cm^{-1}): *ƒ* = 3440, 3396, 2973, 2927, 1719, 1596, 1498, 1229, 1150, 1073, 828, 750. m/z HRMS (ESI) found $[M+H]^+$ 364.2007, $C_{22}H_{26}N_3O_2^+$ requires 364.2020. HPLC: Chiralpak IC column, 80:20 hexanes/isopropanol, 1 ml/min; t_R = 10.2 min (major), 16.8 min (minor); 99% ee.

tert-butyl (S)-(1-(2,5-diamino-3-methoxyphenyl)naphthalen-2-yl)carbamate (**3h**)

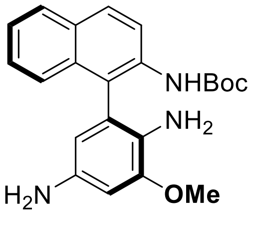

21 mg, 55% yield for two steps. ^{1}H NMR (400 MHz, Chloroform-*d*) δ 8.43 (d, *J* = 9.1 Hz, 1H), 7.93 – 7.66 (m, 2H), 7.46 – 7.29 (m, 3H), 6.69 (s, 1H), 6.42 (d, *J* = 2.4 Hz, 1H), 6.12 (d, *J* = 2.4 Hz, 1H), 3.91 (s, 3H), 3.23 (s, 4H), 1.48 (s, 9H). ^{13}C NMR (101 MHz, $CDCl_3$) δ 153.5, 149.2, 138.9, 134.7, 132.6, 130.6, 129.0, 128.2, 127.7, 126.8, 125.7, 124.7, 121.9, 121.3, 119.8, 109.9, 100.5, 80.9, 55.9, 28.7. $[\alpha]_D^{25}$ = 8.20 (c = 1.0, $CHCl_3$). IR (cm^{-1}): *f* = 3439, 3396, 2982, 1715, 1499, 1481, 1230, 1150, 1074, 820, 750. m/z HRMS (ESI) found $[M+H]^+$ 380.1956, $C_{22}H_{26}N_3O_3^+$ requires 380.1969. HPLC: Chiralpak IA column, 75:25 hexanes/isopropanol, 1 ml/min; t_R = 8.2 min (minor), 9.9 min (major); 99% ee.

dibenzyl(S)-1-(5-amino-2'-((tert-butoxycarbonyl)amino)-6'-methyl-[1,1'-biphenyl]-2-yl)hydrazine-1,2-dicarboxylate (**3i**)

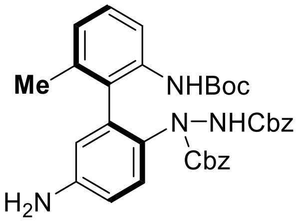

44 mg, 74% yield. ^{1}H NMR (400 MHz, Chloroform-*d*) δ 8.09 – 7.43 (m, 2H), 7.36 – 7.26 (m, 6H), 7.25 – 7.09 (m, 5H), 7.01 – 5.99 (m, 5H), 5.07 (m, 4H), 3.85 (s, 2H), 1.93 (m, 3H), 1.37 (m, 9H). ^{13}C NMR (101 MHz, $CDCl_3$) δ 155.6, 153.3, 152.8, 147.2, 136.9, 135.9, 135.6, 131.2, 130.7, 128.7, 128.6, 128.5, 128.2, 127.7, 127.5, 124.9, 124.7, 118.1, 117.1, 116.5, 116.3, 115.8, 115.6, 80.5, 68.3, 67.9, 28.4, 20.5. $[\alpha]_D^{25}$ = -1.50 (c = 1.0, $CHCl_3$). IR (cm^{-1}): *f* = 3369, 2962, 2928, 1715, 1497, 1455, 1154, 1016, 784, 749, 695. m/z HRMS (ESI) found $[M+H]^+$ 597.2693, $C_{34}H_{37}N_4O_6^+$ requires 597.2708. HPLC: Chiralpak IA column, 75:25 hexanes/isopropanol, 1 ml/min; t_R = 12.0 min (major), 13.4 min (minor); 98% ee.

dibenzyl(R)-1-(5-amino-2'-((tert-butoxycarbonyl)amino)-6'-chloro-[1,1'-biphenyl]-2-yl)hydrazine-1,2-dicarboxylate (**3j**)

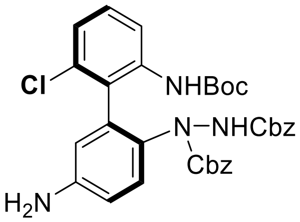

51 mg, 83% yield. ^{1}H NMR (400 MHz, Chloroform-*d*) δ 8.09 – 7.44 (m, 2H), 7.40 – 7.26 (m, 7H), 7.16 m, 5H), 6.89 – 6.22 (m, 4H), 5.04 (m, 4H), 3.85 (s, 2H), 1.40 (m, 9H). ^{13}C NMR (101 MHz, $CDCl_3$) δ 155.9, 155.5, 153.5, 147.2, 138.6, 138.0, 135.9, 135.6, 134.6, 130.9, 129.9, 129.6, 129.3, 128.7, 128.6, 128.5, 128.2, 127.7, 127.4, 124.1, 120.5, 118.0, 116.4, 81.1, 68.3, 67.9, 28.4. $[\alpha]_D^{25}$ = 29.20 (c = 1.0, $CHCl_3$). IR (cm^{-1}): *f* = 3374, 2963, 2928, 1715, 1506, 1218, 1150, 1055, 749, 695. m/z HRMS (ESI) found $[M+H]^+$ 617.2143, $C_{33}H_{34}ClN_4O_6^+$ requires

617.2161. HPLC: Chiralpak IA column, 75:25 hexanes/isopropanol, 1 ml/min; t_R = 15.0 min (minor), 15.8 min (major); 99% ee.

dibenzyl(S)-1-(5-amino-2'-((tert-butoxycarbonyl)amino)-6'-(methoxycarbonyl)-[1,1'-biphenyl]-2-yl)hydrazine-1,2-dicarboxylate(**3k**)

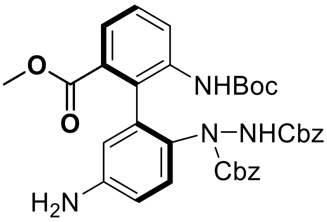

28 mg, 44 % yield. ^{1}H NMR (400 MHz, Chloroform-*d*) δ 8.37 – 6.15 (m, 18H), 5.31 – 4.78 (m, 4H), 3.80 (s, 2H), 3.56 (s, 3H), 1.39 (m, 9H). ^{13}C NMR (101 MHz, $CDCl_3$) δ 155.9, 153.9, 152.8, 146.8, 137.9, 137.7, 136.0, 135.8, 132.5, 131.4, 129.6, 128.6, 128.5, 128.4, 128.2, 128.1, 127.6, 127.3, 126.3, 124.6, 123.5, 116.1, 115.8, 80.4, 68.1, 67.2, 52.4, 28.4. $[\alpha]_D^{25}$ = 55.00 (c = 1.0, $CHCl_3$). IR (cm^{-1}): *ƒ* = 3349, 3290, 2962, 1699, 1504, 1252, 1226, 1010, 798, 740, 696. m/z HRMS (ESI) found $[M+H]^+$ 641.2581, $C_{35}H_{37}N_4O_8^+$ requires 641.2606. HPLC: Chiralpak IA column, 75:25 hexanes/isopropanol, 1 ml/min; t_R = 12.5 min (major), 20.1 min (minor); 95% ee.

Dibenzyl-(S)-1-(4-amino-2-(2-(((benzyloxy)carbonyl)amino)naphthalen-1-yl)phenyl)hydrazine-1,2-dicarboxylate (**3l**)

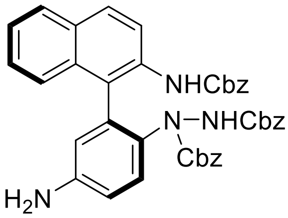

43 mg, 65% yield. ^{1}H NMR (400 MHz, Chloroform-*d*) δ 8.39 – 5.58 (m, 26H), 5.27 – 4.50 (m, 6H), 3.75 (s, 2H). ^{13}C NMR (101 MHz, $CDCl_3$) δ 155.7, 154.3, 153.6, 147.5, 135.8, 135.6, 133.9, 133.4, 132.3, 131.7, 131.3, 130.9, 130.5, 129.2, 128.6, 128.5, 128.4, 128.3, 128.1, 128.1, 127.6, 127.5, 126.6, 125.5, 125.0, 121.7, 120.1, 116.9, 116.2, 116.1, 115.9, 68.2, 67.7, 66.9. $[\alpha]_D^{25}$ = 44.40 (c = 1.0, $CHCl_3$). IR (cm^{-1}): *ƒ* = 3368, 3031, 2957, 1715, 1497, 1213, 736, 694. m/z HRMS (ESI) found $[M+H]^+$ 667.2536, $C_{40}H_{35}N_4O_6^+$ requires 667.2551. HPLC: Chiralpak IB column, 75:25 hexanes/isopropanol, 1 ml/min; t_R = 20.8 min (major), 25.7 min (minor); 99% ee.

Scheme S9. Kinetic resolution of biaryl anilines via asymmetric para-aminations, related to **Scheme 3.**

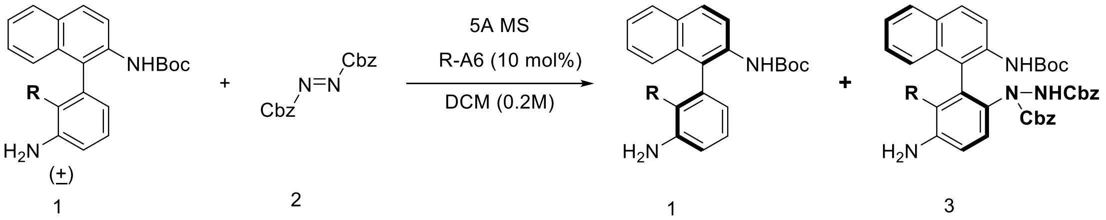

General procedure for the asymmetric synthesis of products 3m to 3o via kinetic resolution: To a solution of **1** (0.1 mmol), **2** (0.06 mmol) in DCM (0.5 mL) was 5 Å MS (30 mg) and (*R*)-**A6** (4 mg, 0.01mmol). After stirring at room temperature for 16 h, the reaction was filtered through celite and the filtrate was concentrated under vacuum to give a residue, which was purified by flash column chromatography to give the product **3** and recovered (*S*)-**1**.

(S)-tert-butyl (1-(3-amino-2-chlorophenyl)naphthalen-2-yl)carbamate (**1m**)

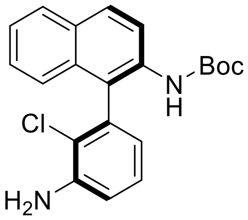

17 mg, 47% yield. HPLC: Chiralpak IA column, 85:15 hexanes/isopropanol, 1 ml/min; t_R = 6.8 min (major), 7.6 min (minor); 95% ee. $[\alpha]_D^{25}$ = 4.40 (c = 0.5, $CHCl_3$)

(S)-tert-butyl (1-(3-amino-2-methoxyphenyl)naphthalen-2-yl)carbamate (**1n**)

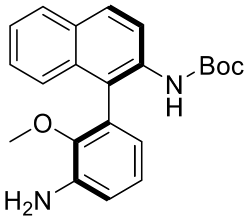

17 mg, 47% yield. HPLC: Chiralpak IA column, 85:15 hexanes/isopropanol, 1 ml/min; t_R = 6.3 min (major), 7.5 min (minor); 89% ee. $[\alpha]_D^{25}$ = 34.40 (c = 0.5, $CHCl_3$)

(S)-tert-butyl (1-(3-amino-2-methylphenyl)naphthalen-2-yl)carbamate (**1o**)

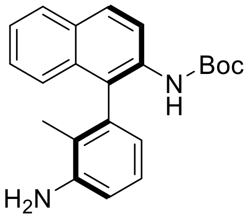

16 mg, 45% yield. HPLC: Chiralpak IA column, 85:15 hexanes/isopropanol, 1 ml/min; t_R = 6.4 min (major), 7.5 min (minor); 88% ee. $[\alpha]_D^{25}$ = -10.00 (c = 0.5, $CHCl_3$)

(S)-tert-butyl (1-(3-amino-2-(methoxymethyl)phenyl)naphthalen-2-yl)carbamate(**1p**)

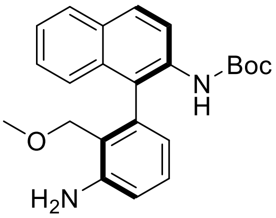

14 mg, 37% yield. HPLC: Chiralpak IA column, 85:15 hexanes/isopropanol, 1 ml/min; t_R = 6.0 min (major), 6.3 min (minor); 93% ee. $[\alpha]_D^{25}$ = -4.00 (c = 0.2, $CHCl_3$)

Dibenzyl-(R)-1-(4-amino-2-(2-((tert-butoxycarbonyl)amino)naphthalen-1-yl)-3-chlorophenyl)hydrazine-1,2-dicarboxylate (**3m**)

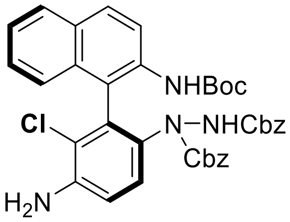

33 mg, 50% yield. ^{1}H NMR (400 MHz, Chloroform-*d*) δ 8.31 – 7.56 (m, 4H), 7.43 – 7.27 (m, 6H), 7.25 – 5.99 (m, 10H), 5.34 – 4.71 (m, 4H), 4.35 (s, 2H), 1.43 (m, 9H). ^{13}C NMR (101 MHz, $CDCl_3$) δ 155.2, 153.7, 153.2, 144.5, 135.9, 135.7, 135.0, 132.4, 131.7, 130.6, 129.7, 129.3, 128.7, 128.6, 128.5, 128.4, 128.3, 128.2, 127.7, 127.6, 126.8, 125.1, 124.8, 122.1, 120.8, 119.5, 116.2, 80.6, 68.3, 67.8, 28.5. $[\alpha]_D^{25}$ = 14.30 (c = 1.0, $CHCl_3$). IR (cm^{-1}): f = 3368, 2962, 1714, 1485, 1223, 1153, 1059, 748, 695. m/z HRMS (ESI) found $[M+H]^+$ 667.2296, $C_{37}H_{36}ClN_4O_6^+$ requires 667.2318. HPLC: Chiralpak IA column, 75:25 hexanes/isopropanol, 1 ml/min; t_R = 10.2 min (major), 11.9 min (minor); 97% ee.

Dibenzyl-(R)-1-(4-amino-2-(2-((tert-butoxycarbonyl)amino)naphthalen-1-yl)-3-methoxyphenyl)hydrazine-1,2-dicarboxylate (**3n**)

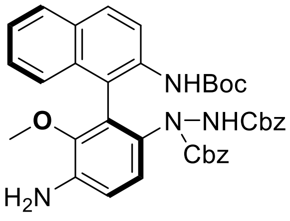

35 mg, 53% yield. ^{1}H NMR (400 MHz, Chloroform-*d*) δ 8.21 – 7.33 (m, 4H), 7.21 (s, 6H), 7.18 – 5.88 (m, 10H), 4.97 (m, 4H), 3.98 (s, 2H), 3.14 (s, 3H), 1.34 (m, 9H). ^{13}C NMR (101 MHz, $CDCl_3$) δ 155.4, 153.7, 153.1, 145.1, 143.5, 141.1, 135.9, 135.6, 132.4, 131.6, 130.4, 129.3, 129.0, 128.6, 128.6, 128.4, 128.2, 128.1, 128.1, 127.7, 127.4, 126.5, 125.2, 124.9, 122.0, 120.7, 116.1, 80.4, 68.1, 67.2, 59.8, 28.4. $[\alpha]_D^{25}$ = 21.60 (c = 1.0, $CHCl_3$). IR (cm^{-1}): *ƒ* = 3368, 2963, 1714, 1487, 1222, 1154, 747, 695. m/z HRMS (ESI) found $[M+H]^+$ 663.2789, $C_{38}H_{39}N_4O_7^+$ requires 663.2813. HPLC: Chiralpak IA column, 75:25 hexanes/isopropanol, 1 ml/min; t_R = 10.2 min (major), 11.9 min (minor); 93% ee.

Dibenzyl-(S)-1-(4-amino-2-(2-((tert-butoxycarbonyl)amino)naphthalen-1-yl)-3-methylphenyl)hydrazine-1,2-dicarboxylate (**3o**)

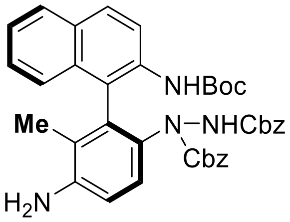

32 mg, 50% yield. ^{1}H NMR (400 MHz, Chloroform-*d*) δ 8.37 – 7.99 (m, 1H), 7.82 (m, 2H), 7.70 – 7.44 (m, 1H), 7.46 – 7.27 (m, 6H), 7.22 – 5.87 (m, 10H), 5.31 – 4.66 (m, 4H), 4.14 – 3.53 (m, 2H), 1.66 (s, 3H), 1.53 – 1.32 (m, 9H). ^{13}C NMR (101 MHz, $CDCl_3$) δ 155.6, 153.7, 153.0, 145.7, 136.0, 135.7, 134.8, 134.1, 132.0, 130.5, 130.4, 129.0, 128.7, 128.6, 128.3, 128.2, 128.0, 127.6, 127.3, 126.5, 125.1, 124.9, 122.4, 122.0, 120.2, 115.9, 115.7, 80.8, 68.0, 28.4, 28.4, 13.8. $[\alpha]_D^{25}$ = 22.90 (c = 1.0, $CHCl_3$). IR (cm^{-1}): *ƒ* = 3378, 2962, 1714, 1484, 1218, 1154, 1072, 747, 695. m/z HRMS (ESI) found $[M+H]^+$ 647.2862, $C_{38}H_{39}N_4O_6^+$ requires 647.2864. HPLC: Chiralpak IB column, 80:20 hexanes/isopropanol, 1 ml/min; t_R = 11.4 min (major), 13.0 min (minor); 92% ee.

Dibenzyl-(S)-1-(4-amino-2-(2-((tert-butoxycarbonyl)amino)naphthalen-1-yl)-3-(methoxymethyl)phenyl)hydrazine-1,2-dicarboxylate (**3p**)

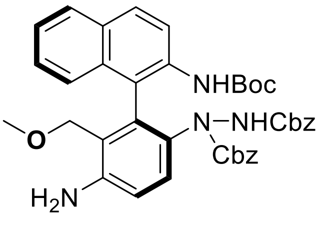

27 mg, 40% yield. ^{1}H NMR (400 MHz, Chloroform-*d*) δ 8.36 – 7.35 (m, 10H), 7.21 – 5.91 (m, 10H), 5.29 – 4.77 (m, 4H), 4.57 (s, 1H), 4.12 – 3.82 (m, 1H), 2.99 (m, 2H), 1.41 (m, 9H). ^{13}C NMR (101 MHz, $CDCl_3$) δ 154.4, 152.5, 151.9, 146.9, 134.8, 134.5, 133.8, 133.3, 131.2, 130.2, 129.4, 129.3, 128.1, 127.6, 127.4, 127.2, 127.0, 126.9, 126.5, 126.2, 125.4, 124.2, 123.8, 121.1, 119.5, 115.7, 115.6, 79.6, 68.5, 66.9, 56.4, 28.7, 27.3. $[\alpha]_D^{25}$ = 35.20 (c = 1.0, $CHCl_3$). IR (cm^{-1}): *ƒ* = 3369, 2927, 1715, 1484, 1217, 1154, 1073, 747, 695. m/z HRMS (ESI) found

$[M+H]^+$ 677.2974, $C_{39}H_{41}N_4O_7^+$ requires 677.2970. HPLC: Chiralpak IA column, 75:25 hexanes/isopropanol, 1 ml/min; t_R = 10.0 min (major), 13.5 min (minor); 94% ee.

dibenzyl3-(3-(2-((tert-butoxycarbonyl)amino)naphthalen-1-yl)phenyl)triazane-1,2-dicarboxylate (**4a**)

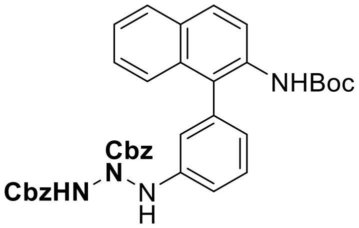

^{1}H NMR (400 MHz, Chloroform-*d*) δ 8.33 (d, *J* = 9.1 Hz, 1H), 7.83 (dd, *J* = 13.8, 8.5 Hz, 2H), 7.58 (s, 1H), 7.43 (t, *J* = 7.8 Hz, 1H), 7.39 – 7.21 (m, 13H), 7.00 – 6.70 (m, 4H), 6.40 (s, 1H), 5.18 (m, 4H), 1.45 (s, 9H). ^{13}C NMR (101 MHz, Chloroform-*d*) δ 156.7, 155.8, 153.2, 146.5, 137.1, 135.3, 135.2, 133.4, 132.8, 130.5, 130.2, 128.8, 128.7, 128.5, 128.4, 128.1, 127.9, 127.8, 127.1, 126.4, 125.6, 124.4, 123.8, 119.8, 115.7, 113.6, 80.9, 69.5, 68.3, 28.4. HRMS (ESI) found $[M+H]^+$ 633.2682, $C_{37}H_{37}N_4O_6^+$ requires 633.2708.

Scheme S10. Asymmetric para-aminations of biaryl phenols, related to **Scheme 4**.

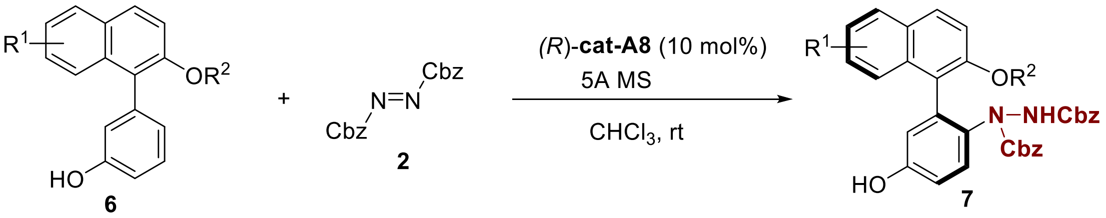

General procedure for synthesis of 7a to 7g: To a solution of **6** (0.1 mmol), **2** (0.3 mmol) in $CHCl_3$ (1 mL) was added 5 Å MS (50 mg) and *(R)*-**A8** (0.01 mmol). After stirring at room temperature for 36 h, the reaction mixture was filtered through celite and concentrated under vacuum to give a residue, which was purified by flash column chromatography to give the products **7**.

Dibenzyl-(S)-1-(4-hydroxy-2-(2-methoxynaphthalen-1-yl)phenyl)hydrazine-1,2-dicarboxylate **(7a)**

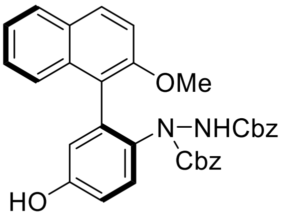

31 mg, 56% yield. ^{1}H NMR (500 MHz, Chloroform-*d*) δ 7.85 (dd, *J* = 9.1, 3.5 Hz, 1H), 7.77 (d, *J* = 8.1 Hz, 1H), 7.66 – 7.27 (m, 7H), 7.24 – 6.65 (m, 9H), 6.37 (m, 1H), 5.40 – 4.16 (m, 4H), 3.66 (d, 3H). ^{13}C NMR (101 MHz, $CDCl_3$) δ 155.9, 153.5, 135.9, 135.7, 135.6, 133.7, 133.3, 130.3, 130.2, 129.3, 128.6, 128.4, 128.3, 128.1, 127.9, 127.9, 127.4, 126.9, 126.6, 125.4, 124.0, 118.6, 115.7, 113.8, 67.9, 67.7, 56.8. IR (cm-1): *ƒ* = 3018, 1214, 1005, 928, 746, 668. $[\alpha]_D^{25}$ = 5.05 (c = 2.0, $CHCl_3$). m/z HRMS (ESI) found $[M+H]^+$ 549.2011, $C_{33}H_{29}N_2O_6^+$ requires 549.2020. HPLC: Chiralpak IA column, 70:30 hexanes/isopropanol, 1 ml/min; t_R= 11.1 min (major), 13.0 min (minor); 86% ee.

Dibenzyl-(S)-1-(4-hydroxy-2-(2-(methoxymethoxy)naphthalen-1-yl)phenyl)hydrazine-1,2-dicarboxylate **(7b)**

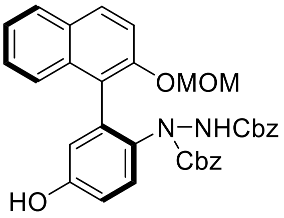

27 mg, 84% yield. ^{1}H NMR (400 MHz, Chloroform-*d*) δ 7.85 – 7.73 (m, 2H), 7.71 – 7.27 (m, 8H), 7.23 – 6.77 (m, 8H), 6.71 (d, *J* = 3.1 Hz, 1H), 5.85 (m, 1H), 5.24 – 4.79 (m, 6H), 3.34 – 3.08 (m, 3H).^{13}C NMR (101 MHz, $CDCl_3$) δ 155.8, 155.4, 135.8, 135.6, 134.0, 133.0, 130.2, 130.1, 129.9, 128.5, 128.3, 128.3, 128.1, 127.7, 127.5, 127.2, 126.4, 125.6, 124.4, 123.3, 118.4, 117.2, 116.8, 115.6, 95.9, 67.7, 67.6, 56.1. IR (cm-1): *ƒ* = 3018, 1214, 1003, 928, 746, 668, 623. $[\alpha]_D^{25}$ = 17.20 (c = 1.0, $CHCl_3$). m/z HRMS (ESI) found $[M+H]^+$ 579.2112, $C_{34}H_{31}N_2O_7^+$ requires 579.2126. HPLC: Chiralpak IA column, 80:20 hexanes/isopropanol, 1 ml/min; t_R= 20.2 min (minor), 21.6 min (major); 84% ee.

Dibenzyl-(S)-1-(2-(2,4-dimethoxynaphthalen-1-yl)-4-hydroxyphenyl)hydrazine-1,2-dicarboxylate **(7c)**

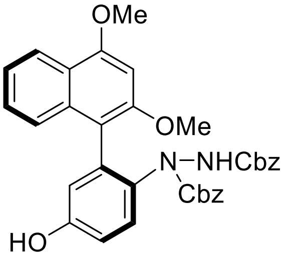

39 mg, 68% yield. ^{1}H NMR (400 MHz, Chloroform-*d*) δ 8.17 (d, *J* = 8.5 Hz, 1H), 7.45 (dd, 6H), 7.23 – 6.46 (m, 12H), 5.85 (d, 1H), 5.35 – 4.72 (m, 4H), 4.02 (s, 3H), 3.65 (d, 3H). ^{13}C NMR (101 MHz, $CDCl_3$) δ 157.1, 155.9, 155.6, 154.0, 135.9, 135.8, 134.3, 133.7, 130.5, 130.4, 128.6, 128.4, 128.1, 127.9, 127.8, 127.7, 127.3, 125.1, 123.4, 122.0, 121.8, 121.6, 119.3, 119.1, 115.5, 93.9, 67.8, 67.6, 55.7, 55.7. IR (cm-1): *ƒ* = 3018, 1214, 1004, 928, 746, 668, 608. $[\alpha]_D^{25}$ = -0.70 (c = 1.0, $CHCl_3$). m/z HRMS (ESI) found $[M+H]^+$ 579.2113, $C_{34}H_{31}N_2O_7^+$ requires

579.2126. HPLC: Chiralpak IB column, 80:20 hexanes/isopropanol, 1 ml/min; t_R = 9.2 min (major), 11.0 min (minor); 87% ee.

Dibenzyl-(S)-1-(2-(2,6-dimethoxynaphthalen-1-yl)-4-hydroxyphenyl)hydrazine-1,2-dicarboxylate (**7d**)

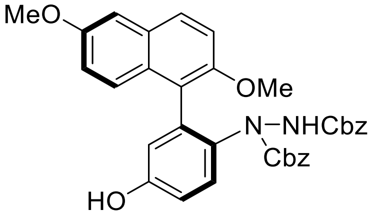

35 mg, 61% yield. ^{1}H NMR (400 MHz, Chloroform-*d*) δ 7.72 (dd, *J* = 9.0, 2.2 Hz, 1H), 7.66 – 7.26 (m, 5H), 7.24 – 6.64 (m, 12H), 6.07 (d, 1H), 5.40 – 4.68 (m, 4H), 3.87 (d, 3H), 3.63 (d, 3H). ^{13}C NMR (101 MHz, $CDCl_3$) δ 156.2, 155.8, 155.7, 152.1, 135.8, 133.8, 130.3, 128.7, 128.6, 128.4, 128.1, 127.9, 127.6, 127.4, 127.0, 119.4, 118.6, 115.7, 114.6, 105.8, 67.9, 67.7, 57.1, 55.4. IR (cm-1): *ƒ* = 3018, 1214, 1006, 928, 746, 668, 608. $[\alpha]_D^{25}$ = 9.40 (c = 1.0, $CHCl_3$). m/z HRMS (ESI) found $[M+H]^+$ 579.2114, $C_{34}H_{31}N_2O_7^+$ requires 579.2126. HPLC: Chiralpak IA column, 75:25 hexanes/isopropanol, 1 ml/min; t_R = 10.7 min (major), 26.2 min (minor); 89% ee.

Dibenzyl-(S)-1-(4-hydroxy-2-(2-methoxy-6-methylnaphthalen-1-yl)phenyl)hydrazine-1,2-dicarboxylate (**7e**)

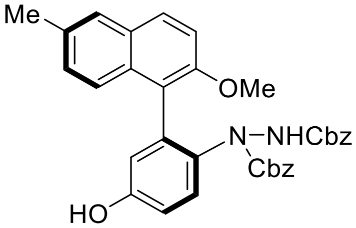

37 mg, 66% yield. ^{1}H NMR (400 MHz, Chloroform-*d*) δ 7.75 (dd, *J* = 9.1, 4.9 Hz, 1H), 7.63 (d, *J* = 8.0 Hz, 1H), 7.53 (d, *J* = 7.9 Hz, 1H), 7.29 (m, *J* = 6.9 Hz, 3H), 7.24 – 6.60 (m, 12H), 5.98 (d, 1H), 5.31 – 4.81 (m, 4H), 3.64 (d, 3H), 2.40 (d, 3H). ^{13}C NMR (101 MHz, $CDCl_3$) δ 155.7, 152.9, 135.9, 135.8, 135.7, 133.9, 133.4, 131.4, 130.3, 129.5, 129.4, 128.9, 128.6, 128.4, 128.1, 127.8, 127.6, 127.4, 126.8, 125.2, 67.9, 67.7, 56.9, 21.4. IR (cm-1): *ƒ* = 3018, 1214, 1006, 747, 668. $[\alpha]_D^{25}$ = 15.00 (c = 1.0, $CHCl_3$). m/z HRMS (ESI) found $[M+H]^+$ 563.2160, $C_{34}H_{31}N_2O_6^+$ requires 563.2177. HPLC: Chiralpak IA column, 70:30 hexanes/isopropanol, 1 ml/min; t_R = 6.9 min (major), 13.7 min (minor); 89% ee.

Dibenzyl-(S)-1-(4-hydroxy-2-(2-methoxy-6-phenylnaphthalen-1-yl)phenyl)hydrazine-1,2-dicarboxylate (**7f**)

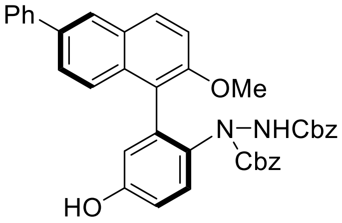

35 mg, 56% yield. ^{1}H NMR (400 MHz, Chloroform-*d*) δ 7.98 (d, *J* = 7.5 Hz, 1H), 7.91 (d, *J* = 9.0 Hz, 1H), 7.73 – 7.27 (m, 12H), 7.24 – 6.65 (m, 9H), 5.78 (d, 1H), 5.24 – 4.79 (m, 4H), 3.69 (d, 3H). ^{13}C NMR (101 MHz, $CDCl_3$) δ155.7, 153.7, 140.9, 136.6, 135.9, 135.7, 134.0, 132.4, 130.5, 129.5, 128.9, 128.6, 128.4, 128.1, 127.9, 127.4, 127.3, 127.3, 126.2, 125.9, 125.7, 118.6, 115.7, 114.1, 67.9, 67.7, 56.88. IR (cm-1): *ƒ* = 3018, 1214, 1004, 928, 747, 668. $[\alpha]_D^{25}$ = 10.70 (c = 1.0, $CHCl_3$). m/z HRMS (ESI) found $[M+H]^+$ 625.2317, $C_{39}H_{33}N_2O_6^+$ requires 625.2333. HPLC: Chiralpak IC column, 70:30 hexanes/isopropanol, 1 ml/min; t_R = 8.9 min (major), 12.8 min (minor); 89% ee.

Dibenzyl-(R)-1-(2-(2,7-dimethoxynaphthalen-1-yl)-4-hydroxyphenyl)hydrazine-1,2-dicarboxylate (**7g**)

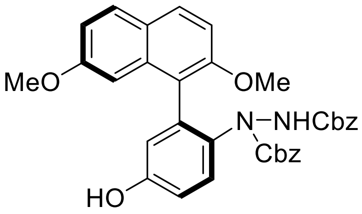

39 mg, 68% yield. ^{1}H NMR (400 MHz, Chloroform-*d*) δ 7.77 (d, *J* = 9.0 Hz, 1H), 7.67 (m, 2H), 7.29 (m, 3H), 7.24 – 6.52 (m, 12H), 5.87 (d, 1H), 5.42 – 4.74 (m, 4H), 3.79 – 3.16 (m, 6H). ^{13}C NMR (101 MHz, $CDCl_3$) δ 158.4, 158.1, 155.7, 154.1, 135.8, 135.6, 133.9, 130.6, 130.3, 129.7, 129.5, 128.5, 128.3, 128.0, 127.7, 127.1, 124.7, 124.3, 118.6, 118.3, 116.5, 115.5, 110.9, 110.5, 103.6, 102.9, 67.8, 67.5, 55.1, 54.8. IR (cm-1): *ƒ* = 3018, 1214, 1007, 746, 668. $[\alpha]_D^{25}$ = 29.20 (c = 1.0, $CHCl_3$). m/z HRMS (ESI) found $[M+H]^+$ 579.2114, $C_{34}H_{37}N_2O_7^+$ requires 579.2126. HPLC: Chiralpak IC column, 8020 hexanes/isopropanol, 1 ml/min; t_R = 11.3 min (major), 20.1 min (minor); 87% ee.

Gram-scale preparation of 3a:

Scheme S11. Gram-scale preparation of **3a**, related to Scheme **6**.

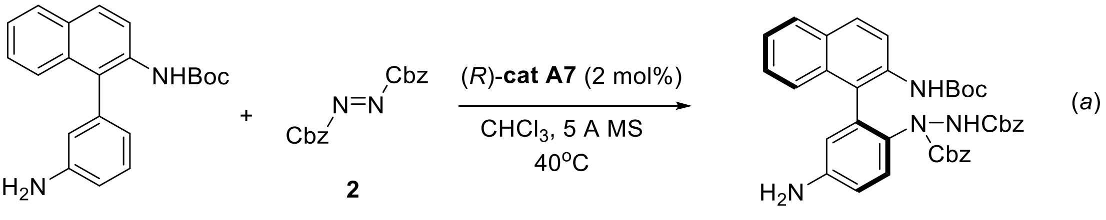

1a, 1002 mg

3a, 70% yield, 99% ee

To a solution of **1** (1.002g 3 mmol), **2** (1.03g 3.45mmol) and 5 Å MS (300 mg) in $CHCl_3$ (15 mL) was added (*R*)-**A7** (60 mg 0.06 mmol). After stirring at 40 ℃ overnight, the reaction mixture was filtered through celite and the filtrate was concentrated under vacuum to give a residue, which was purified by flash column chromatography (petroleum ether/THF = 5: 1) to give the product **3a** (1.326 g, 70%, 99% ee).

Derivatizations of chiral products:

Scheme S12. Transformations of the amino group in product, related to **Scheme 6**.

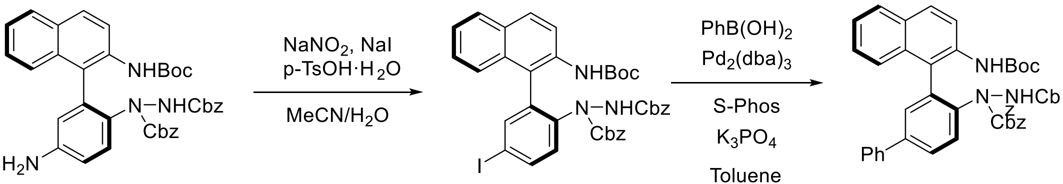

3a, 99 %ee

8a, 50%, 99% ee

9a, 81%, 99% ee

Dibenzyl-(S)-1-(2-(2-((tert-butoxycarbonyl)amino)naphthalen-1-yl)-4-iodophenyl)hydrazine-1,2-dicarboxylate (**8a**)

To a solution of *p*-TsOH.H_2O (180mg, 0.95 mmol) in MeCN (4 mL) was added **3a** (200 mg, 0.31 mmol). The resulting suspension of amine salt was cooled to 5-10 °C and to this was gradually added a solution of $NaNO_2$ (44 mg, 0.63mmol) and NaI (118 mg, 0.8mmol) in H_2O (0.3 mL). The reaction mixture was stirred for 10 min then allowed to warm to 20 °C. After stirring for 30 min, the reaction mixture was then added H_2O (2 mL), $NaHCO_3$ (1 M; until pH = 9-10) and $Na_2S_2O_3$ (2 M, 1 mL). The mixture was extracted with EtOAc for 3 times. The combined organic layer was dried over Na_2SO_4 and concentrated under vacuum to afford a residue, which was purified by column chromatography (petroleum ether/EtOAc = 10:1) as eluent to give the product **8a** (115 mg, 50% yield). ^1H NMR (400 MHz, Chloroform-*d*) δ 8.10 (s, 1H), 7.86 (m, 3H), 7.74 – 7.52 (m, 2H), 7.31 (s, 7H), 7.24 – 6.92 (m, 6H), 6.78 – 5.91 (m, 2H), 5.04 (m, 4H), 1.48 (s, 9H). ^{13}C NMR (101 MHz, $CDCl_3$) δ 155.8, 154.7, 153.6, 141.1, 140.7, 139.0, 135.6, 135.4, 135.3, 132.7, 132.0, 131.3, 130.4, 130.0, 129.4, 128.6, 128.6, 128.5, 128.3, 128.2, 128.1, 127.6, 126.8, 125.0, 124.8, 122.3, 94.7, 80.8, 68.4, 68.0, 28.4. $[\alpha]_D^{25}$ = 33.55 (c = 2.0, $CHCl_3$). IR (cm^{-1}): *ƒ* = 3307, 2973, 1716, 1496, 1222, 1153, 1023, 746, 695. m/z HRMS (ESI) found $[M+H]^+$ 744.1561, $C_{37}H_{35}IN_3O_6^+$ requires 744.1565. HPLC: Chiralpak IB column, 95:05 hexanes/isopropanol, 1 ml/min; t_R = 9.8 min (major), 11.2 min (minor); 99% ee.

dibenzyl(S)-1-(3-(2-((tert-butoxycarbonyl)amino)naphthalen-1-yl)-[1,1'-biphenyl]-4-yl)hydrazine-1,2-dicarboxylate (**9a**)

A mixture of **8a** (110mg, 0.15mmol), phenylboronic acid (27 mg, 0.22mmol), $Pd_2(dba)_3$ (9.6 mg, 0.01 mmol), S-Phos (8.6mg, 0.02mmol) and K_3PO_4 were suspended in dry toluene (10 mL). The mixture was purged with N_2 for 3 times and then heated to 105 ^{o}C. After stirring at this temperature overnight, the reaction mixture was cooled to room temperature and filtered through celite. The filtrate was concentrated under vacuum to give a residue, which was purified by flash column chromatography (petroleum ether/EtOAc = 10: 1) to give the product **9a** (83mg, 81%). ^{1}H NMR (500 MHz, Chloroform-*d*) δ 8.49 – 7.96 (m, 2H), 7.87 (m, 3H), 7.65 (d, *J* = 7.6 Hz, 2H), 7.56 (s, 1H), 7.51 – 5.94 (m, 18H), 5.32 – 4.78 (m, 4H), 1.45 (m, 9H). ^{13}C NMR (126 MHz, $CDCl_3$) δ 155.9, 155.1, 153.7, 145.6, 142.2, 140.3, 139.6, 135.6, 135.4, 134.5, 134.1, 132.3, 130.5, 130.5, 129.8, 129.0, 128.9, 128.6, 128.6, 128.4, 128.2, 128.1, 127.6, 127.2, 126.6, 125.1, 124.9, 124.5, 122.1, 120.4, 109.6, 80.5, 68.3, 67.9, 28.4. $[\alpha]_D^{25}$ = 28.70 (c = 2.0, $CHCl_3$). IR (cm^{-1}): *ƒ* = 3412, 2975, 1716, 1486, 1221, 1153, 748, 695. m/z HRMS (ESI) found $[M+H]^+$ 694.2903, $C_{43}H_{40}N_3O_6^+$ requires 694.2912. HPLC: Chiralpak IB column, 95:05 hexanes/isopropanol, 1 ml/min; t_R = 11.6 min (major), 13.2 min (minor); 99% ee.

(S)-4-amino-3-(2-methoxynaphthalen-1-yl)phenol (**10a)**

Scheme S13. Hydrogenation of products **7a**, related to **Scheme 6**.

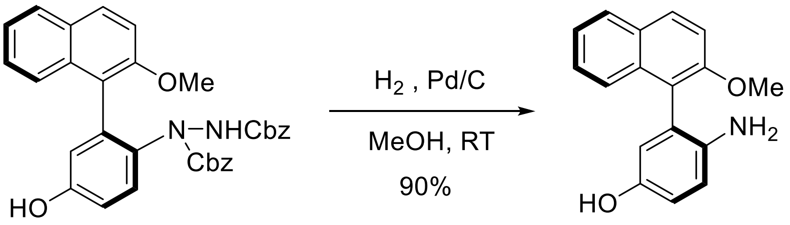

7a, 86 % ee

10a, 86% ee

To a solution of **7a** (27 mg, 86% ee, 0.05 mmol) in MeOH (1 ml) was add Pd/C (10 mg, 10 % Pd, 55% w/w water). After stirring under H_2 atmosphere (1 atm) overnight, the reaction mixture was filtered through celite and concentrated under vacuum to give a residue, which was purified by flash column chromatography (Petroleum ether/EtOAc = 1:1) to give the product **10a** (12 mg, 90% yield). ^{1}H NMR (400 MHz, Chloroform-*d*) δ 7.91 (d, *J* = 9.0 Hz, 1H), 7.85 – 7.77 (m, 1H), 7.49 – 7.43 (m, 1H), 7.40 – 7.32 (m, 3H), 6.79 (d, *J* = 2.5 Hz, 2H), 6.63 (dd, *J* = 2.2, 1.0 Hz, 1H), 3.88 (s, 3H). ^{13}C NMR (101 MHz, $CDCl_3$) δ 154.3, 148.1, 138.5, 133.2, 129.7, 129.2, 127.9, 126.8, 124.9, 123.8, 123.4, 121.0, 118.4, 117.0, 115.8, 113.8, 56.8. IR (cm-1): *ƒ* = 3018, 1214, 1005, 746, 668. $[\alpha]_D^{25}$ = -6.00 (c = 0.25, $CHCl_3$). m/z HRMS (ESI) found $[M+H]^+$ 266.1165, $C_{17}H_{16}NO_2^+$ requires 266.1176. HPLC: Chiralpak IA column, 80:20 hexanes/isopropanol, 1 ml/min; t_R = 12.6 min (major), 17.5 min (minor); 86% ee

(*R*)-2-(2-aminonaphthalen-1-yl)-3-methoxybenzene-1,4-diamine (**11n)**

Scheme S14. Hydrogenation of product **3n**, related to Scheme **6**.

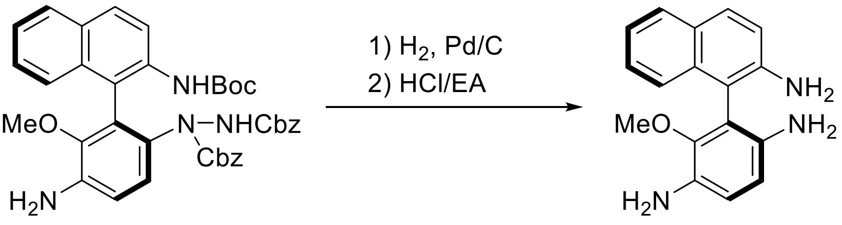

3n, 96% ee **11n**, 82%, 96% ee

To a solution of **3n** (158 mg, 0.24 mmol) in MeOH (4 mL) was add 10% Pd/C (15 mg,). After stirring under H_2 atmosphere (1 atm) overnight at room temperature, the reaction mixture was filtered through celite and concentrated under vacuum to give a residue, which was then dissolved in HCl/EA solution (2.0 M, 4ml). After stirring for 1 h at room temperature, the reaction was quenched by adding saturated $NaHCO_3$ solution. The mixture was extracted with EtOAc for three times and the combined organic layers were dried over Na_2SO_4 and concentrated under vacuum to give a residue, which was purified by flash column chromatography (petroleum ether/EtOAc = 1: 3) to give the product **11n** (55mg, 82%). ^{1}H NMR (500 MHz, Chloroform-*d*) δ 7.73 (t, *J* = 7.9 Hz, 2H), 7.38 – 7.28 (m, 2H), 7.23 (ddd, *J* = 8.1, 6.0, 1.9 Hz, 1H), 7.06 (d, *J* = 8.8 Hz, 1H), 6.78 (d, *J* = 8.4 Hz, 1H), 6.56 (d, *J* = 8.4 Hz, 1H), 3.45 (s, 6H), 3.28 (s, 2H). ^{13}C NMR (126 MHz, $CDCl_3$) δ 147.0, 142.5, 138.0, 133.5, 131.9, 129.5, 128.3, 128.2, 126.9, 123.9, 122.4, 118.4, 117.5, 116.2, 112.3, 111.8, 59.9. $[\alpha]_D^{25}$ = -21.00 (c = 0.5, $CHCl_3$). IR (cm^{-1}): *ƒ* = 3422, 3337, 3185, 2930, 2828, 1616, 1485, 1259, 1011, 811, 749. m/z HRMS (ESI) found $[M+H]^+$ 280.1434, $C_{17}H_{18}N_3O^+$ requires 280.1444. HPLC: Chiralpak IA column, 50:50 hexanes/isopropanol, 1 ml/min; t_R = 11.3 min (major), 12.1 min (minor); 96% ee.

Scheme S15. Preparation of amine-thiourea catalyst from **3a**, related to Scheme **6**.

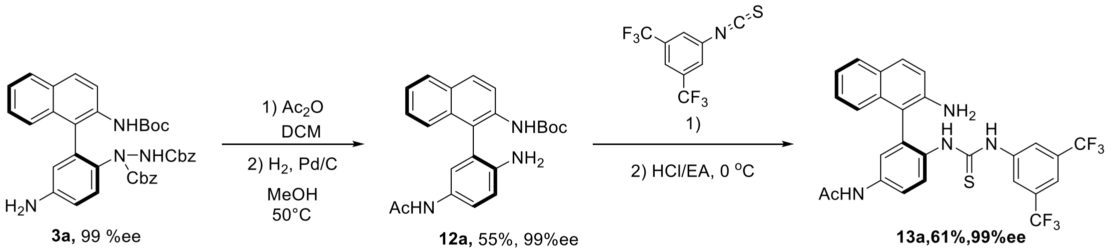

3a, 99 %ee **12a,** 55%, 99%ee **13a,61%,99%ee**

Tert-butyl (S)-(1-(5-acetamido-2-aminophenyl)naphthalen-2-yl)carbamate (**12a**)

To a solution of **3a (**400mg, 0.63mmol**)** in dry DCM (10mL) was added acetic anhydride (65μL, 0.7mmol) at room temperature. After stirring for 3 h, the solvent was removed under vacuum to give a residue, which was purified by flash column chromatography (petroleum ether/EtOAc = 2: 1) to give the product.

To a solution of above product in MeOH (4 mL) was add 10% Pd/C (60 mg,). After stirring under H_2 atmosphere (1 atm) overnight at 50 ^{o}C, the reaction mixture was filtered through celite and concentrated under vacuum to give a residue, which was purified by flash column chromatography (petroleum ether/EtOAc = 2: 1) to give the product **12a** (136mg, 55%). ^{1}H NMR (400 MHz, Chloroform-*d*) δ 8.33 (d, *J* = 9.1 Hz, 1H), 7.81 (dd, *J* = 18.1, 8.6 Hz, 2H), 7.65 (s, 1H), 7.56 (dd, *J* = 8.7, 2.5 Hz, 1H), 7.41 – 7.27 (m, 3H), 6.96 (d, *J* = 2.5 Hz, 1H), 6.76 (d, *J* =

8.6 Hz, 1H), 6.58 (s, 1H), 3.40 (s, 2H), 2.04 (s, 3H), 1.45 (s, 9H). ^{13}C NMR (101 MHz, $CDCl_3$) δ 168.6, 153.3, 141.8, 134.4, 132.5, 130.5, 129.9, 129.0, 128.1, 126.7, 125.2, 124.7, 123.7, 122.9, 121.5, 120.2, 120.0, 116.4, 80.9, 28.4, 24.3. $[\alpha]_D^{25}$ = 19.60 (c = 0.5, $CHCl_3$). IR (cm^{-1}): *f* = 3307, 2976, 1716, 1597, 1496, 1227, 1151, 1072, 820, 747. m/z HRMS (ESI) found $[M+H]^+$ 392.1957, $C_{23}H_{26}N_3O_3^+$ requires 392.1969. HPLC: Chiralpak IA column, 90:10 hexanes/isopropanol, 1 ml/min; t_R = 16.3 min (minor), 17.3 min (major); 99% ee.

(*S*)-*N*-(3-(2-aminonaphthalen-1-yl)-4-(3-(3,5-bis(trifluoromethyl)phenyl)thioureido)phenyl)acetamide (**13a**)

To a solution of **12a** (99 mg, 0.25 mmol) in THF (2mL) was added 3,5-bis(trifluoromethyl)phenyl isothiocyanate (51 μL, 0.28 mmol) at rt. After stirring overnight at this temperature, the solvent was removed under vacuum to give a residue, which was purified by flash column chromatography (petroleum ether/EtOAc = 2: 1) to afford the product.

The above product was dissolved in HCl/EA solution (2.0 M, 4mL) at 0 °C. After stirring for 1h at this temperature, the reaction mixture was quenched by adding saturated $NaHCO_3$ solution. The mixture was extracted with EtOAc for three times and the combined organic layer was dried over Na_2SO_4 and concentrated under vacuum to give a residue, which was purified by flash column chromatography (petroleum ether/EtOAc = 1: 1) to give the product **13a** (87mg, 61%). ^{1}H NMR (500 MHz, Acetone-*d*$_6$) δ 9.32 (s, 1H), 9.16 (s, 1H), 8.57 (s, 1H), 7.91 (s, 2H), 7.78 (dd, *J* = 8.8, 2.5 Hz, 1H), 7.66 (d, *J* = 8.8 Hz, 1H), 7.60 (d, *J* = 8.8 Hz, 2H), 7.57 – 7.50 (m, 2H), 7.20 (d, *J* = 8.4 Hz, 1H), 7.08 (ddd, *J* = 8.3, 6.6, 1.4 Hz, 1H), 7.06 – 6.97 (m, 2H), 4.67 (s, 2H), 2.01 (s, 3H). ^{13}C NMR (126 MHz, Acetone-*d*$_6$) δ 181.8, 169.3, 144.3, 142.8, 140.1, 135.3, 134.6, 133.0, 131.6 (q, *J* = 33.2 Hz), 130.2 (d, *J* = 2.2 Hz), 129.0, 128.6, 127.3, 125.5, 124.8, 124.4, 123.7, 123.4, 122.5, 120.2, 119.5, 118.0 (q, *J* = 3.9 Hz), 114.8, 24.4. $[\alpha]_D^{25}$ = 13.10 (c = 1, $CHCl_3$). IR (cm^{-1}): *f* = 3297, 2962, 1615, 1514, 1273, 1120, 812, 750, 678. m/z HRMS (ESI) found$[M+H]^+$ 563.1327, $C_{27}H_{21}F_6N_4OS^+$ requires 563.1335. HPLC: Chiralpak IA column, 80:20 hexanes/isopropanol, 1 ml/min; t_R = 7.3 min (minor), 15.6 min (major); 99% ee.

Application of amine-thiourea catalyst 13a:

Scheme S16. Application of amine-thiourea catalyst **13a**, related to Scheme **6**.

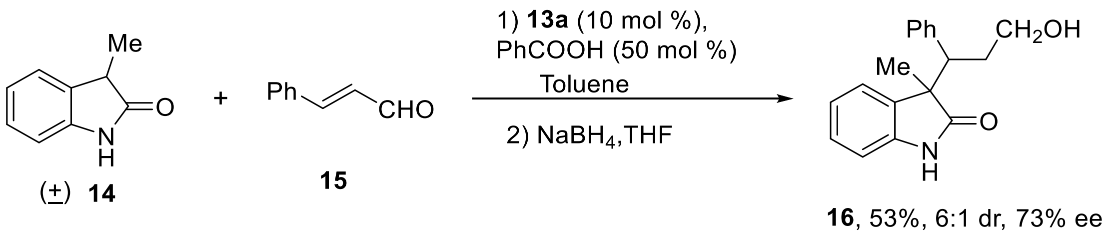

The procedure was adopted from the reported literature (Galzerano et al., 2009) by using the catalyst **13a.**

3-(3-hydroxy-1-phenylpropyl)-3-methylindolin-2-one (**16**)

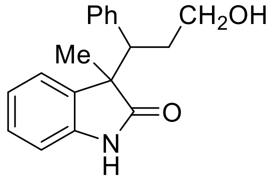

53%, 6:1 dr. The major diastereomers: ^{1}H NMR (400 MHz, Chloroform-*d*) δ 7.97 (s, 1H), 7.30 (d, *J* = 7.3 Hz, 1H), 7.24 – 7.15 (m, 1H), 7.12 – 6.99 (m, 4H), 6.87 – 6.79 (m, 2H), 6.70 (d, *J* = 7.7 Hz, 1H), 3.45 (ddd, *J* = 11.4, 7.3, 4.3 Hz, 1H), 3.32 (ddd, *J* = 10.7, 8.2, 6.4 Hz, 1H), 3.21 (dd, *J* = 12.6, 2.8 Hz, 1H), 2.30 (ddt, *J* = 15.7, 7.8, 3.8 Hz, 1H), 2.09 (dddd, *J* = 12.9, 8.5, 6.4, 3.2 Hz, 1H), 1.46 (s, 3H). $[\alpha]_D^{25}$ = -25.80 (c = 1.0, $CHCl_3$). HPLC: Chiralpak IB column, 90:10 hexanes/isopropanol, 1 ml/min; t_R = 9.6 min (major), 11.2 min (minor); 73% ee.

Supplemental Reference

Galzerano, P., Bencivenni, G., Pesciaioli, F., Mazzanti, A., Giannichi, B., Sambri, L., Bartoli, G., and Melchiorre, P. (2009). Asymmetric Iminium Ion Catalysis with a Novel Bifunctional Primary Amine Thiourea: Controlling Adjacent Quaternary and Tertiary Stereocenters. Chem. Eur. J.*15*, 7846-7849.

Narute, S., Parnes, R., Toste, F.D., and Pappo, D. (2016). Enantioselective Oxidative Homocoupling and Cross-Coupling of 2-Naphthols Catalyzed by Chiral Iron Phosphate Complexes. J. Am. Chem. Soc. *138*, 16553-16560.

Oguma, T., and Katsuki, T. (2012). Iron-Catalyzed Dioxygen-Driven C–C Bond Formation: Oxidative Dearomatization of 2-Naphthols with Construction of a Chiral Quaternary Stereocenter. J. Am. Chem. Soc. *134*, 20017-20020.

Pan, C., Zhu, Z., Zhang, M., and Gu, Z. (2017). Palladium-Catalyzed Enantioselective Synthesis of 2-Aryl Cyclohex-2-enone Atropisomers: Platform Molecules for the Divergent Synthesis of Axially Chiral Biaryl Compounds. Angew. Chem. Int. Ed. *56*, 4777-4781.

Zuo, Z., Wang, H., Fan, L., Liu, J., Wang, Y., and Luan, X. (2017). Modular Assembly of Spirocarbocyclic Scaffolds through Pd0-Catalyzed Intermolecular Dearomatizing [2+2+1] Annulation of Bromonaphthols with Aryl Iodides and Alkynes. Angew. Chem. Int. Ed. *56*, 2767-2771.